SIZE EXCLUSION CHROMATOGRAPHY (SEC) IN AQUEOUS MEDIA

© SUNNY N.E. OMORODION

BSc (HONS.) CHEMISTRY
BSc (HONS.) CHEMICAL ENGINEERING
MEng CHEMICAL ENGINEERING

A Thesis

submitted to the School of Graduate Studies

in Partial Fulfilment of the Requirements

for the Degree

Doctor of Philosophy

McMaster University

12th December 1980

DOCTOR OF PHILOSOPHY (1980)
(Chemical Engineering)

McMASTER UNIVERSITY
Hamilton, Ontario

TITLE: Size Exclusion Chromatography (SEC) in Aqueous Media.

AUTHOR: SUNNY NOSAKHARE EBILAMIAGBON OMORODION
B.Sc. (Hons) Chemistry (University of Ibadan, Nigeria)
B.Sc. (Hons) Chemical Engineering (University of Alberta, Canada)
M.Eng. (McMaster University, Canada)

SUPERVISORS: Professors A.E. Hamielec and J.L. Brash.

NUMBER OF PAGES: xiv , 205

ABSTRACT: This thesis deals with the different aspects of the successful application of size exclusion chromatography (SEC) for the molecular weight distribution (MWD) measurement of water soluble polymers. These aspects include methodology of mobile-phase development, selection of packing pore-sizes and methodology of molecular weight calibration and chromatogram interpretation. Qualitative understanding of ion-exclusion and adsorption, two of the more important and least understood complex phenomena in aqueous SEC was also provided.

The polar nature and unique physical properties of water-soluble polymers in solution were found to be critically important in selection of mobile-phases and pore sizes. Due to the active sites present with most porous packing materials adequately suited for aqueous SEC application, adsorption, one of the resulting complications, was reduced preferentially, by addition of non-ionic surfactants such as Tergitol or polyethylene oxide to the mobile-phase. Ion-exclusion was controlled and reduced by addition of varying amounts of salt and/or acid to the mobile-phase. The optimal pH and ionic strength of the mobile-phase depended on the type of polymer being investigated. No common mobile-phase was found for the four polymers investigated (dextran, hydrolysed and non-hydrolysed polyacrylamide, and sodium polystyrene sulfonate).

From viscosity data, these polymers were found to cover a very wide range of sizes in solution, with dextran being exceptionally very compact in solution when compared to polyacrylamide of the same molecular weight (MW). For this reason, selection of pore sizes was found to be critically important in achieving minimum peak broadening and maximum separation. Selection of one multi-column SEC system for general application to different water-soluble polymers was found not to be possible.

Two powerful methods of molecular weight calibration, where simultaneously the peak broadening correction factors and the true molecular weight calibration curve are obtained, were developed. These methods require the use of multiple polydisperse MW standards, with known ($\bar{M}_n$, $\bar{M}_w$) or ($\bar{M}_n$, $[\eta]$). From these methods, a new shape of the instrumental spreading function was found. This more general symmetric exponential type of spreading function provides a very simple definition of axial dispersion coefficient, which was shown not to be the most important fundamental parameter in SEC. With this shape function, apart from D2, the slope of the true MW calibration curve, the most important fundamental parameter (in the absence of skewing) was found to be the polyplatykurtic coefficient, its importance increasing with increasing polydispersity of polymer samples.

This Thesis

is lovingly dedicated

to my sons

David and Sidney.

ACKNOWLEDGEMENTS

The author wishes to express his gratitude to those who contributed in every way, to the success of this work. He is particularly indebted to his research directors, Professors A.E. Hamielec and J.L. Brash for their enthusiastic, guiding, encouraging and profound advice and interest throughout the course of this study.

The author also wishes to express his thanks to his fellow graduate students who were always willing to discuss academic problems. The financial support and assistance of the National Sciences and Engineering Research Council of Canada and McMaster University are gratefully acknowledged.

Special thanks are due to Mrs Cathy Moulder for her patience and conscientiousness in typing this thesis, and finally to my wife, Francisca, for her moral support and forbearance throughout the study.

Publications Based on PhD Research

The following are some of the papers already accepted for publication during the course of study:

(1) Hamielec, A.E. and S.N.E. Omorodion, 1980. Molecular Weight and Peak Broadening Calibration in SEC - Use of Multiple Broad Molecular Weight Distribution Standards for Linear Polymers. ACS Symp. Series, Washington, D.C., September (1979) - to be issued.

(2) Omorodion, S.N.E., A.E. Hamielec and J. Brash, 1980. Optimization of Peak Separation and Broadening in Aqueous Gel Permeation Chromatography - Nonionic Polyacrylamide. ACS Symp. Series, Washington, D.C., September (1979) - to be issued.

(3) Omorodion, S.N.E., A.E. Hamielec and J. Brash, 1980. Optimization of Peak Separation and Broadening in Aqueous Gel Permeation Chromatography - Dextrans. Accepted for publication in the Journal of Liquid Chromatography (1980).

TABLE OF CONTENTS

SIZE EXCLUSION CHROMATOGRAPHY (SEC) IN AQUEOUS MEDIA

TABLE INDEX

FIGURE INDEX

SIZE EXCLUSION CHROMATOGRAPHY (SEC) IN AQUEOUS MEDIA

1. INTRODUCTION TO SIZE EXCLUSION CHROMATOGRAPHY

Size exclusion chromatography, formerly referred to as gel permeation chromatography, provides the molecular weight distribution (MWD) of polymers, by sorting the polymer molecules in solution according to size. The chromatogram obtained in this process, contains a great deal of information about the performance of the chromatographic process itself, as well as the polymer sample molecular weight distribution.

Water-soluble polymers are of great importance in many areas of technology (1). Recently, they have been the subject of accelerated study, because of the prospect that they can aid in recovery of petroleum from underground formations (2-4). Their optimum use for most applications, requires a knowledge of their molecular weight averages and molecular weight distribution (MWD). Obtaining this information from SEC has a number of inherent difficulties, and new methods such as field-flow fractionation (FFF) (5) are being developed to overcome these problems. However, the FFF method is subject to other disadvantages as are most methods of fractionation.

For SEC of polymers in aqueous media the problem areas include complications arising from polyelectrolytic behaviour, and interpretations of the chromatographic response in terms of MWD curves. Most water soluble polymers exhibit polyelectrolytic effects in chromatographic systems, the majority of which are still not understood. These include ion-inclusion (6-10), ion-exclusion (6, 7, 11-13), polyelectrolytic

expansion of coils in solution (14,15) and adsorption (16-18). Most packing materials suited for aqueous SEC applications have surface active sites. Where ionic solutes and mobile phases are involved, care is needed to establish that the mechanism of separation is only on the basis of size.

The literature is replete with studies on aqueous SEC, dating back to 1964 (19, 20) when the process was known as gel filtration. At that time, the discipline was mostly in the hands of bio-chemists, whose interests were limited to biological materials. Some of these include proteins, amino acids, viruses and carbohydrates. Other polymers which have also been studied include natural polymers such as lignin sulfonates, inorganic solutes and other polymers such as dextran, sucrose and polyvinyl alcohol. Very few studies have been reported on water-soluble synthetic polymers.

Because of the lack of suitable packing and mobile phases for high resolution separations of synthetic water-soluble polymers and the lack of appropriate methodology for calibration and chromatogram interpretation, this investigation was undertaken with the following objectives:

(i) to develop mobile-phases and packing for the SEC of dextrans, non-ionic and anionic polyacrylamides and sodium polystyrene sulfonates.

(ii) to provide at least a qualitative understanding of ion-exclusion and adsorption, two of the more important and least understood phenomena in aqueous SEC

(iii) to develop methodology for molecular weight calibration and chromatogram interpretation suitable for aqueous SEC.

These polymers were chosen for the present investigation, because they have a broad range of properties relevant to most water-soluble polymers.

Thus, they include polymers which are branched, linear, polydispersed in molecular weight, neutral, slightly charged, highly charged, and with compact and highly expanded coils in solution.

2. THEORETICAL DEVELOPMENT

Two methods of molecular weight calibration, where simultaneously the peak broadening correction factors and the molecular weight calibration curve are obtained, have been developed. These methods require the use of multiple polydispersed molecular weight standards, with known ($\bar{M}_N$, $\bar{M}_W$) or ($\bar{M}_N$,$[\eta]$). The first method assumes that the molecular weight calibration curve is linear on a semi-log plot and should be employed where universal calibration is not valid or available as with aqueous SEC. The second and more general method employs the universal molecular weight calibration curve obtained using narrow MWD polystyrene standards. If the universal calibration curve is non-linear, the molecular weight calibration curve for the polymer in question will also be non-linear.

In the following section the theoretical basis for the proposed methods will be established. Several variants of methods involving different molecular weight data for the standards are also discussed. However, before describing these methods, it is appropriate to describe the analytical solutions after Hamielec and Ray (21) of Tungs axial dispersion equation, (22). This analytical solution provides peak broadening correction factors which are employed in the present calibration methods.

2-1. The Analytical Solution of Hamielec and Ray -- Tung's Axial Dispersion Equation

When the molecular size distribution, W(V) is obtained, it can be converted to the molecular-weight distribution, $F_W(M)$ with the following

equation. ($F_W(M)$ and $W(V)$ are normalised.)

$$W(V).dV = -F_W(M)dM$$

and
$$F_W(M) = -W(V).\frac{1}{\left\{\frac{dM}{dV}\right\}} \qquad (2.1.1)$$

where dM/dV is the slope of the molecular weight calibration curve.

The average molecular weights can then be calculated using

$$\bar{M}_W(t) = \frac{\int_o^\infty MF_W(M)dM}{\int_o^\infty F_W(M)dM} = \frac{\int_o^\infty M(V)W(V)dV}{\int_o^\infty W(V)dV} \qquad (2.1.2a)$$

$$\bar{M}_N(t) = \frac{\int_o^\infty F_W(M)dM}{\int_o^\infty \frac{1}{M}F_W(M)dM} = \frac{\int_o^\infty W(V)dV}{\int_o^\infty \frac{W(V)}{M(V)}dV} \qquad (2.1.2b)$$

In general,

$$\bar{M}_K(t) = \frac{\int_o^\infty M(V)^{K-1}W(V)dV}{\int_o^\infty M(V)^{K-2}W(V)dV} \qquad (2.1.2c)$$

where K = 1,2,3, ... corresponds to number -, weight -, z - average molecular weight. Subscript (t) stands for true value or value corrected for peak broadening. These are the absolute values. A knowledge of the calibration curve, M versus V is necessary to perform the above integrations. The direct use of F(V) the raw detector response instead of W(V) leads to the uncorrected or apparent molecular weight averages.

$$\bar{M}_K(\text{app}) = \frac{\int_o^\infty M^{K-1}(V).F(V)dV}{\int_o^\infty M^{K-2}(V).F(V)dV} \qquad (2.1.3)$$

The process of obtaining W(V) from F(V) involves a solution of Tung's integral equation. The ratio of absolute average molecular weights to the apparent ones can be written as

$$\frac{\bar{M}_K(t)}{\bar{M}_K(\text{app})} = \frac{\int_o^\infty W(V)M^{K-1}(V)dV \;/\int_o^\infty W(V)M^{K-2}(V)dV}{\int_o^\infty F(V)M^{K-1}(V)dV \;/\int_o^\infty F(V)M^{K-2}(V)dV} \qquad (2.1.4)$$

By assuming a linear molecular weight calibration curve of the form,

$$M(V) = D1\ \exp(-D2\ V) \qquad (D_1, D_2 > 0) \qquad (2.1.5)$$

where D1 and D2 are the intercept and slope of the true calibration curve respectively, and substituting in eqn (2.1.4),

$$\frac{\bar{M}_n(t)}{\bar{M}_n(\text{app})} = \frac{\int_{-\infty}^{\infty} F(V)e^{D2V}dV}{\int_{-\infty}^{\infty} W(V)e^{D2V}dV} = \frac{\bar{F}(-D2)}{\bar{W}(-D2)} \qquad (2.1.5a)$$

$$\frac{\bar{M}_W(t)}{\bar{M}_W(\text{app})} = \frac{\int_{-\infty}^{\infty} W(V)e^{-D2V}dV}{\int_{-\infty}^{\infty} F(V)e^{-D2V}dV} = \frac{\bar{W}(D2)}{\bar{F}(D2)} \qquad (2.1.5b)$$

where $\bar{F}$ and $\bar{W}$ are the bilateral Laplace transforms of F and W, and there is no loss in generality in letting V=o to V=-∞. These transforms do exist since

$$\lim_{V\to\infty}\left\{F(V)e^{D2V}\right\} < \infty \text{ and } \lim_{V\to\infty}\left\{W(V)e^{D2V}\right\} < \infty$$

Then by assuming a uniform Gaussian instrumental spreading function G(V-y), Tungs axial dispersion equation (2.2) becomes

$$G(V-y) = \sqrt{\frac{h}{\pi}}\exp\left\{-(V-y)^2h\right\} \tag{2.1.6}$$

$$F(V) = \sqrt{\frac{h}{\pi}}\int_{-\infty}^{\infty} W(y)\exp\left\{-h(V-y)^2\right\}dy \tag{2.1.6a}$$

By performing Laplace transformation on this equation, the following is obtained

$$\overline{F}(S) = \overline{W}(S)\sqrt{\frac{h}{\pi}}\int_{-\infty}^{\infty}\exp(-hV^2)\exp(-Sx)dx$$

$$= \overline{W}(S)\sqrt{\frac{h}{\pi}}\exp\left\{\frac{S^2}{4h}\right\}\int_{-\infty}^{\infty}\exp(-hx^2)dx$$

$$= \overline{W}(S)\sqrt{\frac{h}{\pi}}\exp\left\{\frac{S^2}{4h}\right\}\cdot\sqrt{\frac{\pi}{h}}$$

$$= \overline{W}(S)\exp\left\{\frac{S^2}{4h}\right\} \tag{2.1.7}$$

Applying this equation to Equations (2.1.5a) and (2.1.5b) one obtains,

$$\frac{\overline{M}_n(t)}{\overline{M}_n(app)} = \exp\left\{\frac{D2^2}{4h}\right\} = \exp\left\{\frac{D2^2\sigma^2}{2}\right\} \tag{2.1.8a}$$

$$\frac{\bar{M}_W(t)}{\bar{M}_W(app)} = \exp\left\{\frac{-D2^2}{4h}\right\} = \exp\left\{\frac{-D2^2\sigma^2}{2}\right\} \qquad (2.1.8b)$$

where h represents the sharpness of the distribution and has usually been called the resolution factor. σ^2 $(=\frac{1}{2h})$, is the variance or axial dispersion factor.

In general,

$$\frac{\bar{M}_k(t)}{\bar{M}_k(app)} = \exp\left\{\frac{(3-2k)D2^2\sigma^2}{2}\right\} \qquad (2.1.8c)$$

Thus, once the Gaussian resolution factor h and the slope of the linear calibration curve D2 are given, the true average molecular weights can be immediately obtained from the apparent average molecular weights.

Before proceeding to discuss the effective linear calibration methods relevant to the present investigation in the next section, it is important to emphasize some important features of the Yau, Stoklosa and Bly's (23a) version of validating the analytical solutions of Hamielec and Ray. In this version, the integral equation was solved in a unique manner and correction equations for axial dispersion for the contents of the detector cell rather than for the whole polymer were derived. They presented solutions for $\bar{M}_N(V)$ and $\bar{M}_W(V)$ for polymer in the detector cell under the same restriction that polymer molecules within the same retention volume or size in the mobile-phase have the same molecular weight. Then since the contributions from neighbouring species fall off rapidly when integrating in the detector cell, one can set D2 and σ^2 independent of elution volume with negligible error. In this manner Hamielec (23b) has generalized this analytical solution to the more general situation

where the molecular weight calibration curve is non-linear and where peak broadening parameters change with molecular weight or retention volume.

According to a recent publication by Figini, it is difficult to use any of the shape functions which have been proposed (24). Until a more satisfactory instrumental spreading function which is able to account for the MWD of the polymers is found, he proposed the following. Equations (2.8a to 8c) can be rewritten in a more general form as

$$\frac{\bar{M}_K(t)}{\bar{M}_K(app)} = P_K \qquad (2.1.9)$$

where P_K is the molecular weight correction factor. In this form, the shape and parameters of the instrumental shape function need not be known.

2-2. Linear Molecular Weight Calibration Methods

2-2-1. The Effective Linear Calibration Method (ELC) (25)

Table 2.1 lists previous methods which have been used for molecular weight calibration using broad MWD standards. Most of these methods have been limited by the fact that corrections for peak broadening, have either not been made or have used peak broadening parameters measured for polystyrene.

To illustrate the concept of a true MW calibration curve versus an effective MW calibration curve and to compare the proposed methods, the ELC method is described in some detail. This method which is very simple in principle has attracted more attention than any other method. The GPC V2 method of Yau, Stoklosa and Bly (23a)is an improved version of the ELC method, which accounts for peak broadening in SEC using the analytical

Table 2.1. Broad MWD Standard Methods of Calibration

Method #	Method of Calibration	# of MWD Standards Used	GPC System and (Polymer Used)	Axial dispersion Correction/Method	Ref.
			A. Use of MWD of Standards		
1	Integral Distribution Method	1	Organic GPC (polyisobutylene)	Infinite Resolution	Cantow, Porter, Johnson (26)
2		1	Organic GPC	"	Weiss and Ginsberg (27)
3	A Matching Procedure	1	Organic GPC	"	Wild, Ranganath and Ryle (28)
4		1	Organic GPC (Nylon 66, polyethylene)	"	Swatz, Bly and Edwards (29)
5		1	Aqueous GPC (Hydrolysed and non-hydrolysed polyacrylamide)	"	Abdel-Alim and Hamielec (30)
6		2	Aqueous GPC (dextran)	corrected for retention volume by iteration	Van Dijk, Henkens and Smith (31)
7		>2	Aqueous GPC (dextran)	Infinite Resolution	Granath and Kvist (32)
8		>2	Aqueous GPC (dextran)	"	Hashimoto, Sasaki, Aiura and Kato (33)
			B. Use of MW Averages of Standards		
9	A Graphical Method	1	Organic GPC	Infinite Resolution	Rodriguez, Kulakowski and Clark (34)
10		1	Organic GPC	Infinite Resolution	Frank, Ward and William (35)
11	ELC or GPC VI. An Optimization Method	1	--	Infinite Resolution	Balke, Hamielec, LeClai and Pearce (25)

Table 2-1 continued

Method #	Method of Calibration	# of MWD Standards Used	GPC System and (Polymer Used)	Axial dispersion Correction (Method)	Ref.
			B. Use of MW Averages of Standards		
12	GPCV2. An optimization method	1	Organic GPC (Polystyrene)	(Predetermined method)	Yau, Bly and Stoklosa (23)
13	Non-linear Regression	>2	--	None	McCracklin (36)
14	Two-step method	>2	Aqueous GPC (dextran)	Weak correction for peak retention volume	Bombaugh, Dark and King (37)
15	Iterative method	>2	Aqueous GPC (dextran)	(Reverse flow)	Soeteman, Roels, Van Dijk and Smit (38)
16	Iterative method	>2	Aqueous GPC (dextran)	(Reverse flow)	Vrijbergen, Soetman and Smith (39)
			C. Use of Universal Calibration/MW Averages of Standards		
17	Optimization	1	Organic GPC (Polymethyl methacrylate, polyvinyl acetate and polyamides)	None (empirical)	Provder, Woodbrey and Clark (40)
18	Optimization	1	Organic GPC (polyvinyl chloride)	None (empirical)	Abdel-Alim and Hamielec (41)

solutions of Hamielec and Ray (21). The ELC method is the only method which permits the use of one or two broad MWD standards with the option of using any of the molecular weight averages.

In this method, one broad MWD standard with known $\bar{M}_w$ and $\bar{M}_n$ or two broad MWD standards with either of the $\bar{M}_w$ or $\bar{M}_n$ known, are required. The method assumes that

$$F(V) = W(V) \tag{2.2.1}$$

where F(V) and W(V) refer to the apparent and corrected chromatograms respectively.

$$\therefore \quad \bar{M}_K(app) = \bar{M}_K(t) \tag{2.2.2a}$$

$$\text{Then} \quad \bar{M}_w(t) = \int_0^\infty F(V)M(V)dV \tag{2.2.2b}$$

$$\bar{M}_n(t) = \left\{ \int_0^\infty F(V)/M(V)dV \right\}^{-1} \tag{2.2.2c}$$

where M(V) is the true molecular weight calibration curve, which if linear is given by equation (2.1.5)

$$M(V) = D1 \exp(-D2V) \tag{2.1.5}$$

where D1 and D2 are the intercept and slope respectively and are both greater than zero.

For the case where one broad MWD standard is available, Equations (2.2.2b), (2.2.2c) and (2.1.5) are rearranged to give

$$\frac{\bar{M}_I(t)}{\bar{M}_n(t)} = \left\{\int_o^\infty F(V)e^{-D2V}dV\right\} \cdot \left\{\int_o^\infty F(V)e^{D2V}dV\right\} \qquad (2.2.4)$$

In this equation, there is one unknown D2. Using a single-variable search optimization technique, D2 is obtained. Then D1, the intercept of the calibration curve is obtained using either

$$\bar{M}_W(t) = D1\int_o^\infty F(V)e^{-D2V}dV \qquad (2.2.5a)$$

or $$\bar{M}_n(t) = D1 \Big/ \int_o^\infty F(V)e^{D2V}dV \qquad (2.2.5b)$$

For the case where two standards are available, given one piece of molecular weight information per standard (say $\bar{M}_{W_1}$, $\bar{M}_{W_2}$), D2 is obtained using

$$\frac{\bar{M}_{W_1}(t)}{\bar{M}_{W_2}(t)} = \frac{\int_o^\infty F_1(V)e^{-D2V}dV}{\int_o^\infty F_2(V)e^{-D2V}dV} \qquad (2.2.6)$$

Then D1 is obtained using either

$$\bar{M}_{W_1}(t) = D1\int_o^\infty F_1(V)e^{-D2V}dV \quad \text{or} \quad \bar{M}_{W_2}(t) = D1\int_o^\infty F_2(V)e^{-D2V}dV.$$

Given $\bar{M}_N$ for each standard, D2 is similarly obtained using

$$\frac{\bar{M}_{n_1}(t)}{\bar{M}_{n_2}(t)} = \frac{\int_o^\infty F_2(V)e^{D2V}dV}{\int_o^\infty F_1(V)e^{D2V}dV} \qquad (2.2.7)$$

$$\bar{M}_{n_1}(t) = D1 \Big/ \int_o^\infty F_1(V)e^{D2V}dV \quad \text{or} \quad \bar{M}_{n_2}(t) = D1 \Big/ \int_o^\infty F_2(V)e^{D2V}dV.$$

2-2-2. The GPC V2 Method of Yau, Stoklosa and Bly (23a)

In the method just described, no correction for peak broadening was made. The molecular weight calibration curve thus obtained is the effective one and not the true calibration curve. The GPC V2 method goes a step further by accounting for peak-broadening. It is assumed that the variance of single species chromatograms does not vary with molecular weight. This method was developed using one broad MWD standard, with $\bar{M}_n$ and $\bar{M}_W$ provided.

Employing the analytical solutions of Hamielec and Ray of Tung's axial dispersion equation to correct for peak broadening, the parameters of the molecular weight calibration curve may be obtained by solving the following equations

$$\bar{M}_n(t)\ \exp\left\{\frac{-(D2\,\sigma)^2}{2}\right\} = D1 \Big/ \int_o^\infty F(V)\exp(D2V)dV \tag{2.2.8}$$

$$\bar{M}_W(t)\ \exp\left\{\frac{(D2\,\sigma)^2}{2}\right\} = D1 \int_o^\infty F(V)\exp(-D2V)dV \tag{2.2.9}$$

where σ^2 is the variance which is assumed independent of molecular weight. Dividing equation (2.2.9) by (2.2.8), then

$$\frac{\bar{M}_W(t)}{\bar{M}_n(t)}\ \exp[(D2\,\sigma)^2] = \frac{\int_o^\infty F(V)\exp(-D2V)dV}{\int_o^\infty F(V)\exp(D2V)dV} \tag{2.2.10}$$

Given σ^2 (from narrow MWD polytyrene standards) (23a), and using Equation (2.2.10), a single-variable search gives D2. D1 is then obtained by direct calculation of either of Equations (2.2.8) or (2.2.9).

2-2-3. Proposed Linear Two Broad MWD Standards Molecular Weight Calibration Method (TBS)

The equations to be solved follow:

$$\bar{M}_{n_1}(t)\exp\left\{\frac{-(D2\,\sigma_1)^2}{2}\right\} = D1\left\{\int_o^\infty F_1(V)\exp(D2V)dv\right\}^{-1} \qquad (2.2.11)$$

$$\bar{M}_{n_2}(t)\exp\left\{\frac{-(D2\sigma_2)^2}{2}\right\} = D1\left\{\int_o^\infty F_2(V)\exp(D2V)dV\right\}^{-1} \qquad (2.2.12)$$

$$\bar{M}_{W_1}(t)\exp\left\{\frac{(D2\sigma_1)^2}{2}\right\} = D1\left\{\int_o^\infty F_1(V)\exp(-D2V)dV\right\} \qquad (2.2.13)$$

$$\bar{M}_{W_2}(t)\exp\left\{\frac{(D2\sigma_2)^2}{2}\right\} = D1\left\{\int_o^\infty F_2(V)\exp(-D2V)dV\right\} \qquad (2.2.14)$$

Rearrangement of these equations to eliminate D2 , one obtains

$$\bar{M}_{n_i}\bar{M}_{W_i}(t) = D1^2\left\{\int_o^\infty F_i(V)\exp(-D2V)dV\right\}\left\{\int_o^\infty F_i(V)\exp(D2V)dV\right\}^{-1} \qquad (2.2.15)$$

where i is either standard 1 or 2. From this equation, it is seen that the root mean square average molecular weight, defined as $(\bar{M}_n\bar{M}_W)^{\frac{1}{2}}$ is independent of the magnitude of imperfect resolution. This method is valid not only for the case where the instrumental spreading function of a single species is Gaussian, but also for other symmetric spreading functions. It is not valid when the instrumental spreading function is

skewed, however.

Taking the ratios of both standards using Equation (2.2.15) yields

$$\frac{\bar{M}_{rms_1}(t)}{\bar{M}_{rms_2}(t)} = \frac{\left\{\int_0^\infty F_1(V)\exp(-D2V)dV\right\}^{\frac{1}{2}}\left\{\int_0^\infty F_2(V)\exp(D2V)dV\right\}^{\frac{1}{2}}}{\left\{\int_0^\infty F_1(V)\exp(D2V)dV\right\}^{\frac{1}{2}}\left\{\int_0^\infty F_2(V)\exp(-D2V)dV\right\}^{\frac{1}{2}}} \qquad (2.2.16)$$

Therefore, a single-variable search provides D2. This is followed by a direct calculation of D1 using Equation (2.2.15) for either of the broad standards. Finally, Equations (2.2.11) or (2.2.12) and (2.2.13) or (2.2.14) can now be used to calculate σ_i^2 for each broad MWD standard. Or better still P_K, if the instrumental spreading function is unknown.

2-3. Methods Based on Universal MW Calibration Curve - Non-Linear MW Calibration Curve

A non-linear universal molecular weight calibration curve may be expressed as

$$[\eta](V)M(V) = \phi(V) \qquad (2.3.1)$$

where $[\eta]$ is intrinsic viscosity.

The molecular weight calibration curve for the polymer in question may be expressed as

$$M(V) = \alpha\phi(V)^{\beta} \qquad (2.3.2)$$

where $\beta = \frac{1}{1-a}$

and $\alpha = K^{-\beta}$ (2.3.3)

and K and a are Mark-Houwink constants for linear polymer chains.

Hence the analytical solutions to Tung's axial dispersion equation for $\bar{M}_n$, $\bar{M}_W$ and intrinsic viscosity $[\eta]$ of a broad MWD standard in terms of the mass detector response F(V), the true molecular weight calibration curve M(V) and the peak broadening parameter (variance of a single-species chromatogram σ^2) can be written as

$$\bar{M}_n(t)\exp\left\{\frac{-(D2\sigma)^2}{2}\right\} = \alpha\left[\int_o^\infty F(V)\phi(V)^{-\beta}\,dV\right]^{-1} \tag{2.3.4a}$$

$$\bar{M}_W(t)\exp\left\{\frac{(D2\sigma)^2}{2}\right\} = \alpha\left[\int_o^\infty F(V)\phi(V)^{\beta}\,dV\right] \tag{2.3.4b}$$

$$[\eta](t)\exp\left\{\frac{(aD2\sigma)^2}{2}\right\} = \bar{\alpha}\left[\int_o^\infty F(V)\phi(V)^{\bar{\beta}}\,dV\right] \tag{2.3.4c}$$

where $\bar{\beta} = \frac{a}{1+a}$ and $\bar{\alpha} = K^{1-\bar{\beta}}$ (2.3.5)

2-3-1. Method of Provder, Woodbrey and Glark - Neglect of Peak Broadening Correction

This method like the ELC method assumes that σ^2 as well as other corrections are negligible (ie. $\sigma^2 \simeq 0$). Therefore, equations (2.3.4a) and (4b), given one broad MWD standard with known $\bar{M}_W$ and $\bar{M}_n$, become after manipulation

$$\frac{\bar{M}_W(t)}{\bar{M}_n(t)} = \left\{\int_o^\infty F(V)\phi(V)^{-\beta}\,dV\right\}\left\{\int_o^\infty F(V)\phi(V)^{\beta}dV\right\} \tag{2.3.6}$$

and $$\bar{M}_W(t) = \alpha\left\{\int_o^\infty F(V)\phi(V)^{\beta}\,dV\right\} \tag{2.3.7}$$

From Equation (2.3.6), one is left with a single-variable search for β. Then, this is followed by a direct calculation of α using Equation (2.3.7) or that based on $\bar{M}_n(t)$. In some circumstances, it may be desirable to use the intrinsic viscosity, $[\eta](t)$ in place of $M_W(t)$. The Mark-Houwink constants thus obtained are effective rather than true values.

2-3-2. Present Method Based on the Universal Calibration Curve-Peak Broadening Corrections Incorporated

In equations (2.3.4a to 5), there are three unknowns, K, a and σ^2. In principle, one could solve these equations for these unknowns. Unfortunately, $\bar{M}_W$ and $[\eta]$ are often highly correlated and therefore it has usually been recommended that only one of these data be used per standard. Given one broad MWD standard, a practical procedure is to estimate σ^2 using narrow MWD polystyrene standards, leaving two unknowns, K and a. Now suppose $\bar{M}_W$ and $\bar{M}_n$ or $\bar{M}_n$ and $[\eta]$ data are available for this single broad MWD standard, β is obtained using for example Equation (2.3.8) below

$$\frac{\bar{M}_W(t)}{\bar{M}_n(t)} \exp[(D\sigma)^2] = \left\{\int_0^\infty F(V)\phi(V)^{-\beta}\, dV\right\}\left\{\int_0^\infty F(V)\phi(V)^{\beta}\, dV\right\} \quad (2.3.8)$$

Then this is followed by a direct calculation of α using either of equations based on $\bar{M}_W$ or $\bar{M}_n$.

Given two broad MWD standards with one piece of molecular weight data per standard, the following possibilities arise

Case 1 $\bar{M}_{n_1}$ and $\bar{M}_{n_2}$-

$$\bar{M}_{n_1} \exp\left\{\frac{-(D2\sigma_1)^2}{2}\right\} = \alpha\left[\int_o^\infty F_1(V)\phi(V)^{-\beta}\,dV\right]^{-1} \tag{2.3.9}$$

$$\bar{M}_{n_2} \exp\left\{\frac{-(D2\sigma_2)^2}{2}\right\} = \alpha\left[\int_o^\infty F_2(V)\phi(V)^{-\beta}\,dV\right]^{-1} \tag{2.3.10}$$

Case 2 $\bar{M}_{n_1}$ and $\bar{M}_{W_2}$-

$$\bar{M}_{n_1} \exp\left\{\frac{-(D2\sigma_1)^2}{2}\right\} = \alpha\left[\int_o^\infty F_1(V)\phi(V)^{-\beta}\,dV\right]^{-1} \tag{2.3.9}$$

$$\bar{M}_{W_2} \exp\left\{\frac{(D2\sigma_2)^2}{2}\right\} = \alpha\left[\int_o^\infty F_2(V)\phi(V)^{-\beta}\,dV\right] \tag{2.3.11}$$

Case 3 $\bar{M}_{n_1}$ and $[\eta]_2$-

$$\bar{M}_{n_1} \exp\left\{\frac{-(D2\sigma_1)^2}{2}\right\} = \alpha\left[\int_o^\infty F_1(V)\phi(V)^{-\beta}\,dV\right]^{-1} \tag{2.3.9}$$

$$[\eta]_2 \exp\left\{\frac{(aD2\sigma_2)^2}{2}\right\} = \bar{\alpha}\left[\int_o^\infty F_2(V)\phi(V)^{\bar{\beta}}\,dV\right] \tag{2.3.12}$$

There are many additional combinations which may be employed. In any of these combinations, after assuming an independent estimate of σ^2, division of one equation by the other eliminates α and one is left with a single variable search for β. This is then followed by direct calculation of α.

Now, given two pieces of MW data per standard with the TBS method (linear), with proper modification to equations (2.3.4a to 4c), the peak broadening parameter σ^2 or the instrumental spreading functions parameters in the absence of skewing vanish. The equations for two broad MWD standards

for the case where $\overline{M}_n$ and $\overline{M}_W$ are known follow:

$$\overline{M}_{n_i}\overline{M}_{W_i}(t) = \alpha^2 \left\{ \int_o^\infty F_i(V)\phi(V)^\beta \, dV \right\} \left\{ \int_o^\infty F_i(V)\phi(V)^{-\beta} \, dV \right\}^{-1} \qquad (2.3.13)$$

where subscript i represents the standard. A single-variable search for β results when equation (2.3.13) for i = 1 is divided by the equation i = 2,3, ... to eliminate α. Once β is obtained, a direct calculation using equation (2.3.13) gives α. This is then followed by direct calculation for the peak broadening parameters σ_i^2 or the molecular weight correction factors, if the true shape of the instrumental spreading function is unknown, using equation (2.3.4a) or (2.3.4b) or any modified form of it.

Of all the methods described above, only the TBS (linear) and TBS (non-linear) methods do not require the identification of the instrumental spreading parameters, to obtain the true molecular weight calibration curve. However, the instrumental spreading function must either be Gaussian or at least symmetric in shape. For the non-Gaussian symmetric case more than one parameter is needed to describe the shape. Thus, the validity of the analytical solutions of Hamielec and Ray of Tung's axial dispersion equation becomes questionable when the instrumental spreading function is non-Gaussian.

Before proceeding to the next chapter, it is appropriate to describe the analytical solutions of the second case for which the TBS methods also apply. To do this, Provder and Rosen's (42) proposed shape function will first be introduced.

2-4. The Instrumental Spreading Function

Apart from the use of a Gaussian shape function, many non-symmetric shape functions have been proposed and applied (42-45). The general nature of the statistical shape function makes the work of Provder and Rosen of special significance.

2-4-1. The Statistical Shape Function Proposed by Provder and Rosen (42)

The statistical shape function which accounts for deviation from the Gaussian shape has the form

$$G(V,y) = G(V-y) + \sum_{n=3}^{\infty} (-1)^n \frac{An}{n!} \frac{G^n(V-y)}{(2h)^n} \qquad (2.4.1a)$$

where $G(V-y) = \sqrt{\frac{h}{\pi}} \exp[-h(V-y)^2]$ is the Gaussian part of the distribution and $G^n(V-y)$ denotes its n-th order derivative. The coefficients A_n are functions of μ_n, the n-th order moments about the mean retention volume μ_1 of the observed SEC chromatograms. For practical purposes, the series were truncated at the third term neglecting A_5, A_7, A_8 .... and setting A_6 equal to $10A_3^2$. This gives a model with three parameters σ^2, A_3 and A_4 as follows

$$G(v,y) = G(v-y).\left\{1+\frac{A_3}{6}.\ H_3\left[\frac{(v-y)}{\sigma}\right] + \frac{A_4 H_4}{24}\left[\sigma\ (v-y)\right]\right\} \qquad (2.4.1b)$$

where $H_3[x] = x^3 - 3x$ (2.4.2a)

$$H_4[x] = x^4 - 6x^2 + 3 \qquad (2.4.2b)$$

The coefficients A_3 and A_4 are related to the moments as

$$A_3 = \frac{\mu_3}{(\sigma^2)^{3/2}} \qquad (2.4.3a)$$

$$A_4 = \frac{\mu_4}{(\sigma^2)^2} - 3 \qquad (2.4.3b)$$

The coefficient A_3 or μ_3 provides a measure of skewness. When A_3 is positive, the chromatogram is skewed to higher volumes with a lowering of the $\bar{M}_n$ and $\bar{M}_w$. When A_3 is negative, the opposite is true. Similar behaviour is also found with the skewing factor SK in the equations of Balke and Hamielec (44). Finite values of A_4 give a symmetrical distribution but provide a statistical measure of the flattening or kurtosis of the chromatogram of the ideal monodisperse standard. The kurtosis coefficient measures the excess flatness or thinness of the chromatogram peak compared to that of a Gaussian curve. In other words it provides a measure of deviation from Gaussian shape. When A_3 and A_4 are zero, the chromatogram is Gaussian in shape. When $A_3 = 0$ and A_4 is greater than zero, the chromatogram is leptokurtic, taller and slimmer than the Gaussian curve. When A_4 is less than zero, the chromatogram observed is platykurtic, flatter or more squat at the centre of the curve than the corresponding Gaussian curve.

The above form of the equation still preserves the merits of the Gaussian function when applied to a linear calibration curve. Using the method of molecular weight averages, the ratio of the absolute average MWs to the apparent values can be analytically expressed as follows

$$\frac{\bar{M}_n(t)}{\bar{M}_n(app)} = \exp\left\{\frac{D2^2\sigma^2}{2}\right\}\left[1 + \frac{(D2\sigma)^3}{6}A_3 + \frac{(D2\sigma)^4}{24}A_4 + \left\{\frac{(D2\sigma)^3}{72}A_3\right\}^2\right] \qquad (2.4.4)$$

$$\frac{\bar{M}_W(t)}{\bar{M}_W(app)} = \exp\left\{-\frac{D2^2\sigma^2}{2}\right\} \Big/ \left[1-\frac{(D2\sigma)^3}{6}A_3 + \frac{(D2\sigma)^4}{24}A_4 + \left\{\frac{(D2\sigma)^3}{72}A_3\right\}^2\right] \tag{2.4.5}$$

$$\frac{[\eta](t)}{[\eta](app)} = \exp\left\{\frac{-a^2D2^2\sigma^2}{2}\right\} \Big/ \left[1-\frac{(aD2\sigma)^3}{6}A_3 + \frac{(aD2\sigma)^4}{24}A_4 + \left\{\frac{(aD2\sigma)^3}{72}A_3\right\}^2\right] \tag{2.4.6}$$

where $[\eta]$ denotes the intrinsic viscosity and a is the exponent in the Mark-Houwink intrinsic viscosity - MW expression. These equations have never been used in the manner shown above in which the coefficients A_4 and A_3 are used in place of μ_4 and μ_3 respectively. For SEC applications where peak broadening is very predominant, each term is expressed in terms of the axial dispersion coefficients rather than in their absence. These versions of the equations preserves the merits of what is to be expected on the basis of chromatographic theory where $(\sigma D2)^n$ (where n = 2,3,4) is a measure of resolution rather than σ^2 or D2 alone.

2-4-2. Proposed Instrumental Shape Function For Application With TBS Methods of Solution

Hamielec (46) reported negative molecular weight averages when applying the Provder-Rosen shape function with large corrections to higher MW averages when skewing was considered. Several workers also share the view that the use of skewing corrections sometimes introduces larger errors than by using the simpler Gaussian distribution as an approximation for all molecular weight species (47)(48)(49).

For a symmetrical instrumental spreading function, Equation (2.4.1b) becomes

$$G(v,y) = \sqrt{\frac{1}{2\pi\sigma_T^2}} \cdot \left\{1+\frac{A_4\sigma_T^4}{24}\left\{\frac{d^4G(v-y)}{dV^4}\right\}\right\} \exp\left\{\frac{(v-y)^2}{2\sigma_T^2}\right\} \qquad (2.4.7)$$

with corresponding analytical solutions of

$$\frac{\bar{M}_K(t)}{\bar{M}_K(app)} = \exp\left\{\frac{-(2K-3)D2^2\sigma_T^2}{2}\right\} \cdot \left[\frac{\left\{1+\frac{A_4}{24}[(K-2)^4D2^4\sigma_T^4]\right\}}{\left\{1+\frac{A_4}{24}[(K-1)^4D2^4\sigma_T^4]\right\}}\right] \qquad (2.4.8)$$

However on the basis of chromatographic theory, equation (2.4.7) is an approximate form of a more general symmetric shape function

$$G_S(v-y) = \sqrt{\frac{1}{2\pi\sigma_T^2}} \exp\left\{\frac{-(v-y)^2}{2\sigma_T^2}\right\} \cdot \left[\exp\left\{\frac{A_K}{24}\sigma_T^4 \frac{d^4G(v-y)}{dV^4}\right\}\right] \qquad (2.4.9a)$$

$$= \sqrt{\frac{1}{2\pi\sigma_T^2}} \exp\left\{\frac{-(v-y)^2}{2\sigma_T^2}\right\} \cdot \left[1+\sum_{n=1}^{\infty}\left[\frac{A_K\sigma_T^4}{24}\frac{d^4G(v-y)}{dV^4}\right]^n\frac{1}{n!}\right]$$

$$= \sqrt{\frac{1}{2\pi\sigma_T^2}} \exp\left\{\frac{-(v-y)^2}{2\sigma_T^2}\right\} \cdot \left(1+\sum_{n=1}^{\infty}\frac{x^n}{n!}\right) \qquad (2.4.9b)$$

where $x = \frac{A_K\sigma_T^4}{24}\frac{d^4G(v-y)}{dV^4}$ $\qquad -\infty < x < 0 \qquad (2.4.9c)$

where A_K is now used in place of A_4 and is the polyplatykurtic coefficient since the proposed function is an infinite series. When n = 1, the equation approximates Provder and Rosen's equation for an instrumental spreading function which is symmetric. Unlike A_4, A_K is always less than zero. The corresponding analytical solutions for which the method of molecular weight averages is also applicable are given by

$$\frac{\bar{M}_K(t)}{\bar{M}_K(app)} = \exp\left\{ \frac{-(2K-3)D2^2\sigma_T^2}{2} \right\} \exp\left\{ \frac{-(2K-3)D2^4\sigma_T^4}{24} A_K \right\} \qquad (2.4.10)$$

For K = 1,

$$\frac{\bar{M}_n(t)}{\bar{M}_n(app)} = \exp\left\{ \frac{D2^2\sigma_T^2}{2} \right\} \exp\left\{ \frac{D2^4\sigma_T^4}{24} A_K \right\} \qquad (2.4.10a)$$

and K = 2,

$$\frac{\bar{M}_W(t)}{\bar{M}_W(app)} = \exp\left\{ \frac{-D2^2\sigma_T^2}{2} \right\} \exp\left\{ \frac{-D2^4\sigma_T^4}{24} A_K \right\} \qquad (2.4.10b)$$

$$= \exp\left\{ \frac{-D2^2}{2} \left(\sigma_T^2 + \frac{D2^2\sigma_T^4}{12} A_K \right) \right\}$$

$$= \exp\left\{ \frac{-D2^2\gamma}{2} \right\} \qquad (2.4.10c)$$

Similarly

$$\frac{\bar{M}_n(t)}{\bar{M}_n(app)} = \exp\left(\frac{D2^2\gamma}{2} \right) \qquad (2.4.10d)$$

where $\gamma = \sigma_T^2 + \frac{D2^2\sigma_T^4}{12} A_K$ (2.4.11)

Also from Equations (2.4.10c) and (2.4.10d),

$$\frac{\bar{M}_W(t)}{\bar{M}_W(app)} \cdot \frac{\bar{M}_n(app)}{\bar{M}_n(t)} = \exp\{ -D2^2\gamma \}$$

and taking $\log_e$ of both sides

$$\gamma = \frac{\ln P(app)}{D2^2} - \frac{\ln P(t)}{D2^2} \qquad (2.4.12)$$

where $P(app) = \frac{\bar{M}_w(app)}{\bar{M}_n(app)}$, $P(t) = \frac{\bar{M}_w(t)}{\bar{M}_n(t)}$ (2.4.13)

Comparing equations (2.4.12) and (2.4.11),

$$\sigma_T^2 = \frac{\ln P(app)}{D2^2} \quad \text{and} \qquad (2.4.14a)$$

$$A_K = \frac{-12 \ln P(t)}{D2^4 \sigma_T^4} = \frac{-12 K_S}{D2^4 \sigma_T^4} \qquad (2.4.14b)$$

where $K_S = \ln P(t)$. (2.4.14c)

Therefore Equation (2.4.12) can be written as

$$\gamma = \sigma_T^2 - \frac{K_S}{D2^2} \qquad (2.4.15)$$

since σ_T^2 is a constant and independent of D2.

Thus when the instrumental spreading function is symmetric as given by equation (2.4.9b), σ_T^2, the overall axial dispersion coefficient can be obtained either from equation (2.4.14a) or by plotting γ versus $D2^{-2}$ as per equation (2.4.15). γ is the overall instrumental spreading correction factor, a function of two parameters.

To illustrate the power and versatility of the TBS methods,

experimental investigations using both aqueous and non-aqueous SEC systems were done. The second TBS method based on the universal calibration curve of polystyrene, was applied to polyvinyl chloride and this is contained in a recent publication (50). Therefore it will not be described here, since the present thesis is restricted to aqueous SEC systems alone, for which the universal concept is not proven valid. The TBS method (linear) will be applied to dextran standards, which are the best characterized of many water-soluble polymers. The $\bar{M}_n$ and $\bar{M}_w$ are known for each of the many broad MWD dextran standards.

3. EXPERIMENTAL

3-1. Experimental Details

SEC measurements were carried out on a Waters ALC/GPC model 301 high pressure liquid chromatograph designed for room temperature operation. Major plumbing alterations were made to the equipment, replacing most of the 1/16" tubing with 1/8" 312 stainless steel tubings. Without these changes, problems ranging from occasional plugging, wide variation of flow-rates, acidic effects, to unstable base-line control were common. A special filter (2 micrometer, Rheodyne Model 7302) for aqueous SEC application was originally installed after the injection valve, but later removed due to plugging problems. In doing this, it was important to minimize axial dispersion resulting from extra tubing, keeping lengths of extra tubing as short as possible.

This model is equipped with a differential refractometer as the concentration detector. A six-way injection valve was installed with a 2ml injection loop, as the equipment was to be originally designed for conversion as well as MWD measurements. The elution volume scales were measured on a recorder at intervals of 4.4 to 5.3 ml, using a 5 ml siphon dump flow counter. A Milton-Roy 5000 psi pump was used to pump the mobile-phase through the columns.

Commercially available and inexpensive column packing materials or stationary-phase compatible with water include porous glass and silica. Apart from their rigid pore structure, chemical inertness and mechanical stability, porous glass and silica have several additional advantages, which are described in manufacturers' guides. However, the presence of

surface active sites and the complex nature of the pore network are serious disadvantages and searches for improved stationary phases continue. Nonetheless, untreated CPG-10 (a porous glass) was used in this investigation. These packing materials offer a wider range of particle-size and pore-size selectivity than most other packing materials and they have been widely used for aqueous SEC although with mobile phases which were rather far from optimum.

In a preliminary investigation, other packing materials such as deactivated Porasil, silanized Bioglass (51), Bio-beads and Fractosil were used. For the reasons mentioned above, added to the problem of having to deal with a system with packing materials from different sources, this investigation was completed using CPG-10 packings.

Most of the columns were dry-packed. The internal diameter of all the columns was 3/8 inch with length ranging from 2 feet to 4 feet 3 inches. Table 3-1 contains a list of the characteristics of each packing material employed. Table 3-2 is a description of some of the singly packed columns. Columns were used in series in the traditional manner, with the mobile-phase flowing from the smallest to the largest pore-size. However as shown in Table 3-1, the small pore-sizes have very large specific surface areas and these tend to increase polymer/surface interaction during size separation. Therefore, the effect of reversing the flow on the separation process was also experimentally investigated.

More than four hundred mobile-phase compositions were studied in an attempt to find one most suited for polyacrylamide analysis. Details of the most important mobile-phases will be described during the presentation of results. However, of all the additives used in the mobile-phase, apart from salt, non-ionic surfactants were found to be the most important. Non-

ionic surfactants used included Tergitol (T), an alkylphenoxypolyethoxyethylene (from Union Carbide Corp.), Triton X-165 and Triton X-100, both alkyl-phenoxypolyethoxy ethanol (from Rohm and Haas Ltd.). The analytical reagents used for preparing the mobile-phases were used as received.

For studies involving MW calibration using dextrans, twenty five systems were investigated ranging from 3 to six columns combined in series. The systems are listed in Table 3-3. It contains the code designations. The first letter of the four character code (eg. S6AC), represents the series combination, the next number is the number of columns in series, the third character is the number of times the same number of columns (not necessarily the same type) have been combined in series in alphabetical order. The last letter in the code is the order in which the pore-sizes have been arranged, C for the traditional order and R the reversed flow arrangement. The length of each combination is listed in the last column of Table 3-3. The same code was used for the other water soluble polymer SEC systems.

The operating conditions of each case studied are listed in Table 3-4. It contains the case-study number designation, the mobile-phases, flow-rates and concentration of dextran injected.

Table 3-5 contains a list of the MW data supplied by the manufacturers of the polyacrylamide, sodium polystyrene sulfonate and dextran standards. Most of the polyacrylamide standards were purchased from Polysciences, the sodium polystyrene sulfonates from Pressure Chemical Company and the dextrans from Pharmacia Fine Chemicals.

The height of the chromatograms (F(V)s) were measured directly by hand on a large scale and on a special Digitiser. Finally numerical

Table 3-1. Characteristics of Packing Materials

Type	Norminal Pore Diameter (Å)	Mesh Size	Mean Pore Diameter (Å)	Pore Volume (cc/gm)	Surface Area (m^2/gm)	Pore Distr. ± %
CPG-10	69	120/200	69.0	--	--	--
	88		88.0	0.53	170.00	15.30
	120	200/400	116.0	0.73	155.00	8.60
	125	--	--	--	--	--
	240	200/400	257.0	1.09	111.00	3.50
CPG-10	327	120/200	327.0	1.02	73.50	--
	370	--	--	--	--	--
	500	200/400	493.0	1.25	52.40	7.70
	700	200/400	668.0	1.18	38.20	6.90
	700	120/200	729.0	0.98	33.90	8.60
	1000	200/400	1038.0	1.22	27.90	7.30
	2000	200/400	1989.0	0.71	9.20	8.40
	2000	200/400	1902.0	0.80	10.00	12.30
	3000	200/400	2734.0	0.82	7.80	8.80
Bio-glass	1500	100/200	1500.0	--	--	--
Bio-glass	2500	100/200	2500.0	--	--	--
Bio-beads SX-12	--	--	--	--	--	--
Bio-beads SX-2	--	--	--	--	--	--
Bio-beads SX-1	--	--	--	--	--	--
CPG-10	2000B	120/200	1944	0.99	13.30	4.97
Porasil DX	400-800	--	--	--	--	--
Fractosil	5000	120/230	4900	--	--	--

Table 3-2. Description of Singly Packed Columns

Column Designation	Packing Material	Pore Size Å	Length of Column (ins)
C88/120	CPG-10	88/120	31.75
C88	"	88	29.37
C120/240 B	"	120/240	46.75
C120	"	120	32.12
C125	CPG-10	125	48.00
C125/240/370	CPG-10	125/240/370	48.00
C240 A	"	240	48.00
C370/327	"	370/327	48.40
C370	"	370	45.00
C500 A	"	500	45.12
P4/8 (deactivated)	Porasil DX	400-800	48.00
BB12	Bio-Beads SX12	--	48.00
C240 B	CPG-10	240	36.00
C2000	CPG-10	2000	48.00
BB2	Bio-Beads SX2	--	48.00

Table 3-2. Continued

Column Designation	Packing Material	Pore Size Å	Length of Column (ins)
C240 B	CPG-10	240	36.00
C2000	CPG-10	2000	48.00
BB1	Bio-Beads SX1	-	48.00
C2000 D	CPG-10	2000	48.00
C2000 B'	CPG-10	2000	48.00
C729/700 A,B	"	729/700	47.25 , 48.00
C700/500/370	CPG-10	700/500/370	46.37
C1000	"	1000	45.87
C729	"	729	45.50
BG1500	Bio-glass	1500	48.00
BG2500	"	2500	48.00
C327	CPG-10	327	48.00
EM5000	EM-gel	4900	48.00
C3000 A	CPG-10	3000	
C500 B	CPG-10	500	25.00
C120/240 A		120/240	47.00

Table 3-3. Description of Column Combinations for Dextran Studies

#	Code No. (a)	Columns Combined in Series	# of Columns	Length (ft)
1	S6AC	C125/240/370, C370, P4/8, BG1500, BG2500, EM500	6	24.0
2	S9AC	BB12, BB2, BB1, C125/240/370, C370, P4/8, BG1500, BG2500, EM500	9	36.0
3	S5AC	C125, C240A, C370, C2000, C200QB	5	19.7
4	S4AC	C120/240, C370, C500B, C500/700B	4	13.75
5	S5BC	C120/240, C370, C500B, C500/700B, C3000	5	17.67
6	S3AR	C729/700, C700/500/370, C240/120	3	11.58
7	S4BR	C729/700, C700/500/370, C370/327, C240/120	4	15.58
8	S5CR	C729/700, C700/500/370, C240/120, C120/88, C88	5	16.75
9	S5DR	C729/700, C700/500/370, C370/327, C240/120, C120/88	5	18.25
10	S5ER	C729/700, C700/500/370, C370/327, C240/120, C88	5	18.08

Table 3-3. Continued

#	Code No. (a)	Columns Combined in Series	# of Columns	Length (ft)
11	S5FR	C729/700, C700/500/370, C370/327, C240/120, C125	5	18.41
12	S6BR,C	C729/700, C700/500/370, C370/327, C240/120, C120/88, C88	6	20.75
13	S6CR,C	C729, C500, C327, C240/120, C120, C88	6	19.30
14	S3BC	BG1500, C2000D, EM5000	3	12.00
15	S5GC	BG1500, C2000B', C2000D, BG2500, EM5000	5	20.00
16	S4CR	C729, C500, C240B, C240/120	4	13.18

Table 3-4. Operating Conditions of Case Studies for Dextran

Case Study #	Code # (a)	Mobile-phase	Flow-rate (ml/min)	Conc. wt % Injected
1	S6AC	Doubly distilled water	8.90	0.10
2	S6AC		1.90	0.10
3	S9AC	Triply distilled water	4.00	0.10
4	S9AC		2.25	0.10
5	S5AC	Doubly distilled water and 0.1 MKBr	4.60	0.67
6	S4AC	0.01 MNaF	4.20	0.05
7	S5BC	0.01 MNaF	4.20	0.05
8	S3AR	0.05 MKF/0.02wt%NaN_3/ 1.0gm/24lit Tergitol., (pH=6.6)	4.50	0.05
9	S4BR	same as case study #8	4.50	0.05
10	S5CR	"	4.50	0.05
11	S5DR	"	4.50	0.05
12	S5ER	"	4.50	0.05
13	S5FR	"	4.50	0.05
14	S6BR	"	4.50	0.05
15	S6BC	"	4.50	0.05

Table 3-4. Continued

Case Study #	Code # (a)	Mobile-phase	Flow-rate (ml/min)	Conc. wt % Injected
16	S6CR	0.00833 MNa_2SO_4/1.0% CH_3OH/ Tergitol (pH=3.38)	1.43	0.05
17	S6CR	"	4.30	0.05
18	S6CR	"	7.83	0.05
19	S6CR	0.00417 $MKH_3(C_2O_4)_2.2H_2O$/ 1.0% CH_3OH/1.0gm/24lit Tergitol, (pH=2.66)	4.25	0.05
20	S6CC	"	4.25	0.05
21	S6CC	same as in #17	4.30	0.05
22	S3BC	0.05 $MKH_3(C_2O_4)_2.2H_2O$	4.20	0.05
23	S5GC	"	4.20	0.05
		Reproducibility Test		
24	S4CR	0.00833 MNa_2SO_4/1.0gm/24lit Tergitol pH=7.0	3.00	0.05
25	S4CR	"	1.900	0.05

Table 3-5. Data for Polymer Standards

A. Polyacrylamide Fractions

	Designation	Lot No.	$\bar{M}_N$ x10^{-3}	$\bar{M}_W$ x10^{-3}	$\bar{M}_{rms}$ x10^{-3}	$\bar{M}_W/\bar{M}_N$
	PAM55	03-7	--	55.0	--	--
	PAM100(a)	93-3	--	100.0	--	--
	PAM270(a)	93-3	--	270.0	--	--
*	PAM500	93-5	--	500.0	--	--
	PAM1000	95-6	--	1000.0	--	--
	PAM2000	95-4	--	2000.0	--	--
	PAM5000	94-3	--	5-6000.0	--	--
	Std. A	--	2520.0	5040.00	3560.0	2.00
**	Std. B	--	1600.0	3350.00	2320.0	2.10
	Std. C(b)	--	2400.00	5830.00	3740.0	2.43

Table 3-5. Continued

B. Sodium Polystyrene Sulfonate (c)

Designation	Lot No.	$\bar{M}_N$ x10^{-3}	$\bar{M}_W$ x10^{-3}	$\bar{M}_{rms}$ x10^{-3}	$\bar{M}_W/\bar{M}_N$ ≤
NaPSS31	11	--	31.0	--	1.10
NaPSS88	14	--	88.0	--	1.10
*** NaPSS195	15	--	195.0	--	1.10
NaPSS354	12	--	354.0	--	1.10
NaPSS690	16	--	690.0	--	1.10
NaPSS1060	17	--	1060.0	--	1.10

C. Dextrans

T2000	6038	--	--	--	--
T500	5770	173.0	509.00	296.70	2.94
T250	1343	112.50	231.00	161.20	2.05
T150	921	86.00	154.00	115.10	1.79
T110	9071	76.00	106.00	89.80	1.39
T70	1730	42.50	70.00	54.50	1.65
T40	2540	28.90	44.40	35.80	1.54
T20	7968	15.00	22.30	18.29	1.49
T10	3205	5.70	9.30	7.23	1.63

(a) PAM100 and 270 have the same lot No. and Catalogue No. P100 was used initially in the studies,

(b) Std C is hydrolyzed polyacrylamide (14%)

(c) $\bar{M}_W$ of sodium polystyrene sulfonate is the Norminal MW of polystyrene sulfonate ion. They are reported by the manufacturers to contain sodium sulphate impurities.

* Supplied by Polysciences Inc., Warrington, PA.

** Supplied by McMaster University Chem. Eng. Dept.

*** Supplied by Pressure Chemical Company, Pittsburgh

calculations involving searches for the linear calibration parameters over retention volumes ranges of interest, molecular weight correction factors P_K, molecular weight averages and MWDs were performed on a CDC6400. A single variable search subroutine - Fibonacchi search was used (Optimization Theory and Practice by Beveridge and Schecter; McGraw Hill).

3-2. Viscosity Measurements

Viscosity data were needed to assess the relative sizes of the polymer coils in different solvents of different ionic strengths (I) and pH in the absence or presence of other additives. The solvents were then used as mobile phases in the SEC studies.

The viscometers used were Cannon - Ubbelhode viscometers 75-L352, 75-L181 and 50-A620. Their use for the MW range of polyacrylamide investigated here with distilled water as solvent has been described recently (52). The procedures for viscosity measurements are standard and have been described elsewhere (51)(52).

Viscosities were calculated from the following formula:

$\eta(c,p)$ = viscometer constant X solution density X average flow-time

Specific viscosities were obtained using

$$\eta_{sp} = \frac{\eta_{solution} - \eta_{solvent}}{\eta_{solvent}} \simeq \frac{\text{Flowtime}_{solution} - \text{Flowtime}_{solvent}}{\text{Flowtime}_{solvent}}$$

The intrinsic viscosity was obtained using

$$[\eta] = \left.\frac{\eta_{sp}}{c}\right]_{c \to o}$$

where c is the sample concentration in gm/100 ml. η_{sp}/c was plotted versus c and extrapolated to c = 0 ie. zero concentration to obtain $[\eta]$.

3-3. Methodology of Mobile-Phase Development

Single columns were used almost exclusively to develop mobile-phases for the polymers studied. Of the three polymers studied, polyacrylamide was the most difficult for the following reasons:

(i) Unlike dextran which has no ionizable groups and sodium polystyrene sulfonate which is fully dissociated in solution, non-ionic polyacrylamide is generally slightly hydrolyzed to the free carboxylic acid form (53).

At low pH values (pH < 2) polyacrylamide is partly in its protonated form, thus

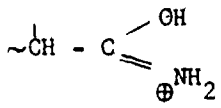

while polyacrylic acid is present in its undissociated form

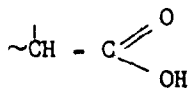

At high pH values (pH > 6.0) polyacrylamide is present in its non-ionic form

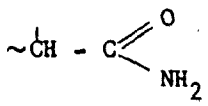

while polyacrylic acid is present in its ionized form as acrylate anion

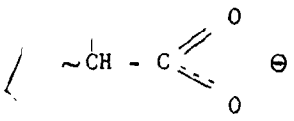

At intermediate pH values ($2.0 < pH < 6.0$), all the different forms co-exist as shown

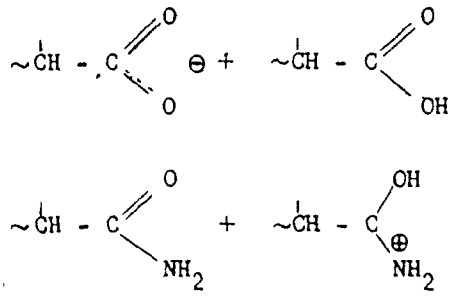

(ii) though they are commercially available, most of the polyacrylamide standards are incompletely characterized as is clear from the lack of data in Table 3-5. When distilled water or very low salt concentrations are used, viscosity data (see below) must be interpreted with care.

In working with single-columns, it was convenient to investigate a wide range of mobile-phase compositions as the retention times were small. Concentrations of the order of 0.025 - 05% by wt. of the readily available salts, ionic surfactants, polar organic solvents and neutral surfactants were consistently used. Ionic surfactants used included: sodium lauryl sulfate, sodium dodecyl sulfate (SDS) and sodium dioctyl sulpho-succinate. Of all these additives, only the neutral surfactants and polyethylene oxide showed promise in reducing adsorption and increasing peak separation.

It was also important to establish that the presence of additives in the mobile-phase did not change the size of the polymer coils. This

was confirmed with viscosity measurements. The different polymers were investigated first in additive-free distilled water. The effects of varying concentrations of salt, acid and neutral surfactants was then investigated. At different stages, the effect of various combinations of salt, acid and surfactants were investigated. The procedures were repeated for each polymer until the optimal mobile phases were established. At each stage, the viscosity data were used to anticipate the SEC behaviour of the polymer molecules in solution.

4. RESULTS AND DISCUSSIONS -- MOBILE-PHASE AND PACKING DEVELOPMENT

Viscosity data are presented first since their use facilitates the interpretation of the SEC behaviour with respect to polymer/surface interactions. Table 4-1 presents summaries of viscosity measurements for polyacrylamide. With distilled water as solvent, two sets of measurements were made eight months apart. Table 4-2 presents results for sodium polystyrene sulfonate and dextran.

Plots of $[\eta]$ versus $\bar{M}_w$, instead of MW, are only approximate relationships, except when the polymers used are either monodispersed or have a most probable distribution. However, the $[\eta]$ versus $\bar{M}_w$ of polyacrylamide and dextran were used and they are shown in Fig. 4-1. Fig. 4-2 contains data for sodium polystyrene sulfonate. Fig. 4-3 are corresponding plots for polyacrylamide and sodium polystyrene sulfonate in water as solvent. It is perhaps surprising that standards P500 and P55 show "anomalous" behaviour in water, behaving as correspondingly larger coils than other polyacrylamides. It cannot be ruled out however, that these polyacrylamides standards which are nominally neutral, become partially hydrolysed when dissolved in distilled water. [The intrinsic viscosity of one of the polyacrylamide standards in water, standard A is found to be in perfect agreement with previous measurements (51)(52), thus validating the experimental procedure.] In the presence of added salt or acid, the polymer coils appear to assume a stable conformation and according to Fig. 4-1, for polyacrylamide, the MW- or $\bar{M}_w$- intrinsic viscosity relationship, like that for dextrans, is independent of the ionic strength and pH of the solvent in the range studied. Therefore,

Table 4-1. Polyacrylamide: Intrinsic Viscosity Data at 25°C

#	Solvent pH	Solvent I	StdA	StdB	P2000	P1000	P500	P270	P55
1	Distilled water		--	--	9.50	5.90	24.5	0.83	2.00
2	6.70	0.171	--	--	5.30	2.88	1.90	0.89	0.43
3	2.75	0.013 (Tergitol, 0.008%wt)	--	--	5.30	--	1.75	1.10	0.35
4	7.00	0.025 (Tergitol, 0.006wt % PEO*)	8.30	8.20	5.35	2.73	1.85	0.85	0.40
5	2.95	0.100 (Tergitol, 0.004%)	8.30	--	5.40	2.85	1.50	0.73	0.40
6	7.00	0.250 (Tergitol, 0.006wt %, PEO*)	8.53	8.40	5.20	2.80	1.93	0.91	0.50
7	3.50	0.025 (Tergitol, 0.006wt % PEO*)	8.50	8.40	5.20	2.80	1.85	0.85	0.45
8	5.43	0.503 (Tergitol, 0.004 wt %)	8.20	--	5.55	2.80	1.80	0.90	0.42
9	6.60	0.053 (Tergitol, 0.004 wt. %)	--	--	5.28	2.70	1.85	0.72	0.51
10	3.25	0.013 (Tergitol, 0.004 wt %)	8.20	--	5.15	2.75	1.80	0.80	0.35
11	2.50	0.063 (Tergitol, 0.004 wt %)	8.10	--	5.30	2.75	1.60	0.73	0.41
12	Distilled water		11.4	--	9.50	6.07	25.8	0.80	1.10

* PEO, 0.025gm/lit ($\bar{M}_w$ = 300,000)

Table 4-2. Sodium polystyrene sulfonate and Dextran intrinsic viscosity data

Solvent pH	Solvent I	$[\eta]$ (at 25°C) Values PS1060	PS690	PS354	PS195	PS88	PS31	#
Distilled water		61.2	46.0	15.0	10.5	5.70	0.20	1
2.95	0.100 (Tergitol) **	4.37	2.32	1.00	0.70	0.20	--	2
3.50	0.025 (Tergitol, PEO)	4.50	3.22	1.43	1.20	0.40	0.15	3
7.00	0.025 (Tergitol, PEO)	5.40	3.70	1.55	1.33	0.52	0.20	4
5.43	0.503 (Tergitol)	1.32	1.15	0.47	0.52	0.26	0.09	5
6.60	0.053 (Tergitol)	4.50	2.72	1.300	0.88	0.40	0.18	6
3.25	0.013 (Tergitol)	8.90	5.72	2.65	1.96	1.00	0.32	7
2.50	0.063* (Tergitol)	5.60	3.90	1.57	1.00	0.42	--	8
2.75	0.013 (Tergitol)	6.45	4.10	2.37	2.00	0.95	--	9

		Dextran			
pH	I	T2000	T500	T250	T70
6.60	0.053	0.80	0.50	0.43	0.27

* The only solvent prepared using organic electrolyte, potassium tetraoxalate $KH_3(C_2O_4)_2 \cdot 2H_2O$.

** Refer to Table 4-1 for the concentration of Tergitol and PEO.

Figure 4-1. Intrinsic Viscosity vs $\bar{M}_W$ for Non-Ionic Polymers - Polyacrylamide and Dextran (25°C)

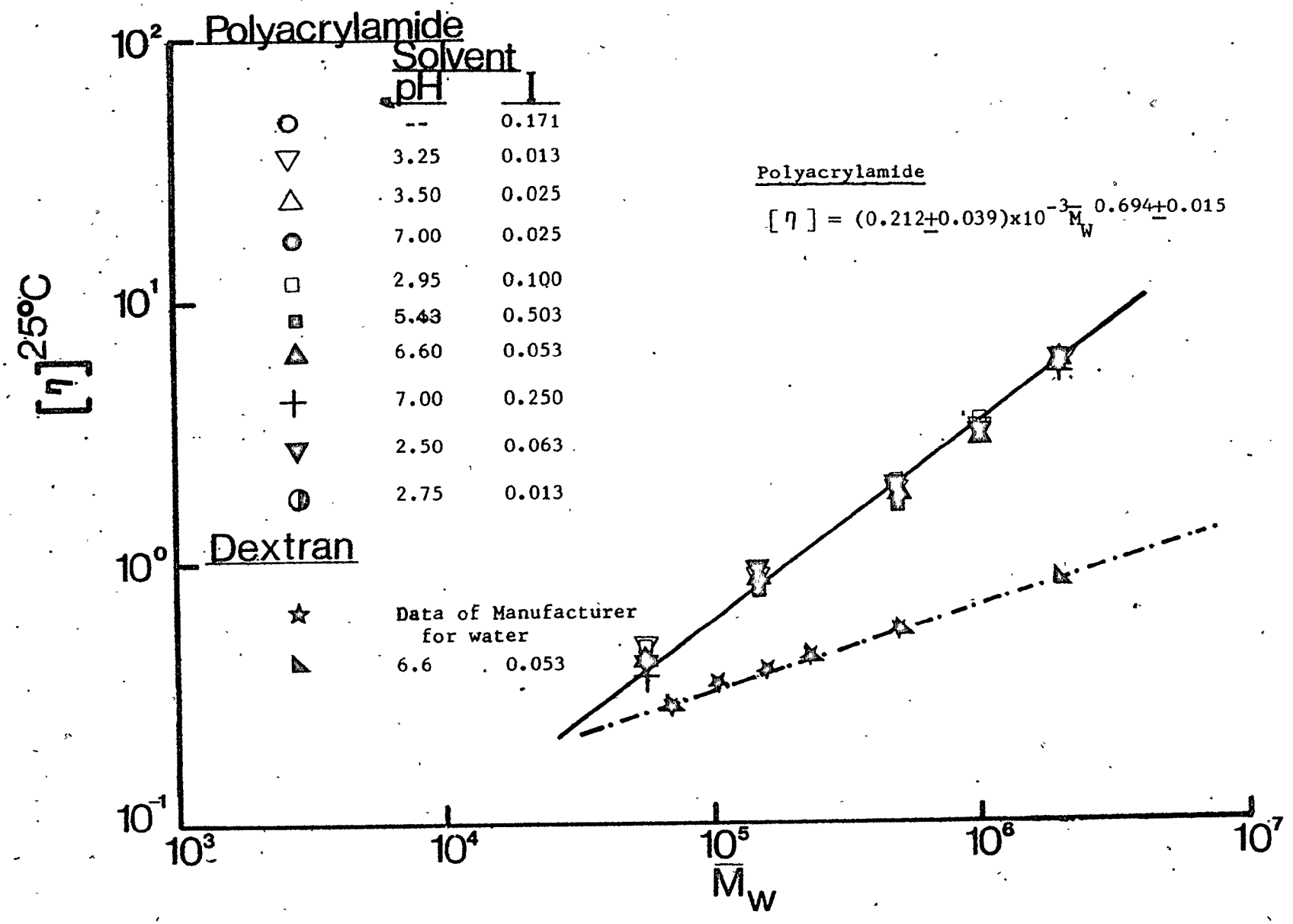

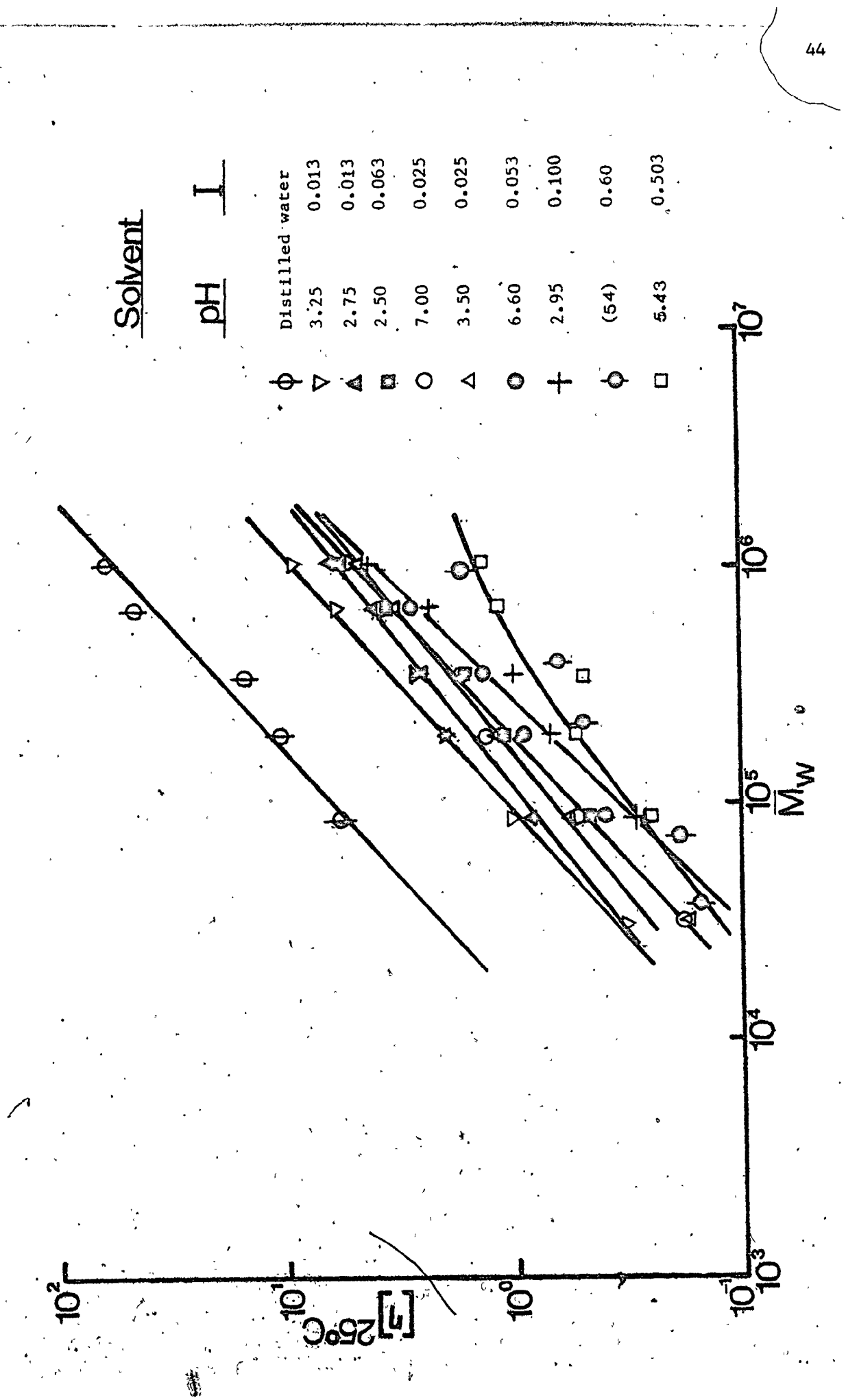

Figure 4-2. Intrinsic Viscosity vs $\bar{M}_w$ for Sodium Polystyrene Sulfonate at 25°C

Figure 4-3. Intrinsic Viscosity vs $\bar{M}_W$ for Non-Ionic Polyacrylamide and Sodium Polystyrene Sulfonate in Water (25°C)

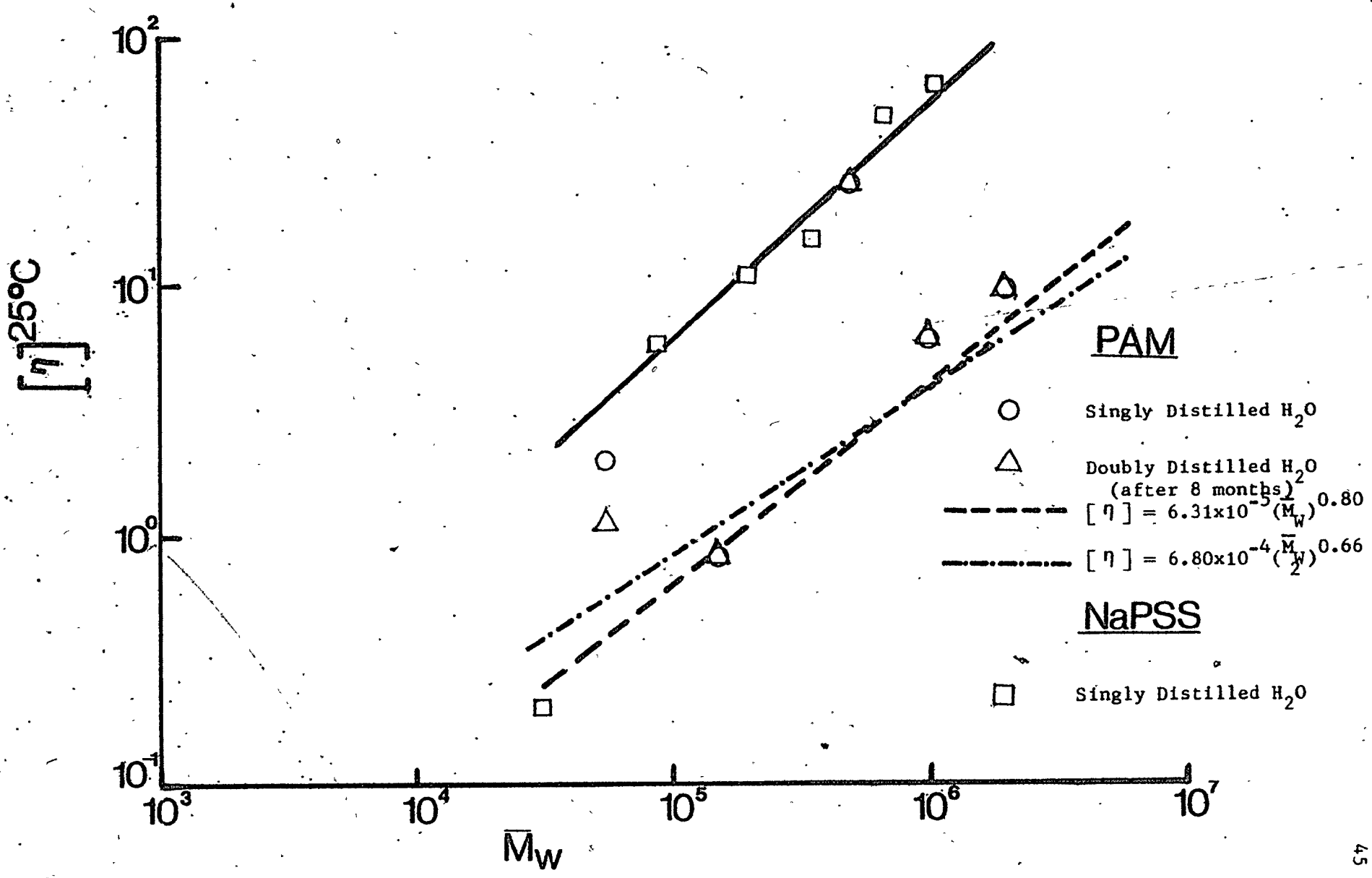

one should expect the molecular weight calibration curve to be independent of ionic strength and pH if a size exclusion mechanism is applicable with SEC.

One of the polyacrylamide standards, standard C which is known to be 14% hydrolyzed was found to be strongly affected by pH and the ionic strength of the solvent as shown in Table 4-3. In water the intrinsic viscosity was too large to measure with available apparatus. At low pH, the coils become quite small compared to the values at high pH. At or close to a pH of 7.0, the size of the coils is independent of ionic strength, except at very high I (compare #1, 3, 4, and 5 in Table 4-3).

Table 4-3.

Effect of Ionic Strength and pH on Intrinsic Viscosities of Anionic Polyacrylamide (Std C 14% hydrolysed) at 25°C

#	pH	I	$[\eta]$
1	7.00	0.250	20.0
2	3.50	0.025	7.00
3	7.00	0.025	25.0
4	5.43	0.503	13.3
5	6.60	0.053	25.0
6	3.25	0.013	10.3
7	2.50	0.063	4.20
8	2.75	0.013	4.13
9	--	0.00	Too large to measure

For dextrans, their very small intrinsic viscosities for even the high molecular weight standards, suggests that they are very compact in solution (54). However with sodium polystyrene sulfonate which are

highly dissociated, the sizes of the coils are strongly dependent on the pH and I of the solvent. At high ionic strength (I = 0.503), there is close agreement with literature results at I = 0.6 (54) and I = 0.5 (55). Excluding the organic based solvent (I = 0.053, pH = 2.5, see Table 4-2), the effect of decreasing pH or increasing I is to decrease the size of the coils. Therefore, one does not expect the MW calibration curves of polystyrene sulfonate to be independent of ionic strength or pH of the mobile-phase. In the absence of adsorption, the trend in size should be apparent in the SEC.

These effects are summarised in Figs. 4-4 and 4-5 for sodium polystyrene sulfonate and polyacrylamide, respectively.

4.1. Reproducibility of Method of Packing

Desirable features of any packing method are:

(i) ease of use

(ii) low cost

(iii) short packing time

(iv) reproducibility of performance and constant control of packing quality.

Glass particles are quite large and therefore dry-packing as opposed to slurry packing was found to be adequate. Data pertaining to reproducibility of performance are shown in Fig. 4-6 for 6 single dry-packed columns. The data are presented in the form of a MW calibration curve. This method of presentation is used throughout for data relating to SEC performance. Two columns were used for each of the three polymers. The lengths and mobile-phases are specified in the figure. As can be seen, the performance of the columns is highly reproducible.

Figure 4-4. Stronger Effect of Increasing Ionic Strength on the Intrinsic Viscosity of Sodium Polystyrene Sulfonates at pH > 3.0

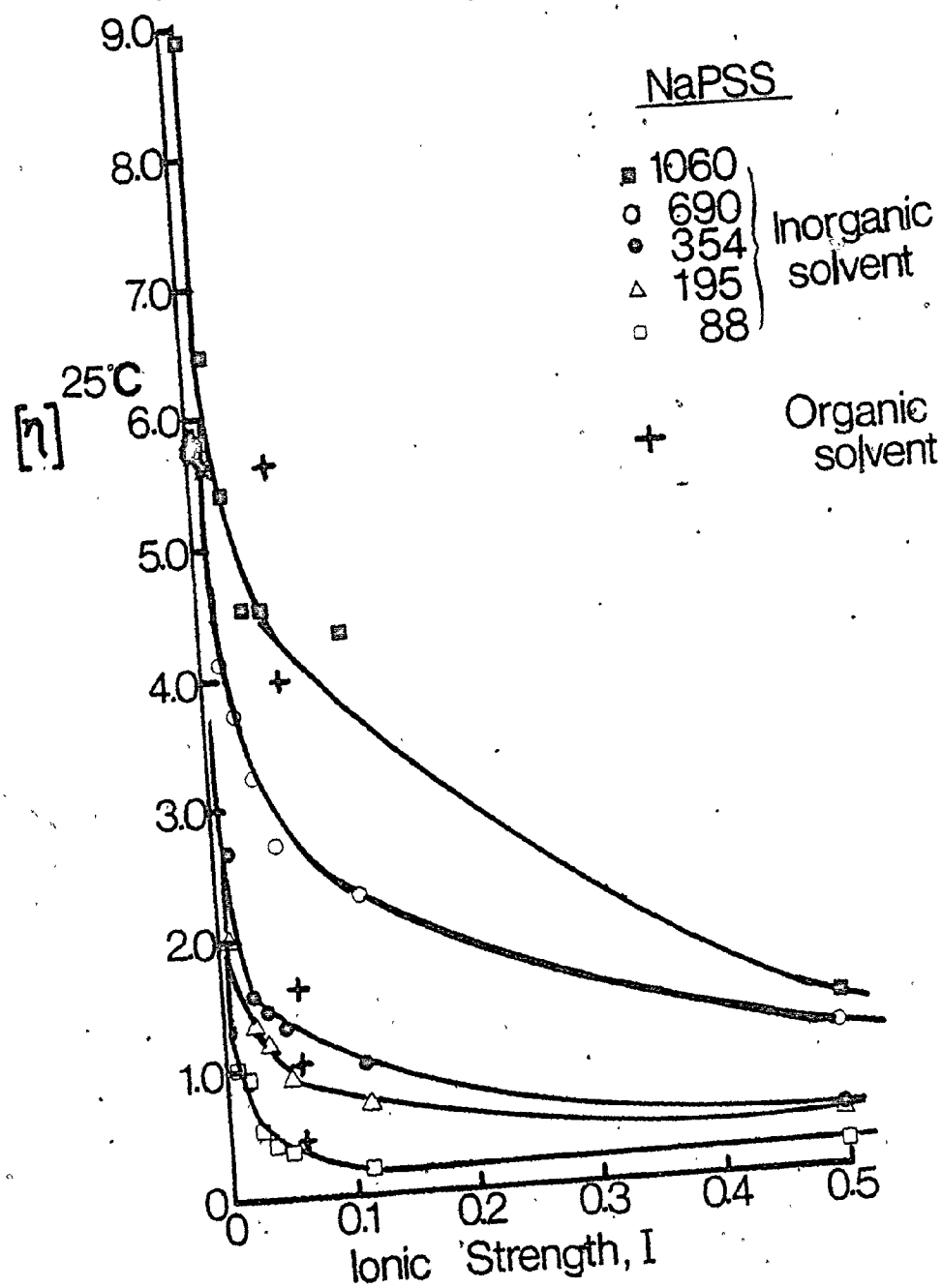

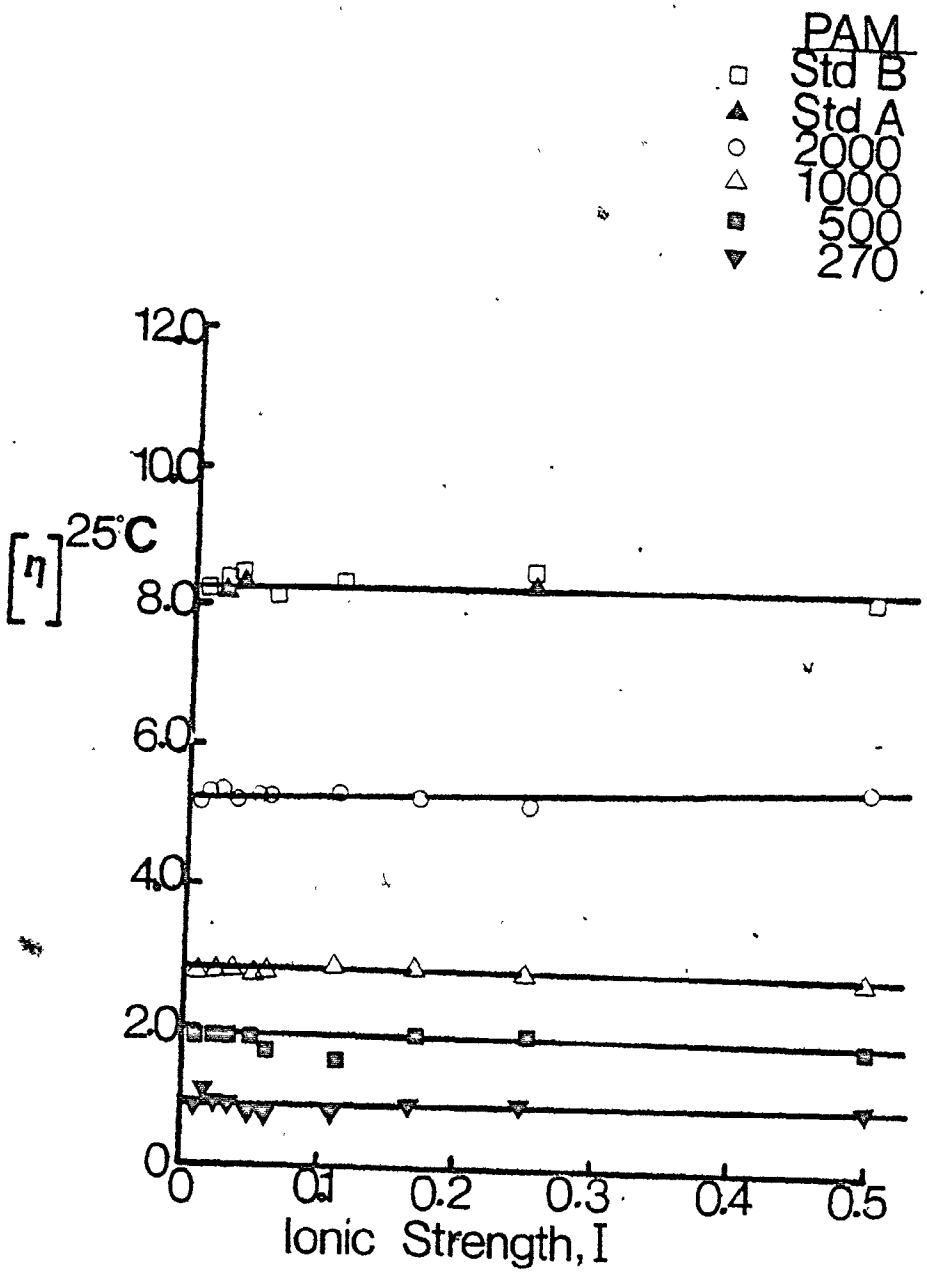

Figure 4-5. Effect of Increasing Ionic Strength on the Intrinsic Viscosity of Non-Ionic Polyacrylamide

Figure 4-6. Reproducibility of Method of Dry Packing

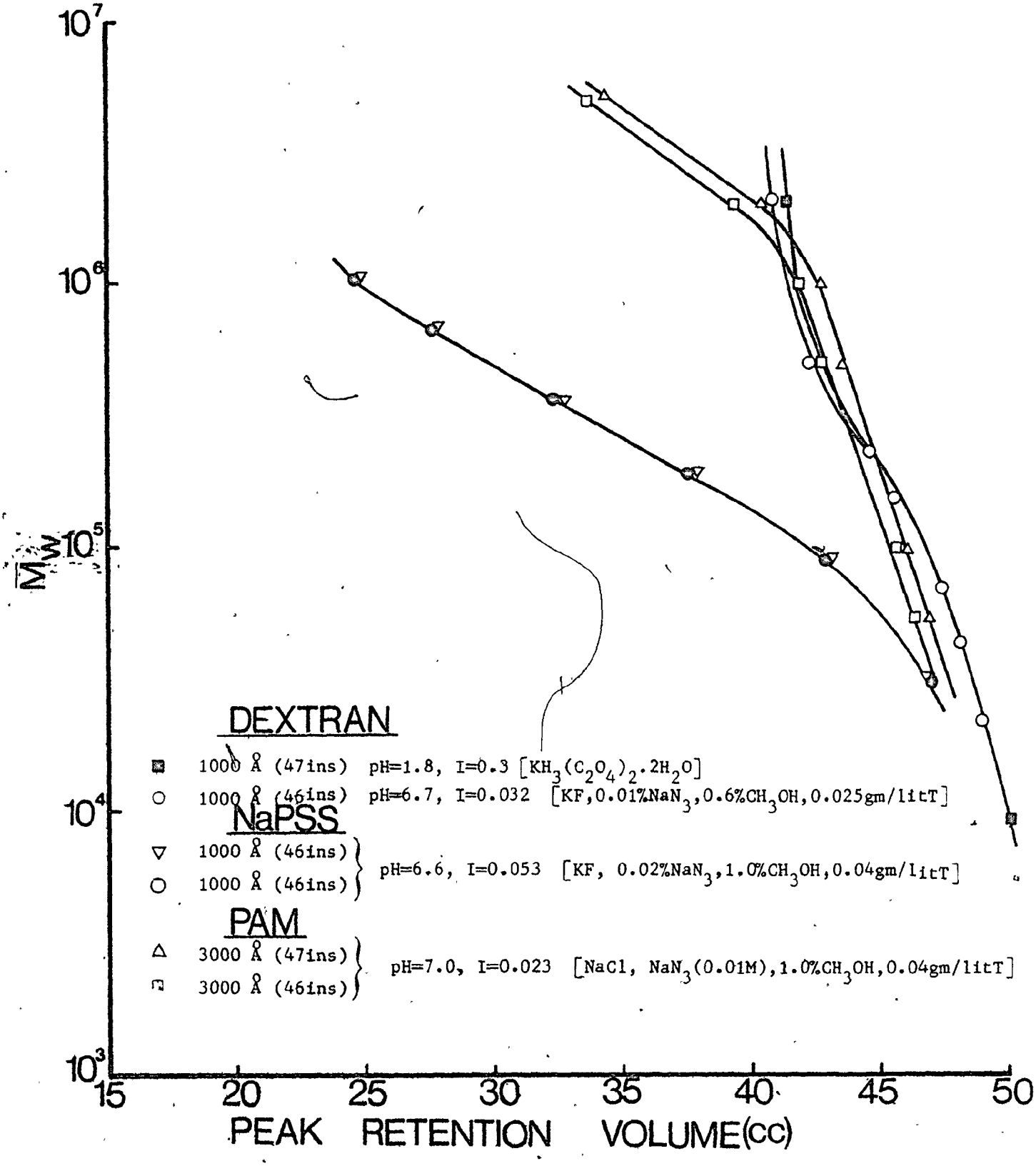

4.2. Effect of Ionic Strength on SEC Elution Volumes

(i) Dextran

The effect of ionic strength I will be shown in the section on development of molecular weight calibration curve.

(ii) Polyacrylamide

For investigation of SEC behaviour, a series of MW calibration curves were obtained at increasing I of the mobile-phase. Above a critical I, a single MW calibration curve should be obtained, according to the viscosity data already discussed. Fig. 4-7 shows MW calibration curves for polyacrylamide in distilled water and in vaious sodium chloride solutions ranging in ionic strength from I = 0.001 to 0.5. Although the pH of the solutions also varied between 5.00 and 6.18, this would be expected to have only a slight effect, if any, on the SEC process since carboxylic acid groups on polyacrylamide are almost fully ionized in this pH range. However, it is possible that in this range the polyacrylamide may be slightly protonated, so that any variation in charge density on the glass surface could result in some polymer/surface interaction. The choice of a single 2000 Å pore size column (4 ft long and 3/8 in ID) emphasizes the wide range of elution volumes in going from water to intermediate or high ionic strength I.

In distilled water, the polymers are completely excluded from the pores and elute at the column void volume. It is unlikely that this exclusion is based on size alone since the pore diameter is relatively large. Also, as already indicated, the intrinsic viscosities in water are only slightly greater than in salt solutions (with the exception of the 500,000 and 55,000 MW polymers). Again one is led to speculate that these polymers are partially hydrolysed. The resulting polyanions would

Figure 4-7. Effect of Increasing I on $\overline{M}_w$ calibration curves of PAM using NaCl

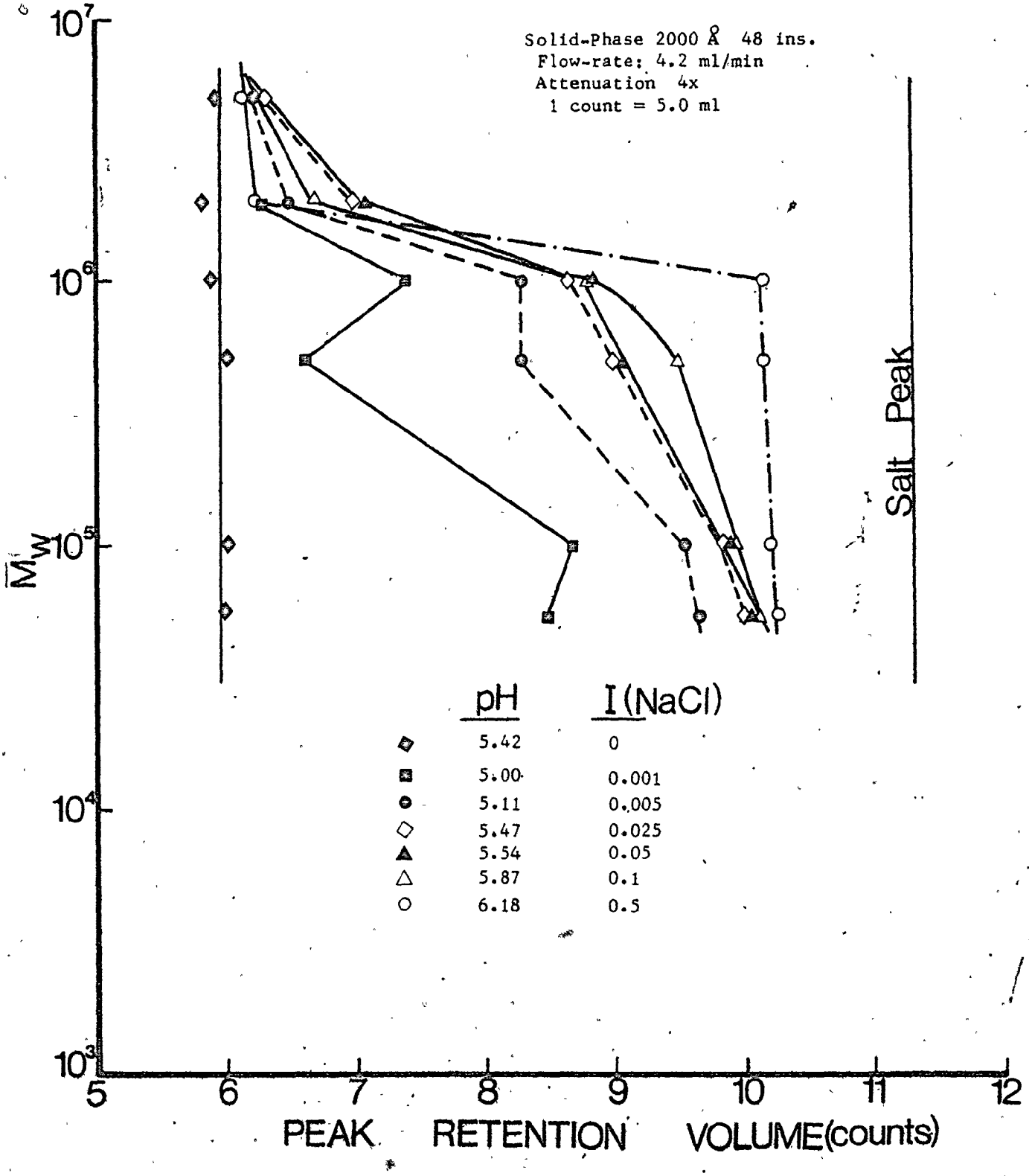

tend to be excluded by charge repulsion from the negatively charged pores of the glass substrate. Chain extension due to charging could also contribute to exclusion at the higher molecular weights.

With addition of NaCl, pore permeation is seen to occur and this is again consistent with polyelectrolyte behaviour, a property which was not reflected in the viscosity data showing independence on I. Addition of salt is, however, observed to attenuate the effect of the surface charge by compression of the associated electrical double layers. The anomalous behaviour of 500,000 and 55,000 MW samples is again evident, particularly at low I. These samples behave as molecular species that are abnormally large relative to the others in the series, again suggesting that they are more highly hydrolysed and thus have a higher charge density.

Pore permeation increases with I, then remains independent of I in the range of 0.01 to 0.1. At very high I (0.5), complete loss of resolution at MW less than one million is noticed, reflecting presumably total permeation. However, the total permeated volume, (which does not change as long as sufficient salt is added to the mobile-phase and measured with any salt) is significantly greater than the polymer elution volume at the highest possible I. Such a volume difference could be explained if a fraction of the pores is inaccessible to even the lowest MW polymer investigated.

It was desirable to show that the SEC behaviour was reproducible with inorganic salts, other than NaCl. Fig. 4-8 shows calibration curves, with potassium fluoride, sodium sulfate and potassium bromide as added salts. Again, at very high I, the total permeation as indicated by samples of MW less than one million is highly reproducible but less than total permeated volume suggesting a bimodal or multimodal nature of the pores. That the multimodal character of the packing is not limited to the 2000 Å pore-size dry-packed column alone, is shown in Fig. 4-9 for a 1000 Å

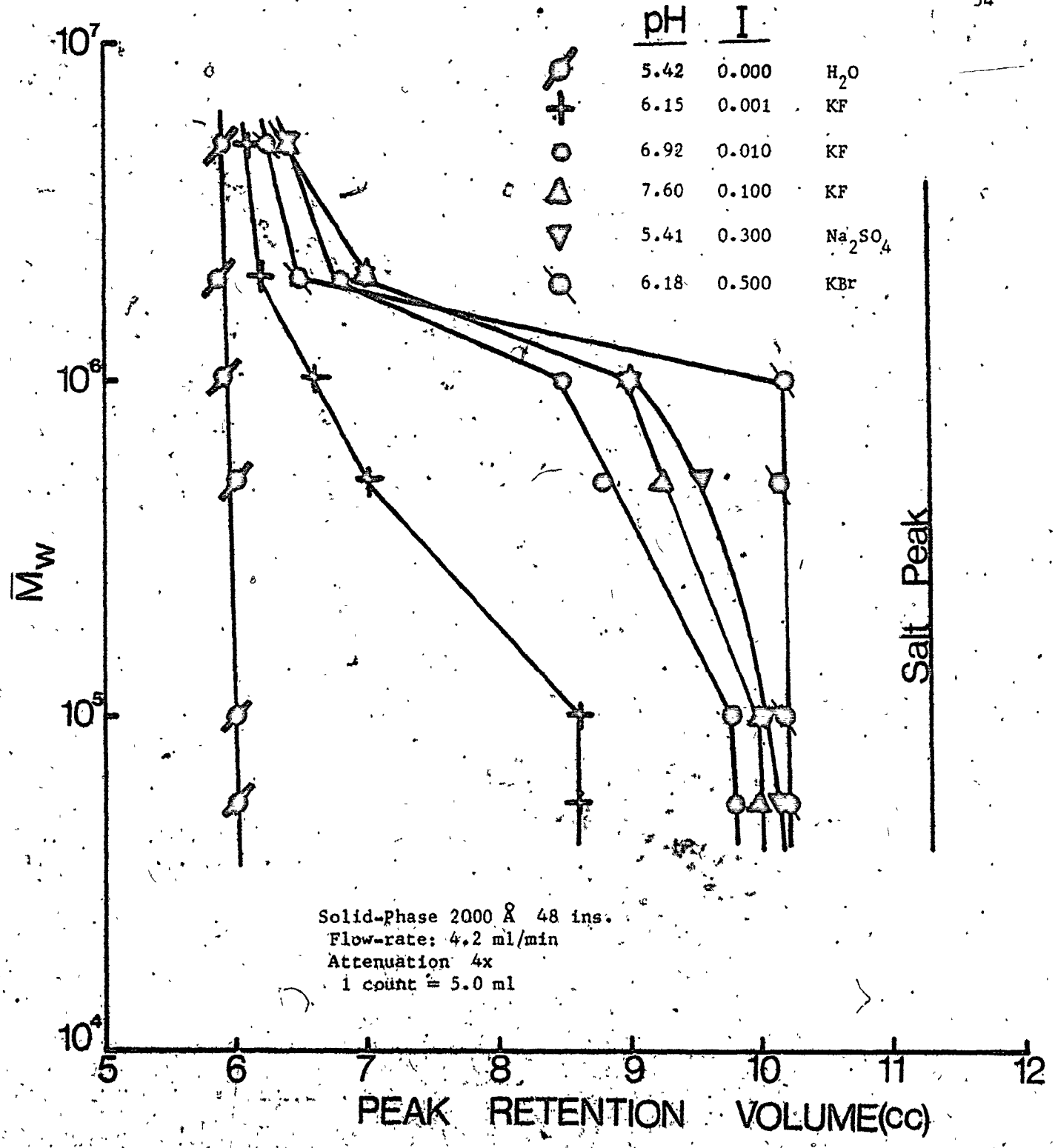

Figure 4-8. Reproducible effect of I on $\bar{M}_w$ calibration curves of PAM using various salts

Figure 4-9. Reproducibility of apparent total Permeated volume on a 1000 Å pore-size column

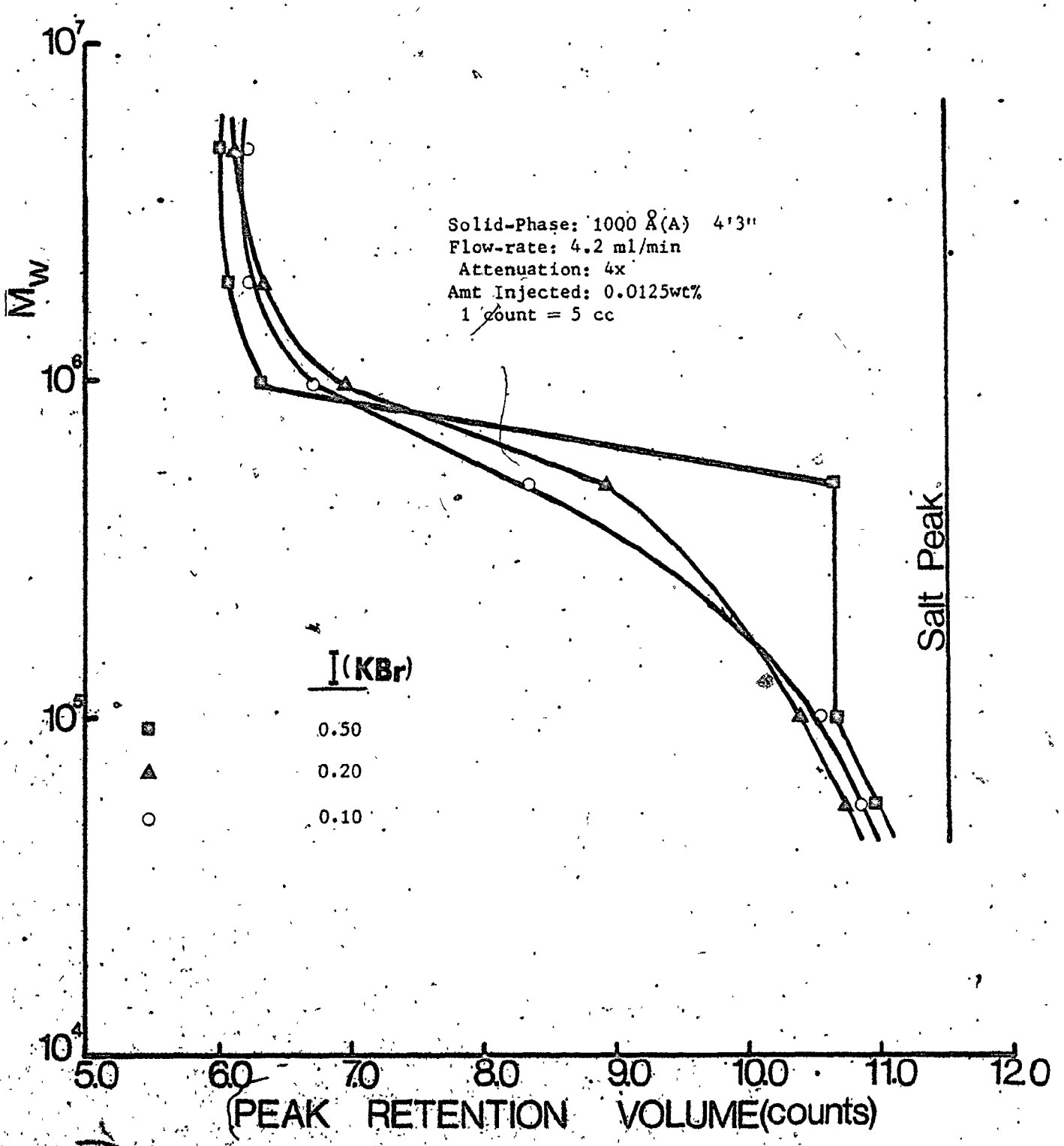

pore-size column.

(iii) Sodium Polystyrene Sulfonate

Fig. 4-10 shows MW calibration curves for a 2000 Å pore-size column for sodium polystyrene sulfonate, using NaCl, KF and sodium sulfate as additives. For this polymer, the MW calibration curve is expected to shift to higher retention volumes with increasing I, and this is reflected in the figure except at high I, where a behaviour similar to that of polyacrylamide is observed.

In distilled water, NaPSS, like polyacrylamide are excluded from the pores by charge repulsion. However, as shown in Fig. 4-3, these polymers are large relative to polyarcylamide, so that one cannot rule out the possibility of exclusion based on size. Unlike polyacrylamides and dextrans, their ionizable groups are fully dissociated in solution, and the low MW standards should not be excluded by size alone from the pore (See Table 4-2).

In the presence of high salt concentrations, the multimodal nature of the pore-network is again apparent, with a more distinct secondary total permeation volume of the polymers.

4.3. Effect of pH on SEC Elution Volumes

(i) Dextrans

The effect of pH is similar to that of I.

(ii) Polyacrylamide

The effect of pH is shown in Fig. 4-11. These data are for the same 2000 Å pore-size column which has been used thus far. The solutions were acidified with sulfuric acid in the presence of sodium sulfate to yield pH values between 2.25 and 1.62, in a range where carboxylic acid

Figure 4-10. Effect of I on the $\bar{M}_w$ calibration curve of NaPSS

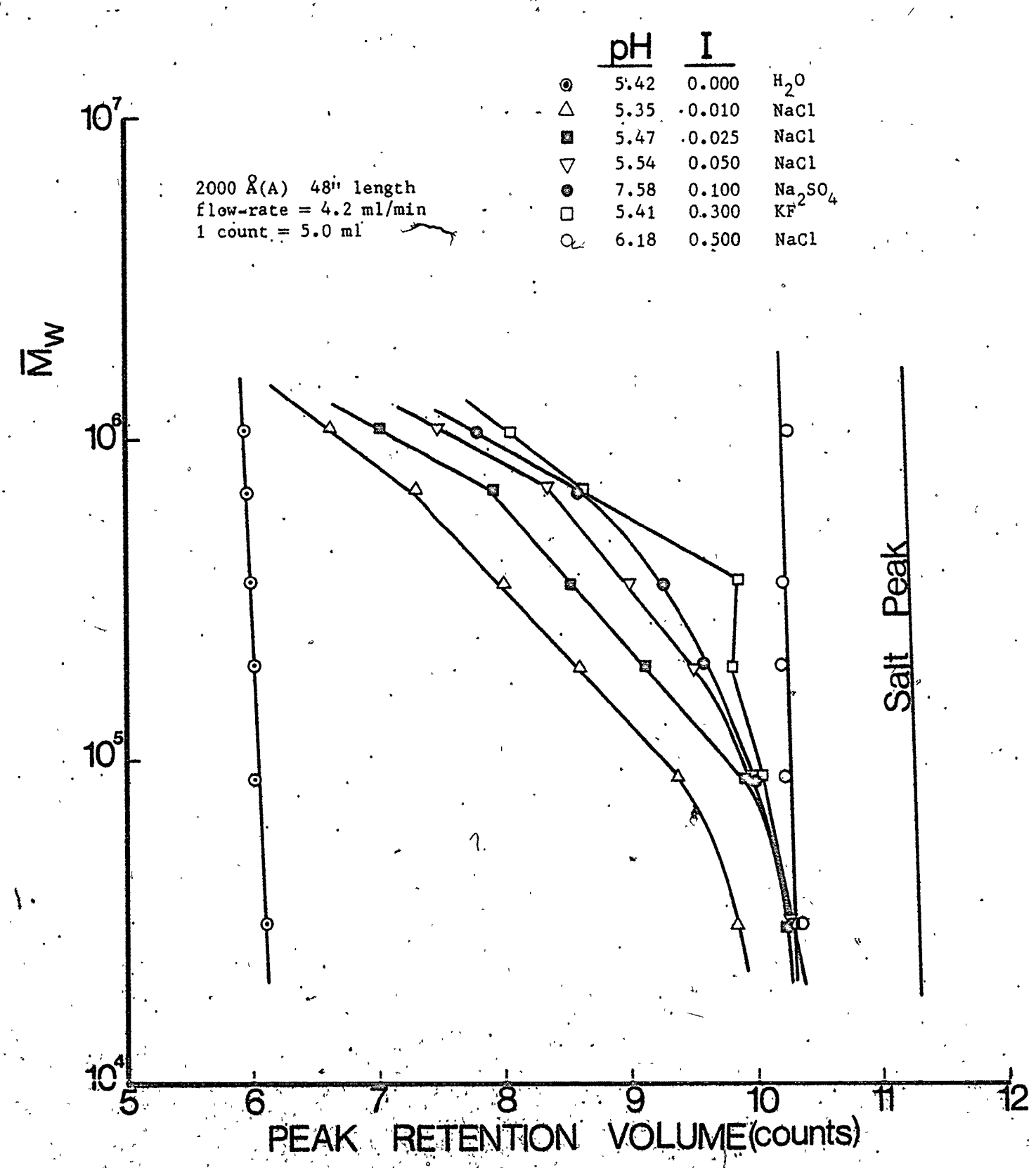

Figure 4-11. Effect of pH on $\bar{M}_w$ calibration curves of PAM in the presence of salt

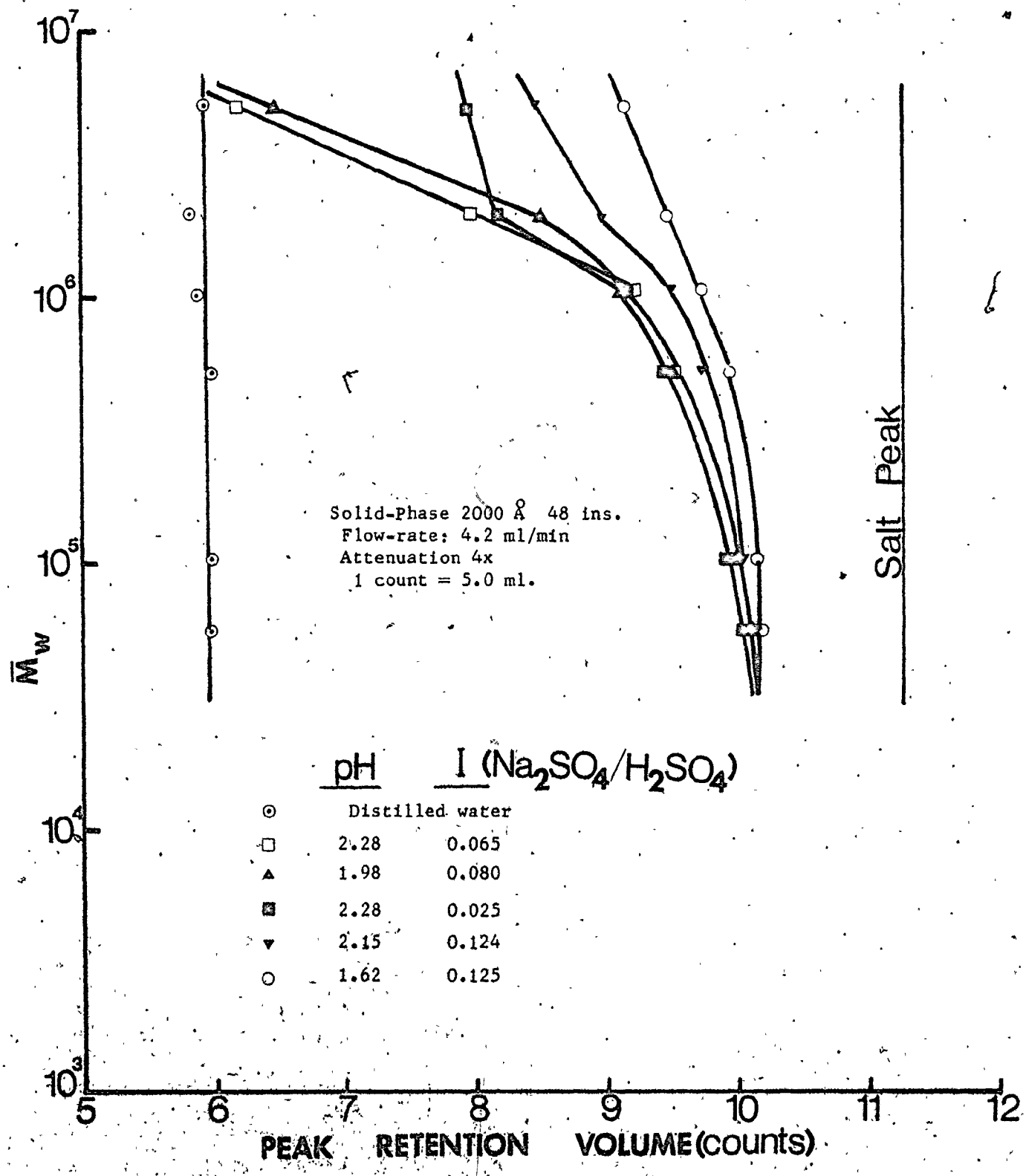

groups on the polymer chain may be expected to be undissociated. As the pH decreases, the curves are seen to shift to higher elution volumes with more extensive pore permeation evident in the higher MW region. For this 2000 Å pore-size column, with properly selected mobile-phase, the molecular weight separation range is between 10^6 and $2x10^6$. Therefore, extensive pore permeation of $2x10^6$ and $5x10^6$ MW samples is not to be expected. At low pH, polyacrylamide is present more in its protonated form. Hence the extensive pore permeation can be explained in terms of a type of "reversible adsorption", caused by the presence of the protons.

The very strong effect of pH in the absence of salt is shown in Fig. 4-12. As in other cases, there is a gap between the apparent total permeated volume and the total permeated volume, which again can only be explained if a fraction of the pores is inaccessible to even the lowest MW sample investigated.

(iii) Sodium Polystyrene Sulfonate

The effect of decreasing pH in the presence and absence of salt are shown in Figs. 4-13 and 14 respectively. The MW calibration curves are seen to shift to very high retention volumes with decreasing pH. At very low pH, the same effect as at high I is observed. The SEC behaviour is contrary to the viscosity data where the effect of I on the coil dimensions is stronger than that of pH. At low pH, the packing materials -- glass or silica are supposed to be very stable (14).

For both polyacrylamide and sodium polystyrene sulphonate, the MW calibration curves are very unreproducible at both high I and low pH. However, the effect of the polymer in causing the instability is stronger than the effect of the stationary phase since no similar difficulties were experienced with dextrans. Therefore, the search for mobile-phases

Figure 4-12. Effect of pH alone on $\bar{M}_w$ calibration curves of PAM

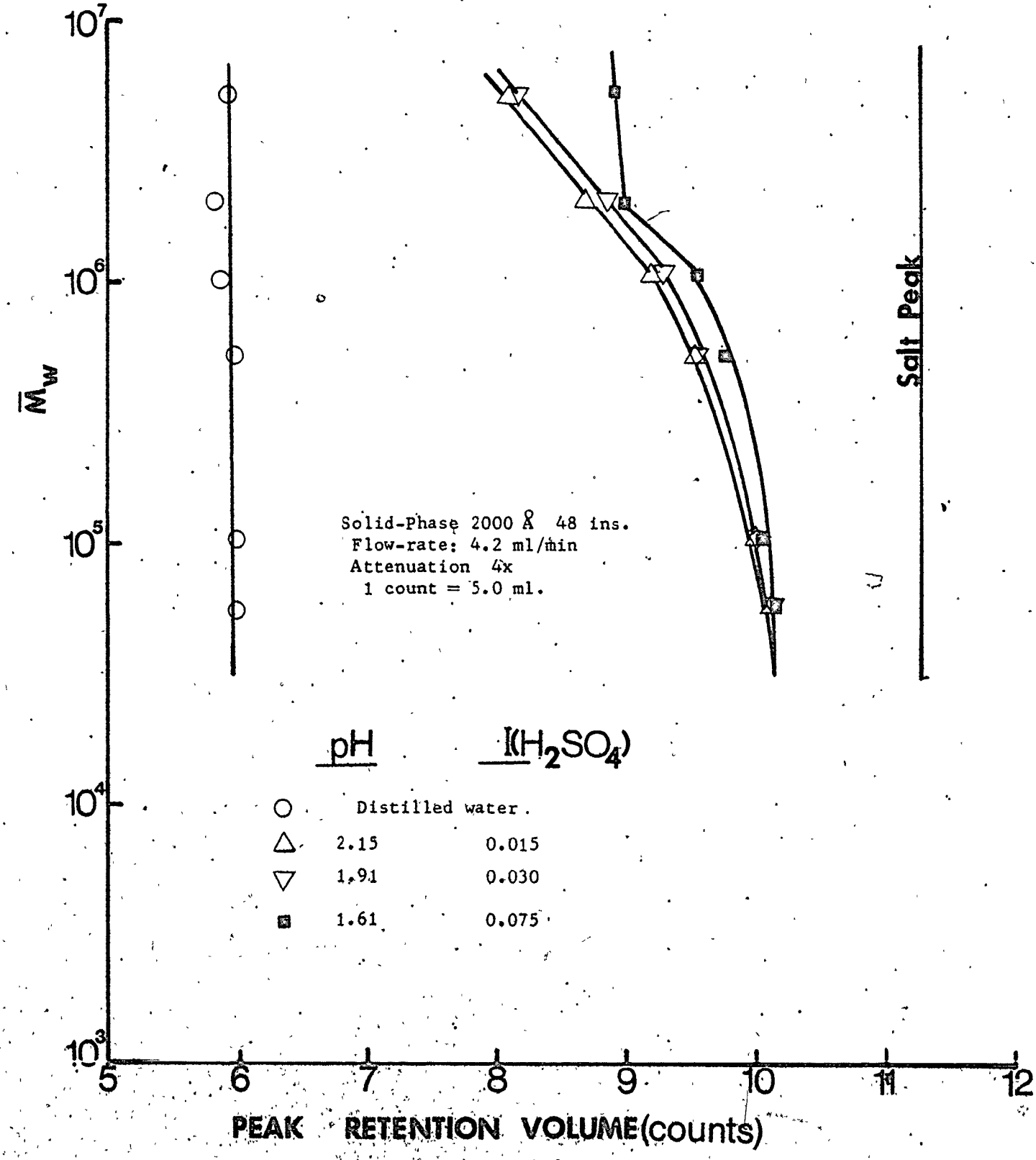

Figure 4-13. Effects of pH on $\bar{M}_w$ calibration curves of NaPSS in the presence of salts

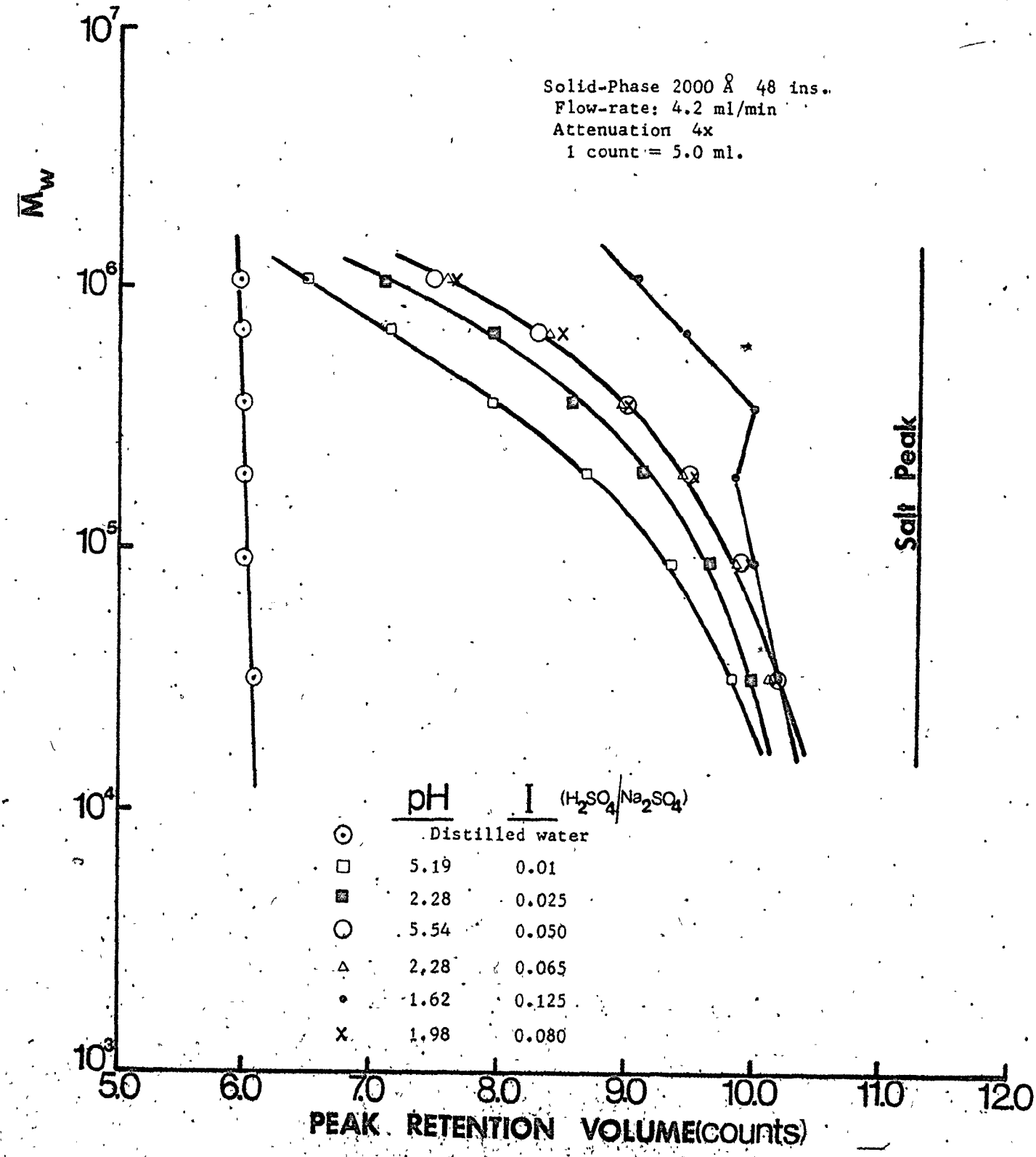

Figure 4-14. Effect of pH alone on the $\bar{M}_w$ calibration curves of NaPSS

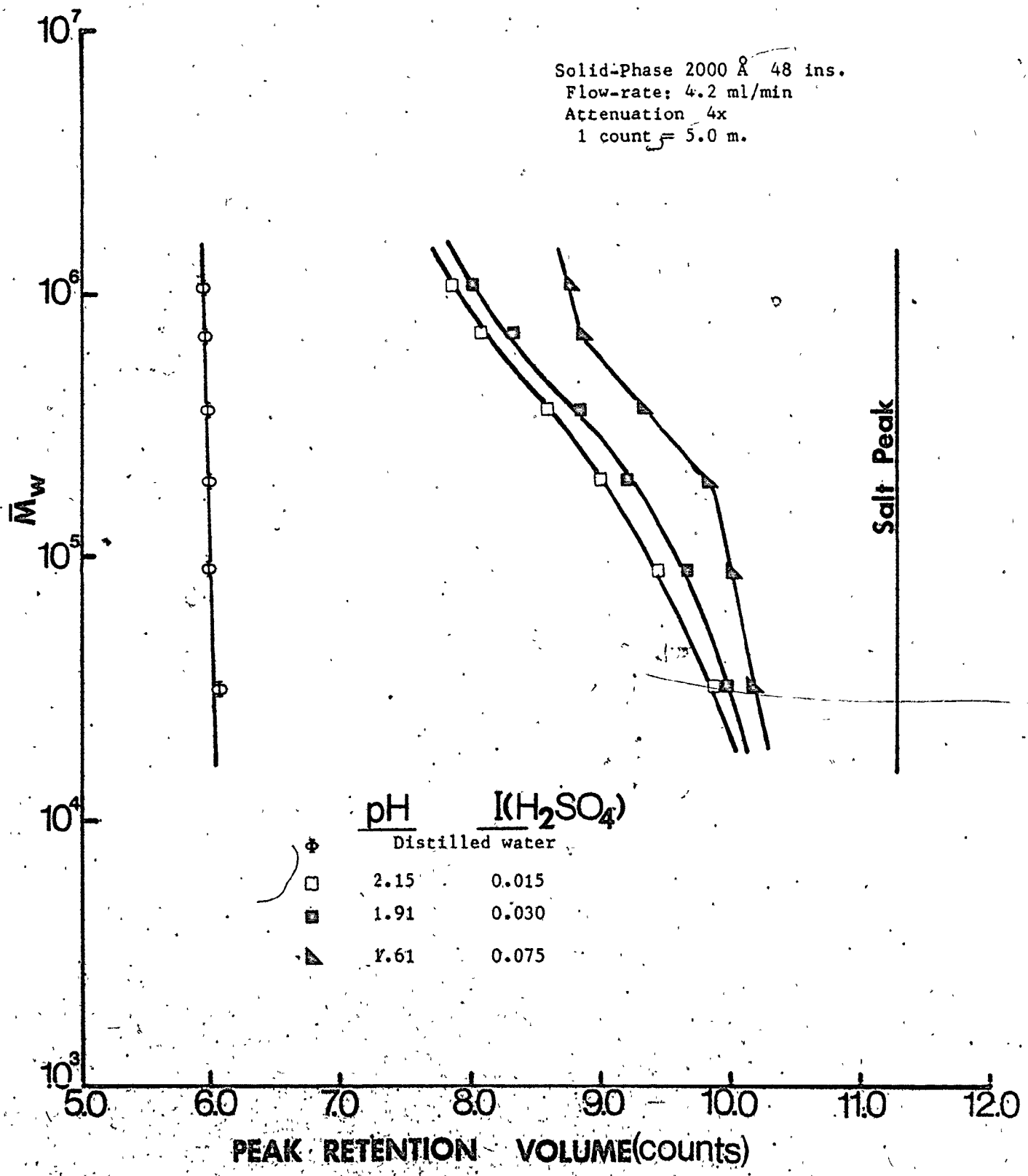

rather than stationary-phases for both polyacrylamide and sodium polystyrene sulfonate was undertaken.

From Figures 4-13 and 4-14 as with other data which have been shown, there is also a gap between the apparent total permeated volume and the total permeated volume as measured with NaCl, which again suggests the bimodal or multimodal nature of the pore size distribution.

4.4. Effect of Neutral Surfactants on SEC Elution Volumes

Apart from the strong adsorption shown by these neutral surfactants, another advantage in their use is that narrower chromatograms are obtained, with distilled water as mobile phase. In the absence of salt or acid, however, ion exclusion could not be completely eliminated.

For most of the experiments reported, Tergitol, at a concentration of less than 50 ppm was used. Even at such a low concentration, the elimination of adsorption effects was evident for both polyacrylamide and sodium polystyrene sulfonates.

(i) Polyacrylamide

Fig. 4-15 shows the effect of Tergitol and polyethylene oxide (PEO MW 300,000), on elution volumes for a 2000 Å 4 ft. column. In the presence of Tergitol at various I and pH similar to those which have been used before, the curves are seen to cluster within a very narrow range of retention volumes. In fact, except at low pH, the MW calibration curves are independent of I.

In the presence of polyethylene oxide, the peak retention volumes or the $\bar{M}_w$ calibration curves shown in Fig. 4-15, are independent of pH and ionic strength (values shown in Table 4-4). Except at low pH, the effect of polyethylene oxide is similar to that of Tergitol. The

Figure 4-15. Effect of neutral sufactants on $\bar{M}_w$ calibration curves of PAM

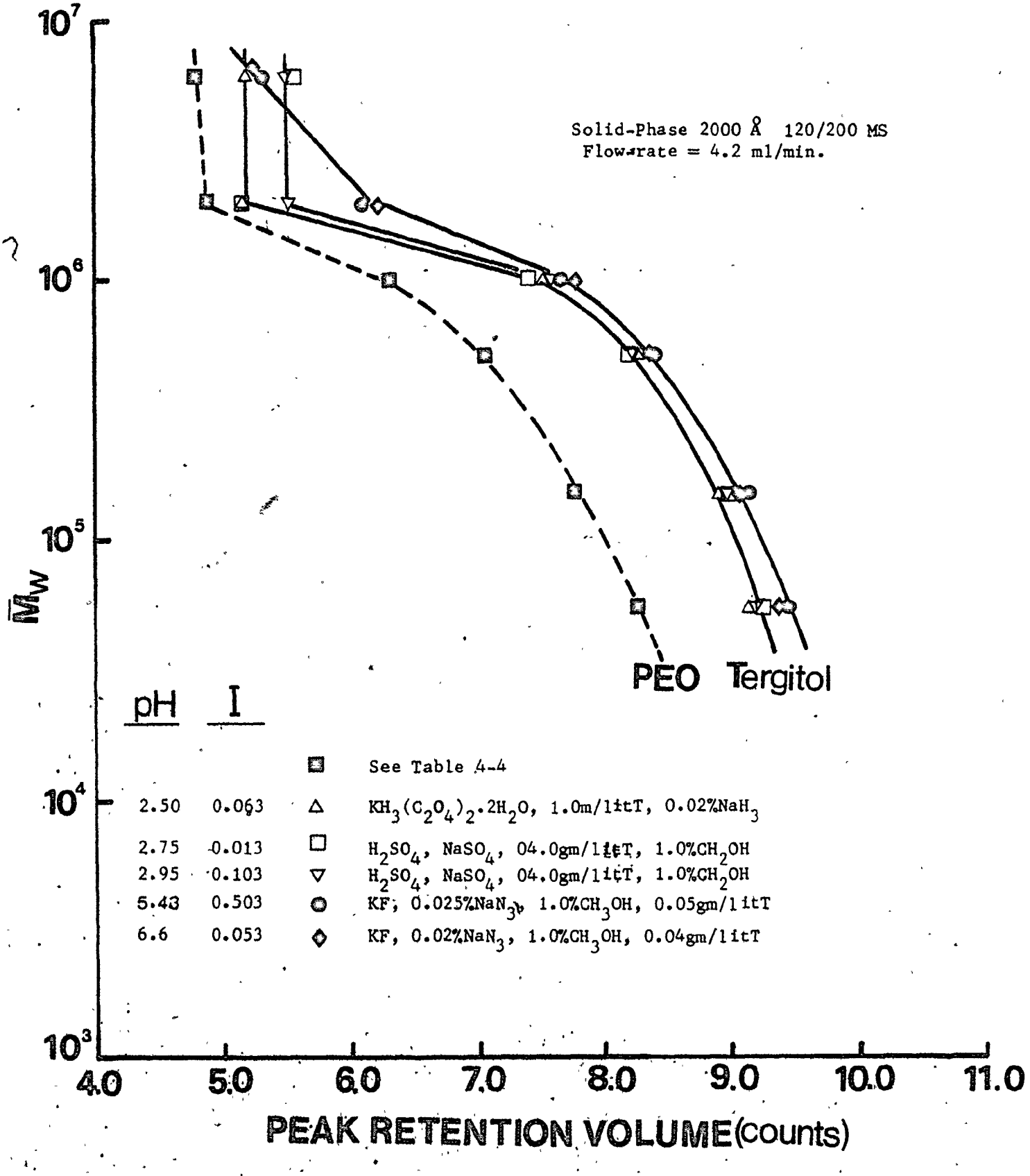

Table 4-4. PRV of polyacrylamide with PEO (300,000 $\bar{M}_w$) in mobile-phase.

Mobile-Phase*	Peak Retention Volumes (PRV) (counts)				
pH=	4.05	7.00	3.50	7.00	3.40
I=	0.025	0.025	0.025	0.250	0.100
Sample					
PAM55	8.30	8.33	8.30	8.32	8.30
PAM270	7.80	7.82	7.80	7.82	7.80
PAM500	7.10	7.13	7.10	7.13	7.10
PAM1000	6.35	6.40	6.35	6.40	6.35
PAM2000	4.90	4.92	4.90	4.91	4.90
Std A	4.80	4.80	4.80	4.80	4.80
ml/count	5.05	5.00	5.05	5.00	5.05

* Mobile-phase contains 0.025 gm/lit PEO (300,000 $\bar{M}_w$)

Pore-size: 2000 Å CPG-10 120/200 Mesh Size

detergents appear to reduce charge effects, with modification of the active sites on the glass surface. With polyethylene oxide, however, the effective pore diameter and volume are reduced. This interpretation is in accord with the fact that the elution volumes are smaller with polyethylene oxide than with Tergitol. This is to be expected since Tergitol is a much smaller molecule than polyethylene oxide.

(ii) Sodium Polystyrene Sulfonate

Fig. 4-16 shows the effect of Tergitol on the elution volumes using the same 2000 Å pore-size column used for polyacrylamide. In the presence of Tergitol at various pH and I, the $\bar{M}_w$ calibration curves are seen to shift in accordance with viscosity data. The unexpected larger dimensions of the coils at I = 0.063 and pH = 2.5 for the oxalate containing mobile phase than at I = 0.053, pH = 6.6 for the KF-containing mobile phase, is in accordance with the pore-permeation in the SEC (Fig. 4-16).

It is important to point out, however, that in the presence of Tergitol or PEO, it was not possible to obtain a response of sodium polystyrene sulfonate at I greater than 0.2, as complete adsorption resulted. Some response was obtained by continued lowering of the pH of the mobile-phase. While adsorption occurred at low pH in the absence of Tergitol or PEO at intermediate I, it was eliminated in the presence of these detergents. Thus, for the analysis of sodium polystyrene sulfonate, while addition of Tergitol or PEO and salt at intermediate I were desirable, it was also important to control pH.

In developing mobile-phase for the difficult polymers, large-pore size single columns were used. For application to smaller pore size packings, the high specific surface areas should be kept in mind (see Table 3-1). The extremely high surface-to-volume ratios can accentuate even minimal adsorption effects.

Figure 4-16. Effect of neutral surfactant on $\bar{M}_W$ calibration curves of NaPSS

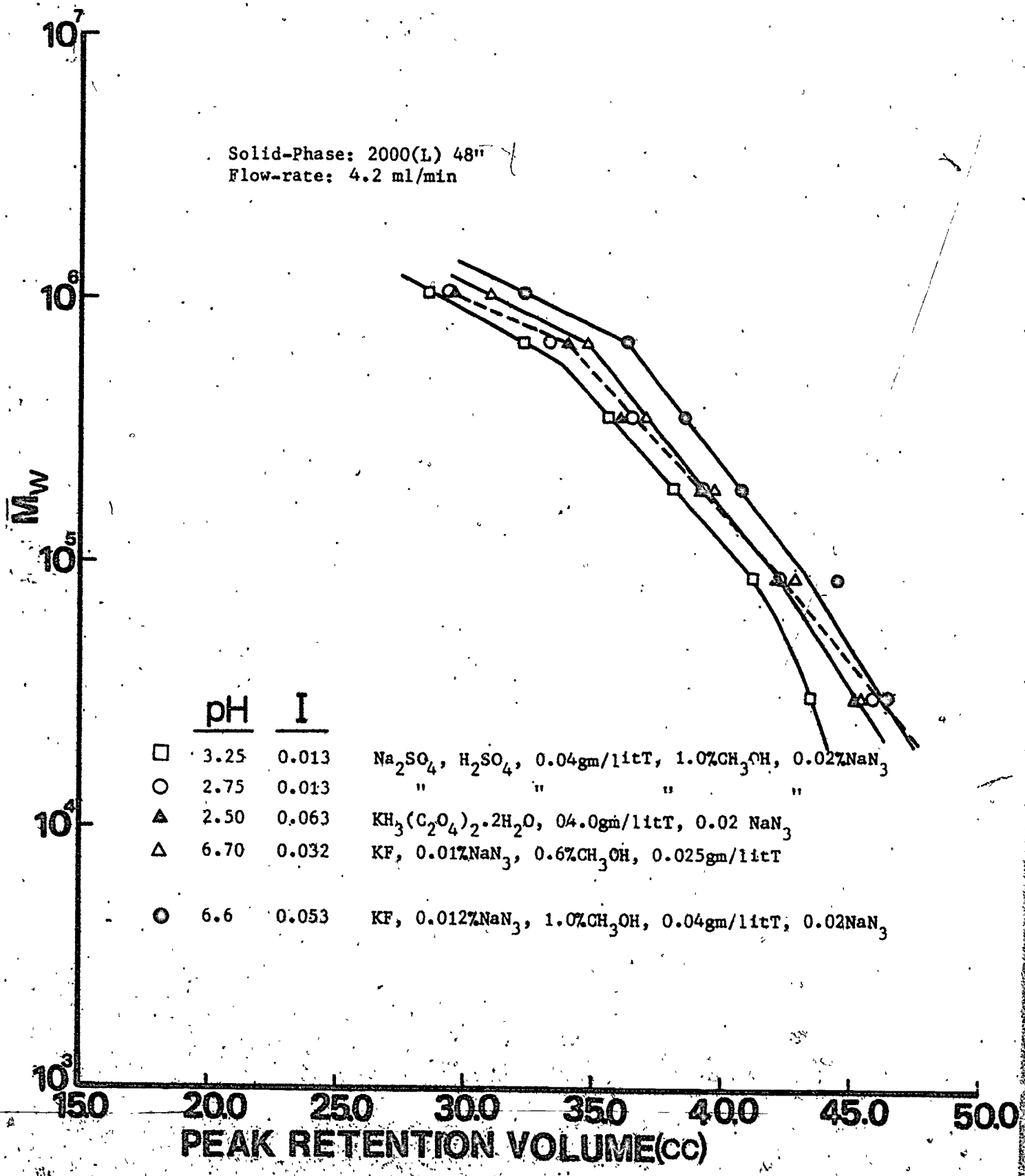

4.5. Reproducibility of the SEC Behaviour for Small and Intermediate Pore-Size Dry-Packed Columns

Fig. 4-17 shows $\bar{M}_w$ calibration curves of polyacrylamide at various pH and ionic strength on a 370/327 Å pore-size 4 ft column, all in the presence of Tergitol. For polyacrylamide, in the presence of Tergitol, as indicated above the use of low pH is not desirable. As shown in figure 4-17 the effect is largely magnified with small pore-sizes. Fig. 4-18 shows $\bar{M}_w$ calibration curves for a 500/700 Å 200/400 Mesh Size, 4 ft column, both in the absence and presence of varying amounts of Tergitol. From this figure, it is obvious that there is no dependence on Tergitol concentration in the range studied. However, low pH is not desirable as there is more pore permeation than desired. The anamalous behaviour of Std C is shown in Fig. 4-19 for a 1000 Å 200/400 Mesh Size column. The lack of dependence of the calibration curve of polyacrylamide on I at neutral pH conditions is also shown.

Fig. 4-20 is a corresponding plot for sodium polystyrene sulfonate for small/intermediate pore-size 700/500/370 Å single pore-size column. The relative positions of these curves are in agreement with intrinsic viscosity data.

4.6. Effect of PEO on the Effective Pore Volume of Packing Materials

When PEO is added to the mobile-phase, the pore volume is reduced, to an extent which depends on the PEO concentration. The extent of reduction of pore volume or diameter is very important as this could diminish the usefulness of the packing materials with respect to molecular weight separation range. With Tergitol there is no reduction in pore volume or diameter, and it is therefore the material of choice.

Figure 4-17. Surface-area effect on $\bar{M}_w$ calibration curves of PAM

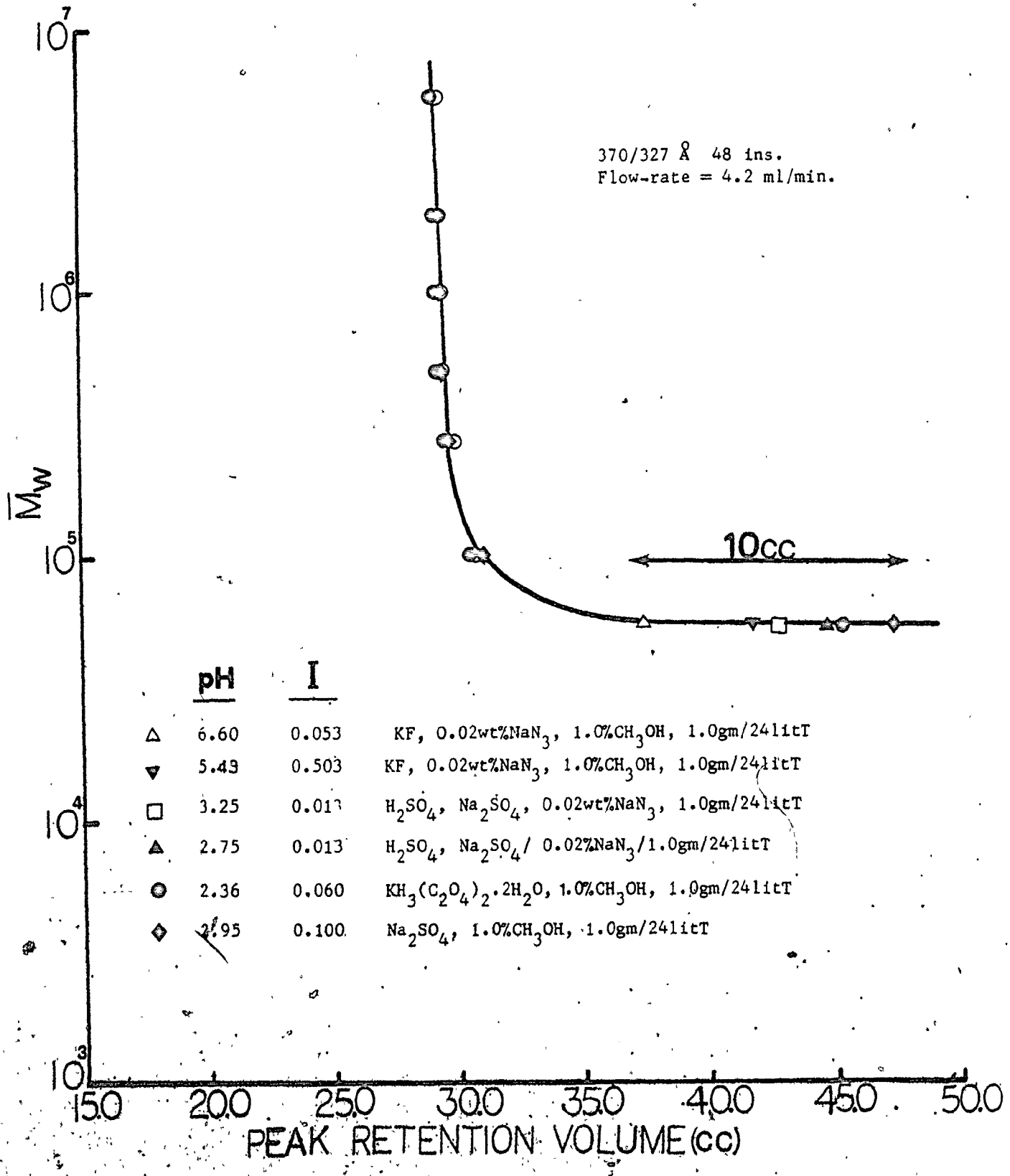

Figure 4-18. Effect of different amounts of Tergitol and pH on $\bar{M}_w$ calibration curves of PAM

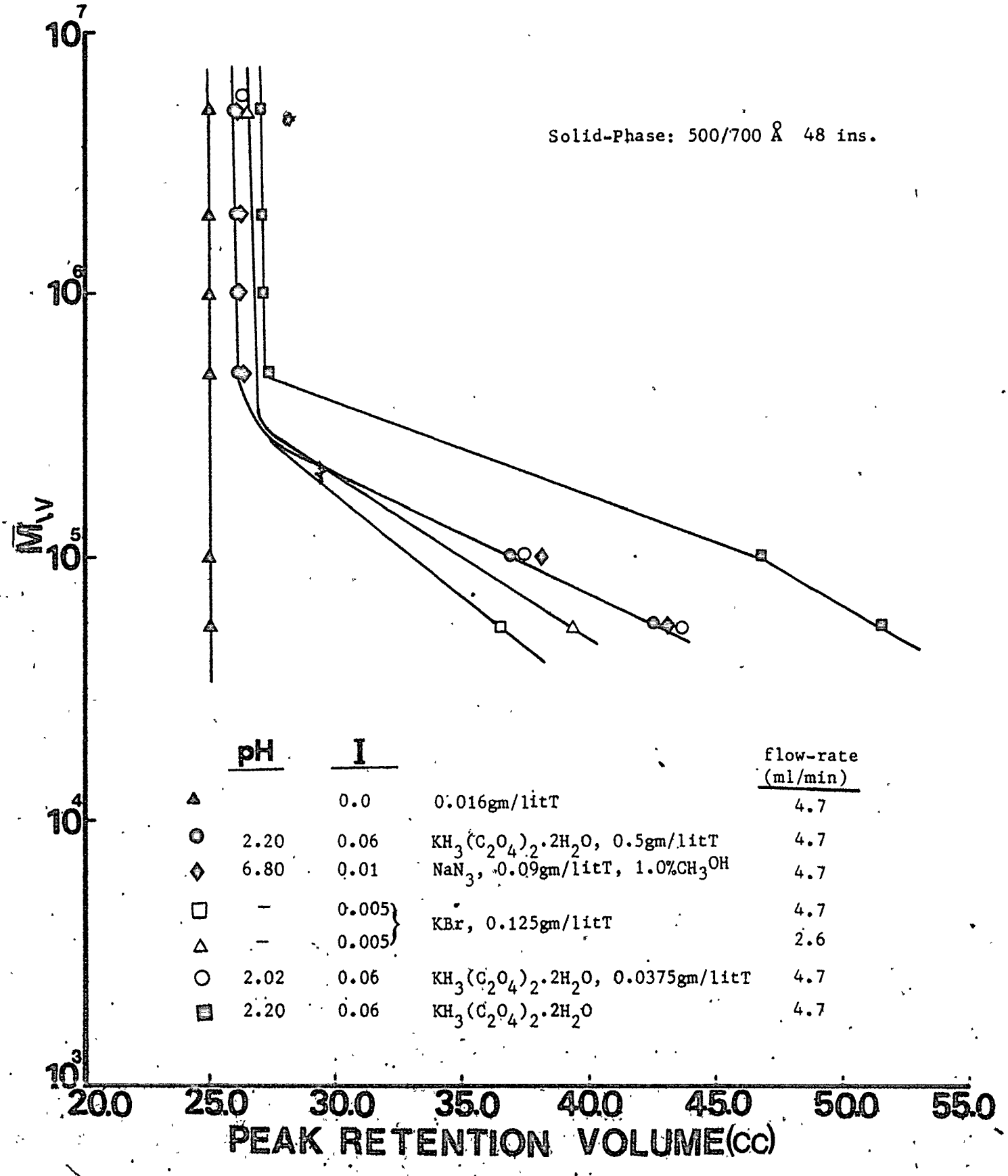

Figure 4-19. Effect of neutral surfactant on $\bar{M}_w$ calibration curves of PAM

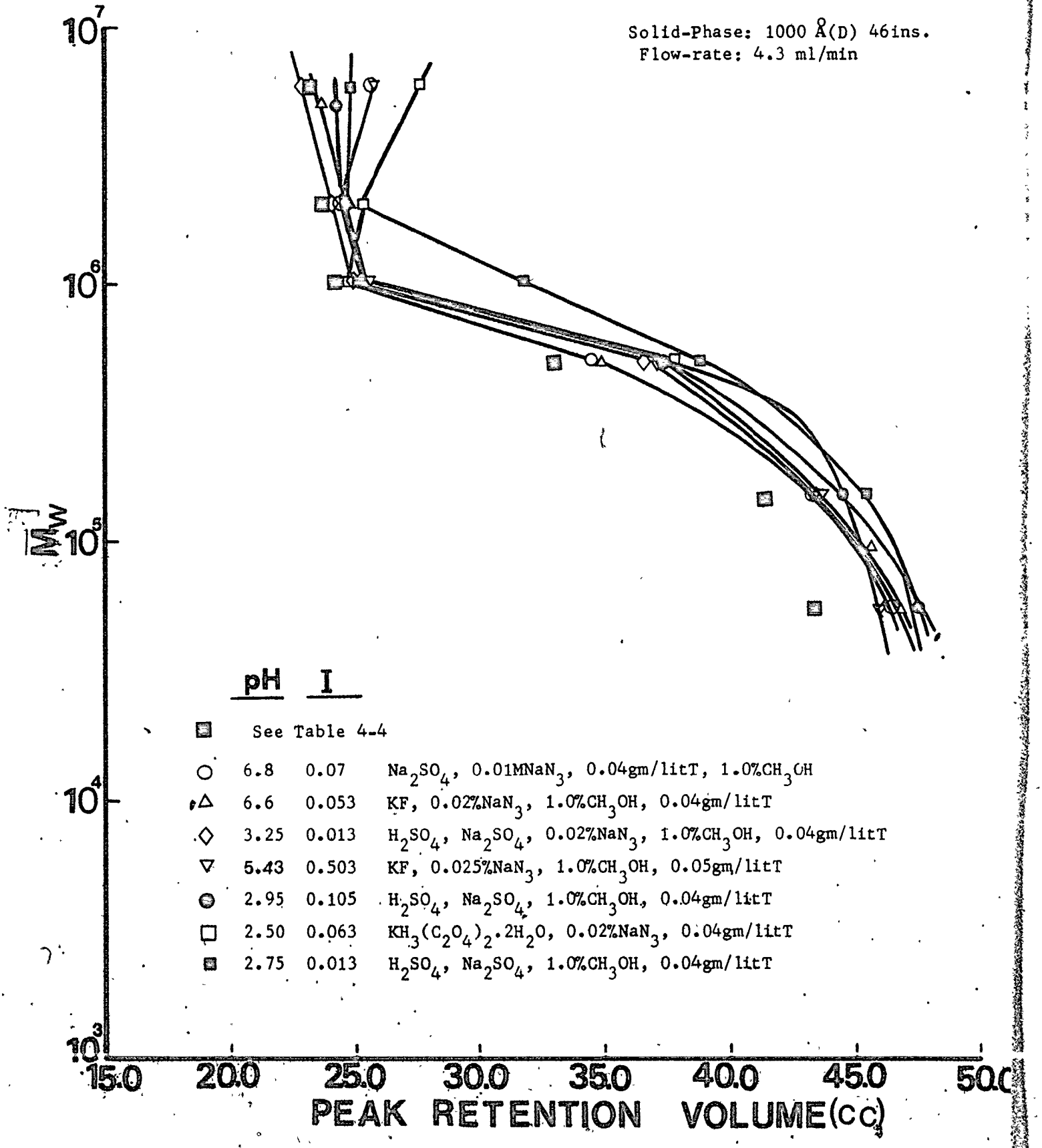

Figure 4-20. Effect of neutral surfactant on $\bar{M}_w$ calibration curves of NaPSS

pH	I		
4.75	0.013	▽	Na_2SO_4, 0.02%NaN_3, 1.0%CH_3OH, 0.04gm/litT, H_2SO_4
3.25	0.013	△	Na_2SO_4, 0.02%NaN_3, 1.0%CH_3OH, 0.04gm/litT, H_2SO_4
2.38	0.063	○	$KH_3(C_2O_4)_2 \cdot 2H_2O$, 0.02wt%$NaN_3$, 1.0%$CH_3OH$, 0.04gm/litT
2.50	0.063	▼	$KH_3(C_2O_4)_2 \cdot 2H_2O$, 0.02wt%$NaN_3$, 0.04gm/litT
6.80	0.032	◆	KF, 0.012%NaN_3, 0.6%CH_3OH, 0.025gm/litT
6.6	0.050	□	KF, 1.0%CH_3OH, 0.04gm/litT
6.6	0.053	●	KF, 0.02%NaN_3, 1.0%CH_3OH, 0.04gm/litT

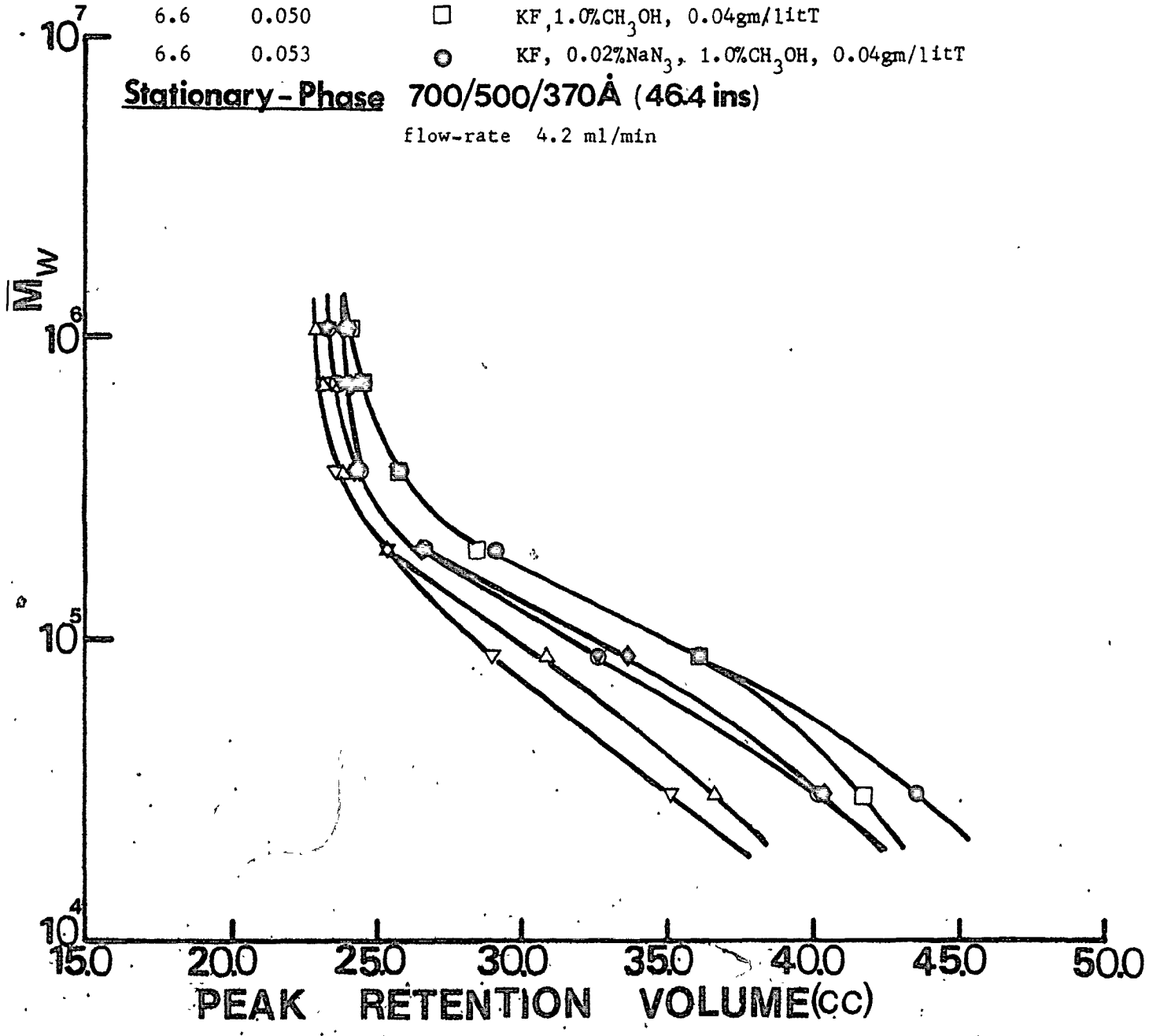

Since the effect of I or pH in the absence of Tergitol or PEO on the MW calibration curves of dextran is quite unlike polyacrylamide and sodium polystyrene sulfonate, $\bar{M}_w$ calibration curves for dextran were obtained for conditions where Tergitol (0.08 gm/l), PEO (0.5 gm/l), and salt alone (0.05 M NaCl) were used as additives. The amount of Tergitol used here was the maximum possible for the 3000 Å pore-size column. At higher concentrations of Tergitol, for packing materials with pore-size greater than 1000 Å, it was difficult to maintain a stable base-line. The only explanation that can be offered for this behaviour was the availability of more volume within the pores for formation of micro bubbles. However, as shown in Fig. 4-21, the addition of polyethylene oxide is seen to effectively reduce the pore-size and volume. One cannot rule out the possibility that the 300,000 $\bar{M}_w$ PEO is too large for preferential adsorption purposes. In a more recent investigation, the effect of MW of PEO grafted on silica based packing material for SEC, was reported (56). Although the investigation was incomplete, intermediate MW (20,000) were found to be most suited for grafting on the silica.

4.7. Methodology and Role of Column Combination Development

The discussion thus far has dealt with composition of mobile-phase and its effects on deviations from ideal SEC behaviour, for individual polymers investigated, and data for a single column and single pore size were presented in order to simplify interpretation of these effects. Working with single columns, ion-inclusion of salt is highly magnified, whereas this is not the case with column combinations. Also, with single columns, polymer-surface interactions may be visible and sometimes not detected, whereas with 3 or more columns combined in series, the phenomenon

Figure 4-21. Effect of PEO and Tergitol on the effective pore volume of packing materials

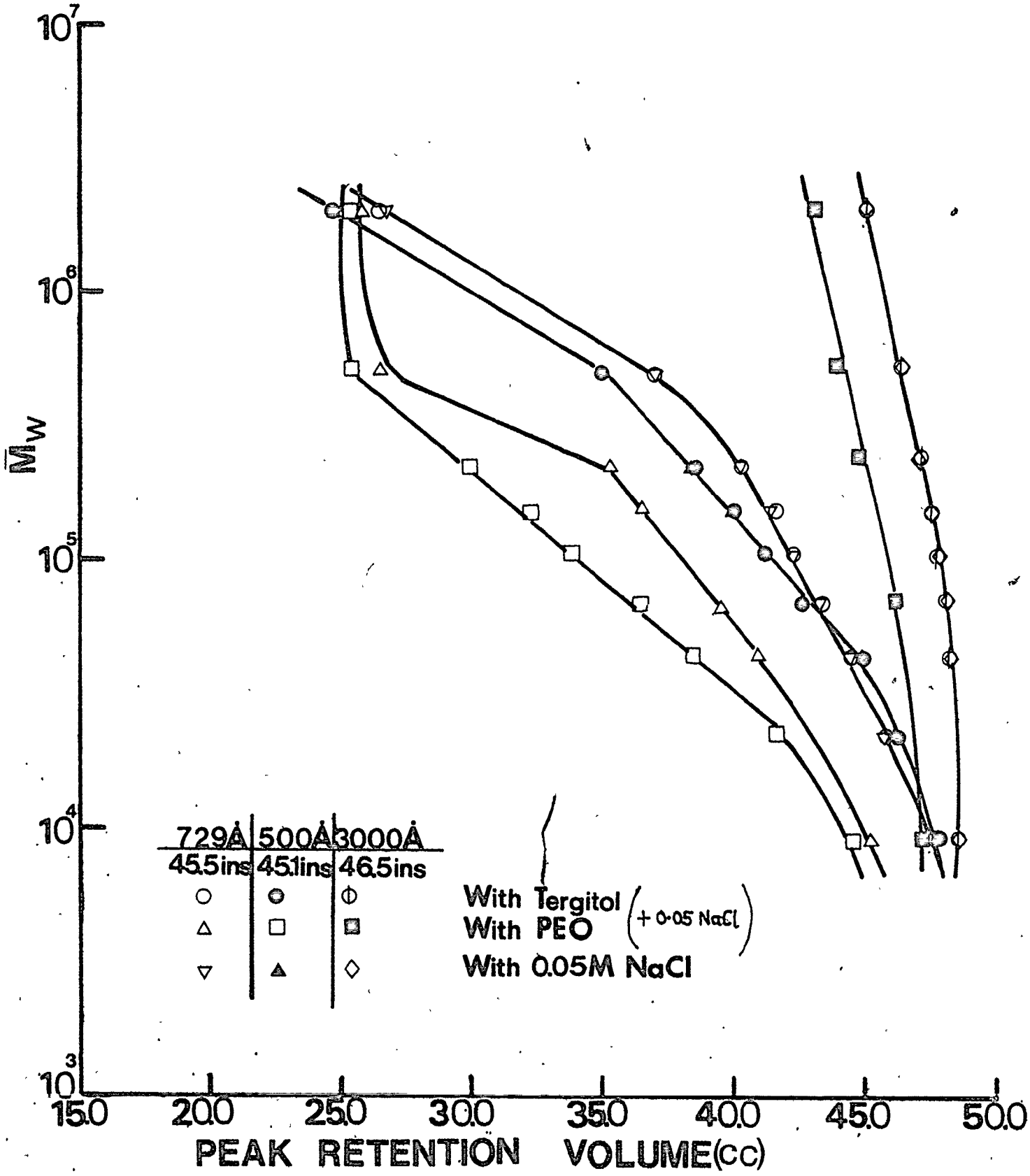

is highly magnified.

Clearly if a useful calibration curve is to be obtained over a wide range of MW, it is necessary to use a multi-column system with a range of pore sizes corresponding to the molecular weight range of interest.

(i) Polyacrylamide

As was pointed out in Section 4.5, surface-areas of packing materials is of considerable importance in studies involving aqueous SEC. Arranging columns in the traditional order could lead to stronger polymer surface interactions, than reversed flow arrangement, even when the mobile-phase has been properly selected.

Data relevant to the question of multi-column system for CPG-10/polyacrylamide are shown in Fig. 4-22 which represents calibration curves on single columns of different pore-sizes. The mobile-phase is an aqueous solution of 0.02 M Na_2SO_4 containing 0.02 gm/l Tergitol, alcohol and sodium azide preservative at pH of 6.65. Under these conditions charge and adsorption effects should be minimal. However, as shown in Fig. 4-23 for a set of 3 columns combined in series and pore-sizes selected, calibration R is about what one would expect. The loss in peak separation of about 2.35 counts (ie 11.75 cc) can be due to nothing other than the difference in polymer/surface area distribution in operation during the process of SEC in both methods of column arrangements. When the mobile-phase has not been properly selected, the effect is very strong as shown in Fig. 4-24 for six columns, with two different mobile-phases. At low pH, presence of reversible adsorption or polymer surface interaction is clearly apparent.

As shown in Fig. 4-22, the 120 Å mostly filled pore size column, provides little or no separation. The effect of including such a passive column into a system of column combinations is shown in Fig. 4-25, which

Figure 4-22. $\bar{M}_w$ range of separation of different pore-sizes for PAM

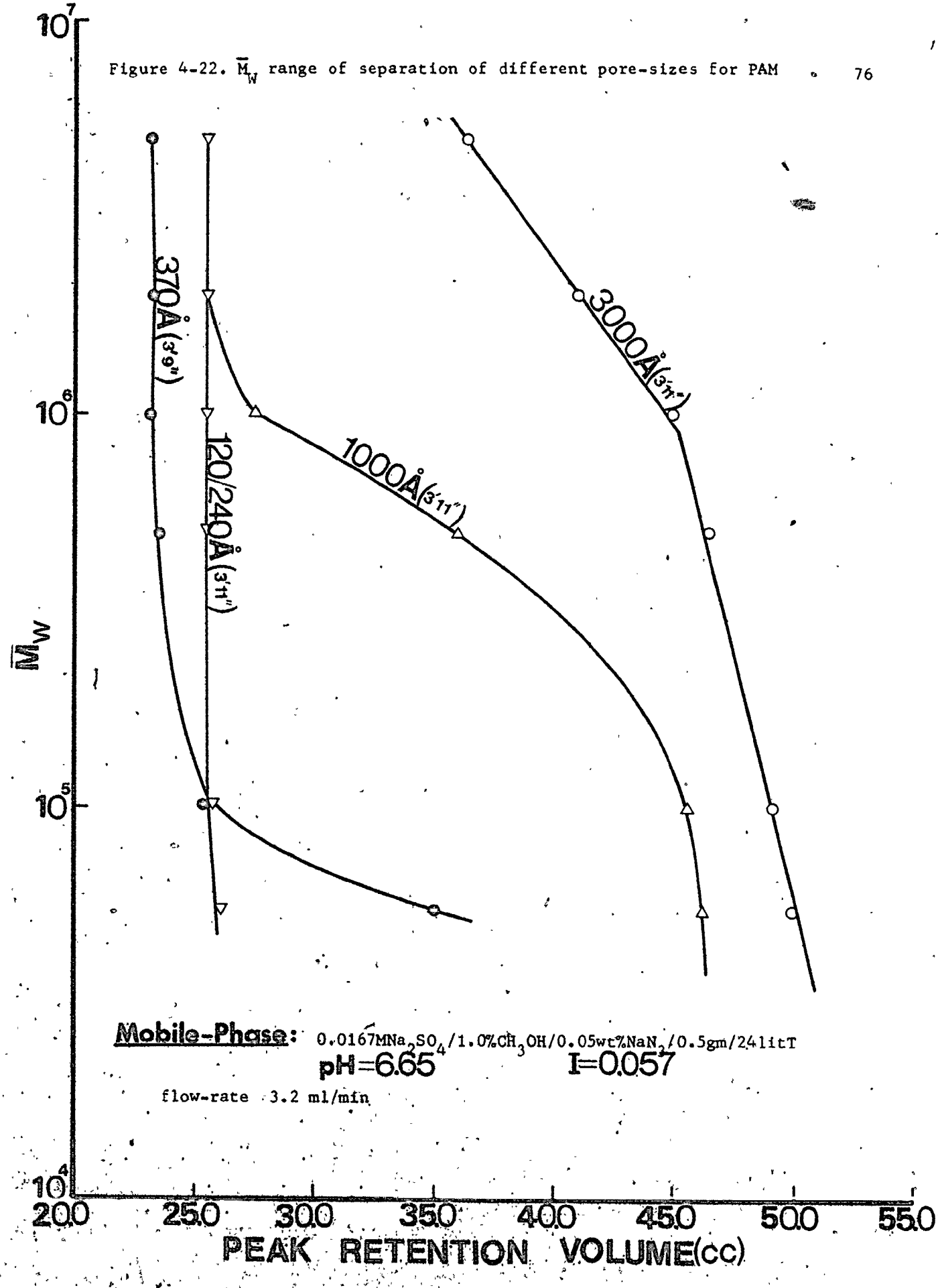

Figure 4-23. Effect of order of column arrangement on $\bar{M}_w$ calibration curves of PAM

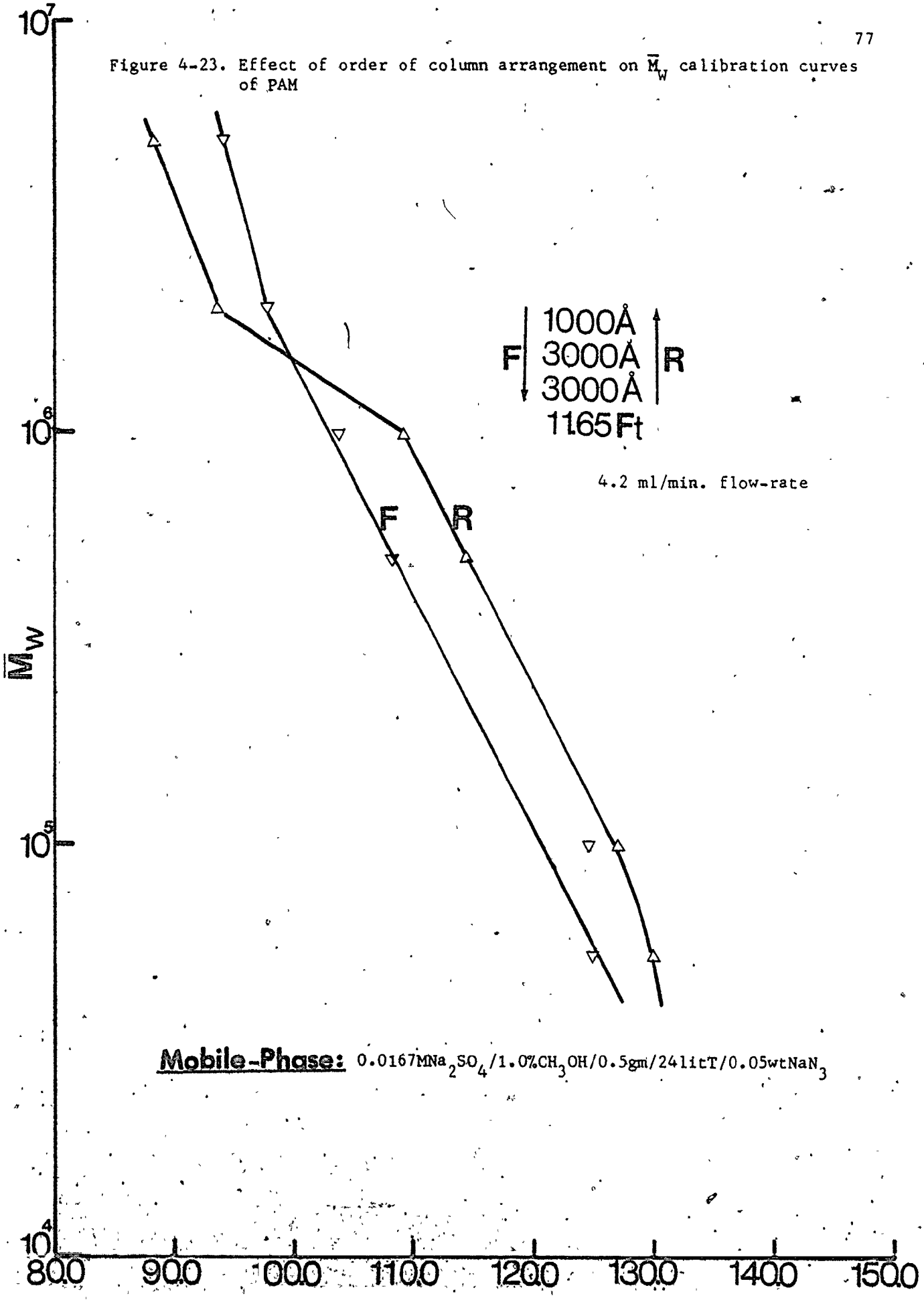

Figure 4-24. Effect of poorly selected mobile-phase and order of column arrangement on $\bar{M}_w$ calibration curve of PAM for a six column combination

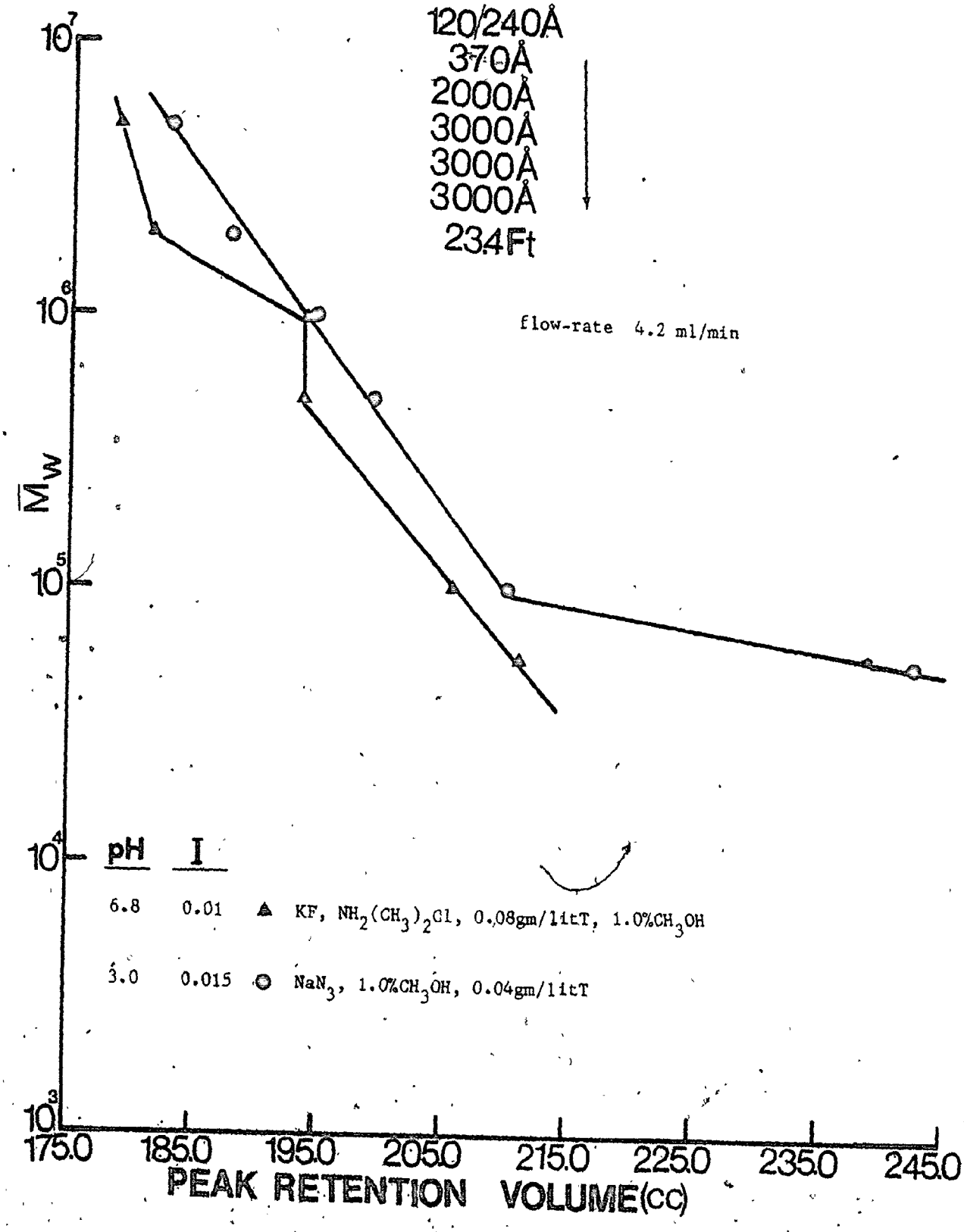

Figure 4-25. Effect of undesirable small pore-size column on peak separation of PAM (see Table 4-5 for description of systems)

Mobile-Phase: 0.0167MNa_2SO_4/1.0%CH_3OH/0.05wt%NaN_3/0.5gm/24litT
flow-rate: 3.2 ml/min pH=6.65
1 count = 5.2cc

Case Study # 31

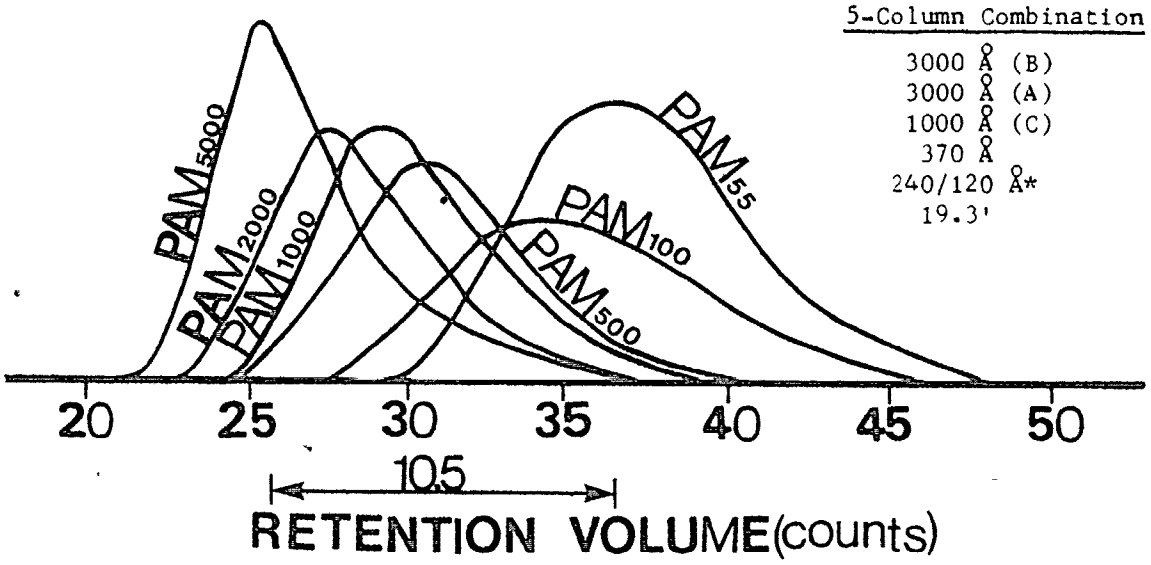

Case Study # 26

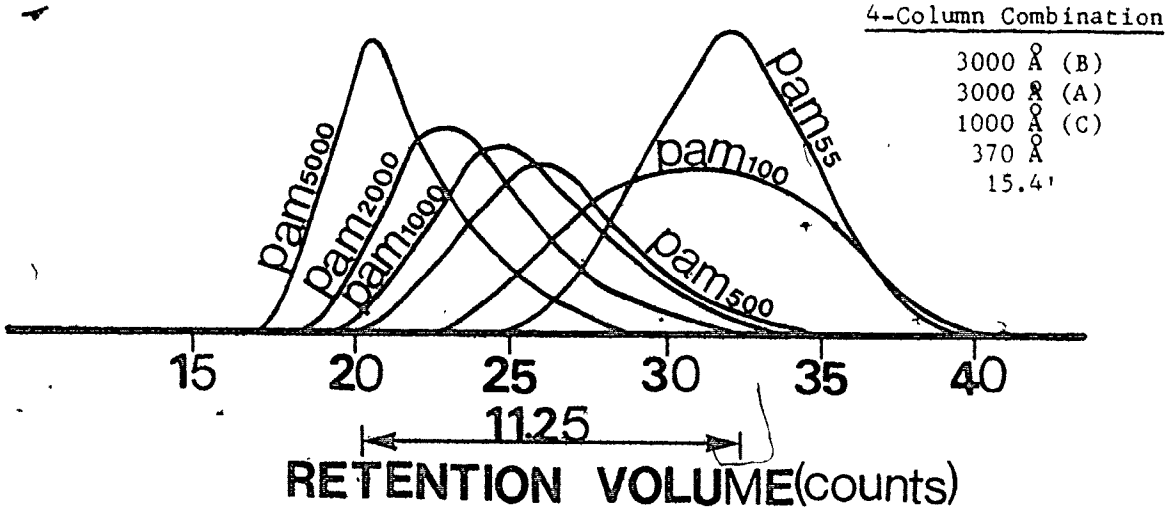

contains chromatograms of polyacrylamide for four and five column-combinations under the same operation conditions. There is a loss in peak separation of about 4.0 cc.

Finally, using the optimum selected mobile-phases, ten systems shown in Table 4-5 were chosen for calibration of polyacrylamide. These systems were finally chosen to illustrate the variables pertinant to maximum peak separation and minimum peak broadening. Figs. 4-26 to 28 contain their corresponding $\bar{M}_W$ calibration curves. Using linear least square regression and non-linear regression analysis where applicable, their $\bar{M}_W$ calibration constants were obtained. These were applied to the chromatograms to obtain $\bar{M}_W$ and $\bar{M}_n$. These values are listed in Table 4-6. From the measured polydispersities, it is obvious that these systems are quite adequate, covering a wide range of molecular weights ($5x10^5$ to $4.0x10^6$). In almost all cases, P100 and P270, are seen to have the broadest MWD. However from the measured MWs, it is obvious that:

(i) a true molecular weight calibration curve is very important as will be shown with application to well characterised dextrans (ie $\bar{M}_W$ and $\bar{M}_n$ known)

(ii) the peak broadening correction or instrumental spreading correction is very important especially when the true molecular weight calibration curve is not known (as will be shown with application to well characterised dextrans using both the ELC and TBS methods of calibration).

The width of each chromatogram for the different systems or cases studied are listed in Table 4-7. Data in this important Table will be compared with data for other polymers and their corresponding slopes (D2) to provide relative or qualitative measures of molecular weight

Table 4-5. Description of column combination characteristics for polyacrylamide studies

Case Study #	Column Combination	Code No.	Mobile-phase	Flow-rate (ml/min)
26	3000Å(B), 3000Å(A), 1000Å (C), 370Å 15.4 ft.	S4DR	0.0167MNa_2SO_4/ 1.0% CH_3OH/0.05 wt% NaN_3/0.5gm/ 24lit T. pH=6.65, I=0.056	3.20 (0.025wt%)
27	3000A(D), 3000Å(E), 2000Å (B), 1000Å(D), 700Å(A), 370Å(B), 240/120Å(B) 20.95 ft.	S7AR	0.02MNa_2SO_4/0.01 MNaN_3/1.0% CH_3OH/ 1.0gm/24lit T pH=5.0 (H_2SO_4)	4.20 (0.050wt%)
28	3000Å(D), 3000 (E), 2000Å (B), 1000Å(D), 500/370Å(B) 19.25 ft.	S5HR	0.05MKF/0.02wt% NaN_3/1.0% CH_3OH/ 1.0 gm/24lit T. pH=6.6, I=0.053	4.70 (0.0375wt%)
29	3000Å(E), 3000Å(D), 1000Å (D), 500/370 (C) 14.2 ft.	S4ER	same as in 28	4.2 (0.0375wt%)
30	3000Å(E), 3000Å(D), 1000Å (D), 700/500/370Å, 370/ 327Å 19.6 ft.	S5IR	same as in 28	4.2 (0.025wt%0
31	3000Å(B), 3000Å(A), 1000Å (C), 370Å, 240/120Å 19.3 ft.	S5IR	same as in 26	3.20 (0.0375wt%)
32	3000Å(E), 3000Å(D), 1000Å (D), 700/500/370Å 15.5 ft.	S4FR	same as in 28	4.2 (0.025wt%)
33	3000Å(D), 3000Å(E), 2000Å (L), 1000Å(D), 729Å 19.0 ft.	S5KR1	0.00833MNa_2SO_4/ 1.5gm/24litT./0.25 gm/l PEO/2.5% CH_3OH, pH=7.0	2.50 (0.05wt%)
34	Same as in 33	S5KR2	0.0833MNa_2SO_4/ 1.5gm/24litT./0.25 gm/l PEO/2.5% CH_3OH pH=7.0	2.50 (0.05wt%)
35	Same as in 33	S5KR3	same as in 35, except pH=3.5	2.50 (0.05wt%)

Figure 4-26. $\bar{M}_w$ calibration curves of PAM for Case Studies #27, 28 and 30

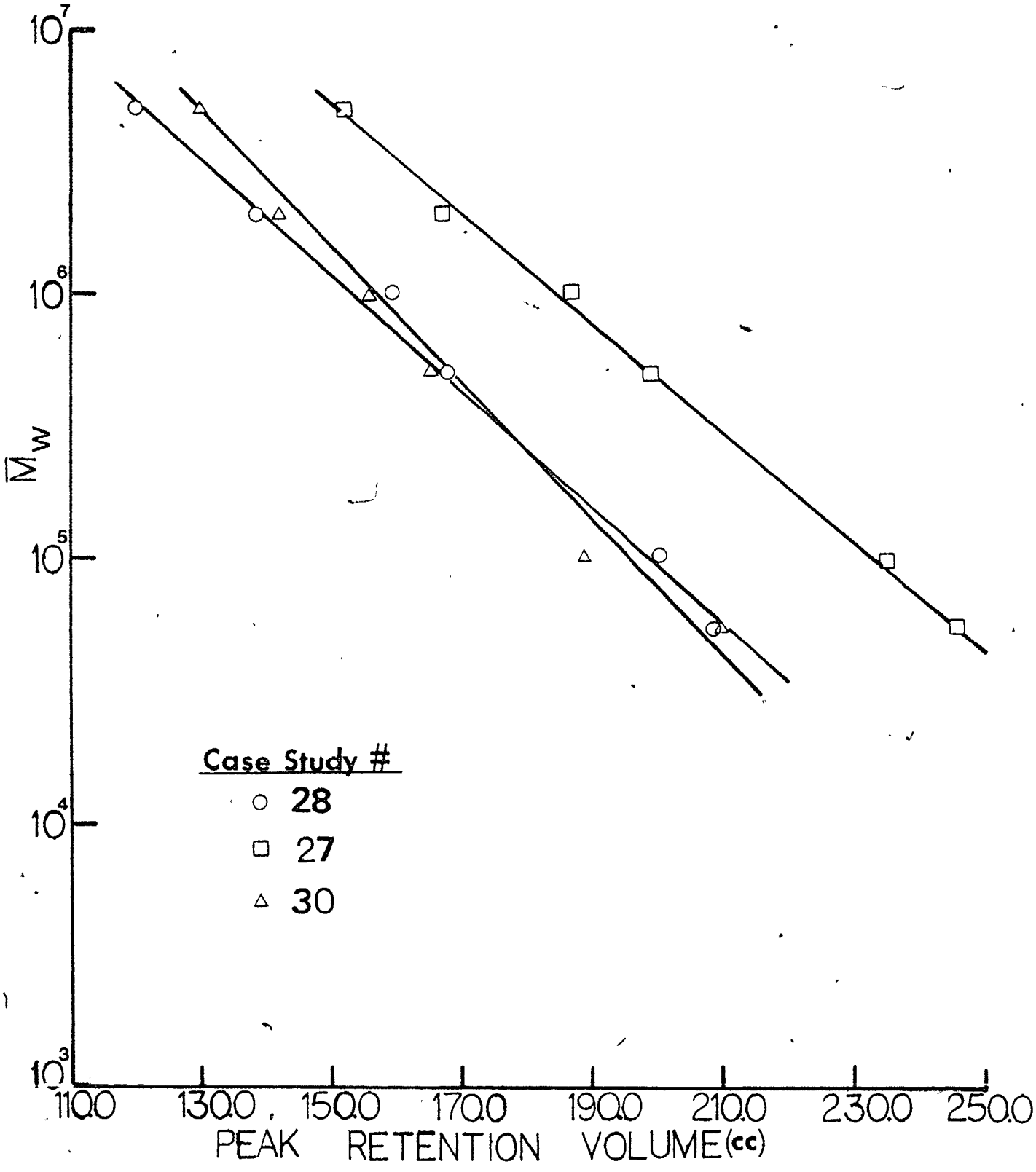

Figure 4-27. $\bar{M}_w$ calibration curves of PAM for Case-Studies #26, 29, 31 and 32.

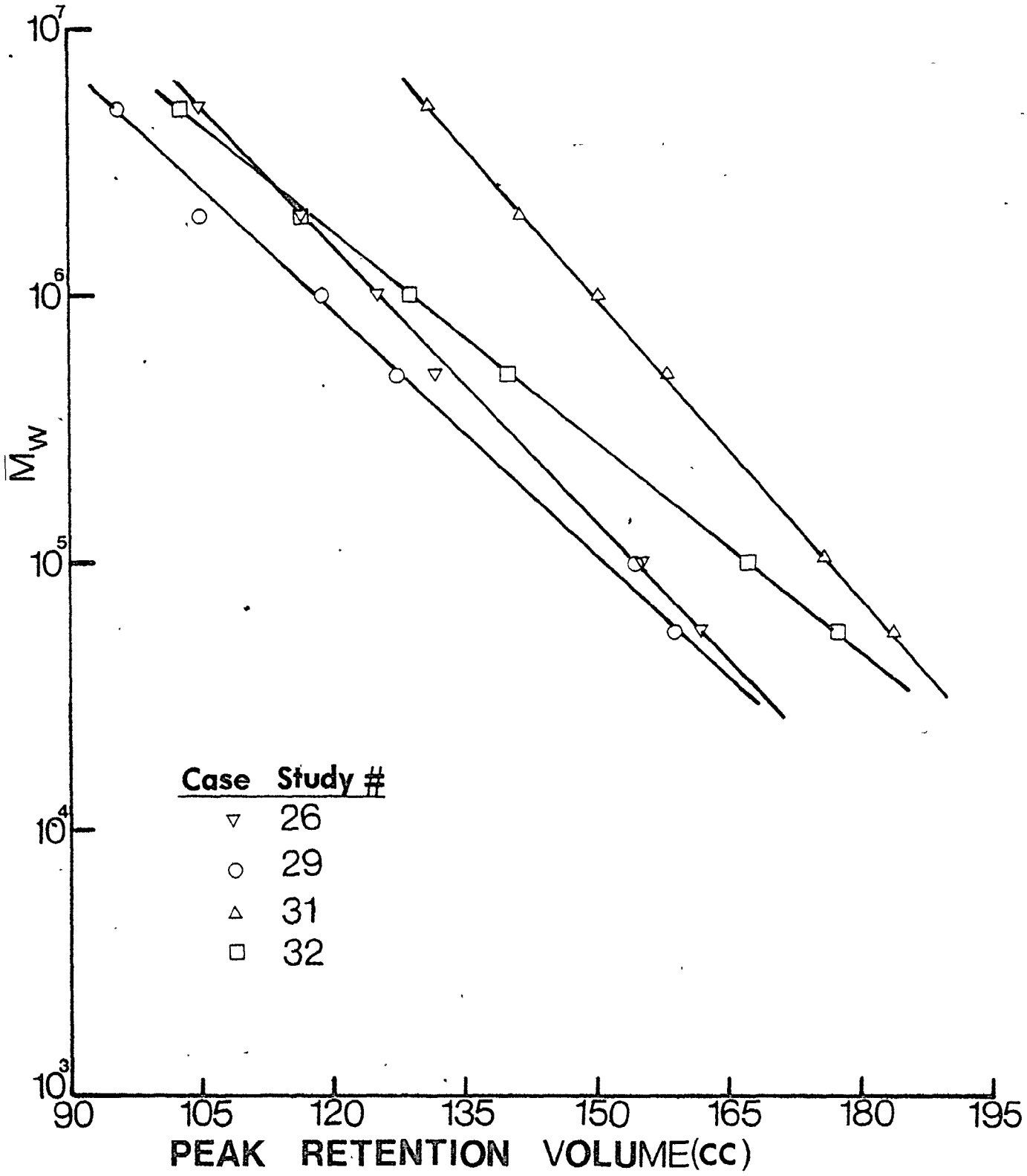

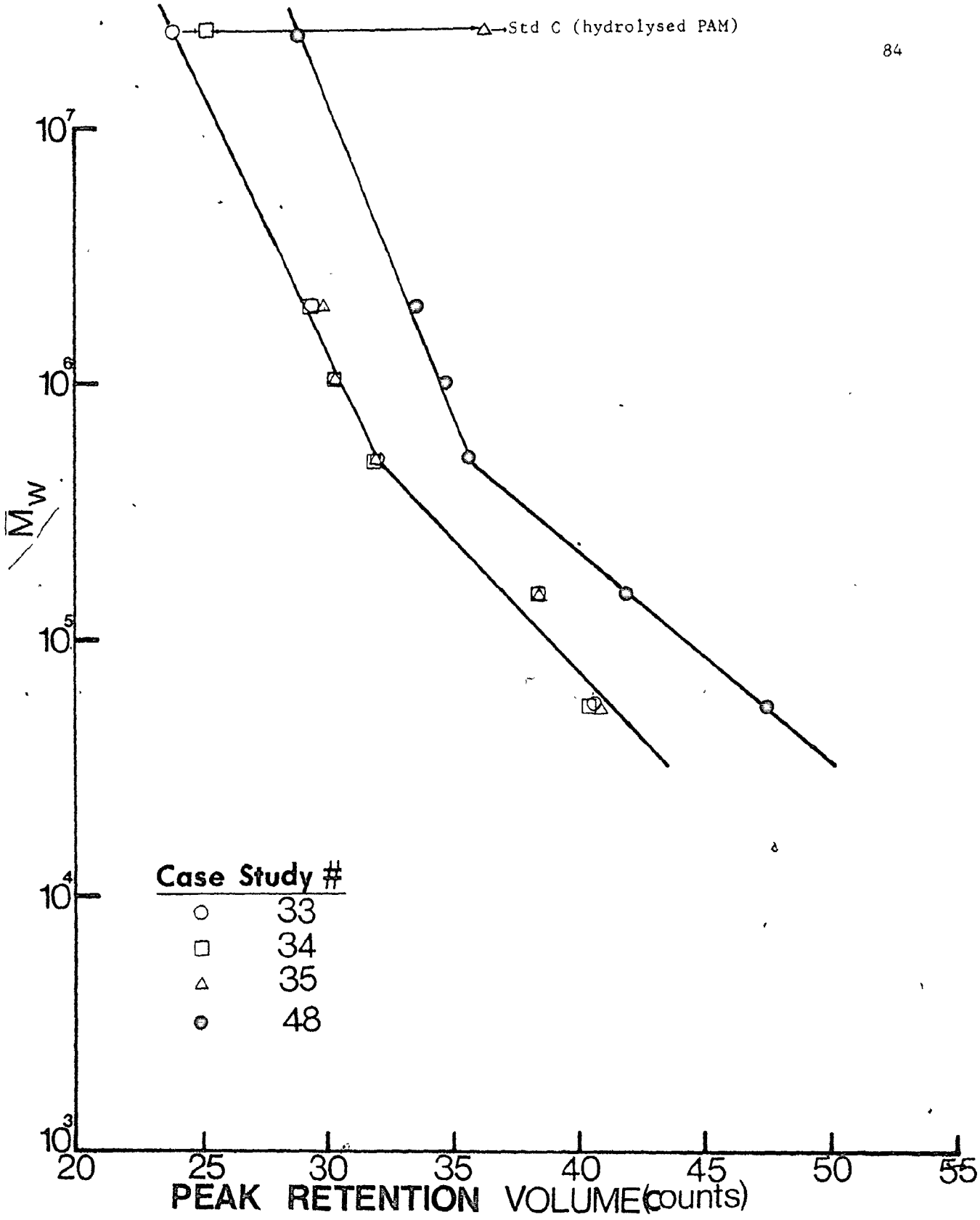

Figure 4-28. $\bar{M}_w$ calibration curves of PAM for Case-Studies #33, 34, 35 and 48

Table 4-6. Measured GPC $\bar{M}_W$, $\bar{M}_N$ values of case-studies for PAM

Case Study M(V)=	[26] $0.141\times10^{11}EXP(-0.390V)$			[27] $0.431\times10^{10}EXP(-0.247V)$			[28] $0.234\times10^{10}EXP(-0.272V)$			[29] $0.292\times10^{10}EXP(-0.358V)$		
Sample	$\bar{M}_W\times10^{-3}$	$\bar{M}_n\times10^{-3}$	P(t)	$\bar{M}_W\times10^{-3}$	$\bar{M}_n\times10^{-3}$	P(t)	$\bar{M}_W\times10^{-3}$	$\bar{M}_n\times10^{-3}$	P(t)	$\bar{M}_W\times10^{-3}$	$\bar{M}_n\times10^{-3}$	P(t)
PAM55	92.00	33.00	2.741	76.00	43.00	1.757	92.00	60.00	1.542	86.00	51.00	1.6900
PAM100	191.00	36.00	5.324	172.00	59.00	2.915	189.00	76.00	2.498	186.00	69.00	2.691
PAM270	--	--	--	184.00	58.00	3.193	206.00	82.00	2.522	196.00	73.00	2.677
PAM500	798.00	316.00	2.528	729.00	298.00	2.449	666.00	324.00	2.058	666.00	298.00	2.236
PAM1000	1016.00	392.00	2.590	897.00	340.00	2.638	874.00	358.00	2.445	930.00	396.00	2.350
PAM2000	2073.00	1064.00	1.948	1798.00	828.00	2.171	1848	820.00	2.254	1917.00	789.00	2.429
PAM5000	3869.00	1977.00	1.957	3214.00	2420.00	1.329	--	--	--	2769.00	1203.00	2.301
M(V)=	[30] $0.732\times10^{10}EXP(-0.310V)$			[31] $0.370\times10^{12}EXP(-0.436V)$			[32] $0.224\times10^{10}EXP(-0.324V)$			[33] $0.200\times10^{11}EXP(-0.341V-0.006V^2)$		
PAM55	74.00	36.00	2.066	73.00	11.00	6.926	81.00	53.00	1.527	76.4	40.7	1.877
PAM100	214.00	45.00	4.735	233.00	32.00	7.305	188.00	72.00	2.607	--	--	--
PAM270	--	--	--	--	--	--	197.00	75.00	2.621	--	--	--
PAM500	--	--	--	929.00	239.00	3.893	618.00	223.00	2.777	761.0	302.0	2.520
PAM1000	932.00	376.00	2.479	1197.00	299.00	4.007	912.00	373.00	2.447	958.0	416.0	2.303
PAM2000	1782.00	840.00	2.121	2416.00	806.00	2.996	1848.00	1077.00	1.716	2090.0	1060.0	1.972
PAM5000	3077.00	1680.00	1.832	4815.00	1640.00	2.936	3209.00	2140.00	1.500	--	--	--

Table 4-7. Measured W_d of PAM standards of the selected systems

Case Study #	W_d (counts)									
	26	27	28	29	30	31	32	33	34	35
Sample										
PAM55	10.65	12.75	10.22	8.00	11.60	13.00	8.00	10.90	10.70	10.65
PAM100	14.55	18.30	15.30	12.30	17.00	13.95	13.00	--	--	--
PAM270	--	18.50	15.35	12.00	--	--	12.95	13.80	15.50	15.70
PAM500	10.15	16.25	13.40	10.95	11.90	10.85	13.15	14.65	14.60	--
PAM1000	10.35	16.65	15.15	11.40	11.00	10.55	12.00	12.30	13.30	14.00
PAM2000	9.10	12.40	13.50	9.00	9.40	9.65	8.50	9.80	10.20	11.10
PAM5000	6.00	7.75	--	6.60	6.80	8.60	7.30	--	--	--
Std A	--	--	--	--	--	--	--	10.00	10.10	10.35
Std C	--	--	--	--	--	--	--	6.10	8.70	--
Std B	--	--	--	--	--	--	--	8.80	--	--
D2	0.390	0.247	0.272	0.358	0.310	0.436	0.324	Non-Linear		
# of Columns	4	7	5	4	5	5	4	5	5	5
Length of System (ft)	15.40	20.90	19.25	14.20	19.60	19.30	15.50	19.00	19.00	19.00
pH	6.65	5.0	6.60	6.60	6.60	6.65	6.60	7.0	7.0	3.50
I	0.056	0.07	0.053	0.053	0.053	0.056	0.053	0.025	0.250	0.025

resolution correction with respect to peak broadening.

(ii) Sodium Polystyrene Sulfonate

With this polymer, it was found that more caution was needed when dealing with ionic strength I (ie amount of added salt) than pH. At very high I, in the presence of Tergitol or PEO, the polymer was completely or partially adsorbed, depending on the pH of the mobile-phase. Therefore, the effect of I was considered important, though, it could not be easily assessed from single column analysis.

The sodium polystyrene sulfonate standards contain impurities of sodium sulfate. Any adequately selected multicolumn system should be capable of resolving the sodium sulfate impurities from the lowest MW standard investigated ($\bar{M}_w$ = 31,000). With polyacrylamide, it was possible to resolve included salt peaks from any of the polymers. With dextrans which are very compact in size in solution, it was also possible to keep the included salt away from the lowest MW standard used ($\bar{M}_w$ = 9,300), with properly chosen systems of pore-sizes.

At intermediate ionic strength in the presence of Tergitol but no added acid, data relevant to the question of multi-column system for CPG-10/sodium polystyrene sulfonate are shown in Fig. 4-29 which represents calibration curves on single columns of different pore-sizes. One should expect the inclusion of 120/240 Å or 120/88 Å pore size columns in a system of more than five well selected pore-sizes to adequately separate the sodium sulphate impurities from any of the narrow MWD polystyrene standards. However, this is not the case, as shown in Fig. 4-30, even for nine multi-column system. In this figure the chromatogram of the lowest MW standard $\bar{M}_w$ = 31,000 is shown for sets of 9(A), 6(B) and 6(C) column combinations. With a mobile-phase of low

Figure 4-29. $\bar{M}_w$ range of separation of different pore-sizes for NaPSS in poorly selected mobile-phase

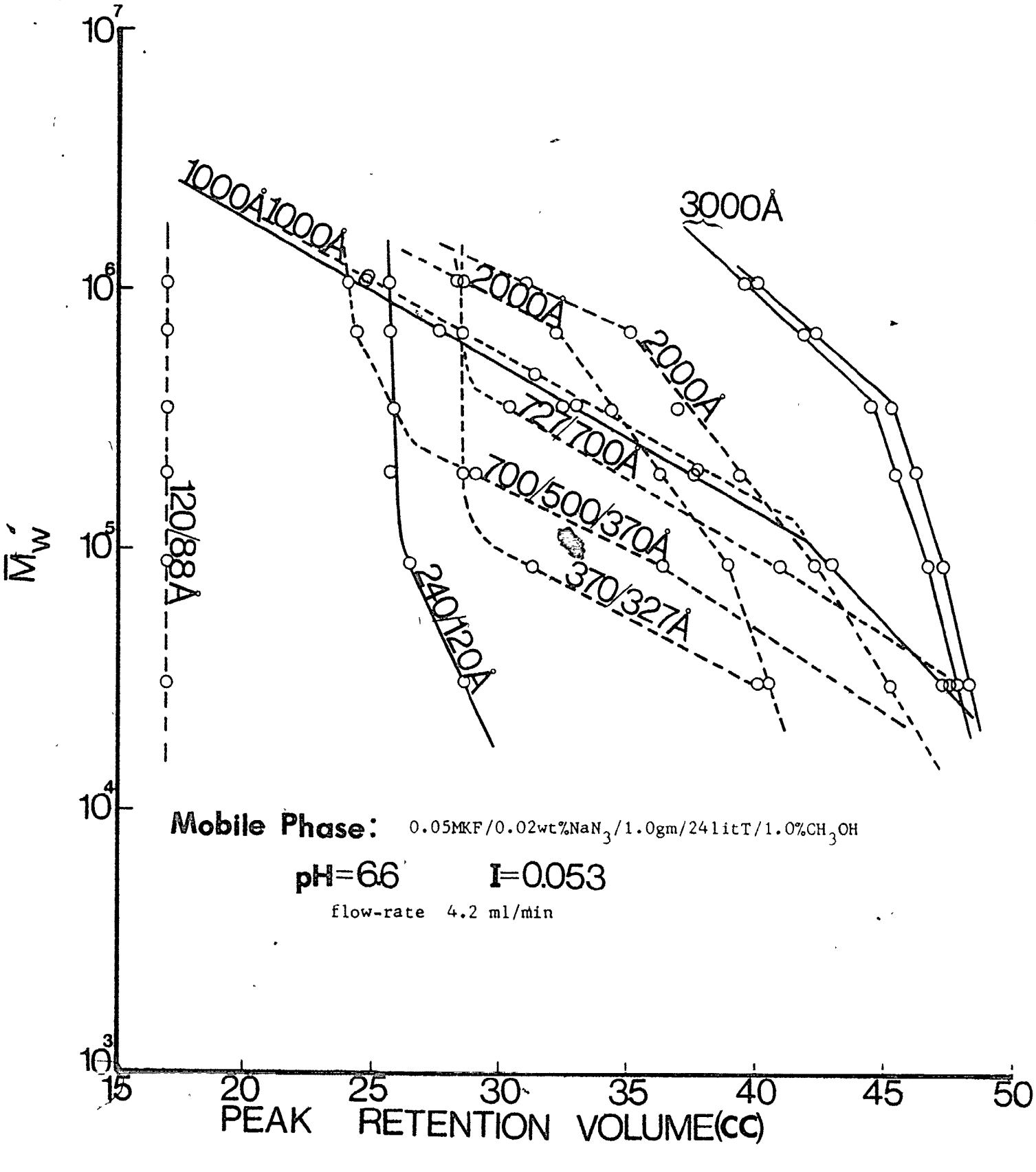

Figure 4-30. Resolution between NaPSS $\bar{M}_w$ (31,000) and Na_2SO_4 impurities in 3 different systems

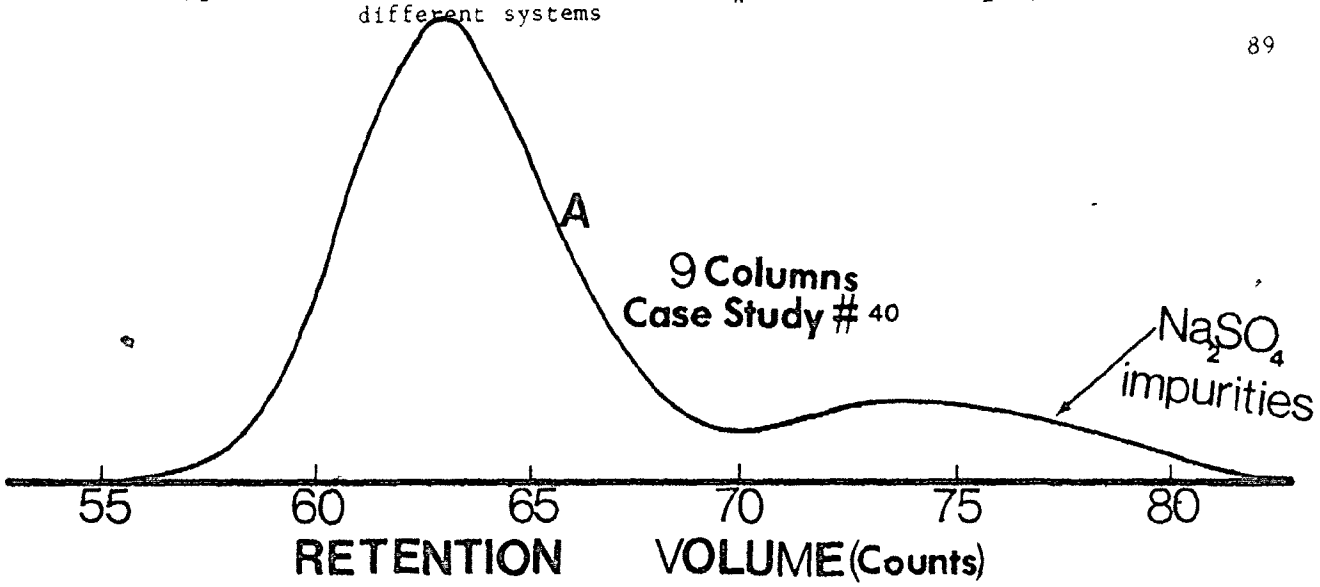

Mobile-Phase: 0.05MKF/0.02wt%NaN_3/1.0gm/24litT/1.0%CH_3OH.(A&B)
pH=6.6

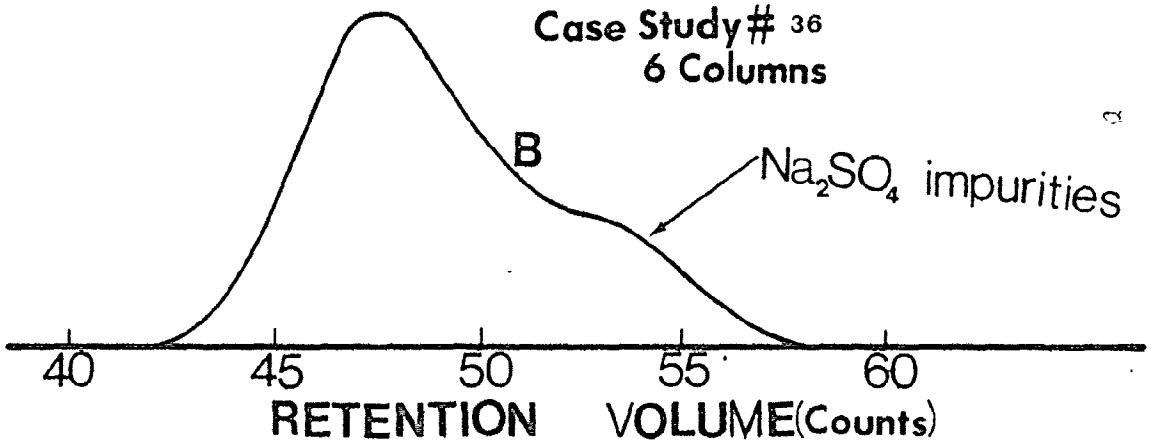

Mobile-Phase: 0.05MKF/0.02wt%NaN_3/1.0gm/24litT/1.0%CH_3OH. pH=6.6 (A&B)

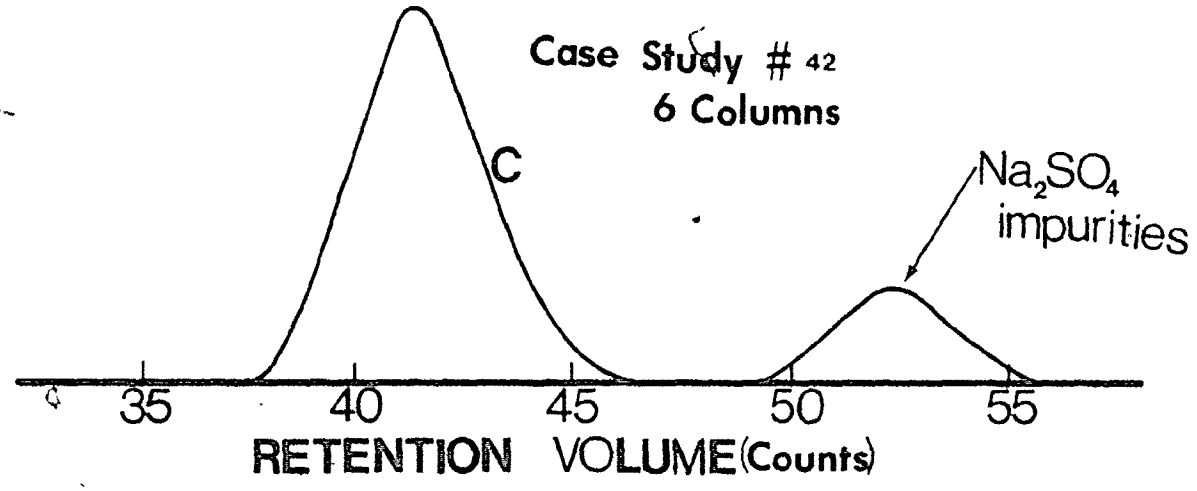

Mobile-Phase: 0.00833MNa_2SO_4/1.0%CH_3OH/1.0gm/24litT pH=3.42(with H_2SO_4)

pH, there is no doubt that there is indeed an excellent separation between the impurities and the polymer. Thus the lowering of the pH of the mobile phase is very important for the analysis of the polymer. At low pH, relevant data for multi-column system corresponding to Fig. 4-29 are shown in Fig. 4-31.

Finally eleven systems were chosen and these are listed in Table 4-8. This Table like the one which has been shown for polyacrylamide contains the operating conditions as well as the description of the systems. Only four of the cases studied here, involved the use of its corresponding mobile-phase (at low pH). Their $\bar{M}_w$ calibration curves are shown in Figs. 4-32 to 34. Using linear least square regression analysis, their $\bar{M}_w$ calibration constants were obtained and used to estimate the $\bar{M}_w$ and $\bar{M}_n$ of each sample. Their calculated values are shown in Table 4-9. From the uncorrected or SEC polydispersities of these standards, it is obvious that they are very narrow compared to polyacrylamide standards. The measured width of each chromatograms are listed in Table 4-10. The slopes of their molecular weight ($\bar{M}_w$) calibration curves, D2, of most of the systems are noticed to be smaller or flatter than those corresponding to systems for polyacrylamide analysis. This observation, when combined with their measured W_d, indicates that there is more molecular weight resolution correction with respect to peak broadening for polyacrylamide than for sodium polystyrene sulfonate. However, from the measured molecular weight averages of the sodium polystyrene standards, just like with polyacrylamide, the following points may be made:

(1) the need of a true molecular weight calibration curve is very important for the accurate analysis of the $\bar{M}_w$ and $\bar{M}_n$ of these samples

Figure 4-31. $\bar{M}_w$ range of separation of different pore-sizes for NaPSS in a well selected mobile-phase

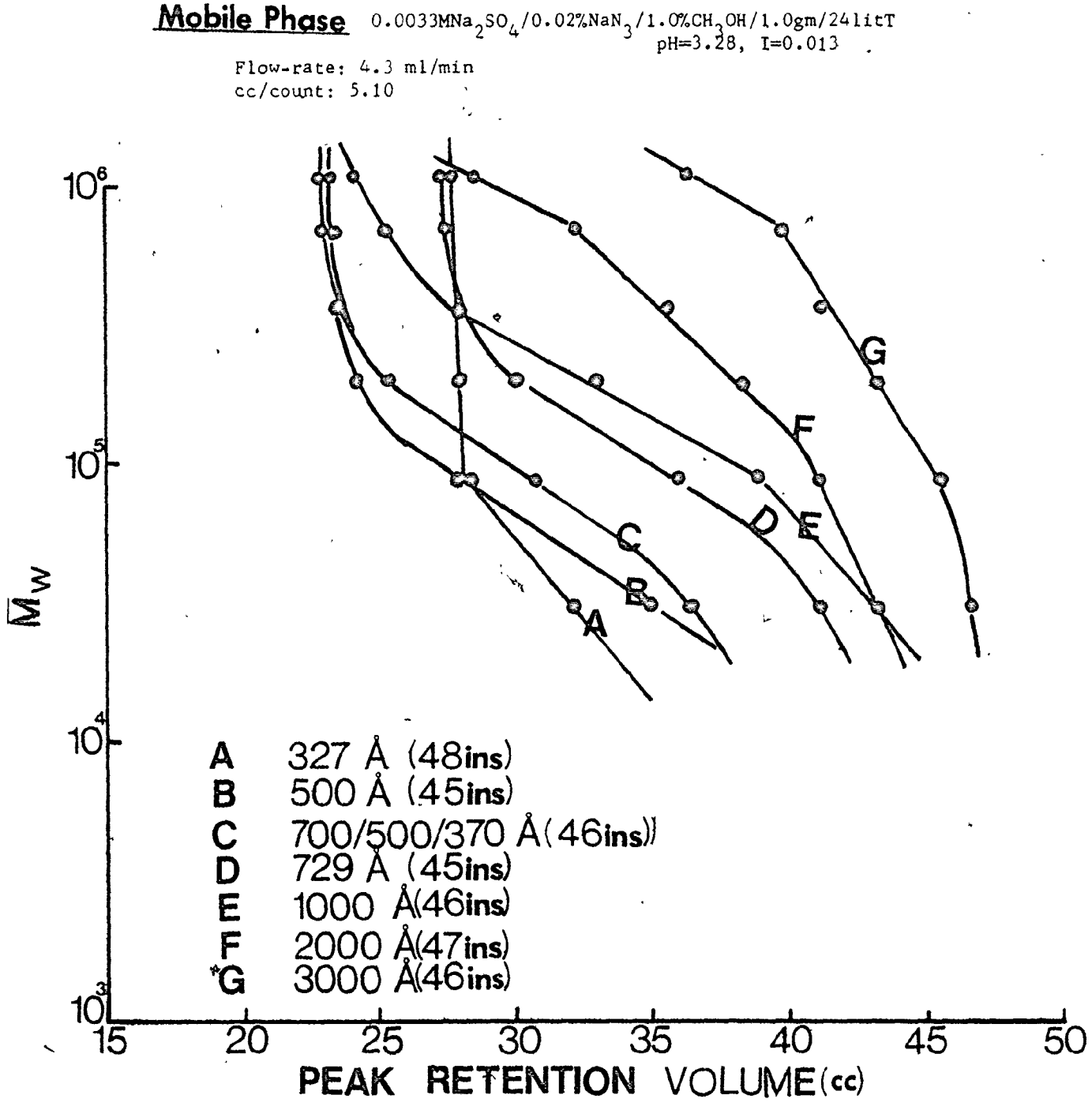

Table 4-8. Description of column combination characteristics for Na Polystyrene Sulfonate and Hydrolysed PAM Studies

Case Study #	Column Combination	Code No.	Mobile-Phase	Flow-rate (ml/min) (conc injected)
36	2000 Å(L), 2000 Å(B), 1000 Å(D), 729/700 Å, 700/500/370 Å, 370/327 Å 23.6 ft.	S6DR	same as 28	4.20 (0.075 wt%)
37	1000 Å(E), 1000 Å(D), 729/700 Å, 700/500/370 Å, 370/327 19.7 ft.	S5LR	same as 28	4.20 (0.05 wt%)
38	2000 Å(B), 1000 Å(D), 729/700 Å, 700/500/370 Å, 370/327 Å 19.7 ft.	S5MR	"	4.20 (0.05 wt%)
39	2000 Å(L), 2000 Å(B), 1000 Å (E), 1000 Å(D), 727/700 Å, 700/500/370 Å, 370/327 Å, 240/120 Å 28.67 ft.	S8AR	"	3.20 (0.075 wt%)
40	All in #39 + 120/88 Å 31.3 ft.	S9BR	"	3.20 (0.1 wt%)
41	Same as in #39 28.67 ft.	S8BR	"	3.20 (0.1 wt%)
42	3000 Å(D), 2000 Å(E), 1000 Å(D), 500 Å, 327 Å, 240/120 Å 21.35 ft.	S6ER	0.00833 MNa_2SO_4/1.0% CH_3OH/1.09 m/24 lit T pH=3.42 (H_2SO_4)	4.5 (0.05 wt%)
43	3000 Å(D), 3000 Å(E), 2000 Å(E), 2000 Å(L), 1000 Å(D), 500 Å 20.8 ft.	S6FR	0.0033 MNa_2SO_4/0.02 wt% NaN_3/1.0% CH_3OH/1.0 gm/24 lit T pH=3.25 (H_2SO_4)	4.2 (0.10 wt%)
44	2000 Å(L), 1000 Å(D), 1000 Å(E), 729 Å, 500 Å, 327 Å, 240/120 Å 25.8 ft.	S7BR	0.00417 M$KH_3(C_2O_4)_2$.$2H_2O$/1.0% CH_3OH/1.0 gm/24 lit T pH=2.66	4.2 (0.1 wt%)
45	Same as in #44 25.8 ft.	S7BR2	Same as in #44	4.2 (0.1 wt%)
46	Same as in #33 19.0 ft.	S5NR	Same as in #33	2.5 (0.05 wt%)
47	Same as in #33 19.0 ft.	S5NR	Same as in #46	2.5 (0.05 wt%)
	Hydrolysed Polyacrylamide			
48	3000 Å(D), 3000 Å(E), 2000 Å(L), 1000 Å(D), 729 Å, 500 Å 22.8 ft.	S6GR	Same as in #33	2.5 (0.02-.025%)

Figure 4-32. $\bar{M}_w$ calibration curves of NaPSS for Case-Studies #36, 37, 38, 42 and 43

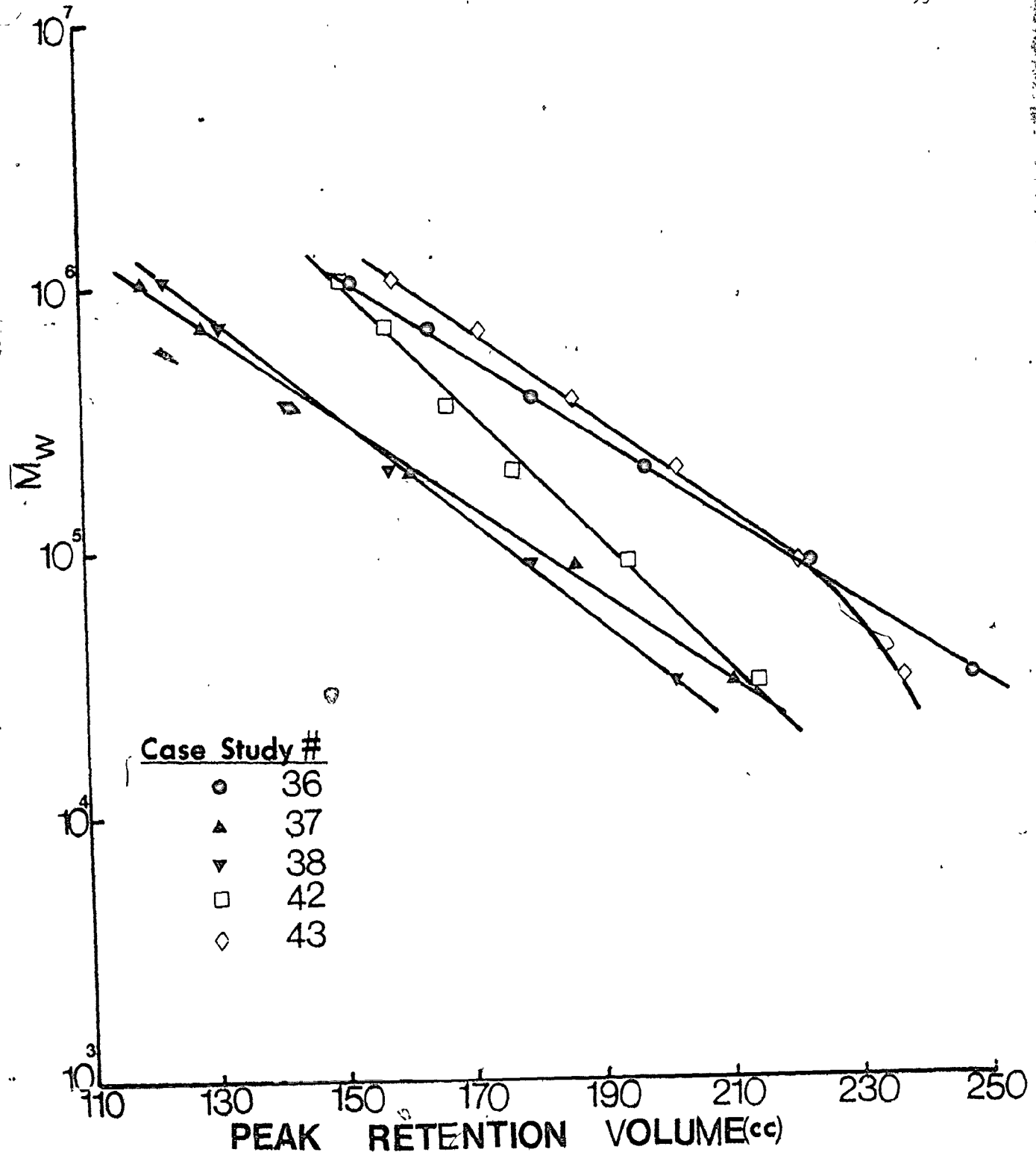

Figure 4-33. $\bar{M}_w$ calibration curves of NaPSS for Case-Studies #41, 39 and 40

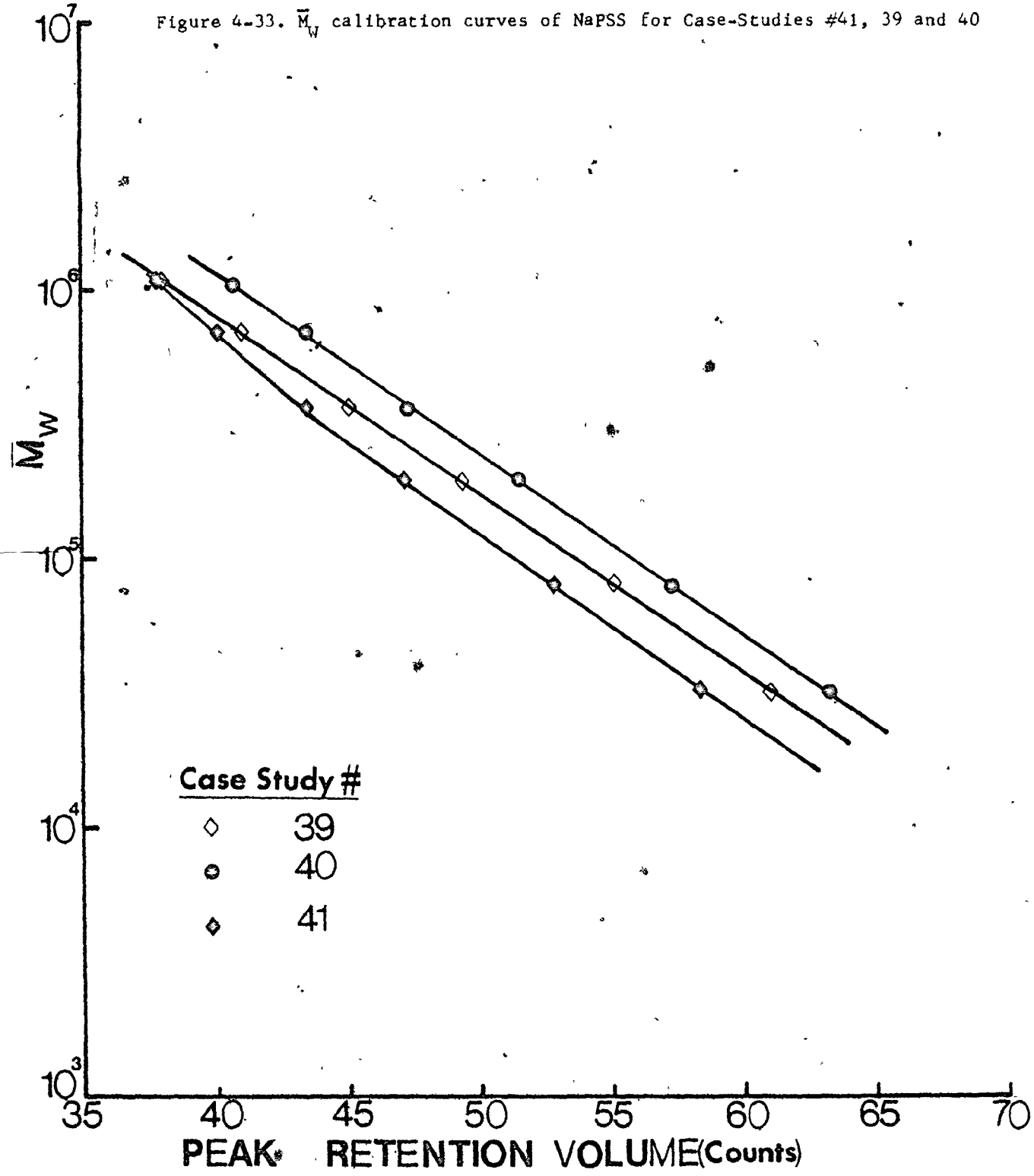

Figure 4-34. $\bar{M}_w$ calibration curves of NaPSS for Case-Studies #44, 45, 46 and 47

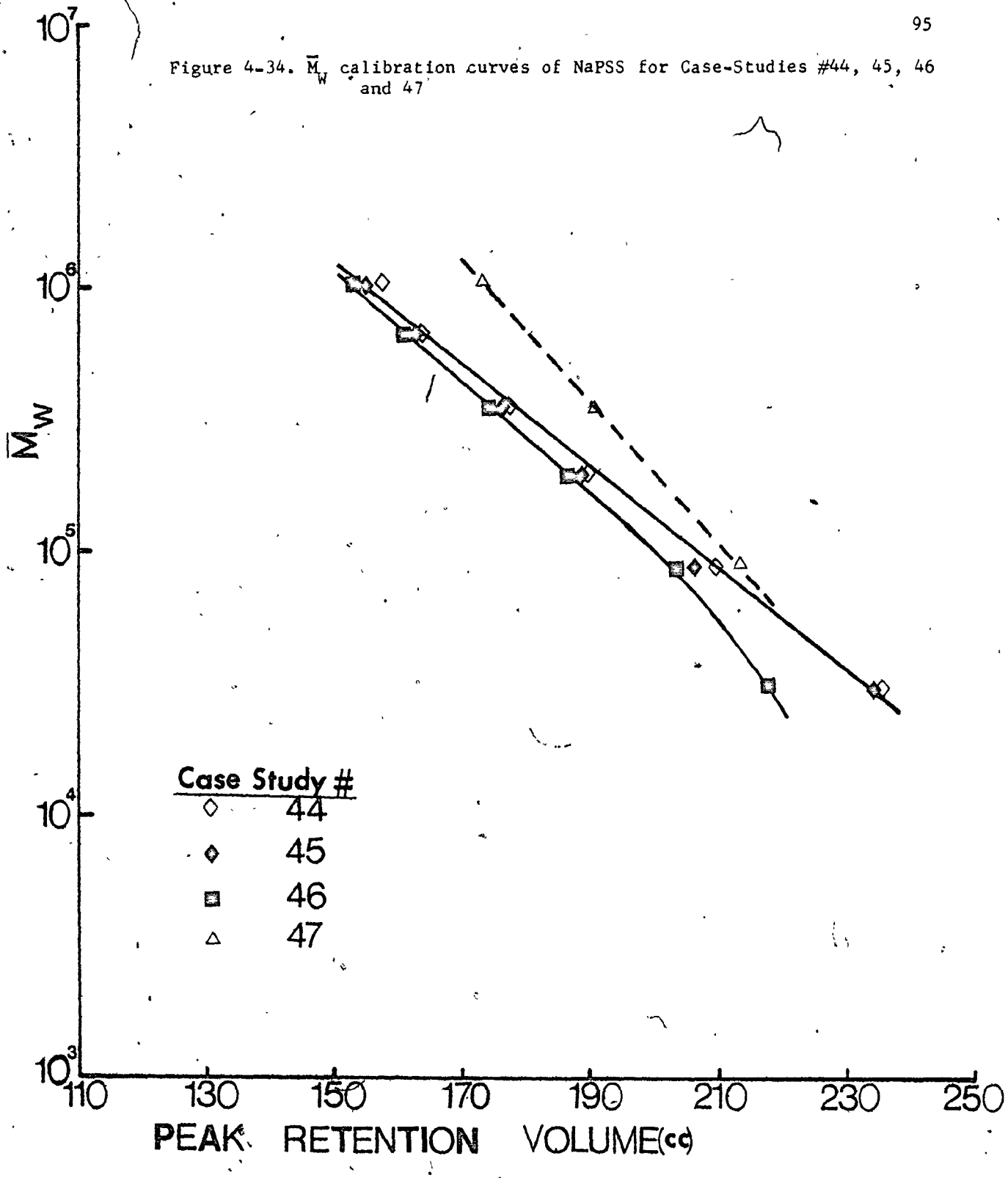

Table 4-9. Measured SEC MW averages of systems selected for NaPSS analysis

Case-Study M(V)=	9^{36} 0.277x10 EXP(-0.190V)			8^{37} 0.827x10 EXP(-0.193V)			9^{38} 0.190x10 EXP(-0.224V)			9^{39} 0.339x10 EXP(-0.151V)		
Sample	$\bar{M}_w$ x10^{-3}	$\bar{M}_n$ x10^{-3}	P(t)	$\bar{M}_w$ x10^{-3}	$\bar{M}_n$ x10^{-3}	P(t)	$\bar{M}_w$ x10^{-3}	$\bar{M}_n$ x10^{-3}	P(t)	$\bar{M}_w$ x10^{-3}	$\bar{M}_n$ x10^{-3}	P(t)
NaPSS31	--	--	--	--	--	--	--	--	--	32.60	27.90	1.170
NaPSS88	81.00	68.00	1.189	81.9	71.3	1.150	81.00	66.90	1.211	81.50	73.30	1.128
NaPSS195	209.00	178.00	1.173	215.9	188.2	1.147	211.00	178.00	1.184	194.00	171.00	1.138
NaPSS354	381.00	323.00	1.180	387.4	333.0	1.164	388.00	336.00	1.155	366.00	327.00	1.118
NaPSS690	615.00	482.00	1.276	653.2	561.9	1.162	589.00	464.00	1.270	606.00	470.00	1.290
NaPSS1060	931.0	746.00	1.248	884.0	776.0	1.138	885.00	751.00	1.178	965.00	812.00	1.189
	9^{40} 0.568x10 EXP(-0.155V)			9^{41} 0.636x10 EXP(-0.170V)			10^{42} 0.347x10 EXP(-0.283V)			10^{43} 0.131x10 EXP(-0.227V)		
NaPSS31	33.10	28.20	1.173	33.40	28.90	1.158	31.80	26.90	1.183	52.10	47.00	1.108
NaPSS88	80.30	70.90	1.132	81.30	70.80	1.148	89.00	73.20	1.216	97.40	86.80	1.122
NaPSS195	199.00	176.00	1.129	204.00	178.00	1.142	231.00	195.00	1.186	199.00	172.00	1.158
NaPSS354	371.00	333.00	1.112	392.00	342.00	1.144	383.00	317.00	1.207	360.00	299.00	1.207
NaPSS690	622.00	513.00	1.213	605.00	453.00	1.338	602.00	447.00	1.346	582.00	389.00	1.497
NaPSS1060	936.00	771.00	1.213	889.00	698.00	1.273	819.00	561.00	1.459	904	572.00	1.581

Case-Study M(V)=	10^{44} 0.107x10 EXP(-0.228V)			10^{45} 0.107x10 EXP(-0.228V)			10^{46} 0.205x10 EXP(-0.2525V)		
	$\bar{M}_w$ x10^{-3}	$\bar{M}_n$ x10^{-3}	P(t)	$\bar{M}_w$ x10^{-3}	$\bar{M}_n$ x10^{-3}	P(t)	$\bar{M}_w$ x10^{-3}	$\bar{M}_n$ x10^{-3}	P(t)
NaPSS31	28.41	24.51	1.159	29.96	25.75	1.163	--	--	--
NaPSS88	83.22	68.66	1.212	85.43	70.86	1.206	103.17	87.09	1.185
NaPSS195	220.75	171.74	1.285	223.06	166.83	1.337	231.76	189.29	1.224
NaPSS354	289.49	177.65	1.630	311.47	199.89	1.558	359.09	261.94	1.371
NaPSS690	448.81	286.20	1.568	--	--	--	663.46	412.96	1.607
NaPSS1060	705.20	461.52	1.528	708.94	461.25	1.537	1003.27	512.28	1.958

Table 4-10. Measured W_d of samples for NaPSS

Case Study #	W_d (counts)										
	36	37	38	39	40	41	42	43	44	45	46
Sample											
NaPSS31	9.15	8.05	9.40	9.85	9.75	9.00	5.70	5.90	6.20	6.30	6.50
NaPSS88	8.40	7.40	8.25	9.20	9.15	8.65	5.90	6.25	6.40	6.40	6.90
NaPSS195	7.90	7.20	7.40	8.70	8.50	8.20	5.60	6.60	6.60	6.70	7.05
NaPSS354	7.50	6.00	6.45	8.15	7.95	7.73	5.80	6.90	7.20	7.15	8.80
NaPSS690	8.00	5.90	6.50	9.70	8.25	8.20	5.15	7.80	7.30	--	9.10
NaPSS1060	7.80	4.70	5.85	8.55	8.90	8.25	7.40	10.90	7.00	7.10	13.40
D2	0.190	0.193	0.224	0.151	0.155	0.170	0.283	0.227	0.228	0.228	0.253
# of columns	6	5	5	8	9	8	6	6	7	7	5
length of columns	23.60	19.70	19.70	28.67	31.30	28.67	21.35	20.80	25.80	25.80	19.00
pH	6.60	6.60	6.60	6.60	6.60	6.80	3.42	3.25	2.66	2.66	7.00
I	0.053	0.053	0.053	0.053	0.053	0.031	0.025	0.013	0.025	0.025	0.025

(ii) correction for peak broadening or instrumental spreading function is very important particularly when the true molecular weight calibration curve is not known.

(iii) Hydrolysed Polyacrylamide

The anomalous behaviour of Standard C (14% hydrolysed) at low pH has been shown in Figs. 4-15, 19 and 28. Without alluding to the viscosity data, one could be made to reach the wrong conclusions about its polymer surface interaction. However at very low pH < 2.5, there are indications of very strong adsorption of the polymer to the glass surface with little or no response. At low pH, and any I, this polymer like sodium polystyrene sulfonate is a polyelectrolyte. But at neutral pH conditions (pH = 7) and intermediate ionic strength (I = 0.01 - 0.1) the polymer behaves exactly like the non-hydrolysed polyacrylamide standards, since in this region, the intrinsic viscosities of Std C remain the same (Table 4-3). At very high ionic strength and pH of 7.0, weak polyelectrolytic behaviour appears again. From the viscosity data at intermediate I and neutral pH conditions ($[\eta] = 25.0$) and using the $[\eta] - \bar{M}_w$ data based on polyacrylamide, the molecular weight of Std C is observed to be very large (of the order of 10^7 $\bar{M}_w$) in disagreement with previously measured molecular weight averages shown in Table 3-5.

With an approximate measure of the $\bar{M}_w$ of Std C at the optimum mobile phase suited for both hydrolysed and non-hydrolysed polyacrylamide, the $\bar{M}_w$ calibration curve also shown in Fig. 4-28 was obtained for a set of six columns described in Table 4-8. Using this system, five approximately 30% hydrolysed polyacrylamide samples were characterised. The difference between the use of the 6 column system instead of the 5

column system is due to the excellent resolution obtained, for which the use of the upper linear section of the calibration curve of the 6 column system was sufficient to accurately determine the uncorrected or SEC molecular weight averages of these samples. The chromatograms of the samples are shown in Fig. 4-35. Table 4-11 contains the supplied $\bar{M}_w$ of the samples and those obtained using the linear calibration curve. Contained in the Table are also their measured width, W_d, which along with D2, when compared with those of polyacrylamide and sodium polystyrene sulfonate shows that resolution correction for peak broadening is similar to those of polyacrylamide.

Table 4-11. Measured SEC MW averages and W_d of hydrolysed PAM samples

Case Study #48

Sample	% Hydrolysis	$\bar{M}_w$ Supplied from $[\eta]$ $\times 10^6$	Uncorrected Values Measured by Aqueous SEC			
			$\bar{M}_w$ $\times 10^6$	$\bar{M}_n$ $\times 10^6$	P(t)	W_d (counts)
2044-105*	30.00	10.00	17.47	7.31	2.388	7.00
2044-109*	30.00	12.00	13.87	4.33	3.200	7.40
1917-225*	30.00	6.00	28.34	9.00	3.151	7.30
Std C	14.00	5.83	21.82	8.46	2.578	7.10
154-5**	30.00	—	20.67	6.97	2.966	7.20

* data provided by Nalco Chemical Co., Chicago, Ill.

** Unknown, McMaster University

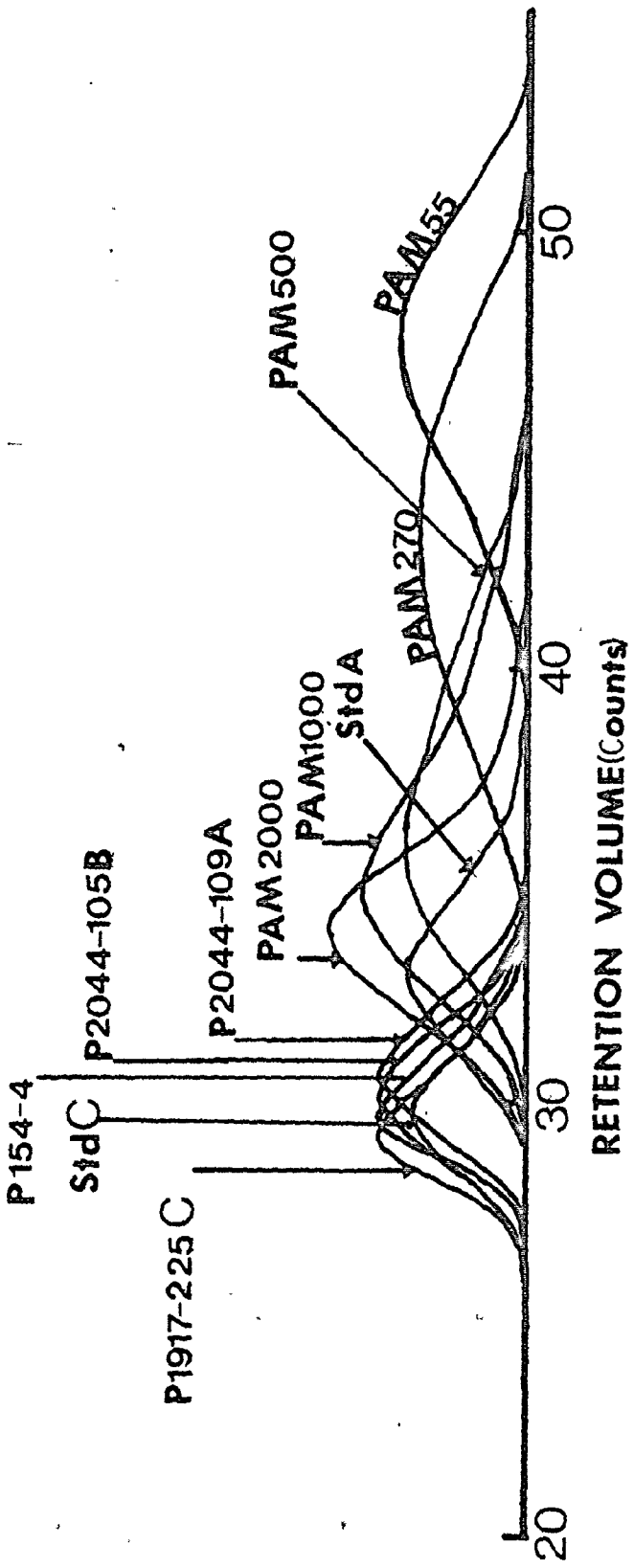

Figure 4-35. Chromatograms of hydrolysed and non-hydrolysed PAM for Case-Study #48

5. RESULTS AND DISCUSSION OF T.B.S. METHOD OF CALIBRATION

For case studies #1 and 2, the same set of columns (6) were employed. The choice of pore-sizes was based on the molecular weight exclusion limits supplied by manufacturers as shown in Table 5-1 below for CPG-10 and Bioglass. The columns used were selected from a set of old columns which have been used before in previous studies (52)(57), all of which were packed by other methods, other than dry packing.

Table 5-1. MW Exclusion Limits of Some Common Stationary-Phases as Supplied by Manufacturers

	CPG-10, 700	CPG-10, 2000	Bio-glass 2500
Avg Pore Size (Å)	700	2000	2500
Exclusion Limit	4×10^5 (a) 1×10^6 (b)	1×10^6 (a) 2×10^6 (b)	9×10^6 (c)
Supplier	WA*	WA*	BR**

(a) Dextran in water
(b) Polystyrene in THF
(c) Polystyrene in Toluene
* Water Associates, Framingham, Mass.
** Bio-Rad Laboratory, Richmond, California

The same mobile phase (double distilled water) was used for both case studies, but at different flow-rates. Though the chromatograms were very broad compared to the linear region of MW separation of the calibration curve, the ELC and TBS methods were applied and the results

are shown in Fig. 5-1 and Table 5-2. Only the $\bar{M}_W$ calibration curves are shown in Fig. 5-1, in counts and cc. According to the P_K values, the molecular weight correction factors, the very excessive correction is reflected in the very broad chromatograms, most of which were also bimodal.

Three additional columns, all dry packed with Bio-beads for low MW separation, were added to the six columns above to improve the D2. These were used for case-studies #3 and #4, both again at different flow-rates. The columns were arranged in the traditional order. Though the chromatograms were also very broad, the peak separation between the lowest and highest MW standards used here, increased by more than 50%. However, this time only two of the chromatograms were bimodal. For Case-Study #4, the system at lower flow-rate, multiple injections were made with some of the standards and the results are shown in Table 5-3, including those of Case-Study #3. The true calibration curve in the linear region were obtained by averaging the D2s and ln of D1 instead of D1s. The $\bar{M}_W$, $\bar{M}_{rms}$ and true MW calibration curves are shown in Fig. 5-2 in counts and cc. The next step was how to improve on the measured P_K values, which were still below 50% but however an improvement over the last two cases studied. The improved P_K values is reflected in the measured D2. In the presence of very large corrections (ie very broad chromatograms), the appearance or occurrence of small high molecular weight shoulder peak could not be explained.

Therefore Case-Study #5 was conducted with six columns, all dry packed with CPG-10, with distilled water and 0.1 M KBr as mobile-phases. Because the breadth of the chromatograms were greatly reduced, the small high MW shoulder peaks were now sharply defined as shown in Fig.

Figure 5-1. $\bar{M}_W$ calibration curves of dextran for Case Studies #1 and 2

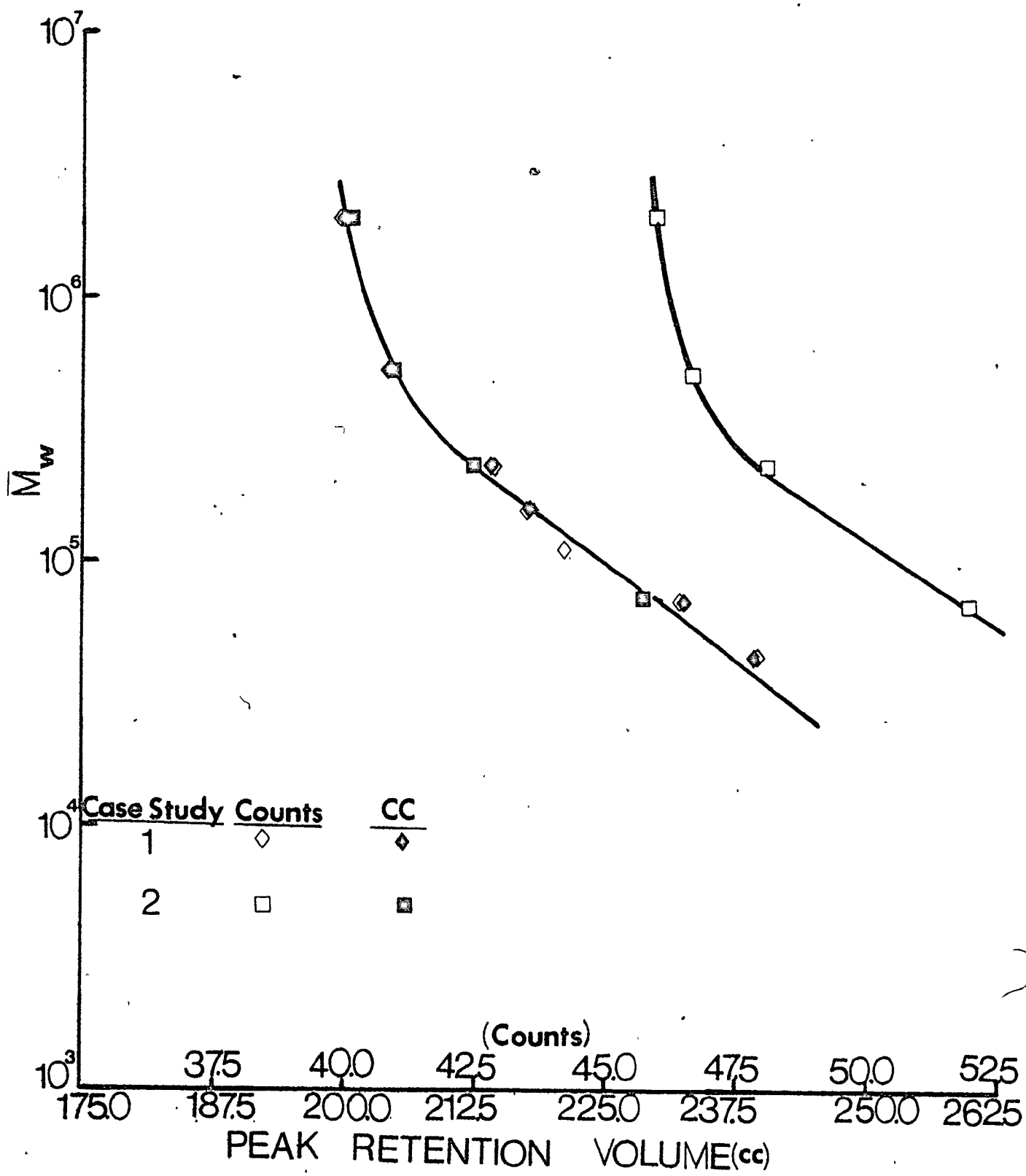

Table 5-2. Application of ELC and TBS methods to Case Studies #1 and 2

Single or Paired Samples	σ^2_{D2} (count)^2	D1	D2 (count)$^{-1}$	P_K	Sample	σ^2_{D2} (count)^2	D1	D2 (count)$^{-1}$	P_K
	ELC Method (Single) 8.9ml/mm (Case Study#1)					1.9ml/mm (Case Study #2)			
T500	--	0.115×10^{10}	0.201	--	T500	--	0.210×10^{10}	0.195	--
T250	--	0.230×10^{9}	0.169	--	T250	--	0.457×10^{9}	0.167	--
T70	--	0.529×10^{8}	0.148	--	--	--	--	--	--
	ELC Method Double $\bar{M}_W$								
T70&T500	--	0.109×10^{14}	0.470	--	T70&T500	--	0.439×10^{12}	0.334	--
T70&T250	--	0.249×10^{15}	0.564	--	T70&T2000	--	0.106×10^{13}	0.356	--
T250&T500	--	0.535×10^{13}	0.448	--	--	--	--	--	--
	ELC Method Double $\bar{M}_N$								
T70&T500		0.1317×10^{13}	0.345		T70&T500	--	0.8013×10^{11}	0.266	--
	(Case Study #1)			TBS Method			(Case Study #2)		
T70	20.75	0.631×10^{12}	0.405	0.182	T70	18.45	0.234×10^{12}	0.299	0.438
T500	19.16	0.631×10^{12}		0.208	T500	15.34	0.234×10^{12}		0.504
T70	20.75	0.596×10^{11}	0.409	0.177	T70	16.95	0.596×10^{11}	0.271	0.536
T250	19.92	0.596×10^{11}		0.189	T250	15.92	0.596×10^{11}		0.557
T250	19.76	0.218×10^{14}	0.399	0.207	T250	20.49	0.218×10^{14}	0.399	0.196
T500	19.01	0.218×10^{14}		0.220	T500	19.46	0.218×10^{14}		0.212
T40	21.34	0.393×10^{23}	0.920	1.17×10^{-4}	--	--	--	--	--
T500	19.38	0.393×10^{23}		2.72×10^{-4}					
T150	23.70	0.273×10^{12}	0.344	0.246					
T500	8.14	0.462×10^{12}		0.618					

Table 5-3. Application of TBS method to Case-Studies #3 and 4

#	Paired Samples	Case Study #3 (4.0 ml/min) σ^2_{D2}	D1	D2	P_K	Paired Samples	Case Study #4 (2.25 ml/min) σ^2_{D2}	D1	D2	P_K
1	T40 T250	21.83 20.00	0.321×10^{13}	0.283	0.418 0.449	T70(IV) T250(VII)	20.41 18.18	0.318×10^{13}	0.272	0.471 0.512
2	T40 T500	22.62 17.99	0.157×10^{14}	0.308	0.343 0.427	T40 T250(VII)	22.83 17.54	0.395×10^{13}	0.294	0.428 0.448
3	T70 T500	21.37 18.66	0.301×10^{14}	0.319	0.338 9.388	T110 T500(VI)	21.55 6.61	0.324×10^{13}	0.278	0.435 0.775
4	T40 T110	21.55 22.12	0.193×10^{13}	0.275	0.443 0.434	T250(II) T500(VII)	18.45 10.10	0.643×10^{13} 0.912×10^{13}	0.286	0.470 0.661
5	T70 T150	21.74 23.37	0.699×10^{14}	0.322	0.302 0.276	T250(II) T500(I)	19.01 18.18	0.127×10^{14}	0.297	0.432 0.448
6	T110 T250	23.04 21.46	0.180×10^{14}	0.312	0.327 0.353	T250(III) T500(VII)	19.53 9.63	0.605×10^{13} 0.870×10^{13}	0.285	0.453 0.676
7	T150 T500	22.52 17.86	0.139×10^{14}	0.306	0.350 0.435	T40 T250(I)	21.74 16.18	0.818×10^{12}	0.252	0.502 0.598
8	T70 T250	20.49 20.49	0.591×10^{13}	0.293	0.415 0.415	T40 T500(II)	23.81 18.18	0.409×10^{14}	0.311	0.317 0.416
9	T70 T110	20.16 22.42	0.391×10^{13}	0.286	0.438 0.399	T40 T500(IV)	23.59 14.21	0.201×10^{14}	0.300	0.346 0.528
10	T110 T500	23.59 20.49	0.306×10^{15}	0.358	0.220 0.267	T70(III) T500(IV)	21.65 15.43	0.667×10^{14}	0.320	0.331 0.455
11	T250 T500	23.37 21.10	0.918×10^{15}	0.377	0.190 0.224	T70(II) T500(VII)	21.55 20.58	0.411×10^{14}	0.310	0.355 0.372

$M(V) = 9.198\times10^{12}EXP(-0.300V)$

$M(V) = 8.749\times10^{12}EXP(-0.288V)$

Figure 5-2. $\bar{M}_w$, $\bar{M}_{rms}$ and MW calibration curves of dextran for Case-Studies #3 and 4

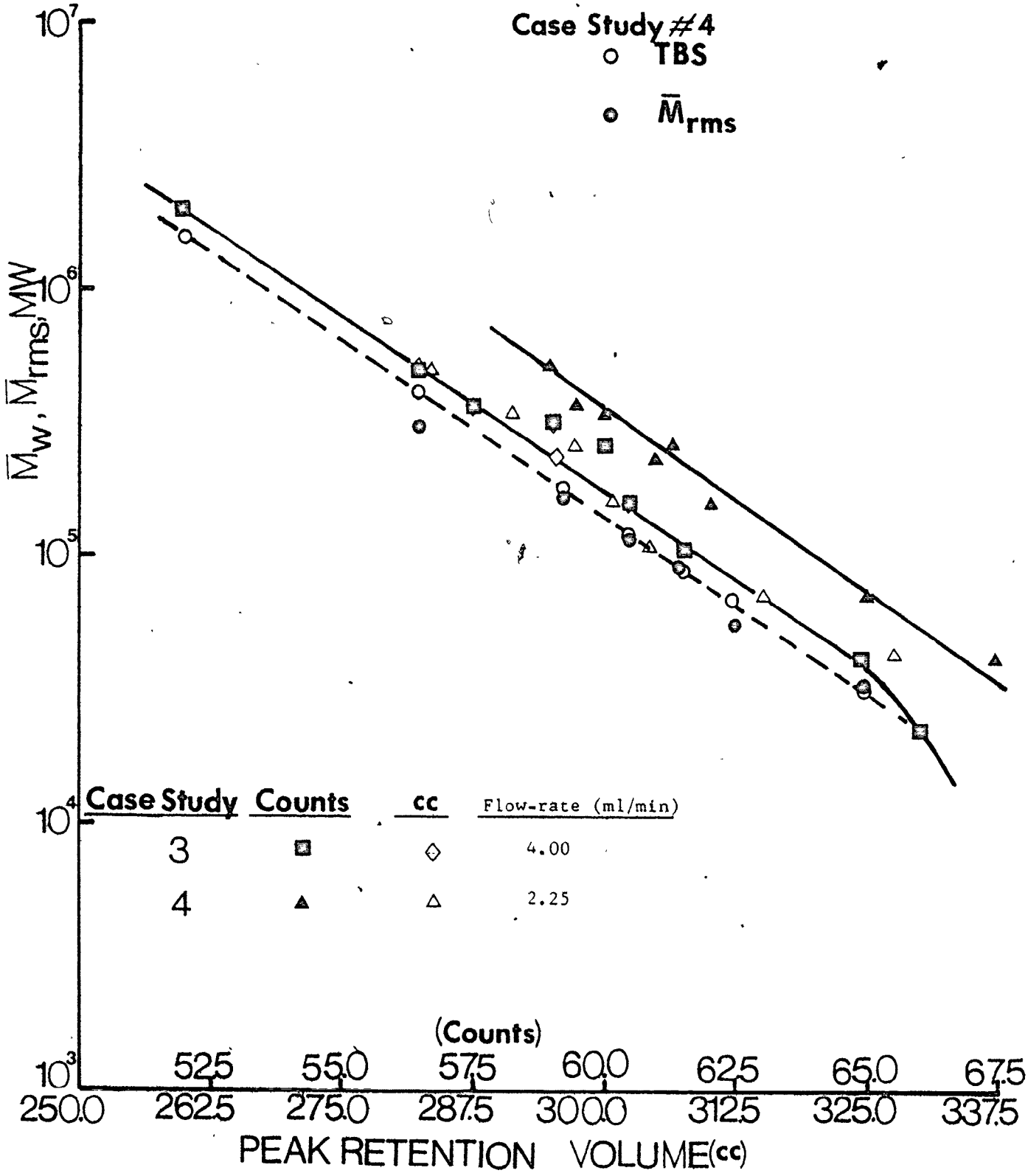

5-3A, with distilled water as mobile-phase. With 0.1 M KBr as mobile-phase the peaks were eliminated as shown in Fig. 5-3B, however to be replaced by small peaks of included KBr at the low MW ends. The chromatograms for this system were used with the TBS method and the results are shown in Table 5-4. One of the chromatograms T150 was deliberately skewed by including some artificial heights from the salt peak, and the results are also shown in Table 5-4. This was done purposely to show the power and versatility of the TBS method in detecting a skewed chromatogram. As shown in Table 5-4, the molecular weight correction factor has greatly improved compared to previous values.

For this system, the void volume was measured with polyacrylamide and sodium polystyrene sulfonate which were totally excluded from the pores by charge repulsion, with distilled water as mobile-phase. Chromatograms of polyacrylamide are shown in Fig. 5-4, where they are compared with the small high MW shoulder peaks of dextrans. The only explanation that could be offered for the appearance of the shoulder peaks was that the dextrans were slightly charged, the very small negative charges resulting in 'partial' ion exclusion from the pores as opposed to 'total' ion exclusion of very polar NaPSS or unique PAMs. The fact that they contain very small amount of negative charges is shown in Fig. 5-5 of the $\bar{M}_w$ calibration curves where apart from the occurrence of the small-shoulder peaks, the peak retention volumes in water/CPG-10 system are only slightly affected. In Fig. 5-5, the $\bar{M}_{rms}$ and the true MW calibration curves using TBS method are also shown.

The need to calibrate each pore-size singly packed column was thought to be a step which could be by-passed since MW exclusion limits are usually supplied. However as shown in Fig. 5-6, which contains MW

Figure 5-3A. 'Partial' ion-exclusion of dextran in water as mobile-phase

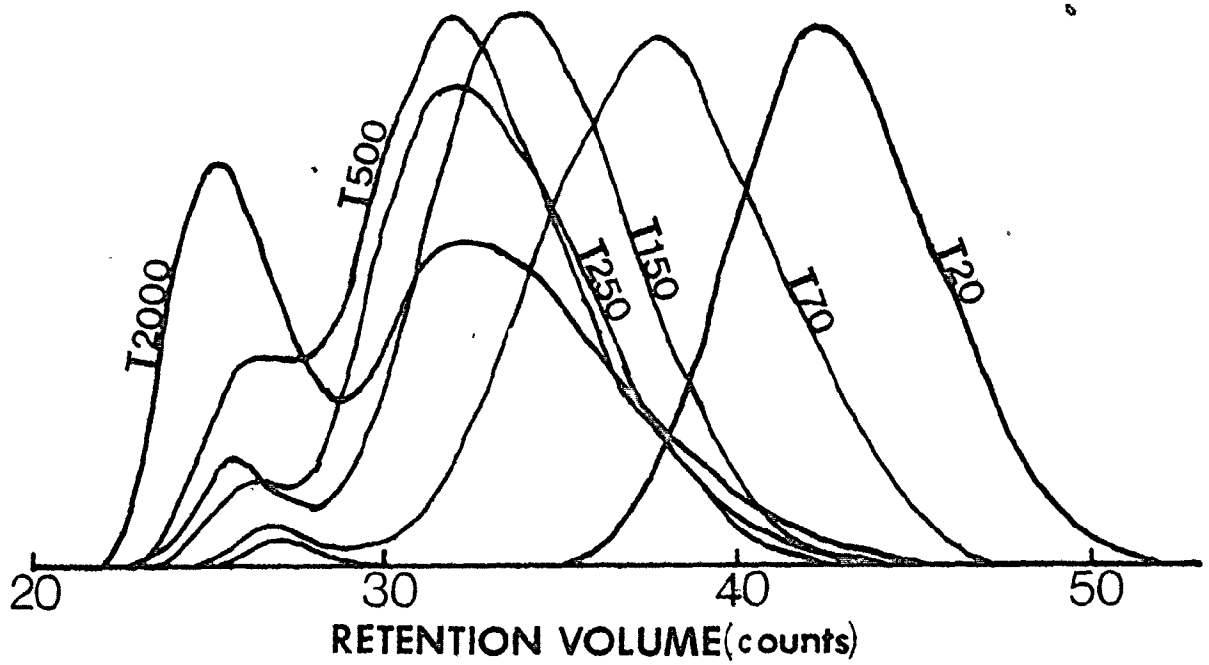

Figure 5-3B. Elimination of 'partial' ion-exclusion of dextran by addition of salt to the mobile-phase

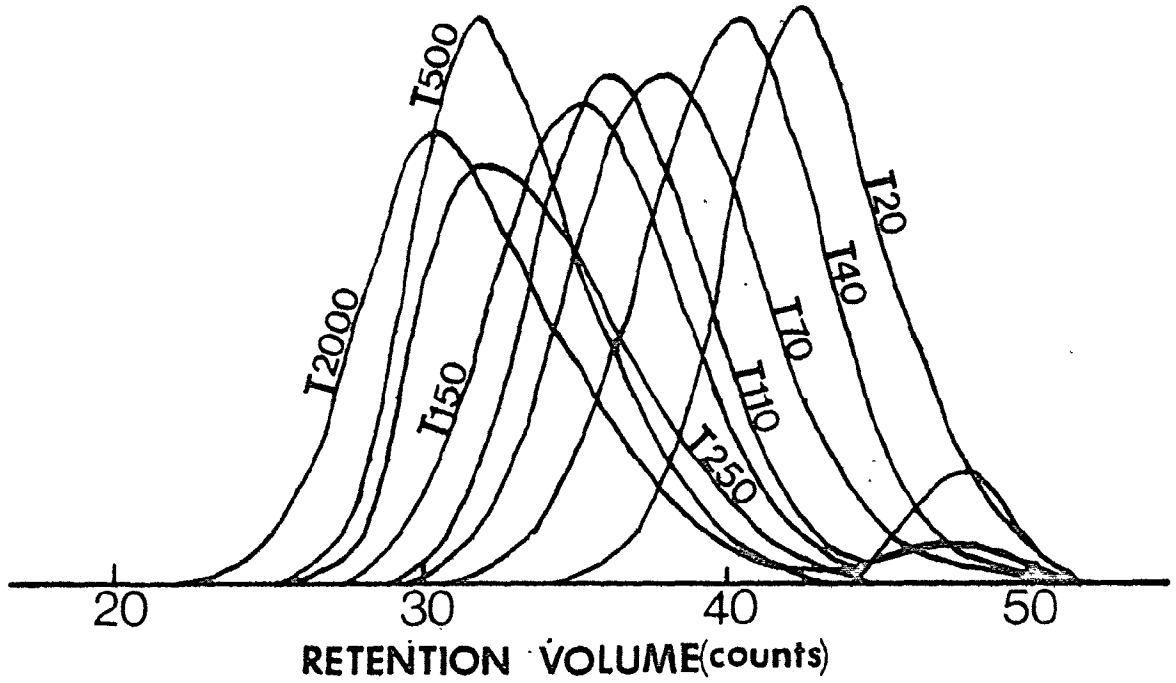

Table 5-4. Application of TBS method to Case Study 5

#	Paired Sample	σ^2_{D2} (count)^2	P_K	D1	D2 (count)$^{-1}$
1	T40	3.150	0.899	0.130×10^{10}	0.261
	T70	3.910	0.876	0.130×10^{10}	
2	T20	2.200	0.929	0.130×10^{10}	0.259
	T250	-0.340	1.012	0.130×10^{10}	
3	T40	3.550	0.879	0.186×10^{10}	0.270
	T250	0.460	0.983	0.186×10^{10}	
4	T70	4.550	0.845	0.206×10^{10}	0.273
	T250	0.670	0.975	0.206×10^{10}	

$$M(V) = 1.652\times10^{9}EXP(-0.266V)$$

Non-Linear Region of Calibration

1	T20	3.120	0.883	0.350×10^{10}	0.282
	T500	-5.110	1.226	0.350×10^{10}	
2	T40	4.700	0.810	0.627×10^{10}	0.300
	T500	-3.580	1.174	0.627×10^{10}	
3	T70	6.090	0.748	0.847×10^{10}	0.309
	T500	-2.890	1.148	0.847×10^{10}	
4	T40	7.16	0.521	0.111×10^{13}	0.427
	T150*	13.41	0.295	0.111×10^{13}	
5	T70	10.12	0.017	0.178×10^{21}	0.900
	T150*	13.30	0.005	0.178×10^{21}	
6	T250	5.91	0.620	0.201×10^{12}	0.402
	T500	1.76	0.867	0.201×10^{12}	

* Deliberately skewed

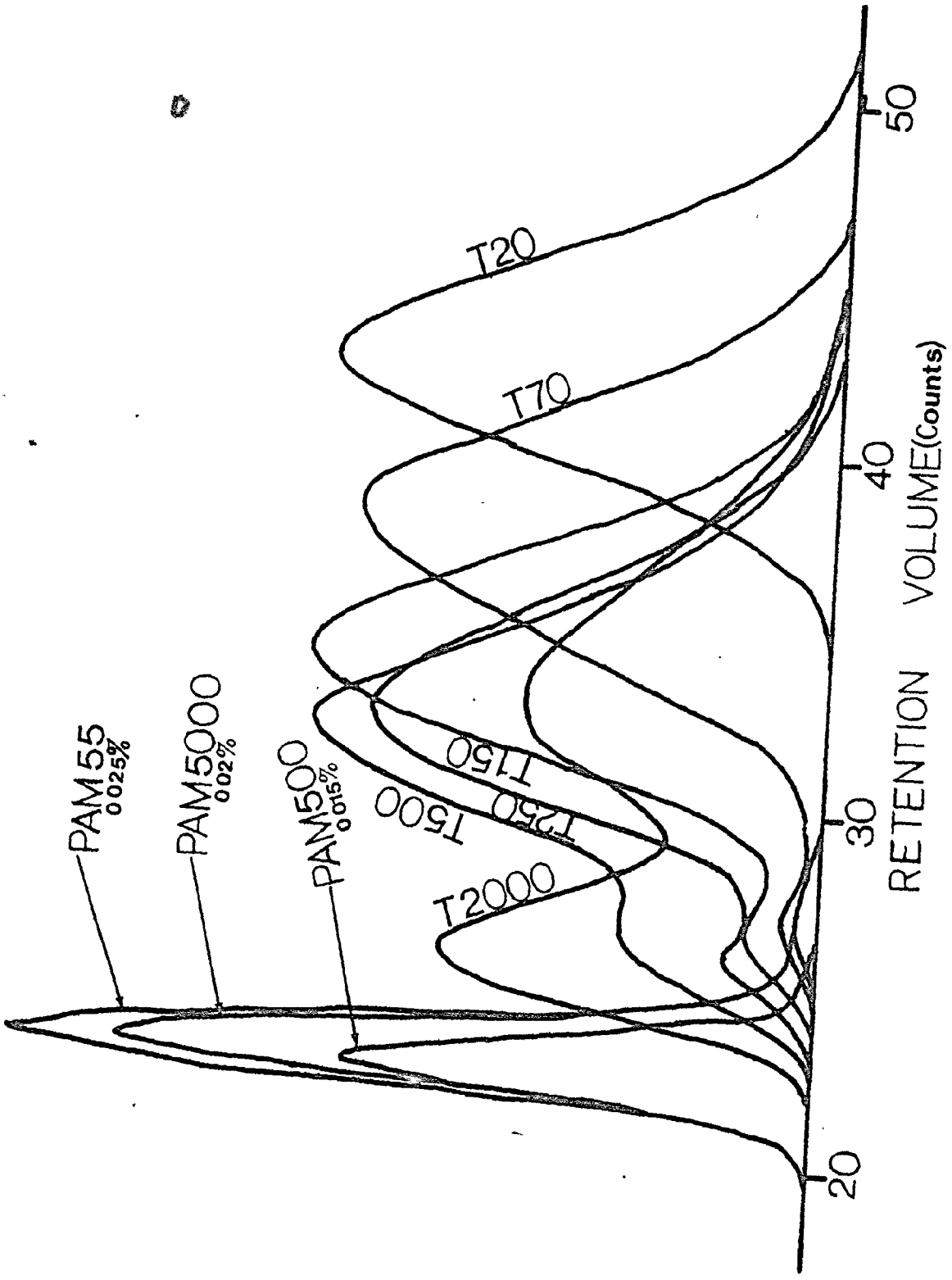

Figure 5-4. 'Total' ion-exclusion of PAM compared with 'Partial' ion-exclusion of dextran with water as mobile-phase

Figure 5-5. $\bar{M}_w$, $\bar{M}_{rms}$ and MW calibration curves of dextran for Case-Study #5

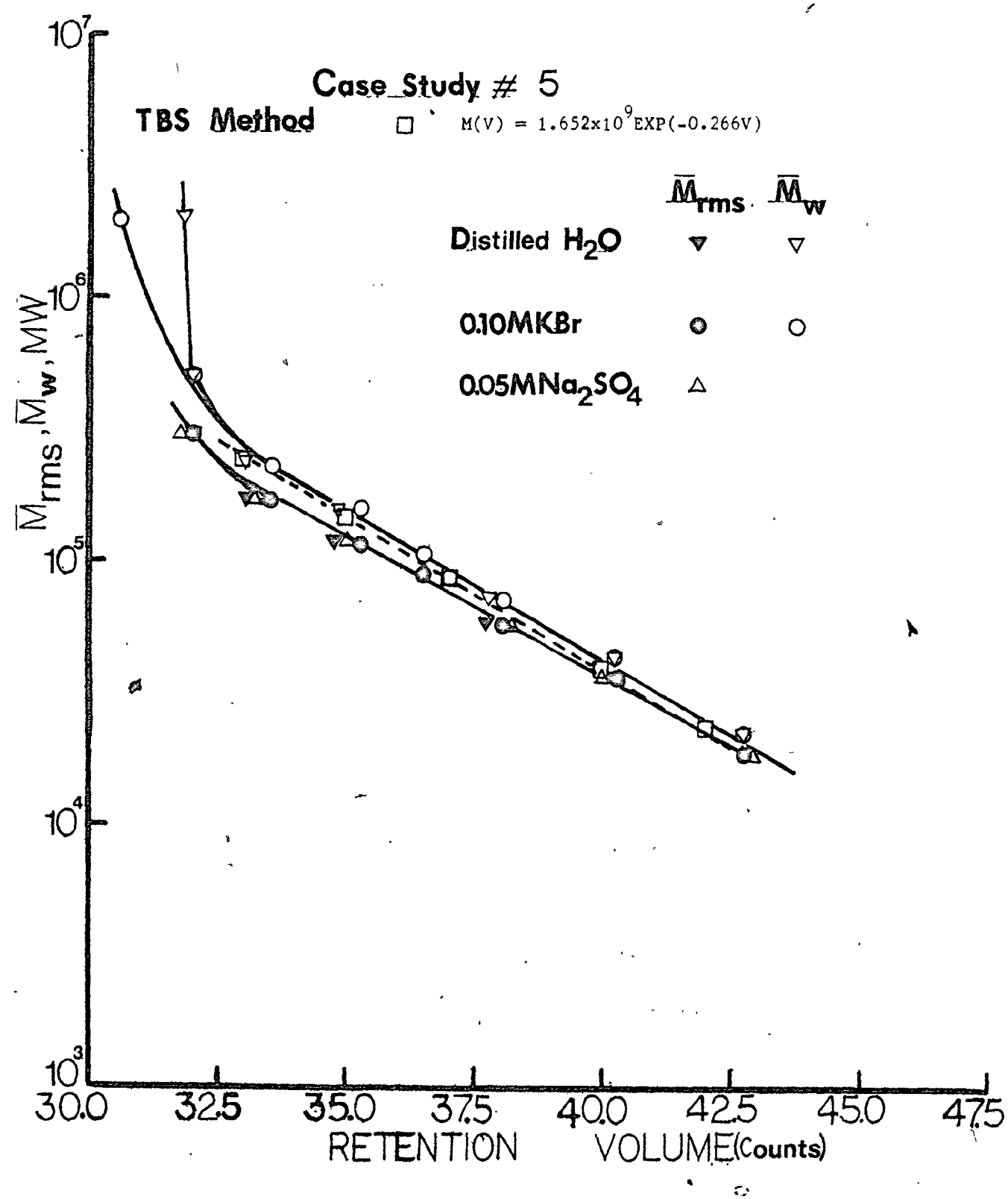

Figure 5-6. $\bar{M}_w$ range of separation of different pore-sizes for dextran

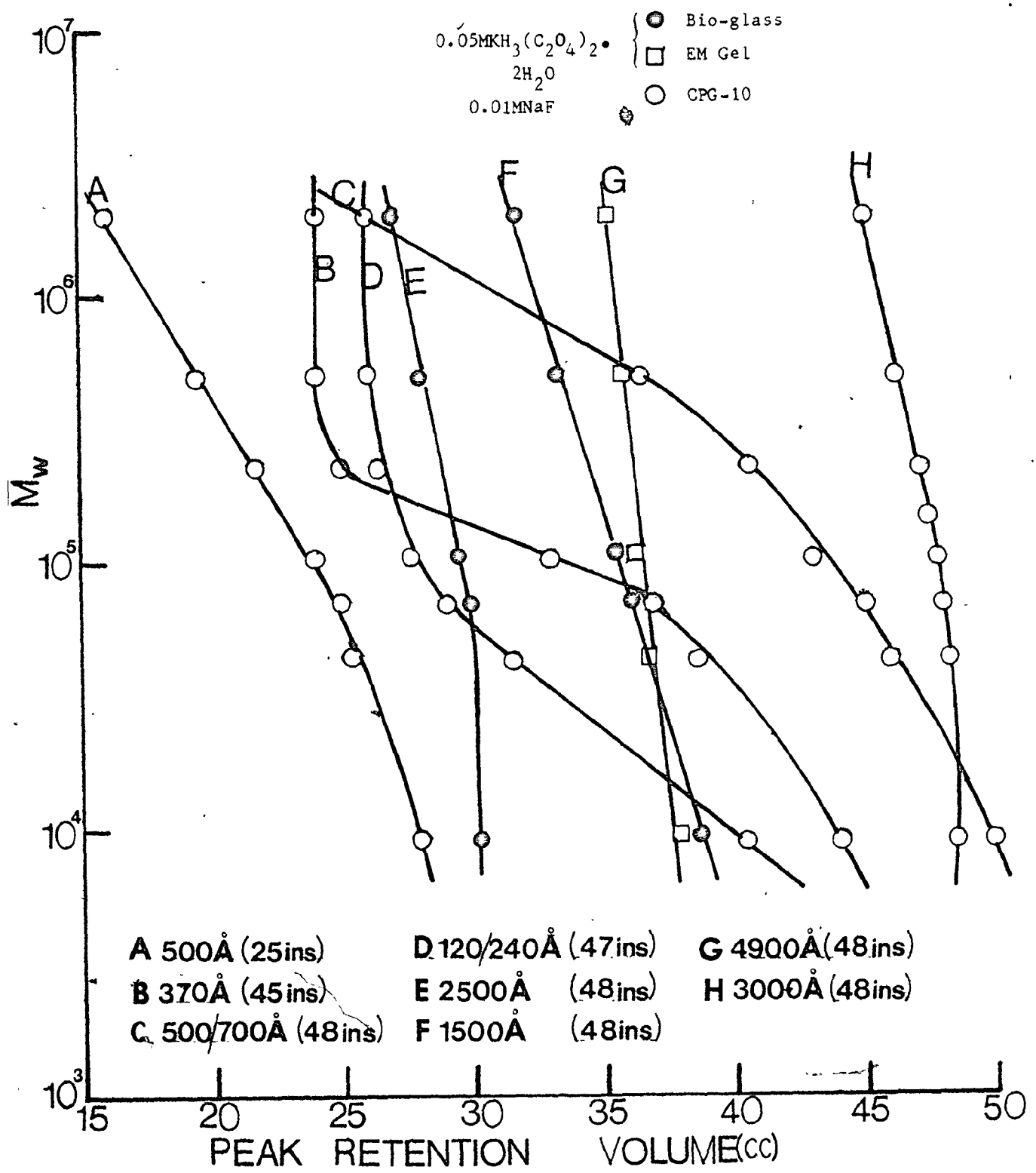

data of singly packed columns some of which were used in the previous systems and the remaining newly dry-packed, the large pore-sizes are seen to provide little or no peak separation. From this figure, systems were chosen for case studies # 6 and 7 using 0.01 M NaF as mobile-phase. (Note: NaF should not be used in mobile-phase as it was found to attack fractosil 4900 with no response obtained when PAM and NaPSS were injected.) Four columns were chosen for case-study #6. To this was added 3000 Å pore-size column (Case-study #7). Using the same operating conditions, the results of the TBS method are listed in Table 5-5, in which for Case-study #7, standard T250 was also deliberately skewed. Their MW, $\overline{M}_W$ and $\overline{M}_{rms}$ calibration curves are shown in Fig. 5-7. For these two systems the molecular weight correction factors are noticed to be greatly improved with the values (P_K) approaching and even greater than 1.0. However, the presence of the 3000 Å large-pore size is reflected in not only widely varying D2, but also more corrections of the SEC MW averages.

For the next eight systems, the same mobile-phase was employed, this time in the presence of Tergitol. With the exception of the last system, the others were arranged in the reversed-flow order. These systems have been described in Tables 3-3 and 4. Beginning with three columns (Case-Study #8), the number was gradually increased to six by addition of smaller pore-size columns one at a time. Undesirable large pore-sizes were excluded from the systems. For two of the systems MW gaps were deliberately introduced into the system by the removal of 370 Å pore-size column (Case Study #8 and #10). In one case study (#13), the pore-size was disorderly arranged at the low MW end. Data relevant to their selection for the new mobile phase are shown in Fig. 5-8. Again large pore-sizes greater than 1000 Å serve no useful purpose. In Tables

Table 5-5. Application of TBS method to Case Studies 6 and 7

#	Paired Samples	Case Study #6 σ^2_{D2} (count)^2	D1	D2 (count)$^{-1}$	P_K	Paired Samples	Case Study #7 σ^2_{D2} (count)^2	D1	D2 (count)$^{-1}$	P_K
1	T110	0.300	0.158×10^{9}	0.315	0.985	T110	0.962	0.149×10^{10}	0.305	0.956
	T500	-4.337	0.158×10^{9}		1.240	T500	-2.931	0.149×10^{10}		1.146
2	T110	-0.456	0.765×10^{8}	0.285	1.019	T110	-12.376	0.780×10^{8}	0.140	1.129
	T250	-2.461	0.765×10^{8}		1.105	T250*	-29.412	0.780×10^{8}		1.334
3	T70	-0.412	0.155×10^{9}	0.314	1.021	T70	0.588	0.177×10^{10}	0.311	0.972
	T500	-4.413	0.155×10^{9}		1.243	T500	-2.489	0.177×10^{10}		1.128
4	T70	-1.020	0.994×10^{8}	0.297	1.046	T70	-8.104	0.306×10^{8}	0.190	1.158
	T250	-1.762	0.994×10^{8}		1.081	T250*	-12.821	0.306×10^{8}		1.260
5	T70	-0.491	0.146×10^{9}	0.312	1.024	T70	1.041	0.290×10^{10}	0.326	0.946
	T110	0.224	0.146×10^{9}		0.989	T110	1.401	0.290×10^{10}		0.928
6	T40	-0.316	0.133×10^{9}	0.310	1.015	T40	-4.753	0.566×10^{8}	0.212	1.113
	T250	-1.079	0.133×10^{9}		1.053	T250*	-8.881	0.566×10^{8}		1.221
7	T40	-0.017	0.179×10^{9}	0.321	1.001	T40	0.331	0.170×10^{10}	0.310	0.984
	T500	-3.946	0.179×10^{9}		1.225	T500	-2.587	0.170×10^{10}		1.132
8	T40	0.172	0.218×10^{9}	0.329	0.991	T40	0.499	0.210×10^{10}	0.316	0.975
	T110	0.567	0.218×10^{9}		0.970	T110	1.199	0.210×10^{10}		0.942
9	--	--	--	--	--	T40	0.177	0.142×10^{10}	0.304	0.992
						T70	0.365	0.142×10^{10}		0.983

$M(V) = 0.136\times10^{9}\,EXP(-0.308V)$

$M(V) = 1.872\times10^{9}\,EXP(-0.312V)$

* Deliberately skewed

Figure 5-7. $\bar{M}_w$, $\bar{M}_{rms}$ and MW calibration curves of dextran for case-studies #6 and 7

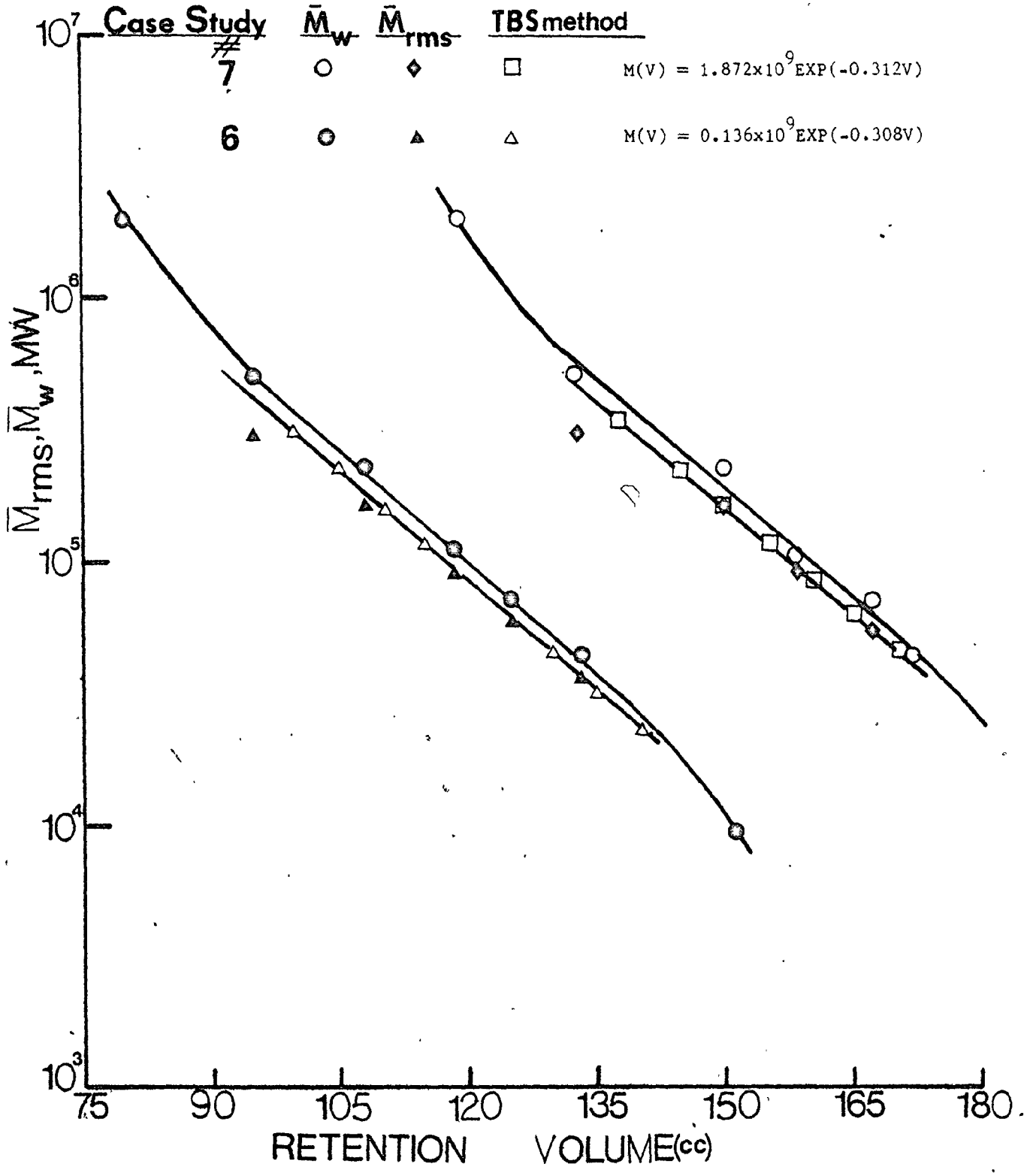

Figure 5-8. $\bar{M}_W$ range of separation of different pore-sizes for dextran

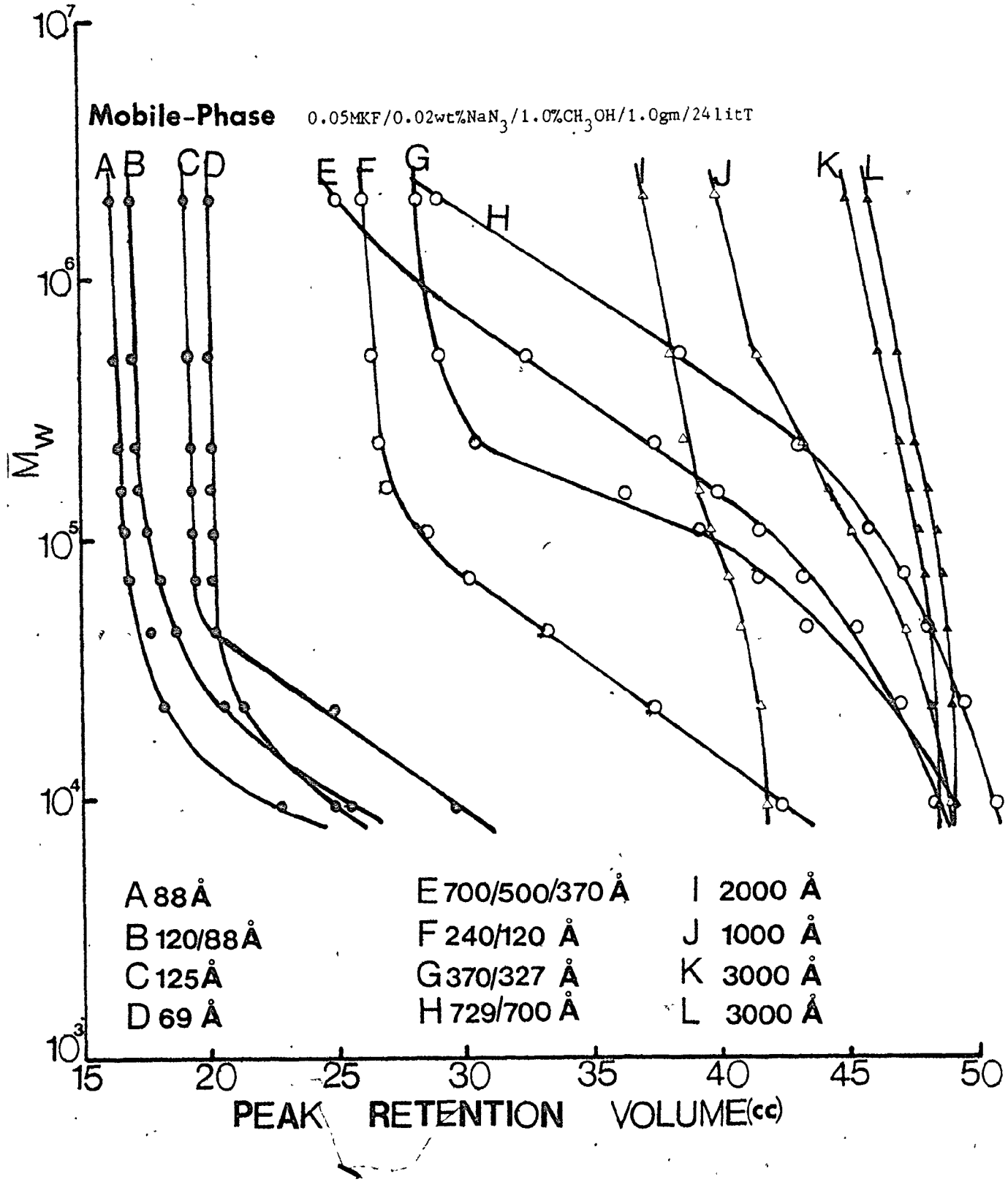

5-6 and 5-7, the $\bar{M}_W$ regions of separation of each pore-sizes are listed. Table 5-6 contains data based on Fig. 5-8 and Table 5-7 those corresponding to Fig. 5-6, which when compared with Table 5-1, clearly shows the important need of working with and calibrating single columns as a first major step in studies involving SEC.

The results of Case-Studies #8, to 15 are shown in Tables5-8 to 10 and their corresponding $\bar{M}_W$, $\bar{M}_{rms}$ and true MW calibration curves are shown in Figs. 5-9 to 12. As shown by these data, as was anticipated, the values D2 for case study #13 are noticed to vary widely. The same but less variation was also observed for Case Studies #8 and 10. In others, almost constant values of D2 were obtained, and in almost all the cases excellent molecular weight correction factors were obtained with P_K usually close to one. For the last two case-studies (#14 and 15), where the same six column combination was used, as shown in Fig. 5-12, for where polymer-surface interaction is non existent or negligible, the MW calibration curves are noticed to be different for both forward and reversed flow arrangements. The forward shift of the MW calibration of the former arrangement, reflects the influence of large surface areas of the small pore-size packing materials.

At this stage when a fully optimized system could now be realised, studies pertaining to flow rate were again investigated. For this purpose case-studies #16, 17 and 18 were conducted at flow-rates of 1.43, 4.30 and 7.83 ml/min respectively. Data relevant to the system selected for the flow-rate studies are shown in Fig. 5-13. For this system there was no MW gap. The results of application of the TBS method are listed in Table 5-11. In Fig. 5-14, the $\bar{M}_W$ calibration curves are shown in counts

Table 5-6. Measured Molecular Weight Exclusion Limit for Dextrans

Average Pore Size Å	Molecular Weight Region of Separation (b) From		To	Length of Column (ft)	Size * Separation (cc)	
69 (a)	Unknown	-	1.5×10^4	2.92	4.80	
88	Unknown	-	2.0×10^4	2.50	6.50	
88/120	Unknown	-	2.3×10^4	2.67	8.50	
125	Unknown	-	5.0×10^4	2.83	10.40	
120/240	Unknown	-	1.2×10^5	3.89 (0.1645)	16.30	
370/327	6.0×10^4	-	2.4×10^5	4.00 (0.0924)	20.10	
700/500/370	9.5×10^4	-	1.2×10^6	3.83	23.40	
727/700	1.7×10^5	-	2.0×10^6	3.92 (0.1444)	22.0	
1000(D)	Two Linear Regions			3.83		
	(i) 5.0×10^4	-	5.0×10^5		7.5	9.10
	(ii) 5.0×10^5	-	2.0×10^6		2.6	
2000(B)	Two Linear Regions			3.92		
	(i) 2.1×10^4	-	2.5×10^5		3.1	4.60
	(ii) 2.5×10^5	-	2.0×10^6		1.5	
3000(D)	1.0×10^5	-	2.0×10^6	3.92	3.50	

* Separation between T2000 and T10 standards.

** Separation between T10 and Intermediate Molecular Weight Exclusion Limit

(a) CPG-10

(b) Mobile-Phase: As specified in Figure 5-8
In parentheses (of the 3rd column) are D2 measured in cc^{-1}

Table 5-7. Measured Molecular Weight Exclusion Limits for Dextrans

Average Pore Sizes Å	Molecular Weight Region of Separation From	To	Length of Column (ft)	Size Separation (cc)	
240/120[a]	Unknown	1.2×10^5	3.92	14.50	
370[a]	6.0×10^4	2.4×10^5	3.75	20.00	
500[a]	1.0×10^5	2.0×10^6	2.08	12.00	
500/700[a]	3.0×10^5	2.0×10^6	4.00	24.00	
1500[b]	Unknown	2.0×10^6	4.00	6.85	
4900[c]	Two Linear Regions		4.00 (2.7726)	1.50 1.20	2.70
	(i) Unknown	7.0×10^4			
	(ii) 7.0×10^4	2.0×10^6			
3000[a](A)	1.0×10^5	2.0×10^6	3.83	3.40	
*1000(E)[a]	Two Linear Regions		3.83		
	(i) 5.0×10^4	5.0×10^5		7.90	9.70
	(ii) 5.0×10^5	2.0×10^6		1.80	
*1000(B)[a]	Two Linear Regions		3.92		
	(i) 5.0×10^4	5.0×10^5		7.50	9.5
	(ii) 5.0×10^4	2.0×10^6		2.00	
2500[b]	6.0×10^4	2.0×10^6	4.00	3.10	

(a) CPG-10 Mobile-phase 0.01 M NaF as shown in Figure 5-6

(b) Bio-glass Previously silanized in previous studies (52). Mobile-phase as in Figure 5-6

(c) EM-Gel of fractosils. Mobile-phase as in Figure 5-6

* Mobile-phase as specified in Figure 5-6

Table 5-8. Application of TBS method to Case-Studies #8, 9 and 10

#	Paired Samples	σ^2_{D2} (count)^2	D1	D2 (count)$^{-1}$	P_K
		Case Study #8			
		Linear Region of Calibration			
1	T110 T150	0.123 -1.11	0.277×10^{9}	0.381	0.991 1.084
2	T40 T250	0.27 -0.30	0.378×10^{9}	0.399	0.979 1.024
3	T40 T150	0.54 -0.40	0.622×10^{9}	0.420	0.953 1.036
4	T40 T110	0.68 0.63	0.823×10^{9}	0.432	0.939 0.943
5	T110 T250	-0.21 -1.45	0.163×10^{9}	0.356	1.013 1.096
6	T70 T150	0.39 -0.22	0.789×10^{9}	0.432	0.964 1.021
7	T70 T250	-0.09 -0.32	0.370×10^{9}	0.398	1.007 1.026
		Non-Linear Region of Calibration			
8	T10 T20	0.75 1.41	0.871×10^{13}	0.816	0.780 0.626
9	T10 T40	0.44 2.11	0.682×10^{12}	0.682	0.903 0.612
10	T10 T70	0.85 1.60	0.245×10^{11}	0.586	0.864 0.760
11	T10 T110	-0.09 1.32	0.113×10^{11}	0.556	1.013 0.815
12	T10 T150	-0.22 0.84	0.630×10^{10}	0.533	1.032 0.888
		Case Study #10			
		Linear Region of Calibration			
	T110 T150	0.009 -1.346	0.101×10^{10}	0.352	0.994 1.087
	T40 T250	0.889 -0.902	0.173×10^{10}	0.371	0.941 1.064
	T10 T110	-0.110 0.176	0.116×10^{10}	0.357	1.007 0.989
	T10 T150	-0.120 -1.225	0.114×10^{10}	0.356	1.008 1.081
	T20 T110	0.151 0.081	0.981×10^{9}	0.351	0.991 0.995
	T20 T150	0.154 -1.373	0.986×10^{9}	0.351	0.991 1.088
	T70 T250	0.936 -0.133	0.379×10^{10}	0.402	0.927 1.011
		Non-Linear Region of Calibration			
	T20 T500	0.410 -2.953	0.157×10^{10}	0.366	0.973 1.219
	T40 T500	0.970 -2.523	0.200×10^{10}	0.376	0.934 1.195
		Case Study #9			
	T40 T250	-0.49 -0.12	0.317×10^{9}	0.295	1.044 1.084

Table 5-8 continued

#	Paired Samples	Case Study #8 $\sigma^2_{D2\,(count)^2}$	D1	$D2_{(count)^{-1}}$	P_K	Paired Samples	Case Study #9 $\sigma^2_{D2\,(count)^2}$	D1	$D2_{(count)^{-1}}$	P_K	#
		Non-Linear Region of Calibration					Linear Region of Calibration				
13	T10 T250	-0.45 1.31	0.276×10^{10}	0.501	1.058 0.848	T70 T250	0.22 -0.04	0.387×10^{9}	0.304	0.990 1.002	2
14	T10 T500	-0.45 1.07	0.281×10^{10}	0.502	1.058 0.874	T40 T150	0.17 0.01	0.417×10^{9}	0.304	0.992 1.000	3
15	T20 T40	0.70 1.58	0.127×10^{11}	0.550	0.900 0.788	T110 T500	0.89 -2.53	0.406×10^{9}	0.304	0.960 1.124	4
16	T20 T70	0.27 0.87	0.215×10^{10}	0.497	0.970 0.906	T40 T500	-0.06 -2.77	0.376×10^{9}	0.301	1.003 1.134	5
17	T20 T110	0.23 0.92	0.193×10^{11}	0.473	0.974 0.902	T40 T110	0.06 -0.72	0.334×10^{9}	0.297	0.997 1.032	6
18	T20 T150	0.12 0.11	0.133×10^{10}	0.457	0.988 0.988	T70 T500	-0.37 -2.21	0.450×10^{9}	0.308	1.018 0.900	7
19	T20 T250	-0.10 0.38	0.741×10^{9}	0.434	1.009 0.965	T150 T500	0.32 -3.12	0.339×10^{9}	0.296	0.986 0.872	8
20	T20 T500	0.02 -0.02	0.100×10^{10}	0.446	0.999 1.002	T110 T250	-0.61 0.64	0.295×10^{9}	0.293	1.026 0.973	9
21	T500 T250	1.13 1.36	0.301×10^{10}	0.506	0.866 0.840		Non-Linear Region of Calibration				
22	T500 T150	-0.58 -0.34	0.668×10^{9}	0.424	1.053 1.031	T10 T20	1.08 1.82	0.146×10^{13}	0.559	0.845 0.753	10
23	T500 T110	-0.87 0.47	0.554×10^{9}	0.414	1.078 0.961	T10 T110	-0.65 2.21	0.379×10^{10}	0.385	1.049 0.849	11
24	T500 T70	-0.48 0.33	0.715×10^{9}	0.427	1.045 0.970	T10 T150	-0.74 2.21	0.317×10^{10}	0.379	1.055 0.853	12
						T10 T500	-1.20 0.55	0.142×10^{10}	0.356	1.079 0.966	13

Table 5-8 continued

#	Paired Samples	σ^2_{D2} $(count)^2$	Case Study #9 D1	D2 $(count)^{-1}$	P_K
			Non-Linear Region of Calibration		
14	T20 T40	0.29 1.75	0.372×10^{10}	0.375	0.980 0.883
15	T20 T70	-0.55 1.02	0.839×10^{9}	0.330	1.030 0.947
16	T20 T110	-0.63 1.35	0.749×10^{9}	0.326	1.034 0.930
17	T20 T150	-0.60 0.85	0.773×10^{9}	0.327	1.033 0.956
18	T20 T500	-0.85 -1.63	0.551×10^{9}	0.317	1.044 1.085
19	T250 T500	0.57 -1.62	0.553×10^{9}	0.317	0.972 1.085

$M(V) = 0.439 \times 10^{9} EXP(-0.403V)$ (Case Study #8)

$M(V) = 0.359 \times 10^{9} EXP(-0.300V)$ (Case Study #9)

$M(V) = 1.080 \times 10^{9} EXP(-0.353V)$ (Case Study #10)

Table 5-9. Application of TBS method to Case Studies #11, 12 and 13

#	Paired Samples	Case Study #11 σ^2_{D2} (count)^2	D1 $\times 10^{-9}$	D2 (count)$^{-1}$	P_K	Paired Samples	Case Study #12 σ^2_{D2} (count)^2	D1 $\times 10^{-9}$	D2 (count)$^{-1}$	P_K
		Linear Region of Calibration					Linear Region of Calibration			
1	T20 T250	-0.64 -0.28	0.575	0.287	1.027 1.012	T20 T250	-0.35 -1.43	0.538	0.289	1.015 1.062
2	T110 T500	1.24 -3.39	0.751	0.295	0.948 1.159	T110 T500	0.42 -5.09	0.497	0.283	0.983 1.226
3	T150 T500	0.51 -2.43	1.052	0.307	0.976 1.121	T150 T500	-0.33 -3.80	0.737	0.298	1.015 1.184
4	T70 T150	0.66 0.03	0.751	0.296	0.972 0.999	T70 T150	0.86 0.06	0.969	0.308	0.960 0.997
5	T20 T500	-0.45 -3.56	0.711	0.293	1.020 1.165	T20 T500	-0.14 -4.03	0.686	0.295	1.006 1.192
6	T20 T150	-0.66 -0.42	0.563	0.286	1.027 1.017	T40 T500	0.67 -4.57	0.579	0.289	0.972 1.210
7	T40 T240	0.23 -0.63	0.490	0.281	0.991 1.025	T40 T250	0.24 -2.12	0.394	0.278	0.991 1.085
8	T70 T250	0.59 0.14	0.711	0.294	0.975 0.994	T70 T250	0.28 -1.25	0.587	0.292	0.988 1.055
9	T110 T250	0.67 -1.03	0.411	0.275	0.975 1.040	T70 T500	0.69 -3.47	0.825	0.302	1.021 1.138
10	T20 T70	-0.88 -0.01	0.448	0.280	1.035 1.000	T20 T150	-0.17 -0.51	0.655	0.294	1.083 1.121
11	T20 T110	-0.50 1.14	0.675	0.291	1.021 0.953		Non-Linear Region of Calibration			
12	T40 T110	0.38 0.98	0.561	0.285	0.985 0.961	T10 T500	-0.68 -2.00	1.451	0.324	1.036 1.111
13	T70 T500	0.88 -2.83	0.911	0.302	0.961 1.138	T250 T500	0.39 -1.87	1.534	0.326	0.980 1.105

Table 5-9. Application of TBS method

#	Paired Samples	σ^2_{D2} (count)^2	D1 x10^{-9}	D2 (count)$^{-1}$	P_K
		Case Study #12 contd.			
		Linear Region of Calibration			
1	T40	0.62	0.670	0.291	0.977
	T500	-2.83			1.172
15	T40	0.14	0.453	0.279	0.995
	T150	-0.79			1.031
		Non-Linear Region of Calibration			
1	T10	0.83	36.860	0.402	0.935
	T20	1.70			0.872
2	T10	-0.10	5.196	0.351	1.006
	T40	2.14			0.876
3	T10	-0.76	1.919	0.325	1.033
	T70	1.62			0.918
4	T10	-0.79	1.841	0.324	1.042
	T110	1.89			0.906
5	T10	-1.01	1.383	0.317	1.052
	T150	0.86			0.958
6	T10	-1.08	1.268	0.314	1.055
	T500	-1.94			1.101
7	T250	1.28	1.383	0.318	0.937
	T500	-1.71			1.091
		Case Study #13			
		Linear Region of Calibration			
1	T10	-1.73	0.699	0.291	1.076
	T150	0.18			0.992
2	T20	-0.12	0.808	0.289	1.005
	T500	-1.91			1.083

Paired Samples	σ^2_{D2} (count)^2	D1 x10^{-9}	D2 (count)$^{-1}$	P_K	#
	Case Study #13 contd.				
	Linear Region of Calibration				
T40	0.88	0.824	0.290	0.964	3
T500	-1.85			1.081	
T10	-1.77	0.670	0.290	1.077	4
T250	0.05			0.998	
T20	-0.19	0.747	0.287	1.008	5
T40	0.78			0.968	
* T150	-0.34	0.509	0.280	1.013	6
T250	-0.53			1.021	
T20	-0.61	0.485	0.275	1.023	7
T110	0.97			0.964	
	Effect of Pore-Size Arrangement				
T40	-0.01	0.377	0.267	1.000	1
T110	0.70			0.975	
T70	0.16	0.238	0.255	0.995	2
T150	-1.87			1.063	
T20	-1.11	0.308	0.263	1.039	3
T250	-1.76			1.063	
T40	-1.87	0.116	0.233	1.052	4
T70	-1.33			1.037	
T20	-1.06	0.321	0.264	1.038	5
T70	0.67			0.977	
* T110	-0.69	0.135	0.234	1.019	6
T250	-4.42			1.129	
T40	-0.67	0.233	0.253	1.022	7
T250	-2.55			1.085	

Table 5-10. Application of TBS method for Case Studies #14 and 15

#	Paired Samples	Case Study #14 σ^2_{D2} (count)^2	Case Study #14 P_K	Case Study #14 D2 (count)$^{-1}$	Case Study #14 D1x10^{-9}	Case Study #15 σ^2_{D2} (count)^2	Case Study #15 P_K	Case Study #15 D2 (count)$^{-1}$	Case Study #15 D1x10^{-9}
				Linear Region of Calibration					
1	T40	0.75	0.97	0.269	0.665	1.64	0.94	0.264	0.633
	T250	-1.56	1.06			-1.24	1.04		
2	T20	-0.63	1.02	0.266	0.621	--	--	--	--
	T150	-1.31	1.05						
3	T40	0.80	0.97	0.270	0.690	1.59	0.95	0.263	0.608
	T150	-1.12	1.04			-0.43	1.02		
4	T150	-1.38	1.05	0.265	0.598	-0.11	1.00	0.268	0.719
	T250	-1.82	1.07			-0.93	1.03		
5	T20	-0.64	1.02	0.266	0.616	1.21	1.04	0.259	0.539
	T250	-1.75	1.06			-1.64	1.06		
6	T20	--	--	--	--	1.65	0.94	0.269	0.812
	T110					1.95	0.93		
7	T110	0.40	0.99	0.257	0.462	--	--	--	--
	T250	-2.48	1.09						
				Non-Linear Region of Calibration					
1	T10	0.49	0.98	0.304	2.687	1.94	0.91	0.314	4.762
	T20	0.65	0.97			3.08	0.86		
2	T10	-0.26	1.01	0.284	1.183	0.76	0.97	0.282	1.225
	T40	1.39	0.95			2.38	0.91		
3	T10	-0.92	1.03	0.270	0.644	--	--	--	--
	T70	0.40	0.99						
4	T10	-0.38	1.02	0.282	1.048	0.85	0.97	0.284	1.334
	T110	1.24	0.95			2.41	0.91		
5	T10	-0.54	1.02	0.278	0.902	0.39	0.99	0.274	0.859
	T150	-0.65	1.03			0.21	0.99		

Table 5-10 contd.

#	Paired Samples	Case Study #14 $\sigma^2_{D2_2}$ count	Case Study #14 P_K	Case Study #14 D2 $(count)^{-1}$	Case Study #14 $D1\times10^{-9}$	Case Study #15 $\sigma^2_{D2_2}$ count	Case Study #15 P_K	Case Study #15 D2 $(count)^{-1}$	Case Study #15 $D1\times10^{-9}$
				Non-Linear Region of Calibration					
6	T10 T250	--	--	--	--	0.36 -0.59	0.99 1.02	0.273	0.837
7	T10 T500	-0.28 -3.96	1.01 1.17	0.284	1.165	0.81 -3.20	0.97 1.14	0.283	1.287
8	T250 T500	1.88 -0.34	0.90 1.02	0.334	5.091	3.42 1.87	0.80 0.89	0.362	13.610
9	T150 T500	0.61 -2.24	0.97 1.11	0.305	2.141	--	--	--	--
10	T110 T500	1.47 -3.45	0.94 1.15	0.290	1.276	2.33 -3.37	0.91 1.14	0.281	1.228
11	T70 T500	1.81 -2.35	0.92 1.11	0.303	2.051	2.38 -1.65	0.90 1.08	0.301	2.223
12	T40 T500	1.36 -3.98	0.95 1.17	0.284	1.165	2.46 -3.11	0.01 1.13	0.284	1.322
13	T20 T500	--	--	--	--	1.84 -4.08	0.93 1.17	0.274	0.985

$M(V) = 0.608\times10^{9}EXP(-0.288V)$ #11

$M(V) = 0.623\times10^{9}EXP(-0.292V)$ #12

$M(V) = 0.672\times10^{9}EXP(-0.286V)$ #13

$M(V) = 0.655\times10^{9}EXP(-0.267V)$ #14

$M(V) = 0.672\times10^{9}EXP(-0.265V)$ #15

Figure 5-9. $\bar{M}_w$, $\bar{M}_{rms}$ and MW calibration curves of dextran for Case-Study #8

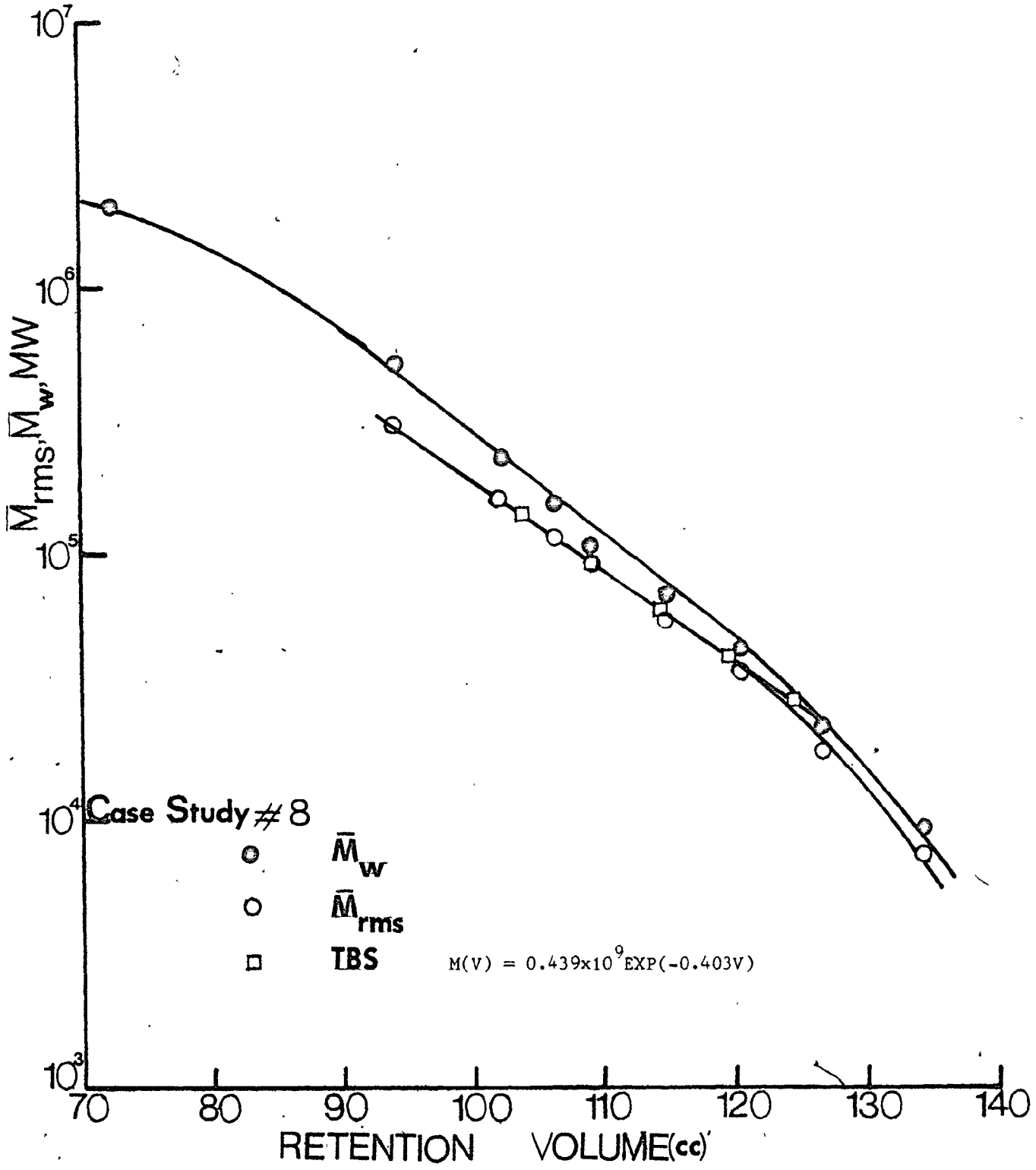

Figure 5-10. $\bar{M}_w$, $\bar{M}_{rms}$ and MW calibration curves of dextran for Case-Studies #9 and 10

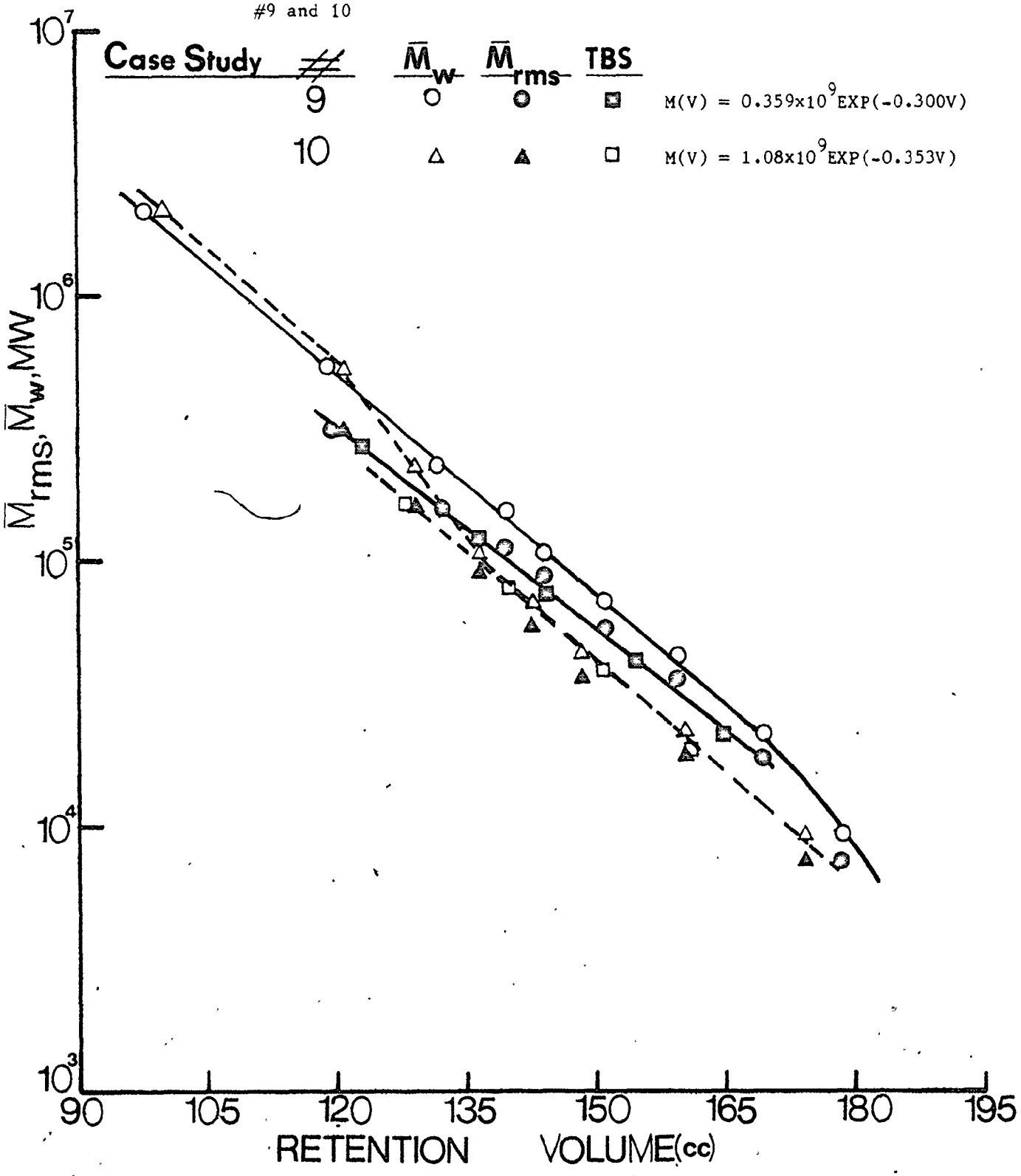

Figure 5-11. $\bar{M}_w$, $\bar{M}_{rms}$ and MW calibration curves of dextran for Case-Studies[129] #11, 12 and 13

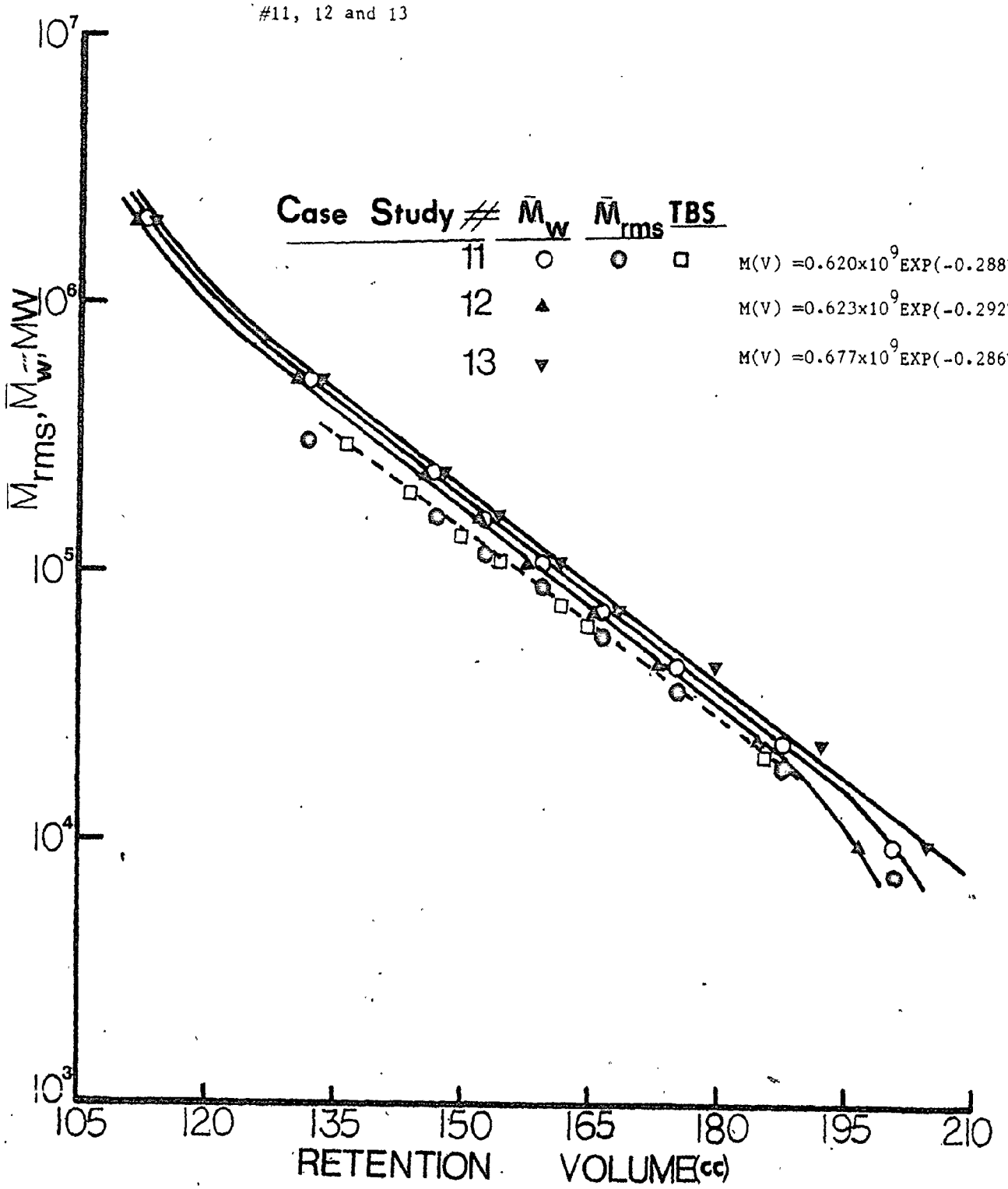

Figure 5-12. $\bar{M}_w$, $\bar{M}_{rms}$ and MW calibration curves of dextran for Case-Studies #14 and 15

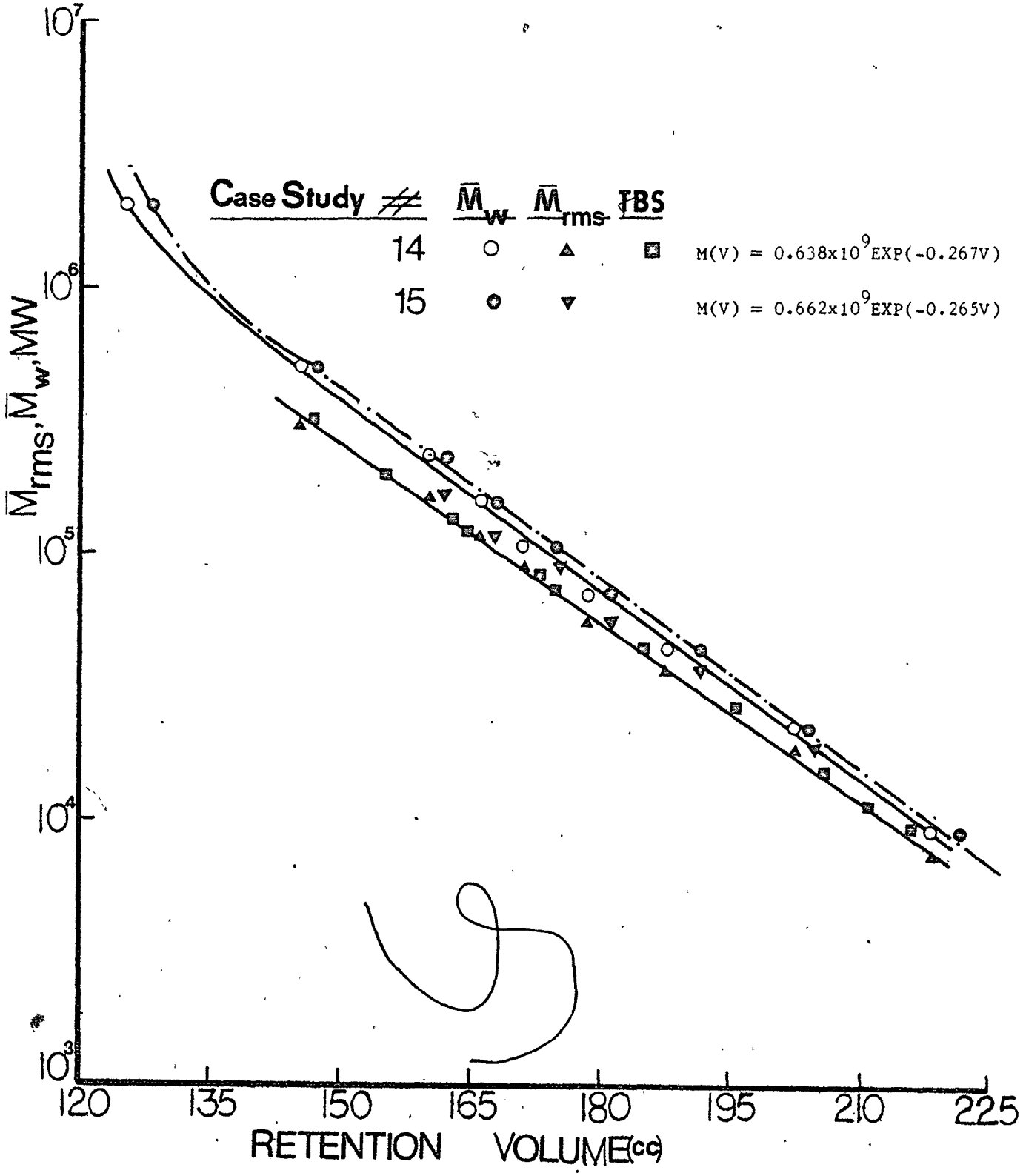

Figure 5-13. $\bar{M}_w$ range of separation of different pore-sizes for dextran

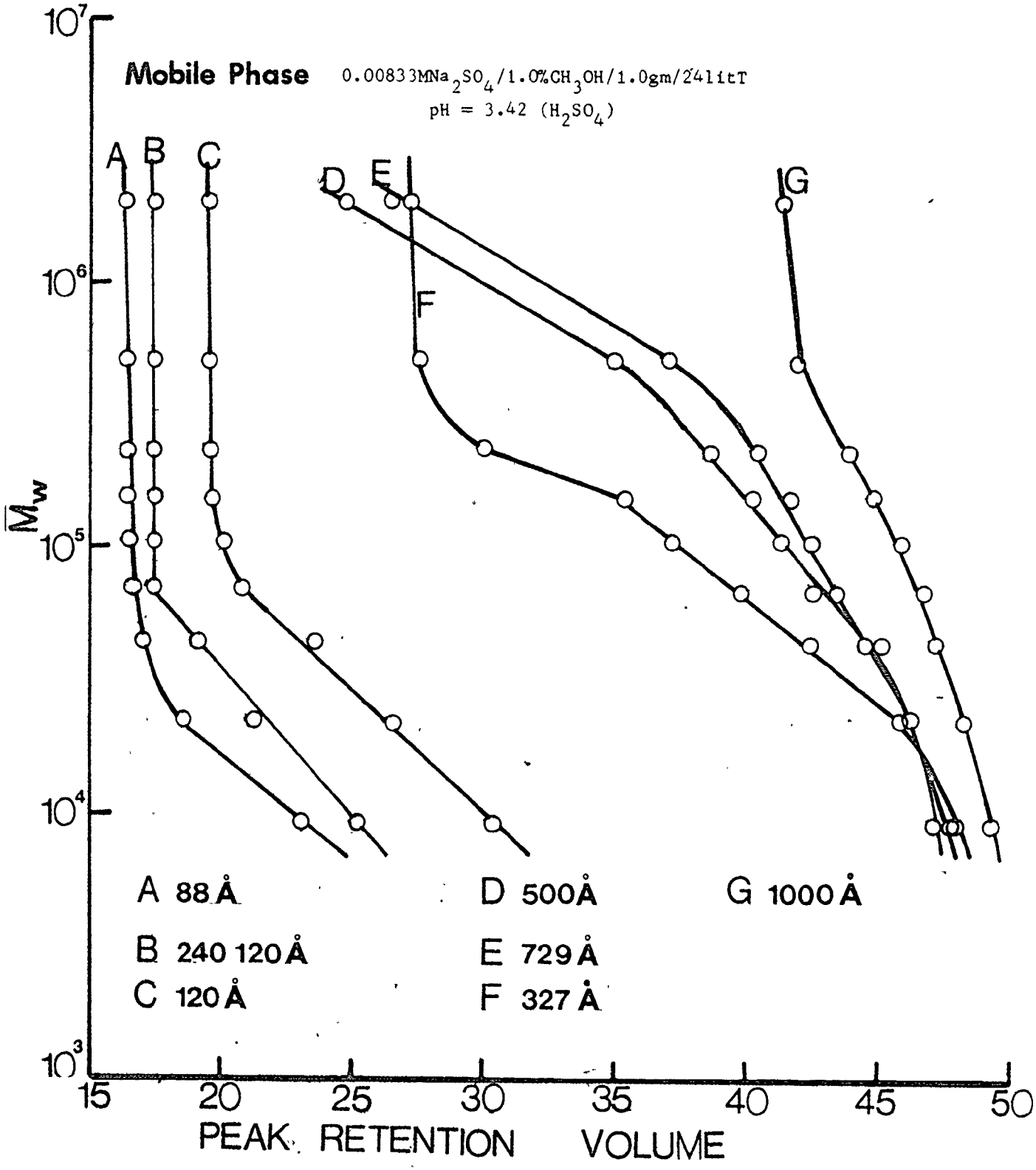

Table 5-11. Application of TBS method to Case-Studies #16, 17 and 18

#	Paired Samples	Case-Study #16 (1.43 ml/min) σ^{-2}_{D2} (count)^2	$D1 \times 10^{-9}$	D2 (count)$^{-1}$	P_K	Paired Samples	Case-Study #17 (4.3 ml/min) σ^{-2}_{D2} (count)^2	$D1 \times 10^{-9}$	D2 (count)$^{-1}$	P_K	#
		Linear Region of Calibration					Linear Region of Calibration				
1	T10 T500	-2.01 -5.68	0.940	0.286	1.09 1.26	T70 T250	-0.33 -2.07	0.510	0.286	1.01 1.09	1
2	T10 T70	-2.12 -0.05	0.843	0.283	1.09 1.00	T150 T250	-1.35 -1.91	0.549	0.289	1.06 1.08	2
3	T10 T110	-2.07 -0.49	0.881	0.284	1.09 1.02	T20 T70	-0.40 -0.47	0.458	0.283	1.02 1.02	3
4	T10 T250	-2.17 -2.40	0.803	0.282	1.09 1.10	T20 T110	-0.16 0.11	0.586	0.290	1.01 0.99	4
* 5	T20 T500	-1.15 -6.73	0.691	0.275	1.04 1.29	T20 T150	-0.36 -1.60	0.474	0.284	1.02 1.07	5
6	T40 T500	-0.54 -6.36	0.767	0.278	1.02 1.28	T20 T250	-0.34 -2.17	0.487	0.285	1.01 1.09	6
7	T70 T500	0.20 -5.39	1.031	0.289	0.99 1.25	T40 T150	0.26 -1.39	0.535	0.288	0.99 1.06	7
8	T110 T500	-0.34 -5.37	1.037	0.285	1.01 1.25	T40 T250	0.27 -1.96	0.538	0.288	0.99 1.09	8
9	T20 T150	-0.78 -2.45	1.023	0.288	1.03 1.11	T70 T150	-0.37 -1.53	0.493	0.285	1.02 1.06	9
10	T70 T110	0.18 -0.36	1.013	0.280	0.99 1.02		Non-Linear Region of Calibration				
11	T70 T250	-0.20 -2.53	0.753	0.277	1.01 1.10	T10 T20	0.30 1.54	8.117	0.363	0.98 0.90	1
		Traces of Non-Linearity				T10 T40	-0.73 1.26	1.600	0.321	1.04 0.94	2
1	T10 T20	-0.68 0.32	4.57	0.320	1.04 0.98	T10 T70	-0.91 0.73	1.279	0.315	1.05 0.96	3

Table 5-11 contd.

#	Paired Samples	σ^{-2}_{D2} (count)^2	D1 $\times 10^{-9}$	D2 (count)$^{-1}$	P_K
		Case Study #16 (1.43 ml/min) Traces of Non-Linearity			
2	T10 T40	-1.61 0.08	1.420	0.296	1.07 1.00
3	T250 T500	-0.91 -3.80	1.813	0.309	1.04 1.20
		Case Study #18 (7.85 ml/min) Linear Region of Calibration			
1	T20 T250	0.58 0.32	0.721	0.320	0.97 0.98
2	T40 T250	1.24 0.37	0.742	0.321	0.94 0.98
3	T110 T250	1.31 0.69	0.915	0.329	0.93 0.96
4	T20 T40	0.52 1.15	0.667	0.318	0.97 0.94
5	T20 T70	0.12 0.40	0.407	0.303	1.00 0.98
6	T20 T110	0.50 1.08	0.651	0.317	0.98 0.95
7	T20 T150	0.48 -0.17	0.629	0.316	0.98 1.01
8	T40 T110	1.12 1.06	0.641	0.316	0.95 0.95
9	T40 T150	1.08 -0.21	0.612	0.315	0.95 1.01

Paired Samples	σ^{-2}_{D2} (count)^2	D1 $\times 10^{-9}$	D2 (count)$^{-1}$	P_K	#
	Case Study #17 (4.3 ml/min) Non-Linear Region of Calibration				
T10 T110	-0.98 0.66	1.177	0.313	1.05 0.97	4
T10 T150	-1.20 -0.60	0.906	0.306	1.06 1.03	5
T10 T250	-1.27 -1.09	0.841	0.304	1.06 1.05	6
T10 T500	-0.99 -3.51	1.169	0.313	1.05 1.19	7
T250 T500	1.40 -0.40	5.531	0.371	0.91 1.03	8
T150 T500	0.44 -2.10	2.136	0.335	0.98 1.13	9
T110 T500	0.65 -3.53	1.156	0.312	0.97 1.89	10
T70 T500	0.56 -3.70	1.086	0.310	0.97 1.20	11
T40 T500	0.87 -3.93	0.996	0.307	0.96 1.20	12
T20 T500	0.12 -4.53	0.809	0.299	1.00 1.23	13

Table 5-11 contd.

#	Paired Samples	σ^2_{D2} (count)^2	Case Study #18 (7.83 ml/min) D1 x10^{-9}	D2 (count)$^{-1}$	P_K
		Linear Region of Calibration			
10	T110 T150	0.92 -0.41	0.529	0.309	0.96 1.02
		Non-Linear Region of Calibration			
1	T10 T20	0.81 1.95	9.471	0.398	0.94 0.86
2	T10 T40	0.11 2.07	2.404	0.359	0.99 0.88
3	T10 T70	-0.34 1.51	1.210	0.339	1.02 0.92
4	T10 T110	-0.28 1.54	1.328	0.342	1.02 0.91
5	T10 T150	-0.36 0.59	1.174	0.339	1.02 0.97
6	T10 T250	-0.34 1.09	1.208	0.339	1.02 0.94
7	T10 T500	-0.18 -1.50	1.511	0.346	1.01 1.10
8	T20 T500	0.84 -2.29	1.056	0.331	0.96 1.13
9	T40 T500	1.61 -2.01	1.192	0.336	0.91 1.12
10	T70 T500	1.84 -1.10	1.845	0.354	0.89 1.07
11	T110 T500	1.75 -1.05	1.893	0.355	0.90 1.07
12	T150 T500	1.43 -0.34	2.837	0.371	0.91 1.02
13	T250 T500	2.48 0.26	4.165	0.386	0.83 0.98

$M(V) = 0.884 \times 10^9 EXP(-0.284V)$ #16

$= 0.510 \times 10^9 EXP(-0.286V)$ #17

$= 0.623 \times 10^9 EXP(-0.316V)$ #18

Figure 5-14. $\bar{M}_w$ calibration curves of dextran for Case-Studies #16, 17 and 18

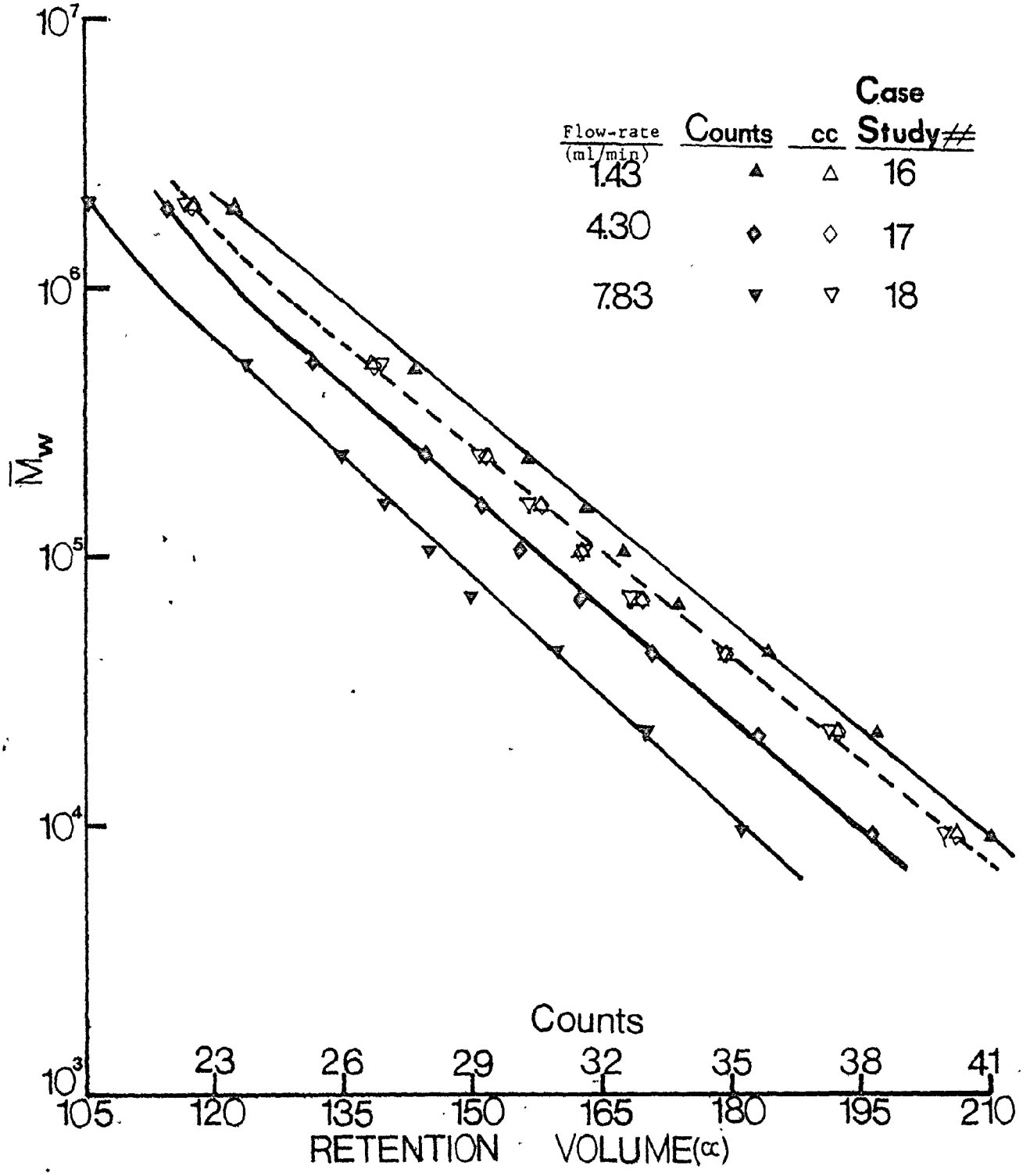

and cc for clarity. The importance of correction of elution volumes in counts, during flow-rate studies is shown in Table 5-12 where the variation of elution volume per count with flow-rate are listed for all the flow-rate cases studied. Thus when the correction is applied, the MW calibration curve is found to be independent of flow-rate. However, the MW correction factors P_K are seen to vary, though the corrections above and below 1.0 are negligible. At very low flow-rate, almost all the P_K values are seen to be greater than 1.0. At intermediate flow-rate, the same is true but at high flow-rate, most the values are less than 1.0.

The unique effect of organic solvent on sodium polystyrene sulfonate was shown and this solvent will now be used with dextran. For the same system used above, organic-based mobile-phase was employed with both reversed and forward flow arrangements. This is compared with inorganic-based mobile-phase using both reversed and forward flow arrangements. These are case-studies #19 and 20, and 17 and 21 respectively, all conducted at the same operating conditions. The results of the TBS method are shown and compared in Tables 5-13 and 5-14. The $\bar{M}_W$, $\bar{M}_{rms}$ and the MW calibration curves are shown in Fig. 5-15. Though the effect of surface area is apparent, it is however almost negligible. Again the P_K values are close to one, with values of P_K greater than one occurring more often with the well optimized systems especially at lower flow-rates.

A large number of the systems have thus far contained only small and intermediate pore-sizes. The role of large pore-sizes cannot however be completely understood without studies involving large pore-size multi-column systems. For this purpose case-studies #22 and 23 were selected with three and five columns respectively and at the same operating conditions. Table 5-15 gives results of the TBS method. Only

Table 5-12. Measured Variation of Elution Volume/count with flow-rate (ml/min)

Case-Studies #16, 17 and 18* (6 columns)

Flow-rate	Elution Volume	Case-Study #
1.43	5.00	17
4.30	5.30	18
7.83	5.82	19

* Mobile-phase: 0.00833 M Na_2SO_4/1.0% CH_3OH/1.0 gm/24 lit Tergitol (pH = 3.42 H_2SO_4)

Case-Studies #1 and 2* (6 columns)

Flow-rate	Elution Volume	Case-Study #
1.9	4.46	2
8.9	5.00	3

* Mobile-phase: Doubly distilled water

Case-Studies #3 and 4* (9 columns)

Flow-rate	Elution Volume	Case-Study #
2.25	4.85	5
4.00	5.00	4

* Mobile-phase: Triply distilled water

Case-Study #24 and 25* (4 columns)

Flow-rate	Elution Volume	Case-Study #
3.00	5.15	25
1.90	5.05	26

* Mobile-phase: 0.00833 M Na_2SO_4/1 gm/24 lit Tergitol (pH = 7.0)

Table 5-13. Application of TBS method to Case Studies #17 and 21

#	Paired Samples	Case Study #17 σ^2_{D2} (count)^2	D1 $\times 10^{-9}$	D2 (count)$^{-1}$	P_K	Paired Samples	Case Study #21 σ^2_{D2} (count)^2	D1 $\times 10^{-9}$	D2 (count)$^{-1}$	P_K
		Linear Region of Calibration					Linear Region of Calibration			
1	T20 T250	-0.34 -2.17	0.487	0.285	1.01 1.09	T20 T250	0.51 -1.74	0.498	0.281	0.98 1.07
2	T40 T150	0.26 -1.39	0.535	0.288	0.99 1.06	T40 T150	0.77 -1.57	0.464	0.280	0.97 1.06
3	T40 T250	0.27 -1.96	0.538	0.288	0.99 1.09	T40 T250	1.08 -1.50	0.612	0.288	0.96 1.06
4	T20 T150	-0.36 -1.60	0.474	0.286	1.02 1.07	T20 T150	0.28 -1.85	0.398	0.275	1.00 1.07
5	T70 T250	-0.33 -2.07	0.510	0.286	1.01 1.09	T10 T70	0.35 -0.16	0.479	0.283	0.99 1.01
6	T150 T250	-1.35 -1.91	0.549	0.289	1.06 1.08	T10 T150	0.60 -1.11	0.608	0.289	0.98 1.05
7	T20 T70	-0.40 -0.47	0.458	0.283	1.02 1.02	T20 T70	-0.50 -1.50	0.204	0.257	1.02 1.05
8	T70 T150	-0.37 -1.53	0.493	0.285	1.02 1.06	T10 T250	-0.51 -0.78	0.798	0.298	1.02 1.04
9	T20 T110	-0.16 0.11	0.586	0.290	1.01 1.00	T20 T110	-0.73 -0.68	0.171	0.252	1.02 1.02
		Non-Linear Region of Calibration					Traces of Non-Linearity			
1	T10 T20	0.30 1.54	8.117	0.363	0.98 0.90	T10 T20	0.94 2.23	5.580	0.347	0.95 0.87
2	T10 T40	-0.73 1.26	1.600	0.321	1.04 0.94	T10 T40	-0.18 1.68	1.151	0.307	1.01 0.92
3	T10 T70	-0.91 0.73	1.279	0.315	1.05 0.96	T150 T70	-0.36 0.73	1.010	0.306	1.02 0.97

Table 5-13. contd.

#	Paired Samples	σ^2_{D2} (count)^2	Case Study #17 D1 $\times 10^{-9}$	D2 (count)$^{-1}$	P_K
		Non-Linear Region of Calibration			
4	T10	-1.20	0.906	0.306	1.06
	T150	-0.60			1.03
5	T10	-1.27	0.841	0.304	1.06
	T250	-1.09			1.05
6	T10	-0.99	1.169	0.313	1.05
	T500	-3.51			1.89
7	T250	1.40	5.531	0.371	0.91
	T500	-0.40			1.03
8	T150	0.44	2.136	0.335	0.98
	T500	-2.10			1.19
9	T110	0.65	1.156	0.312	0.97
	T500	-3.53			1.19
10	T70	0.56	1.086	0.310	0.97
	T500	-3.70			1.2
11	T40	0.87	0.996	0.307	0.96
	T500	-3.93			1.20
12	T20	0.12	0.809	0.299	1.0
	T500	-4.53			1.23

$M(V) = 0.510 \times 10^9 EXP(-0.286V)$

#	Paired Samples	σ^2_{D2} (count)^2	Case Study #21 D1 $\times 10^{-9}$	D2 (count)$^{-1}$	P_K
		Traces of Non-Linearity			
4	T70	0.89	1.171	0.311	0.96
	T250	-0.11			1.01
5	T10	-0.51	0.798	0.298	1.02
	T250	-0.78			1.04
6	T10	-0.32	0.990	0.303	1.02
	T500	-3.51			1.18
7	T250	1.00	2.528	0.338	0.95
	T500	-1.27			1.08
8	T150				
	T500	--	--	--	--
9	T110	2.17	6.889	0.375	0.86
	T500	0.45			0.97
10	T70	1.15	1.542	0.319	0.94
	T500	-2.35			1.13
11	T40	1.48	0.916	0.300	0.94
	T500	-3.73			1.18
12	T20	0.84	0.716	0.291	0.97
	T500	-4.48			1.21

$M(V) = 0.523 \times 10^9 EXP(0.284V)$

Table 5-14. Application of TBS method to Case-Studies #19 and 20

#	Paired Samples	Case Study #19 σ^{-2}_{D2} (count)^2	D1 $\times 10^{-9}$	D2 (count)$^{-1}$	P_K	Paired Samples	Case Study #20 σ^{-2}_{D2} (count)^2	D1 $\times 10^{-9}$	D2 (count)$^{-1}$	P_K
		Linear Region of Calibration					Linear Region of Calibration			
1	T20	-0.32	0.559	0.284	1.01	T20	0.01	0.421	0.277	1.00
	T110	0.49			0.98	T110	0.11			0.97
2	T20	-0.44	0.497	0.280	1.02	T20	0.14	0.478	0.280	1.00
	T150	-1.25			1.05	T150	-0.30			1.05
3	T20	-0.35	0.545	0.283	1.01	T20	0.06	0.433	0.278	1.00
	T250	-1.50			1.06	T250	-2.19			1.09
4	T40	1.09	0.420	0.278	0.95	T40	1.18	0.514	0.283	0.95
	T110	0.34			0.99	T110	0.30			0.99
5	T40	1.12	0.493	0.279	0.96	T40	1.12	0.490	0.282	0.96
	T250	-1.72			1.07	T250	-1.91			1.08
6	T110	0.41	0.515	0.281	0.98	T110	0.20	0.462	0.280	0.99
	T250	-1.62			1.07	T250	-2.04			1.08
7	T40	0.93	0.420	0.275	0.97	T40	1.34	0.597	0.288	0.95
	T150	-1.55			1.06	T150	-0.96			1.04
		In the Neighbourhood of Non-Linear Region								
1	T10	-0.74	1.103	0.304	1.06	T10	0.38	0.875	0.298	0.98
	T500	-3.54			1.18	T500	-4.39			1.22
2	T10	-1.09	0.774	0.295	1.05	T10	-0.10	0.545	0.286	1.00
	T250	-0.78			1.04	T250	-1.68			1.07
3	T10	-1.09	0.762	0.295	1.05	T10	0.03	0.612	0.289	1.00
	T150	-0.54			1.02	T150	-0.92			1.04
4	T10	-0.94	0.887	0.299	1.04	T10	-0.04	0.575	0.287	1.00
	T110	-0.89			1.04	T110	0.41			0.98
5	T10	-1.11	0.744	0.294	1.05	T10	-0.11	0.540	0.285	1.01
	T70	1.10			0.95	T70	0.97			0.96

Table 5-14, contd.

#	Paired Samples	σ^2_{D2} (count)^2	Case Study #19 D1 $\times 10^{-9}$	D2 (count)$^{-1}$	P_K	Paired Samples	σ^2_{D2} (count)^2	Case Study #20 D1 $\times 10^{-9}$	D2 (count)$^{-1}$	P_K
					In the Neighbourhood of Non-Linear Region					
6	T10 T40	-0.48 2.21	1.504	0.312	1.02 0.90	T10 T40	0.05 1.39	0.627	0.289	1.00 1.06
7	T10 T20	0.01 0.92	2.849	0.328	1.00 0.95	T10 T20	0.70 1.06	1.228	0.306	0.97 0.95
8	T250 T500	2.06 0.01	6.076	0.366	0.87 1.00	T250 T500	2.26 0.50	10.371	0.389	0.84 0.97
9	T150 T500	1.09 -1.30	2.862	0.339	0.94 1.08	T150 T500	0.70 -2.21	2.064	0.329	0.97 1.13
10	T110 T500	1.32 -2.61	1.575	0.317	0.94 1.14	T110 T500	1.27 -2.53	1.787	0.324	0.94 1.14
11	T70 T500	1.90 -2.62	1.573	0.317	0.91 1.14	T70 T500	2.02 -3.21	1.341	0.313	0.91 1.17
12	T40 T500	1.80 -3.98	0.944	0.298	0.92 1.19	T40 T500	1.89 -3.86	1.054	0.305	0.92 1.20
13	T20 T500	0.01 -4.12	0.901	0.297	1.00 1.20	T20 T500	0.62 -4.63	0.810	0.295	0.97 1.22

$M(V) = 0.498 \times 10^{9} EXP(-0.280V)$

$M(V) = 0.473 \times 10^{9} EXP(-0.281V)$

Figure 5-15. $\bar{M}_w$, $\bar{M}_{rms}$ and MW calibration curves of dextran for Case-Studies #17, 19, 20 and 21

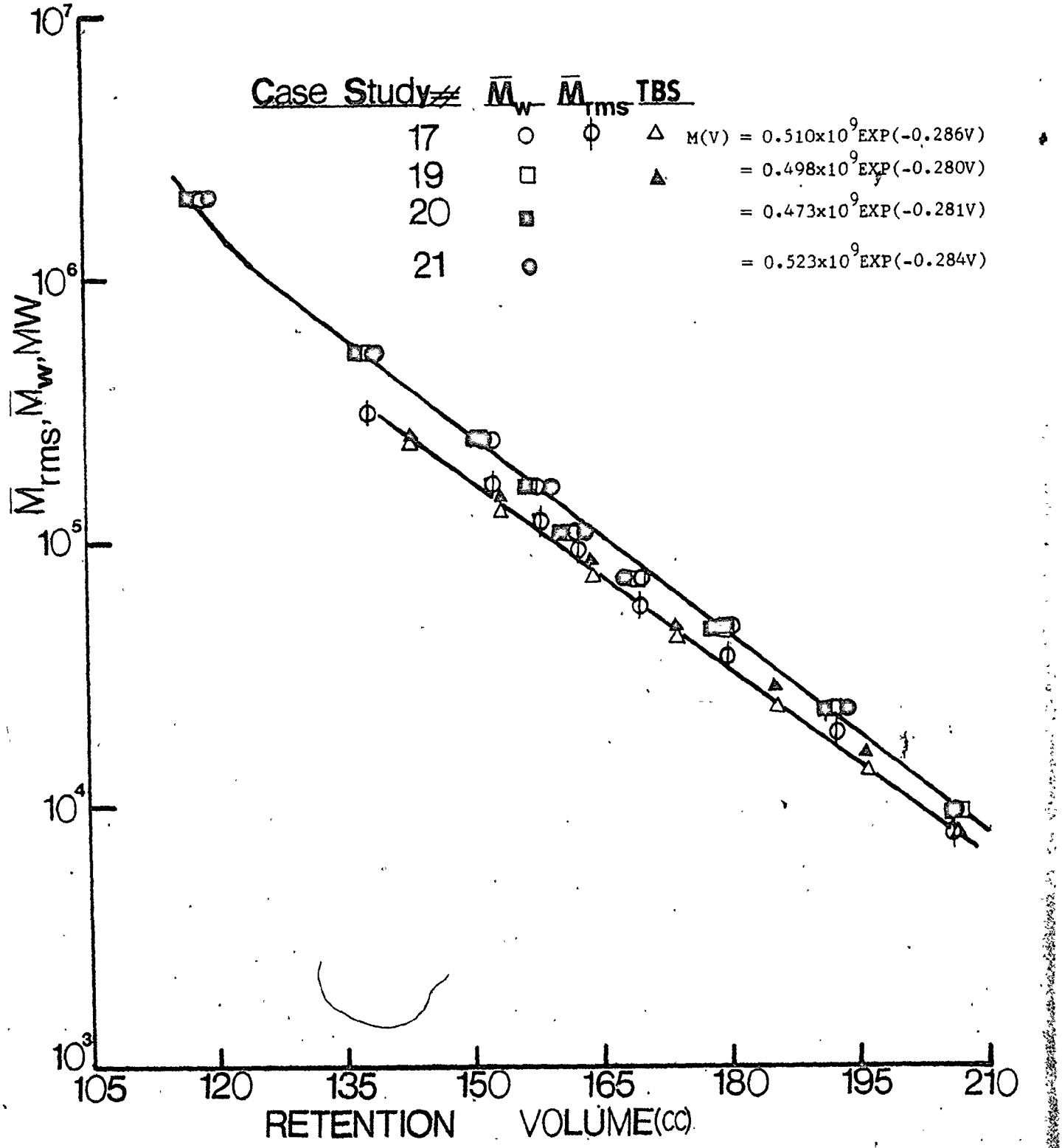

Table 5-15. Application of TBS method to Case-Studies #22 and 23

#	Paired Samples	Case Study #22 σ^2_{D2} (count)^2	D1 $\times 10^{-9}$	D2 (count)$^{-1}$	P_K	Paired Samples	Case Study #23 σ^2_{D2} (count)^2	D1 $\times 10^{-9}$	D2 (count)$^{-1}$	P_K
		Linear Region of Calibration					Linear Region of Calibration			
1	T40	1.11	0.073	1.504	0.29	T10	3.66	5.86	1.120	0.10
	T500	2.00			0.10	T40	4.10			0.08
2	T40	1.13	0.306	1.568	0.25	T40	4.11	3.580	1.105	0.08
	T250	1.49			0.16	T250	5.20			0.04
3	T40	1.19	3105.0	1.985	0.10	T40	4.10	0.38×10^{3}	1.244	0.04
	T110	1.45			0.05	T110	4.55			0.03
4	T40	1.16	251.2	1.768	0.16	T40	4.10	0.015	0.942	0.16
	T70	1.20			0.15	T70	4.42			0.14
5	T70	1.14	0.019	1.438	0.31	T10	3.66	1.213	1.075	0.12
	T500	1.97			0.13	T70	4.44			0.08
6	T70	1.15	0.062	1.492	0.28	T70	4.41	0.80×10^{2}	1.201	0.04
	T250	1.47			0.20	T250	5.17			0.02
7	T110	1.35	0.50×10^{-3}	1.260	0.34	T10	3.66	0.26×10^{2}	1.163	0.08
	T500	1.84			0.23	T110	4.60			0.05
8	T110	1.33	0.14×10^{-3}	1.200	0.39	T110	4.68	0.012	0.927	0.13
	T250	1.33			0.38	T250	5.17			0.11
9	T250	1.41	0.25×10^{-2}	1.338	0.28	T10	3.66	4.576	1.113	0.10
	T500	1.90			0.18	T250	5.20			0.40
		Non-Linear Region of Calibration					Non-Linear Region of Calibration			
1	T10	0.77	1.66×10^{5}	2.200	0.16	T40	3.93	3.74×10^{6}	1.518	0.01
	T40	1.20			0.06	T500	4.88			0.00
2	T10	0.77	1.66×10^{5}	2.200	0.16	T70	4.04	5.64×10^{10}	1.818	0.00
	T70	1.22			0.05	T500	4.61			0.00

Table 5-15. contd.

#	Paired Samples	Case Study #22 σ^2_{D2} (count)^2	$D1 \times 10^{-9}$	$D2$ (count)$^{-1}$	P_K	Paired Samples	Case Study #23 σ^2_{D2} (count)^2	$D1 \times 10^{-9}$	$D2$ (count)$^{-1}$	P_K
3	T10	0.77	1.66×10^5	2.200	0.16	T110	4.11	2.046×10^{10}	1.786	0.00
	T110	1.45			0.03	T500	4.64			0.00
4	T10	0.77	1.66×10^5	2.200	0.16	T250	4.27	7.73×10^{16}	2.200	3.25×10^{-5}
	T250	1.52			0.03	T500	4.24			3.50×10^{-5}
5	T10	0.76	0.37×10^4	2.031	0.21	T10	3.62	8.0×10^3	1.326	0.04
	T500	2.07			0.14	T500	5.03			0.01
6	T70	1.22	3.15×10^5	2.200	0.05	T70	3.96	2.82×10^{14}	1.936	0.00
	T110	1.45			0.03	T110	3.98			0.00
Size Separation between T10 and T2000 (cc)			10.25					21.5		
Length of System.			12 ft.					20 ft.		

the $\bar{M}_W$ calibration curve is shown in Fig. 5-16, because of the widely varying D2. As shown in Table 5-15, the P_K values deviate from unity the most of all the systems studied reflecting the importance of D2. In Fig. 5-17 chromatograms of systems of case-studies #23 and 11 are shown where the importance of well selected pore-sizes can be fully appreciated.

From the fore-gone discussion, P_K values have been very useful in assessing the SEC systems. Based on the analytical solutions of Hamielec and Ray (21) of Tung's axial dispersion equation (22), for an instrumental spreading function which is Gaussian, P_K value can only be less than 1.0 but never equal to or greater than 1.0. To further investigate the validity of the occurence of P_K values greater than one, especially at low flow-rates, two final case-studies were done one and a half years after all the original work with dextrans was completed. The same four column combination was used at two flow-rates, 3.0 and 1.9 ml/min for case-studies #24 and 25 respectively. Of the four columns, one (240 Å pore-size column) was freshly dry-packed and like case-studies #8 and 10, the system was characterised by MW gap. At 3.0 ml/min, T70, T250, T150 and T110 were injected fifteen, fifteen, five and two times respectively over a period of one month.

The results of the TBS method are shown in Table 5-16 and their $\bar{M}_W$, $\bar{M}_{rms}$ and MW calibration curves are shown in Fig. 5-18 in corrected retention volumes. Again their MW calibration curves are independent of flow-rate. At the low and intermediate flow-rates, almost all the P_K values are again greater than one instead of being less than one. Under the conditions where P_K value are greater than one, the instrumental spreading function cannot be Gaussian. A shape that is compatible with the TBS theoretical method of analysis is a symmetrical distribution, with

Figure 5-16. $\bar{M}_w$ calibration curves of dextran for Case-Studies #22 and 23

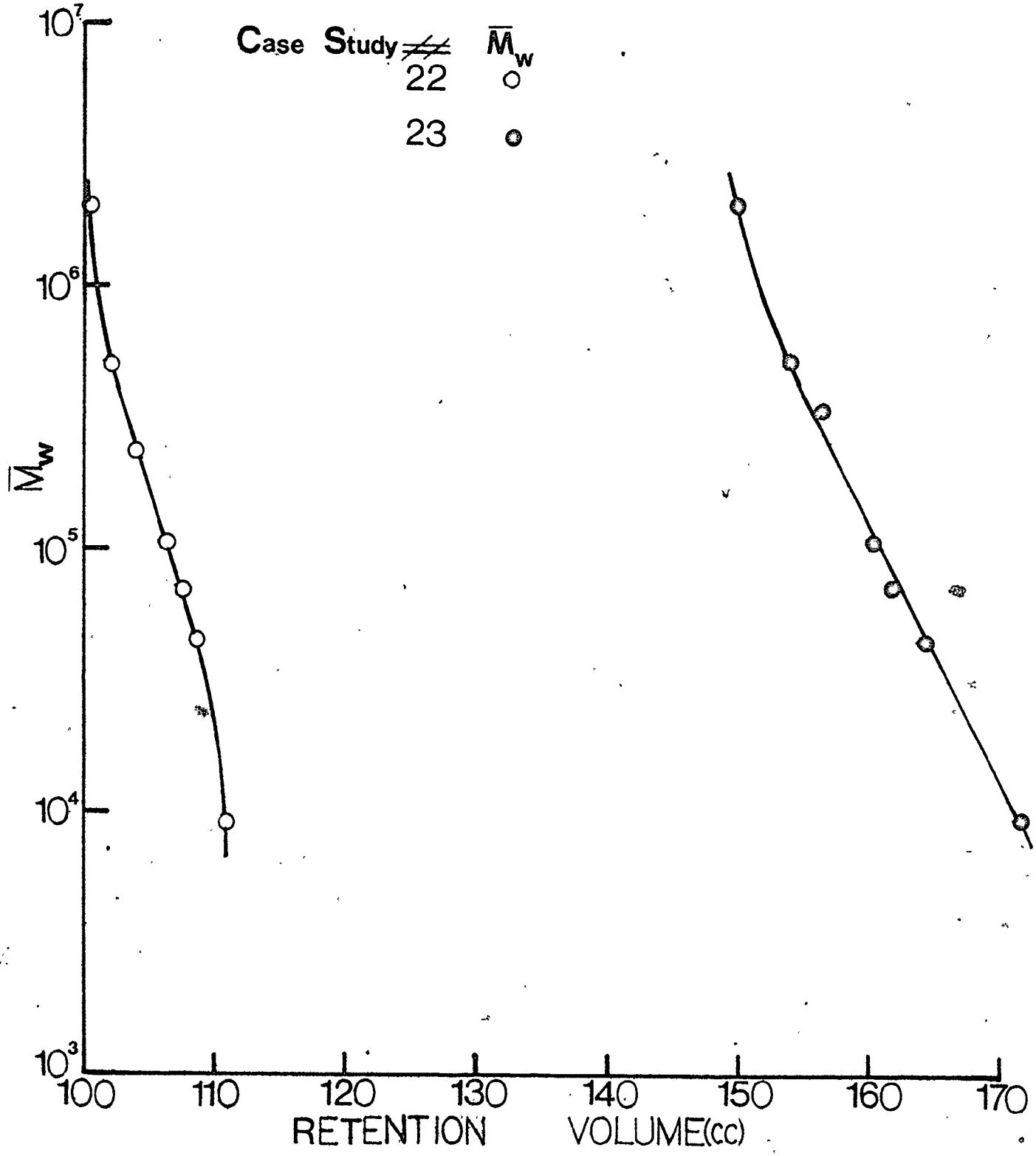

Figure 5-17. Comparison of peak separation and broadening for poorly and well optimized SEC systems for dextran analysis

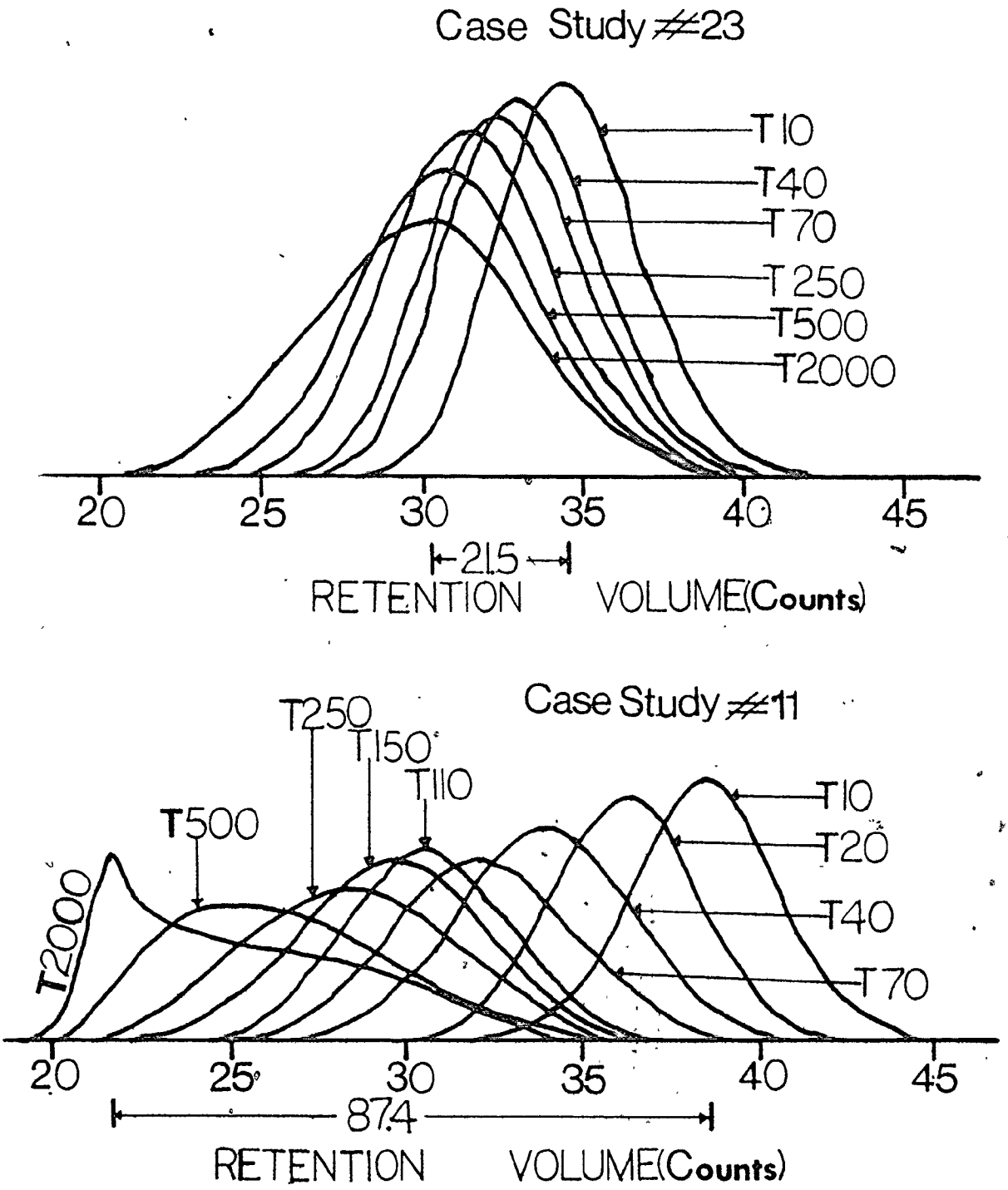

Table 5-16. Application of TBS method to Case-Studies #24 and 25

#	Paired Samples	Case Study #24 σ^2_{D2} (count)^2	Case Study #24 D1x10^{-9}	Case Study #24 D2 (count)$^{-1}$	Case Study #24 P_K	Paired Samples	Case Study #25 σ^2_{D2} (count)^2	Case Study #25 D1x10^{-9}	Case Study #25 D2 (count)$^{-1}$	Case Study #25 P_K
		Linear Region					Linear Region			
1	T40 T70	-0.96 -0.89	0.258	0.358	1.06 1.06	T40 T70	-1.22 -1.12	0.275	0.356	1.08 1.07
2	T40 T150	-0.70 -0.12	0.372	0.373	1.05 1.01	T40 T150	-0.86 -0.34	0.465	0.377	1.06 1.02
3	T40 T250	-0.79 -0.30	0.328	0.368	1.06 1.02	T40 T250	-0.99 -0.20	0.382	0.369	1.07 1.01
4	T70 T250	-0.61 -0.19	0.356	0.371	1.04 1.01	T70 T250	-0.74 -0.05	0.429	0.375	1.05 1.00
5	T150 T250	-0.19 -0.22	0.346	0.370	1.01 1.02	T150 T250	-1.21 -1.04	0.218	0.342	1.07 1.06
6	T110 T500	0.41 -2.28	0.371	0.369	0.97 1.17	T110 T500	0.19 -2.80	0.366	0.361	0.99 1.20
7	T150 T250	0.07 0.15	0.451	0.383	1.00 0.99	--	--	--	--	--
8	T70 T150	-0.43 0.06	0.449	0.381	1.03 1.00	--	--	--	--	--
		Non-Linear Region and Effect of Pore-Size Selection								
1	T10 T20	0.50 0.63	47.350	0.566	0.92 0.90	T70 T110	1.14 1.61	27.310	0.549	0.84 0.78
2	T10 T40	0.37 0.93	25.120	0.543	0.95 0.87	T10 T40	-0.04 0.58	17.360	0.521	1.01 0.92
3	T10 T70	-0.00 0.92	6.017	0.491	1.00 0.89	T10 T70	-0.41 0.59	4.709	0.475	1.05 0.94
4	T10 T110	-0.07 1.42	4.819	0.483	1.01 0.85	T10 T110	-0.31 1.32	6.552	0.487	1.04 0.85

Table 5-16 continued

#	Paired Samples	σ^2_{D2} (count)^2	Case Study #24 D1x10^{-9}	D2 (count)$^{-1}$	P_K	Paired Samples	σ^2_{D2} (count)^2	Case Study #25 D1x10^{-9}	D2 (count)$^{-1}$	P_K
			Non-Linear Region and Effect of Pore-Size Selection							
5	T10 T150	-0.34 1.25	2.240	0.456	1.04 0.88	T40 T110	-0.11 0.97	1.974	0.434	1.01 0.91
6	T10 T250	-0.47 1.30	1.569	0.443	1.05 0.88	T10 T250	-0.83 1.24	1.541	0.435	1.08 0.89
7	T10 T500	-0.48 0.05	1.558	0.443	1.05 1.00	T10 T500	-0.77 -0.16	1.773	0.440	1.08 1.16
8	T20 T40	0.38 0.77	12.880	0.516	0.95 0.90	T20 T40	-0.26 0.21	4.779	0.470	1.03 0.98
9	T20 T70	-0.16 0.46	1.929	0.443	1.02 0.96	T20 T70	-0.74 -0.04	1.205	0.418	1.07 1.00
10	T20 T110	-0.13 1.17	2.071	0.446	1.01 0.89	T20 T110	-0.43 1.08	2.752	0.449	1.04 0.90
11	T20 T150	-0.43 0.69	0.946	0.416	1.04 0.94	T20 T150	-0.87 0.22	0.883	0.406	1.07 0.98
12	T20 T500	-0.48 -0.79	0.844	0.411	1.04 1.07	T20 T250	-1.00 0.46	0.666	0.395	1.08
13	T70 T150	-0.19 0.43	0.719	0.403	1.02 0.97	T70 T500	-0.28 -1.25	0.817	0.401	1.02 1.11
14	T250 T500	1.28 0.02	1.515	0.441	0.88 1.00	T250 T500	1.82 0.61	3.607	0.476	0.81 0.93
	$M(V) = 0.356 \times 10^9 EXP(-0.372V)$					$M(V) = 0.370 \times 10^9 EXP(-0.364V)$				

Figure 5-18. $\bar{M}_w$, $\bar{M}_{rms}$ and MW calibration curves of dextran for Case-Studies #24 and 25

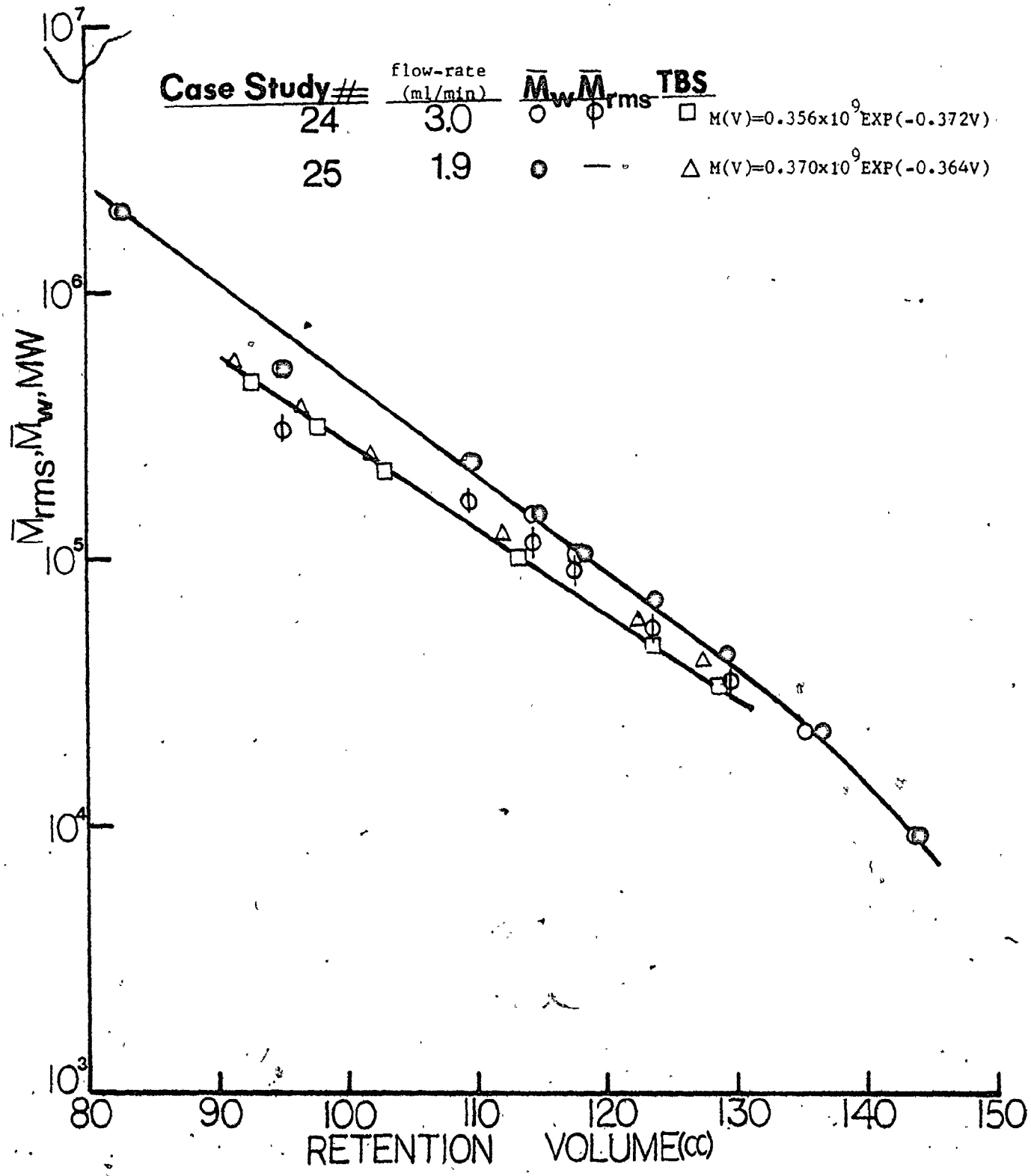

at least two shape parameters to give P_K values greater than unity.

As shown in Table 5-17 (contains the list of average D2s in the linear regions for all the cases studied) the measured relative standard deviations of less than 1.0%, reflects the reproducibility of the aqueous SEC and the minimal error propagation of the TBS method. Table 5-18 contains the peak retention volumes and measured W_d of the multiply injected samples and of case-studies #24 and 25. The measured W_d of the chromatograms of the system studied are listed in Table 5-19. From these Tables, it is important to note that just as with polyacrylamide and sodium polystyrene sulfonate, for the fully optimized SEC systems, W_d is generally seen to decrease with increasing D2. When these W_d in conjunction with D2 for these dextran systems are compared with those corresponding to other water soluble polymers, MW resolution correction with respect to peak broadening for low and intermediate MW dextran are observed to be less than those corresponding to polyacrylamide, but far greater than those for sodium polystyrene sulfonate. The high molecular weight dextran resolution corrections with respect to peak broadening are however similar to those of polyacrylamide, reflecting the influence of MWD or polydispersities of these standards.

5.1. Evaluation of TBS Method

The TBS method is valid only when the instrumental spreading function is symmetric. It is not valid when the spreading function is skewed. With the ELC method, the instrumental spreading function is assumed not to exist, since there is no skewing, no axial dispersion or other effects to account for, whereas, it is well known that for any SEC

Table 5-17. Standard Deviations of $D2_t$ for all Case-Studies

Case-Study #	Avg. $D2_t$	$\pm \sigma_{D2_t}$	No. of Observations
3	0.3000	--	--
4	0.2880	--	--
5	0.2660	0.0071	4
6	0.3080	0.0141	8
7	0.3120	0.0081	6
8	0.4030	0.0280	7
9	0.3000	0.0045	9
10	0.3530	0.0214	7
11	0.2880	0.0078	15
12	0.2920	0.0066	10
13	0.2860	0.0060	7
14	0.2670	0.0045	6
15	0.2650	0.0032	5
16	0.2840	0.0046	11
17	0.2860	0.0025	9
18	0.3160	0.0069	9
19	0.2800	0.0031	7
20	0.2810	0.0037	7
21	0.2840	0.0076	8
22	1.400	--	--
23	--	--	--

Table 5-18. Reproducibility of PRV and W_d of Measurement

#	T70		T250		T150		T110	
	PRV (counts)	W_d (counts)	PRV (Counts)	W_d (Counts)	PRV (counts)	W_d (counts)	PRV (Counts)	W_d (counts)
1	23.85	6.80	21.10	9.70	22.01	7.75	22.65	6.30
2	23.83	7.00	21.10	9.70	22.01	7.68	22.65	6.35
3	23.80	6.80	21.10	9.65	22.01	7.70		
4	23.85	6.90	21.10	9.70	22.01	7.65		
5	23.80	7.00	21.10	9.75	22.01	7.70		
6	23.85	7.00	21.10	9.70				
7	23.85	7.00	21.10	9.75				
8	23.85	6.95	21.10	9.65				
9	23.83	7.10	21.10	9.70				
10	23.85	7.00	21.10	9.75				
11	23.83	6.80	21.10	9.70				
12	23.85	7.00	21.10	9.75				
13	23.83	6.80	21.10	9.70				
14	23.85	6.85	21.10	9.65				
15	23.83	6.90	21.10	9.70				

Case-Study Sample	#24 W_d (counts)	#25 W_d (counts)
T10	5.45	5.15
T20	5.30	5.30
T40	5.80	5.85
T70	7.20	6.75
T110	6.30	6.40
T150	7.70	7.70
T250	9.70	9.80
T500	10.10	10.10

Table 5-19. Measured W_d of each chromatogram

Case-Study # / Sample	W_d (counts) 1	2	3	4	5	6	7	8	9	10	11	12
T10	--	--	--	--	--	7.30	7.40	5.10	6.70	8.15	8.30	8.35
T20	--	--	19.70	--	11.10	--	--	5.58	7.10	7.70	8.60	8.60
T40	17.50	--	20.40	21.40	12.05	8.80	9.50	6.85	8.90	8.50	9.90	9.95
T70	17.90	17.0	20.00	20.55	12.74	9.40	10.75	7.45	9.90	8.50	10.40	10.30
T110	16.60	--	20.10	20.70	11.30	8.50	9.30	6.70	8.75	7.00	9.50	8.80
T150	17.50	--	21.05	21.40	12.55	--	--	7.00	10.30	7.65	10.70	10.35
T250	20.10	16.30	22.33	--	12.50	11.05	12.40	8.90	12.00	8.80	12.60	11.65
T500	22.55	20.00	22.50	--	11.40	11.10	13.10	10.50	12.95	9.90	12.75	12.60
T2000	--	--	26.00	--	12.90	3.50	8.55	2.40	4.00	3.00	4.40	4.20
ml/count	5.00	4.46	5.0	4.85	5.00	5.00	5.00	5.20	5.20	5.20	5.20	5.20
D2	0.390	0.285	0.300	0.288	0.266	0.308	0.312	0.403	0.300	0.353	0.288	0.292
$\frac{Max}{\sigma}$ 2	21.34	17.70	22.95	22.40	4.23	1.08	2.67	1.37	0.62	2.20	1.24	0.69
Length of System (ft)	24	24	36	36	19.7	13.8	17.7	11.6	15.6	16.8	18.3	18.1

Table 5-19 contd.

Case-Study #	W_d (counts)										
Sample	13	14	15	16	17	18	19	20	21	22	23
T10	8.60	8.70	11.10	8.50	8.50	7.80	8.8	9.50	9.51	3.40	9.00
T20	8.90	9.60	11.15	8.60	8.80	8.20	8.70	9.35	9.80	--	--
T40	10.50	10.50	11.60	9.50	9.60	9.25	10.00	10.45	10.45	4.40	9.40
T70	11.50	10.90	11.70	10.50	9.90	9.40	10.30	10.40	10.30	4.80	9.70
T110	9.70	9.50	10.63	7.90	8.50	8.10	8.60	8.75	8.90	4.90	9.55
T150	11.00	10.97	11.80	9.20	9.90	9.30	9.70	10.40	10.30	--	--
T250	12.90	12.60	12.70	11.50	11.00	11.40	11.55	11.85	11.70	5.90	10.25
T500	13.65	13.10	13.60	12.10	12.10	11.70	11.95	12.00	12.20	6.70	11.00
T2000	4.20	4.00	7.00	4.30	4.00	3.30	4.10	4.60	4.60	8.70	13.60
ml/count	5.20	5.20	5.20	5.00	5.30	5.82	5.30	5.30	5.30	5.30	5.30
D2	0.286	0.267	0.265	0.284	0.286	0.316	0.280	0.281	0.284	1.40	1.10
Max σ^2	2.77	1.44	1.68	1.19	1.96	2.10	1.76	1.63	1.66	1.43	5.17
Length of System (ft)	18.4	20.8	20.8	19.3	19.3	19.3	19.3	19.3	19.3	12.0	20.0

system, correction is necessary (26)(27)(58)(43)(59)(60). Therefore, one should expect a plot of $\log_e$ D1 versus D2 obtained by either the ELC or TBS method to be linear if the instrumental spreading function is not skewed, and adequate correction is not made. With the TBS method, one should expect a single point in these plots if the method is capable of providing a true molecular weight calibration curve.

The ELC method with many options, was applied to most of the cases studied. Table 5-20 contains the list of results of four of the systems studied. Case Study #10 was one of the systems with a MW gap, Case-Study #13, that with disorderly arranged small pore-sizes and Case-Studies #12 and 14, systems with no defect. Figs. 5-19 and 21 show the plot of ln D1 versus D2 comparing the TBS with the ELC method. For Case-Studies #12 and 14 there is only a single point (Figs. 5-20 and 21) followed by the system with MW gap (Case-Study #10). Then the widely varying D2 of Case-Study #13 as shown in Fig. 5-19 is the worst case. From these figures, the linear relationship between ln D1 and D2 is apparent. Therefore

$$D1 = J1^* e^{J2^* \times D2'} \tag{5.1.1}$$

where $J1^*$ is the intercept and $J2^*$ is the slope and D2' is to emphasize that there is only one true MW calibration which is being rotated about a 'fixed point', the degree of rotation depending on the Gaussian or symmetric instrumental spreading correction. Substituting Equation (5.1.1.) into the linear MW calibration curve, the following is obtained

$$M(V) = J1^* e^{-D2'(V-J2^*)} \tag{5.1.2}$$

Table 5-20. Application of ELC method to some of the cases studied

Case-Study #10

Single

Sample	$D1 \times 10^{-9}$	$D2^{-1}$ Count	σ_{D2_2} count
T10	1.381	0.362	0.0
T20	0.765	0.343	0.0
T40	0.481	0.327	0.0
T70	0.938	0.352	0.0
T110	0.856	0.345	0.0
T150	5.439	0.417	0.0
T250	4.432	0.409	0.0
T500	15.600	0.463	0.0

Double $\bar{M}_{II}$

Paired Samples			$\sigma_{\bar{M}_{W_2}}$ count
T10	2.324	0.377	0.58
T20			1.17
T40	0.121	0.282	-2.79
T70			-4.52
T110	0.014	0.194	-12.03
T150			-24.10
T250	0.227	0.297	-7.66
T500			-14.18

Double $\bar{M}_{W}$

Paired Samples			$\sigma_{\bar{M}_{n_2}}$ count
--	--	--	--
--			--
--	--	--	--
--			--
--	--	--	--
--			--
--	--	--	--
--			--
T10	2.936	0.385	0.88
T500			-4.32
T40	1.902	0.377	1.96
T110			0.90
T20	1.662	0.367	0.91
T150			-1.86
T250	7.695	0.432	0.903
T70			2.690

Case-Study #12

Single

Sample	$D1 \times 10^{-9}$	$D2^{-1}$ count	σ_{D2_2} count
T10	3.988	0.351	0.0
T20	0.805	0.300	0.0
T40	0.324	0.272	0.0
T70	0.470	0.285	0.0
T110	0.332	0.270	0.0
T150	0.949	0.306	0.0
T250	1.186	0.317	0.0
T500	4.030	0.362	0.0

Double $\bar{M}_{II}$

Paired Samples			$\sigma_{\bar{M}_{W_2}}$ count
T10	271.20	0.516	-4.20
T20			-5.80
T40	0.084	0.233	4.18
T70			6.02
T110	0.027	0.190	9.22
T250			25.18
T500	0.104	0.236	22.05
T150			8.52

Double $\bar{M}_{W}$

Paired Samples			$\sigma_{\bar{M}_{n_2}}$ count
T70	1.469	0.323	2.69
T150			1.24
T40	0.644	0.293	1.64
T250			-2.34
T10	1.839	0.329	-1.05
T500			-3.34
T110	0.740	0.298	1.60
T20			0.15
T500	2.511	0.342	-1.89
T150			2.46
T110	0.563	0.288	1.10
T250			-2.92
T40	0.227	0.261	-1.01
T70			-2.36
T10	40.490	0.415	2.24
T20			4.21

Table 5-20 continued

Case-Study #13

Single

Samples	$D1 \times 10^{-9}$	D2 count^{-1}	$\sigma^2_{D2\ count}$
T10	6.490	0.347	0.0
T20	0.930	0.293	0.0
T40	0.379	0.267	0.0
T70	0.219	0.252	0.0
T110	0.214	0.249	0.0
T150	0.623	0.287	0.0
T250	0.654	0.289	0.0
T500	1.606	0.314	0.0

Double $\bar{M}_n$

Paired Samples			$\sigma^2_{\bar{M}_W\ count}$
T10	144.20	0.423	-2.63
T20			-4.78
T40	0.165	0.244	2.04
T70			1.06
T110	0.002	0.105	49.33
T150			90.99
T250	8.094	0.369	-6.36
T500			-4.08

Double $\bar{M}_W$

Paired Samples			$\sigma^2_{\bar{M}_n\ count}$
T10	6.707	0.348	0.02
T20			2.71
T40	0.098	0.227	-4.58
T70			-3.75
T110	0.215	0.249	0.017
T150			-4.59
T250	56.840	0.461	9.81
T500			11.09

Case-Study #14

Samples	$D1 \times 10^{-9}$	D2 count^{-1}	$\sigma^2_{D2\ count}$
T10	1.543	0.291	0.0
T20	1.192	0.283	0.0
T40	0.373	0.253	0.0
T70	0.494	0.262	0.0
T110	0.337	0.247	0.0
T150	1.364	0.291	0.0
T250	1.421	0.293	0.0
T500	6.110	0.340	0.0

Double $\bar{M}_n$

Paired Samples			$\sigma^2_{\bar{M}_W\ count}$
T10	3.022	0.306	1.13
T20			1.41
T40	0.085	0.214	5.32
T70			7.28
T110	0.008	0.137	24.59
T150			48.24
T250	0.302	0.247	-6.82
T500			-16.54

Double $\bar{M}_W$

Paired Samples			$\sigma^2_{\bar{M}_n\ count}$
T20	2.367	0.301	0.80
T10			1.15
T40	0.212	0.237	-1.90
T70			-3.30
T110	2.024	0.304	3.66
T150			1.15
T250	28.720	0.399	7.43
T500			4.84

Figure 5-19. Evaluation of TBS method for Case Studies #10 and 13

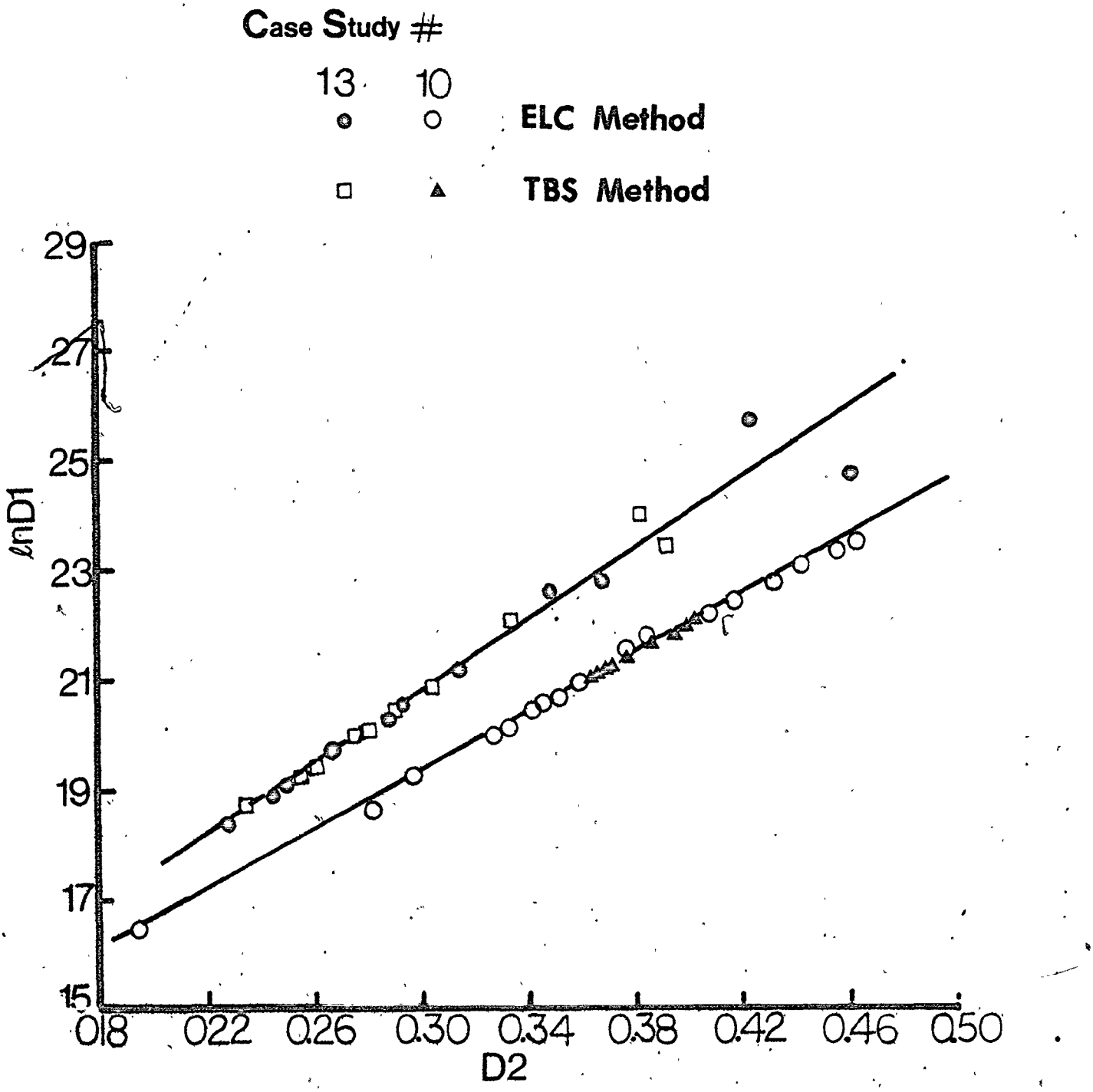

Figure 5-20. Evaluation of TBS method for Case-Study #12

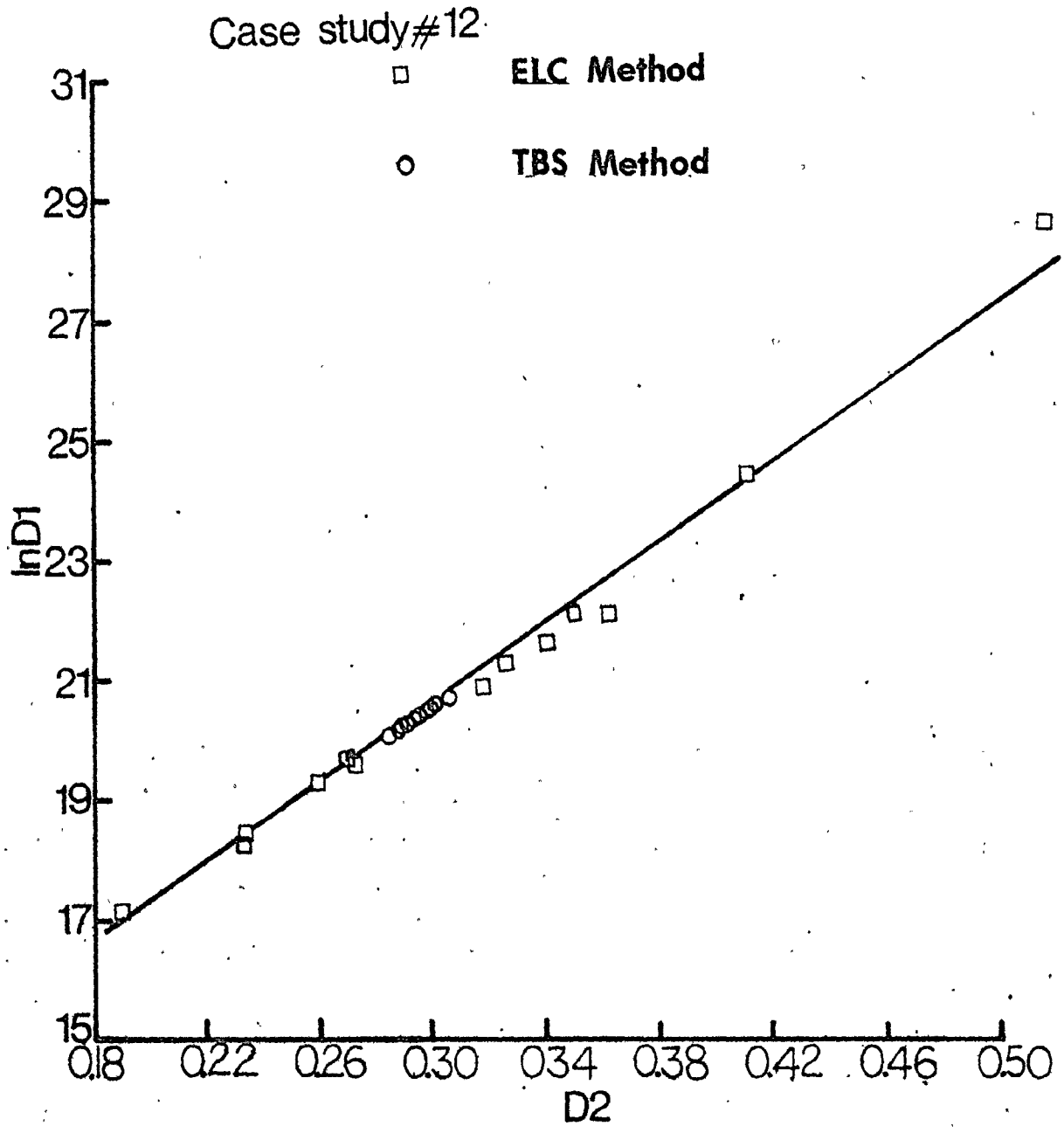

Figure 5-21. Evaluation of TBS method for Case-Study #14

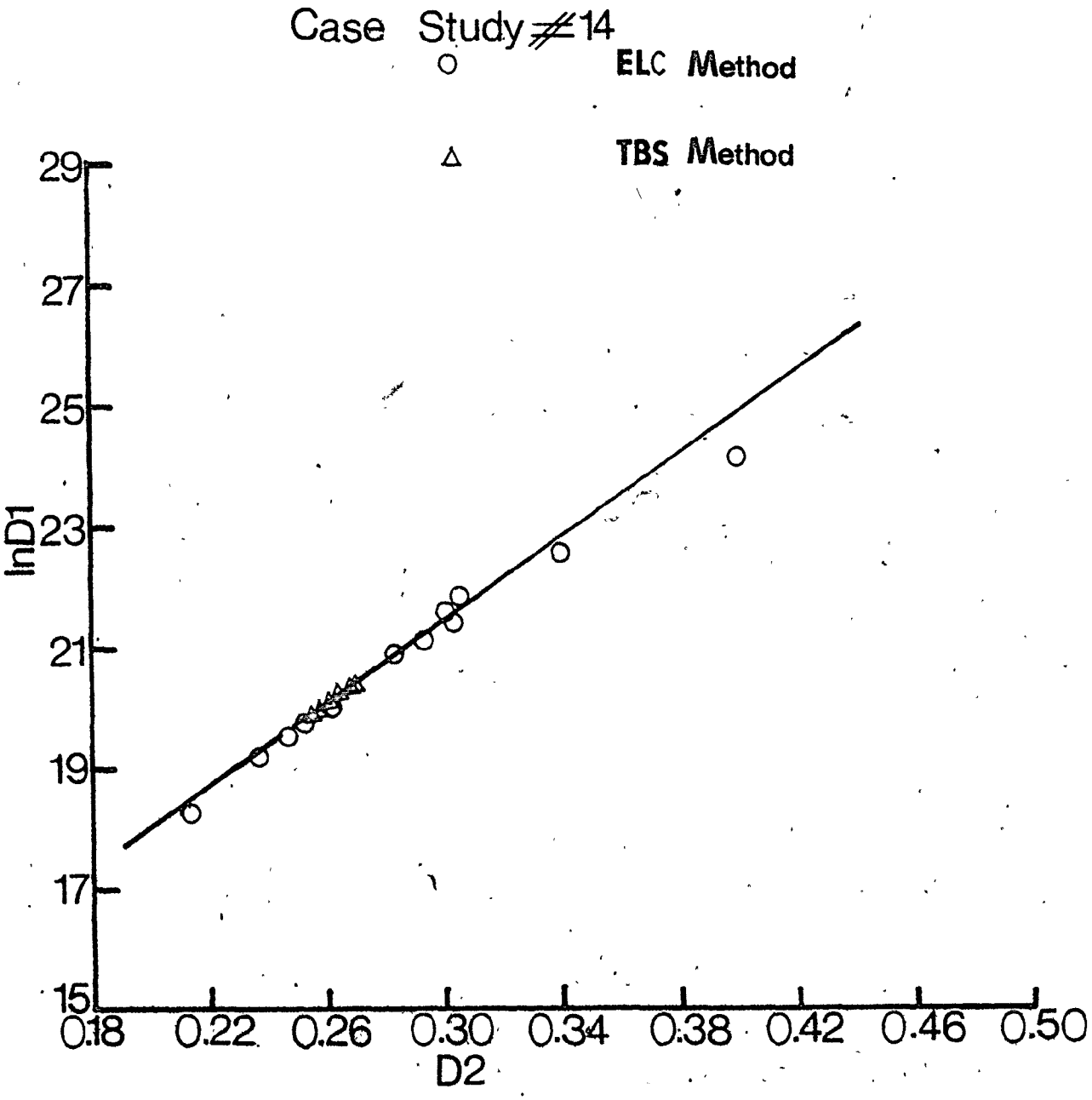

When D2' = D2, the slope of the true MW calibration curve,

$$M(V) = J1^{*}_{e} \; ^{-D2(V-J2^{*})} \tag{5.1.3}$$

$$= (J1^{*}_{e} \; ^{D2*J2^{*}})_{e} \; ^{-D2*V}$$

$$= J3^{*}_{e} \; ^{-D2*V} \tag{5.1.4}$$

where $J3^{*}$ is a constant. According to Equation (5.1.4), the true molecular weight calibration curve remains the same. Thus the effect of neglecting instrumental spreading correction is to rotate the true MW calibration curve about a fixed point.

This fixed point or rotation has been alluded to in the works of Balke and Hamielec (44), Provder and Rosen (42) and Yau, Stoklosa and Bly (23). According to Yau, Stoklosa and Bly, "the ELC method calibration line was found to rotate counterclockwisely relative to the peak position calibration line and the extent of rotation was found to increase with increasing dispersion of the column and with decreasing polydispersity" of the polystyrene standards used.

5.2. Calibration of Molecular Weight Correction Factors

Using the true MW calibration curves, obtained via the TBS method, the MW correction factors, P_K, were obtained. These are listed in Table 5-21 for only one system used for flow-rate studies, Case-Studies #16, 17 and 18. The plot of P_K versus peak retention volumes are shown in Fig. 5-22. These systems according to the TBS method (ref to Table 5-11), show a very constant D2 over a wide molecular weight range, with the system at the lowest flowrate being more linear (10^3 to 10^6 MW) than

Table 5-21. P_K values of Case-Studies #16, 17 and 18 using the true MW calibration curves

Case Study #	16		17		18	
Flow-rate (ml/min)	1.43		4.30		7.83	
Sample	P_K	σ^{-2}	P_K	σ^{-2}	P_K	σ^{-2}
T10	0.965	0.68	0.980	0.30	0.938	0.83
T20	1.032	-0.78	1.021	-0.50	0.963	0.75
T40	1.022	-0.54	0.978	0.54	0.946	1.12
T70	0.973	0.67	1.009	-0.22	0.946	1.11
T110	1.020	-0.49	1.028	-0.67	0.949	1.06
T150	1.092	-2.19	1.054	-1.29	0.980	0.40
T250	1.049	-1.19	1.083	-1.96	1.002	-0.04
T500	1.199	-3.80	1.125	-2.10	0.981	0.26

the system at intermediate flowrate, which in turn is also more linear than the system at highest flow-rate. The same observation was also apparent using Peak position method (Figure 5-14). But the P_K values show the contrary. It is not unlikely that the breadth of the MWD of the polymers is playing a major role, which increases with decrease in flow-rate as shown in Fig. 5-22. It is not possible to use this figure to re-estimate the true MW averages of any of the polydextran standards. Without applying a correction the true MW averages can never be obtained.

When P_K values are greater than 1, on the basis of a Gaussian instrumental spreading shape function, negative variances (σ^{-2}) which are shown in Table 5-21 and have been shown all along in Tables 5-2 to 5-4 and 5-4 to 5-11 and 5-13 to 5-16 would result (an impossible situation). Therefore, the alternative explanation is an instrumental spreading function which may be symmetric. Therefore, on this basis the σ^{-2} values shown in these Tables are γ values of the newly proposed instrumental

Figure 5-22. $\bar{M}_w$ correction factors (P_K) versus peak retention volume for Case-Studies #16, 17 and 18

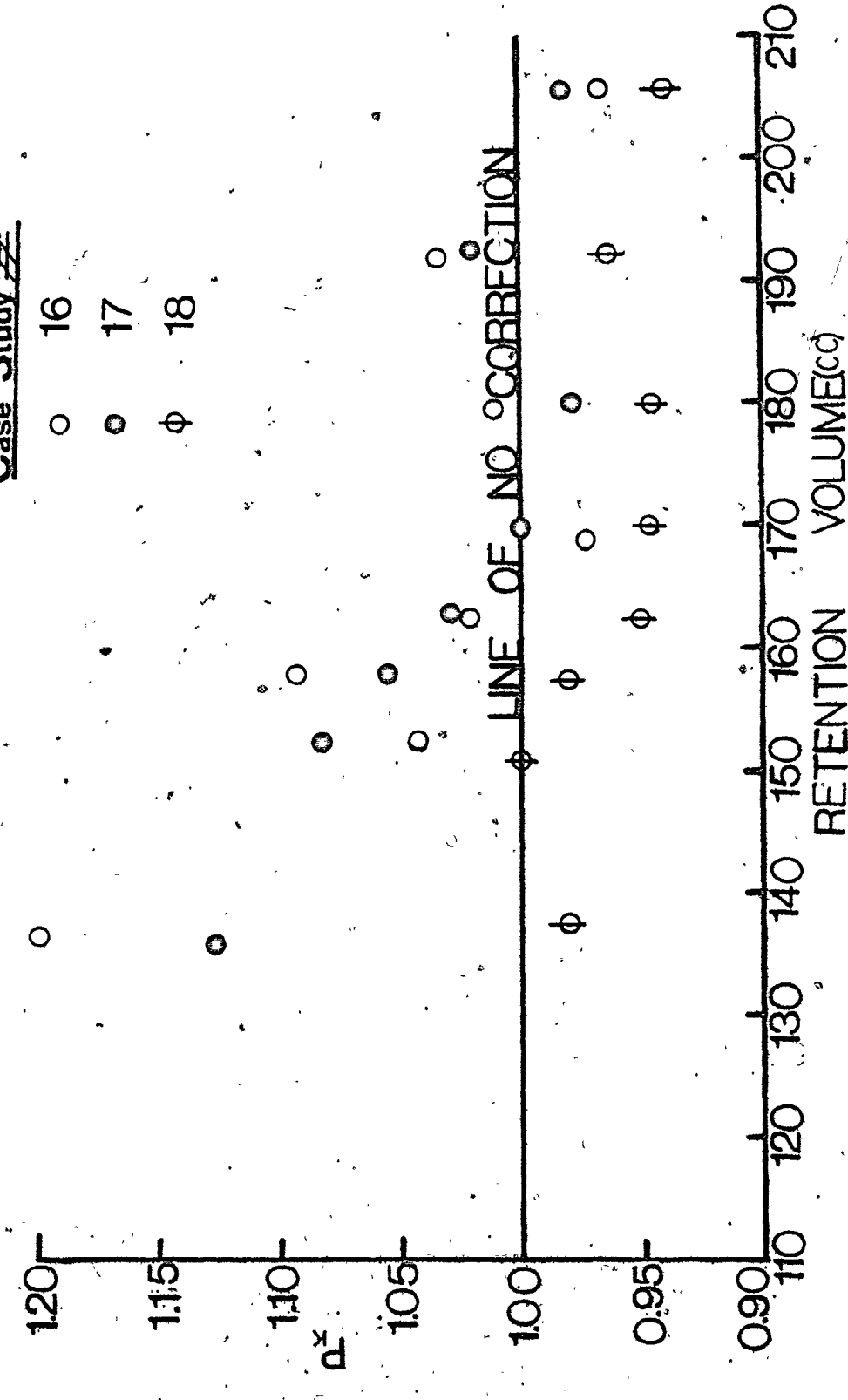

spreading shape function in Section (2.4.2), which in fact was conceived from the data obtained using both the TBS and ELC methods of calibration.

5.3. Re-evaluation of the TBS Method Using the Proposed Instrumental Spreading Function

According to equation (2.4.15), a plot of γ versus $D2^{-2}$ should be linear, with σ^{-2} as intercept and $-K_S$ as the slope. Such is the case in Figs. 5-23, 24 and 25, of Case-Studies 16, 17, 19 and 23. Of all the cases studied, only Case-Study #24 was non-linear as shown in Fig. 5-26. Using the intercepts and slopes of these plots, σ^{-2} and K_S values were obtained. These are listed in Tables 5-22 and 23 for all the last 23 systems studied. In Table 5-23, the $\log_e$ of the true polydispersities of the standards are also shown to compare with the experimentally obtained values. With careful observation, one can conclude that distilled water is not a good mobile-phase for dextran SEC analysis, that some of the standards eg. T110 may not have been well characterised by the manufacturer, and finally that large pore-sizes when not applicable, should not be used.

The MW resolution corrections with respect to the measured axial dispersion coefficients are listed in Table 5-24. From the Table, it is apparent that axial dispersion is an inherent phenomenon, the contributing sources in decreasing order being (i) pore dispersion (large pores) (ii) polymer surface interaction due to improperly packed and selected mobile-phases (Case Studies #1, 2, 3 and 4), (iii) polymer/small pore-size surface area interaction due to traditional method of column arrangement (Case-Studies #14 and 15, 17 and 21, 19 and 20), (iv) increased flow-rate (Case-Studies #16, 17 and 18, 24 and 25, 4 and 5.) As the flow-rate decreases there is decreasing correction for axial dispersion, contrary

Figure 5-23. Overall symmetric spreading parameter (γ_{D2}) versus $D2^{-2}$ for Case-Studies #16, 17 and 18

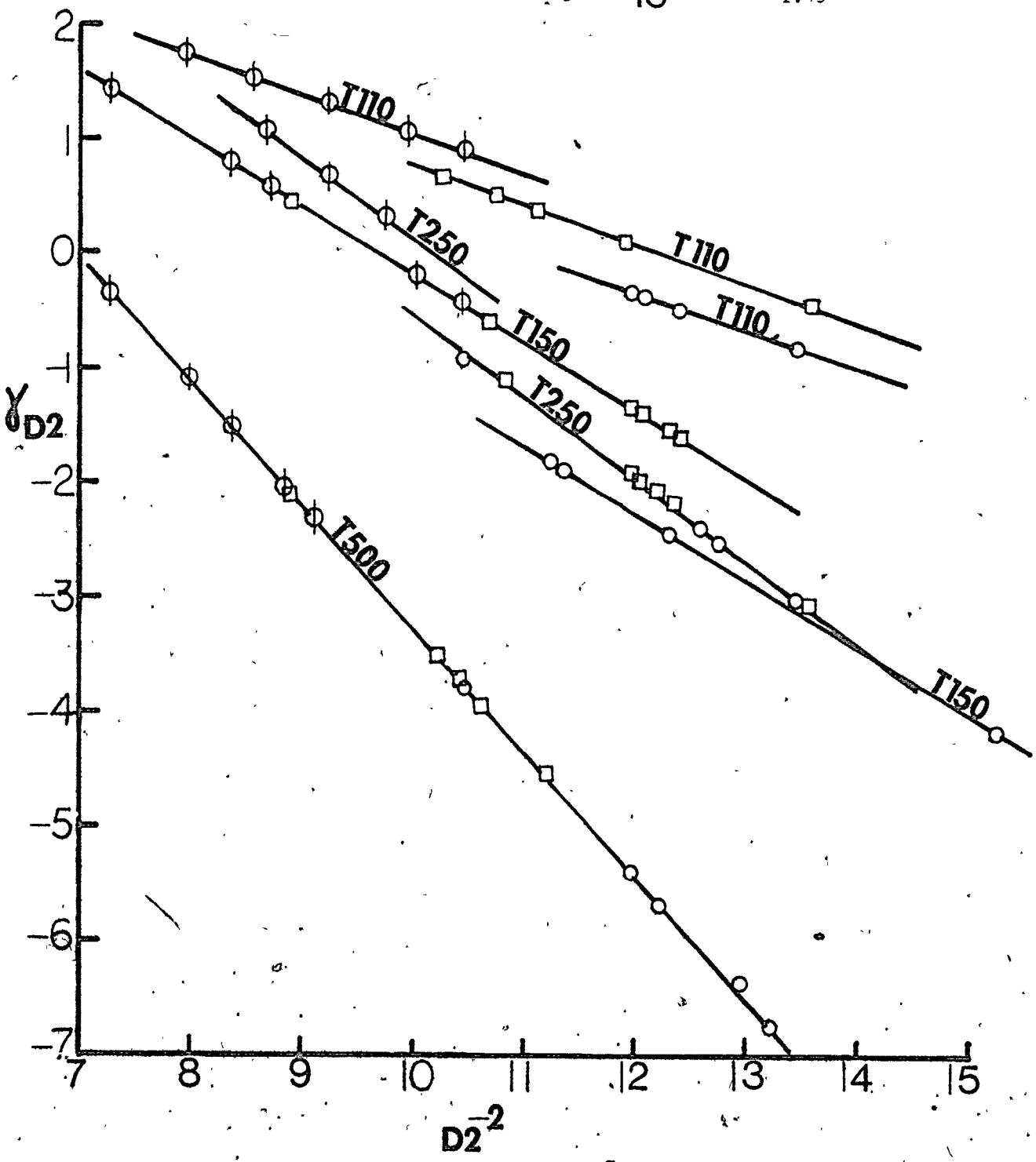

Figure 5-24. Overall symmetric spreading parameter (γ_{D2}) versus $D2^{-2}$ for Case Studies #16, 17 and 18

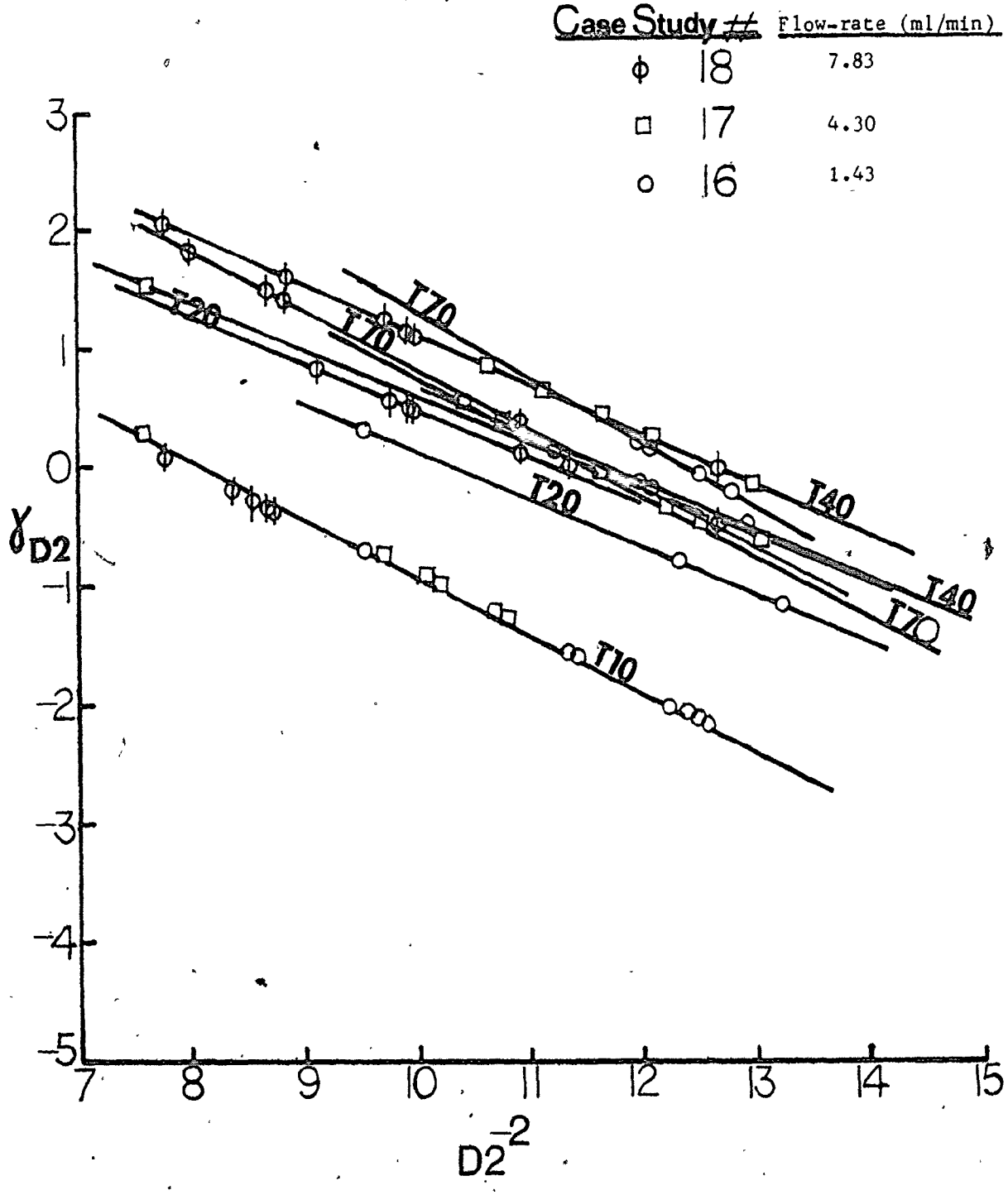

Figure 5-25. γ_{D2} versus $D2^{-2}$ for Case-Study #22

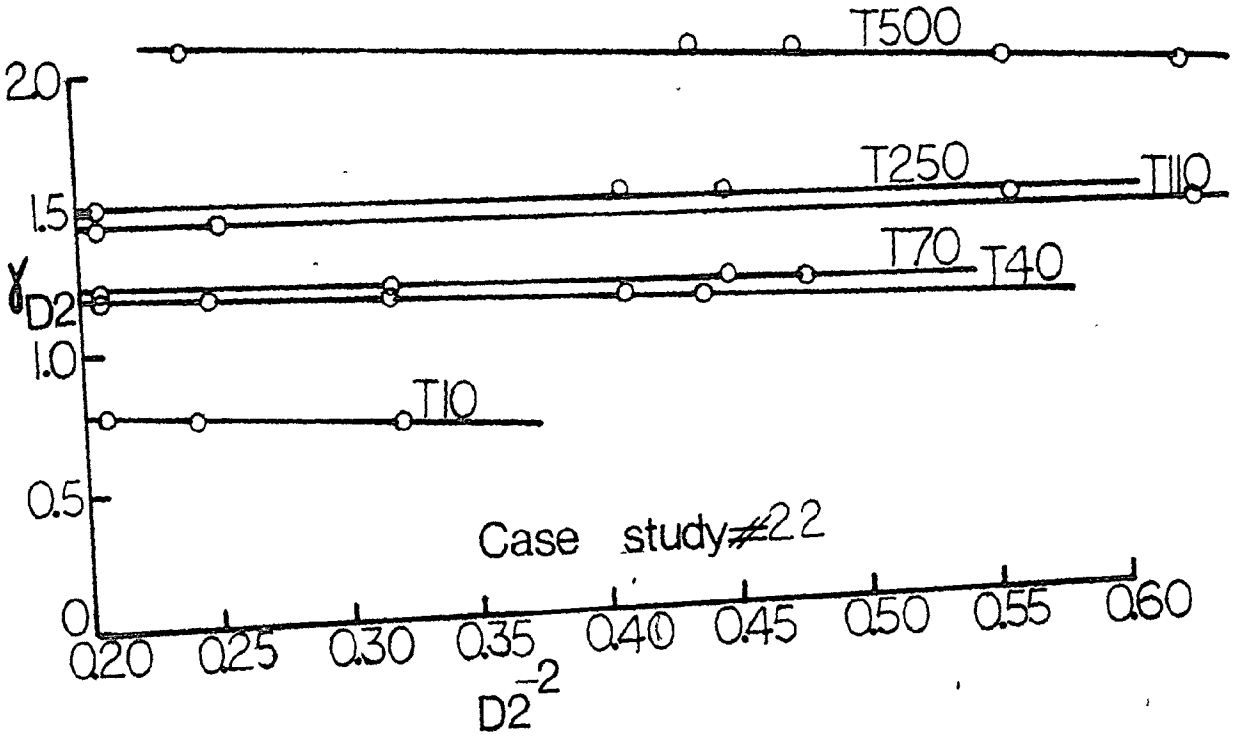

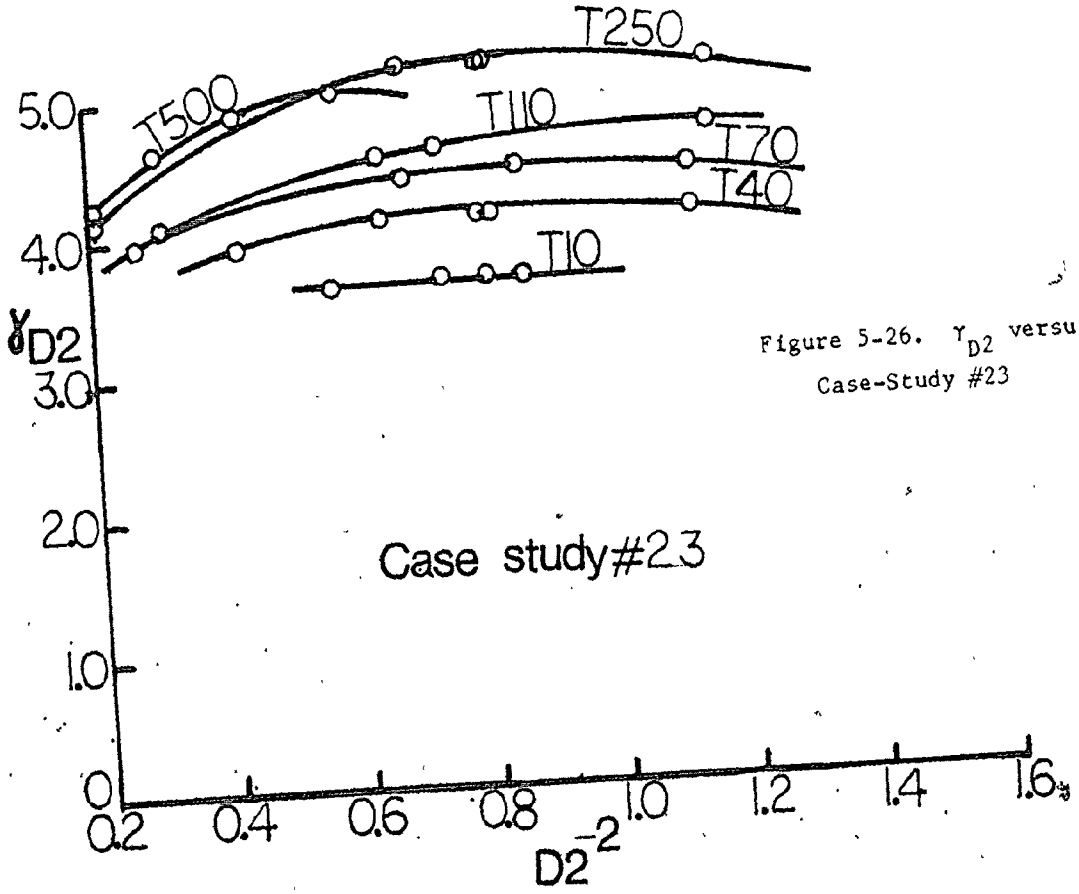

Figure 5-26. γ_{D2} versus $D2^{-2}$ for Case-Study #23

Table 5-22. σ^{-2} values of dextran samples from cases studied

Case Study #	3	4	5	6	7	8	9	10	11	12	13	14
Sample												
T10	--	--	--	3.04	3.04	1.48	2.64	3.72	3.84	3.89	4.16	5.74
T20	--	--	8.10	--	--	1.99	3.08	3.34	4.17	4.43	4.60	4.99
T40	26.8	27.8	9.55	4.10	4.74	3.07	4.78	3.99	5.67	5.82	5.89	6.62
T70	26.2	26.0	11.5	4.62	5.70	3.07	5.58	3.98	6.33	6.03	7.79	7.23
T110	26.1	25.4	--	3.62	4.51	2.40	4.46	2.76	5.03	4.55	5.33	5.39
T150	28.2	--	13.3	--	--	2.88	6.21	3.35	6.71	6.15	6.74	6.97
T250	27.7	26.2	10.4	6.26	7.20	4.08	7.55	4.25	8.22	6.95	8.47	8.21
T500	28.0	28.2	8.41	6.36	8.45	5.20	8.93	4.98	8.82	8.15	10.8	9.27

Case Study #	15	16	17	18	19	20	21	22	23	24	25
Sample											
T10	6.86	4.04	4.08	3.95	4.66	6.01	5.04	0.85	3.66	2.05	1.77
T20	7.10	4.07	4.57	4.43	4.59	5.28	5.51	--	--	1.88	1.53
T40	7.70	4.97	5.40	5.40	6.50	6.49	6.20	1.28	<4.11	2.38	2.15
T70	7.86	6.13	5.72	5.79	6.81	7.06	6.02	1.32	<4.44	2.97	2.79
T110	6.55	3.66	4.10	4.44	4.65	4.48	4.55	1.51	<4.68	2.83	2.76
T150	8.03	4.75	5.61	5.63	6.17	6.08	5.89	--	--	4.02	3.74
T250	8.76	6.50	6.50	7.22	7.34	7.01	7.20	1.80	<5.17	4.84	4.90
T500	10.1	7.35	7.35	7.35	8.03	7.70	8.09	2.47	<5.03	5.41	5.27

Table 5-23. Measured K_s values of dextran samples from cases studied

Case Study #	3	4	5	6	7	8	9	10	11	12	13	14
Sample												
T10	--	--	--	0.500	0.500	0.486	0.486	0.488	0.485	0.480	0.500	0.485
T20	--	--	0.396	--	--	0.392	0.395	0.393	0.395	0.399	0.395	0.392
T40	0.399	0.383	0.435	0.424	0.422	0.446	0.426	0.427	0.430	0.430	0.421	0.422
T70	0.491	0.455	0.519	0.497	0.493	0.500	0.490	0.494	0.496	0.490	0.493	0.498
T110	0.300	0.296	--	0.330	0.330	0.330	0.330	0.330	0.330	0.331	0.330	0.330
T150	0.530	--	0.026	--	--	0.578	0.573	0.582	0.585	0.575	0.570	0.589
T250	0.618	0.629	0.719	0.707	0.723	0.700	0.701	0.710	0.700	0.700	0.707	0.695
T500	0.950	0.985	1.076	1.062	1.060	1.040	1.060	1.061	1.061	1.060	1.067	1.065

Case Study #	15	16	17	18	19	20	21	22	23	24	25	lnP(t)
Sample												
T10	0.490	0.495	0.495	0.495	0.500	0.500	0.500	0.400	--	0.495	0.495	0.489
T20	0.395	0.395	0.395	0.394	0.395	0.395	0.395	--	--	0.401	0.400	0.399
T40	0.423	0.426	0.426	0.426	0.426	0.426	0.426	0.386	--	0.429	0.429	0.432
T70	0.496	0.495	0.495	0.493	0.494	0.495	0.495	0.490	--	0.498	0.497	0.501
T110	0.335	0.335	0.330	0.339	0.335	0.335	0.335	0.300	--	0.330	0.330	0.285
T150	0.585	0.585	0.581	0.578	0.584	0.585	0.585	--	--	0.580	0.580	0.582
T250	0.700	0.707	0.707	0.706	0.707	0.707	0.707	0.700	--	0.700	0.700	0.718
T500	1.063	1.065	1.065	1.065	1.069	1.069	1.065	1.065	--	1.052	1.056	1.078

Table 5-24. Axial dispersion Resolution Correction

$\exp(-D2^2\sigma_T^2/2)$

Case Study #	5	6	7	8	9	10	11	12	13	R* 14	C* 15
Sample											
T10	--	0.865	0.862	0.886	0.888	0.793	0.852	0.847	0.843	0.814	0.786
T20	0.751	--	--	0.850	0.870	0.812	0.851	0.827	0.828	0.837	0.779
T40	0.713	0.823	0.794	0.779	0.806	0.779	0.790	0.780	0.785	0.789	0.762
T70	0.664	0.803	0.757	0.779	0.777	0.780	0.769	0.773	0.728	0.772	0.758
T110	--	0.842	0.803	0.822	0.818	0.842	0.811	0.823	0.804	0.825	0.794
T150	--	--	--	0.791	0.756	0.811	0.757	0.769	0.759	0.780	0.754
T250	0.693	0.743	0.704	0.718	0.711	0.767	0.711	0.743	0.707	0.746	0.735
T500	0.742	0.739	0.662	0.655	0.669	0.733	0.693	0.706	0.642	0.718	0.702

Case Study #	F2 16	17R	18	R 19	C 20	21C	22	F3 24	25	F1 3	4
Sample											
T10	0.849	0.846	0.821	0.833	0.788	0.816	0.434	0.867	0.889	--	--
T20	0.848	0.829	0.801	0.835	0.811	0.800	--	0.877	0.903	--	--
T40	0.818	0.801	0.763	0.775	0.773	0.778	0.285	0.848	0.867	0.299	0.316
T70	0.781	0.791	0.749	0.765	0.756	0.784	0.261	0.814	0.831	0.308	0.341
T110	0.862	0.845	0.801	0.833	0.837	0.832	0.277	0.822	0.836	0.309	0.349
T150	0.825	0.795	0.755	0.785	0.786	0.789	--	0.757	0.781	0.281	--
T250	0.769	0.766	0.697	0.750	0.758	0.747	0.171	0.715	0.723	0.287	0.338
T500	0.743	0.740	0.693	0.730	0.737	0.721	0.088	0.687	0.705	0.283	0.310

* F Flow-rate systems

R Reversed order of column arrangement

C Conventional order of column arrangement

to their P_K values. However the difference is very little hardly worth the expense of long analysis times.

The second parameter of the symmetric instrumental spreading function was estimated using equation (2.4.14b). The estimated values are listed in Table 5-25. As shown, A_K values cannot be positive. The contributing sources of poor values of A_K ($A_K \longrightarrow 0$) are in decreasing order the same as for axial dispersion resolution correction mentioned above. The corresponding MW polyplatykurtic corrections are listed in Table 5-26, which also includes the square root of the true polydispersities of the standards. From this table, it is unquestionable that the polyplatykurtisis is an inherent phenomenon, by far more important than axial dispersion. In one of the systems (Case Study #24), replicate injections were made and on the basis of a Gaussian instrumental spreading function, it was impossible to assess statistically the quality of the TBS method. For the standards which were each injected fifteen times, using the true MW calibration for the system, their γ values were obtained. These were used to estimate σ^2 and A_K values. These are listed in Table 5-27 below, which also contains their average values and the standard deviations. With errors of less than 1.5% for both coefficients and samples, there is no doubt that the TBS method is an important contribution and the instrumental spreading functions for these very compact dextran standards are symmetric in shape as proposed.

From the foregone results and discussions, the physical interpretation of the proposed symmetric instrumental spreading function as applied to dextran, which accounts for both peak broadening and the polydispersity or MWD effects is shown in Figure 5-27, for monodisperse, very narrow and very broad MWD standards.

Table 5-25. Polyplatykurtic coefficient values of dextran for all cases studied

Case Study #	F*1 3	F 1 4	5	6	7	8	9	10	11	12	13	R *1 14
Sample												
T10	--	--	--	70.50	66.95	101.48	103.86	27.29	57.80	53.30	50.64	35.02
T20	--	--	14.57	--	--	45.82	62.28	27.63	40.00	33.54	33.80	37.82
T40	0.89	0.98	11.35	34.25	24.34	20.84	28.00	20.96	23.43	21.04	22.32	23.27
T70	1.08	1.30	9.01	31.28	19.52	24.17	24.34	24.43	21.80	22.73	14.99	22.62
T110	0.65	0.81	--	30.53	18.68	23.70	22.34	30.44	20.66	23.92	18.94	24.38
T150	1.09	--	--	--	--	31.92	22.36	40.08	22.55	25.40	22.98	28.29
T250	1.38	1.83	16.06	24.43	17.54	19.62	18.66	30.71	18.53	24.53	17.95	25.15
T500	2.04	2.36	36.55	35.55	19.13	18.14	20.03	33.61	24.18	26.80	16.58	29.63

Case Study #	C *1 15	F2 16	F(R)2 17	F2 18	R3 19	C3 20	C 2 21	22	23	F3 24	F3 25
Sample											
T10	25.26	55.38	52.64	37.69	43.93	26.04	35.48	2.11	--	73.94	108.05
T20	19.25	44.41	34.25	24.46	36.96	27.53	24.23	--	--	70.73	116.04
T40	17.68	32.25	26.56	17.82	19.95	19.73	20.72	0.82	--	47.44	63.47
T70	19.72	24.58	27.45	19.97	21.08	19.33	25.49	0.90	--	35.34	43.94
T110	17.02	41.31	32.01	18.31	27.09	27.09	26.73	0.41	--	25.82	30.88
T150	21.96	47.58	33.22	22.10	29.85	30.30	30.95	--	--	22.47	28.50
T250	22.76	31.34	30.47	16.57	26.01	28.11	25.54	0.89	--	18.66	19.98
T500	25.83	36.82	35.80	24.02	32.66	35.01	30.39	0.55	--	22.50	26.02

* F Flow-rate systems

R Reversed order of column arrangement

C Conventional order of column arrangement

Table 5-26. Polyplatykurtic MW resolution corrections for dextran

$\exp(-D2^4\sigma^4 A_K/24)$

Case Study #	3	4	5	6	7	8	9	10	11	12	13	14
Sample												
T10	--	--	--	1.283	1.282	1.273	1.275	1.277	1.277	1.274	1.284	1.276
T20	--	--	1.221	--	--	1.213	1.219	1.218	1.205	1.218	1.219	1.220
T40	1.226	1.208	1.243	1.237	1.235	1.251	1.238	1.239	1.229	1.241	1.235	1.236
T70	1.276	1.237	1.297	1.281	1.282	1.283	1.278	1.281	1.282	1.279	1.280	1.283
T110	1.165	1.159	--	1.180	1.180	1.181	1.180	1.179	1.179	1.181	1.179	1.179
T150	1.279	--	--	--	--	1.337	1.331	1.338	1.339	1.335	1.321	1.341
T250	1.368	1.366	1.433	1.440	--	1.419	1.412	1.425	1.419	1.419	1.425	1.423
T500	1.609	1.632	1.710	1.655	1.697	1.688	1.697	1.699	1.688	1.701	1.709	1.706

Case Study #	15	16	17	18	19	20	21	22	23	24	25	$\sqrt{P(t)}$
Sample												
T10	1.273	1.280	1.282	1.279	1.283	1.286	1.282	1.278	--	1.279	1.280	1.277
T20	1.219	1.219	1.222	1.216	1.219	1.224	1.219	--	--	1.223	1.219	1.220
T40	1.237	1.238	1.239	1.239	1.234	1.238	1.238	1.229	--	1.237	1.238	1.241
T70	1.281	1.280	1.282	1.279	1.279	1.281	1.282	1.241	--	1.281	1.281	1.285
T110	1.182	1.182	1.183	1.183	1.182	1.183	1.182	1.147	--	1.179	1.179	1.179
T150	1.342	1.339	1.338	1.334	1.338	1.339	1.336	--	--	1.335	1.335	1.338
T250	1.417	1.423	1.422	1.422	1.424	1.428	1.424	1.423	--	1.416	1.418	1.432
T500	1.699	1.703	1.699	1.698	1.706	1.708	1.702	1.713	--	1.691	1.698	1.715

Table 5-27. Reproducibility of estimation of σ_T^2 and A_K values

T70			T250		
γ	σ_T^2	A_K	γ	σ_T^2	A_K
-0.701	2.877	-37.615	-0.274	4.743	-19.313
-0.717	2.866	-37.909	-0.144	4.874	-18.294
-0.747	2.831	-38.837	-0.184	4.834	-18.595
-0.681	2.897	-37.082	-0.138	4.879	-18.254
-0.644	2.934	-36.161	-0.171	4.846	-18.502
-0.704	2.874	-37.689	-0.206	4.812	-18.770
-0.654	2.924	-36.413	-0.261	4.757	-19.531
-0.628	2.950	-35.772	-0.228	4.789	-18.946
-0.697	2.881	-37.514	-0.274	4.743	-19.314
-0.701	2.877	-37.623	-0.158	4.859	-18.401
-0.702	2.876	-37.657	-0.172	4.845	-18.511
-0.628	2.950	-35.774	-0.261	4.757	-19.534
-0.587	2.991	-34.791	-0.156	4.861	-18.389
-0.696	2.883	-37.464	-0.178	4.839	-18.557
-0.646	2.933	-36.203	-0.205	4.812	-18.768
Avg.	2.903	-36.967	Avg.	4.817	-18.779
σ	$\pm$ 0.042	$\mp$ 1.066	σ	$\pm$ 0.046	$\mp$ 0.445

5.4. Evaluation of Mobile-phases and Application of TBS method.

The importance of improper selection of mobile-phases and the practical limitation of the universal concept for the three water-soluble polymers investigated are shown in Fig. 5-28 for the system used in Case-Study #19 (for dextran analysis). While the system is well suited for the SEC analysis of dextran over a wide range of MWs, because of the limitation of the selected pore-sizes, the same system cannot be applied for polyacrylamide or sodium polystyrene sulfonate analysis. The selected mobile-phase is well suited for both polydextran and sodium polystyrene sulfonate SEC analysis, but not polyacrylamide,

Figure 5-27. Physical interpretation of newly proposed instrumental spreading function

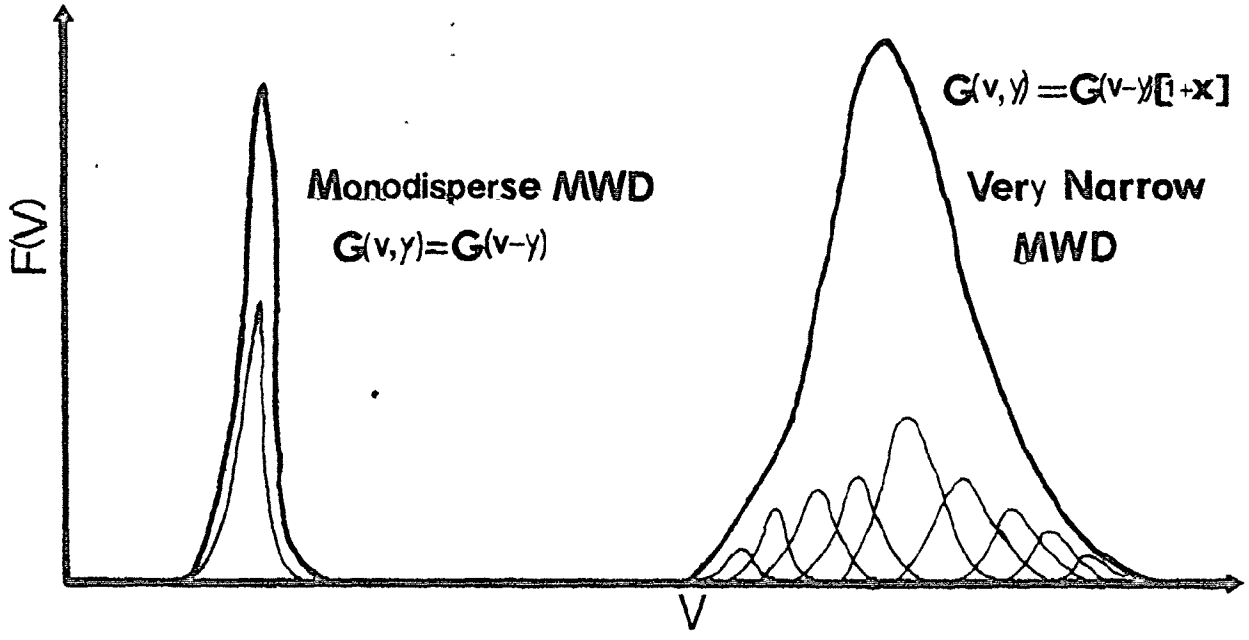

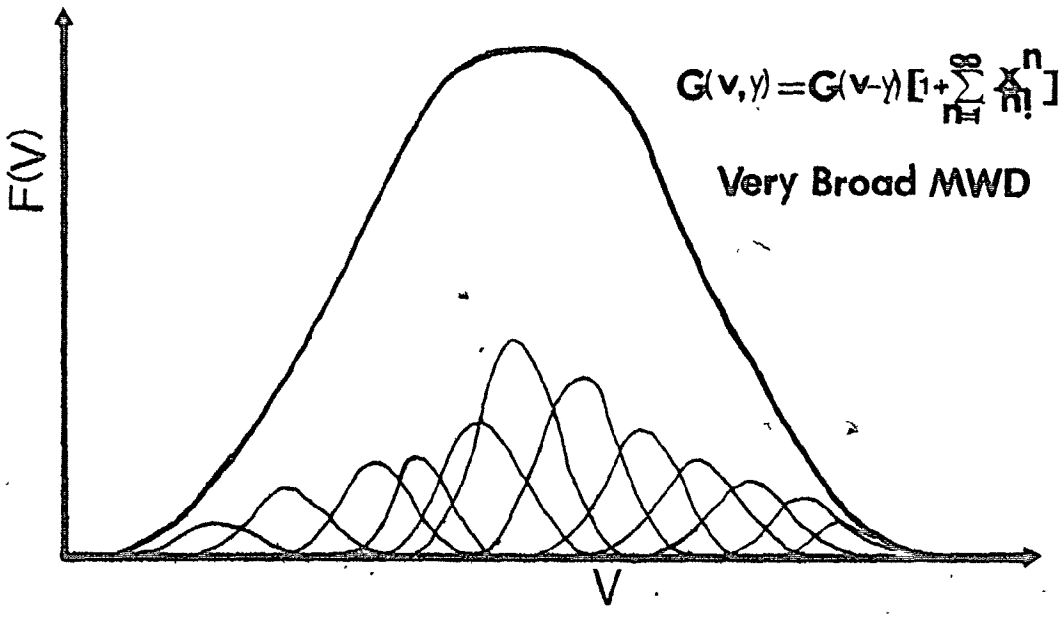

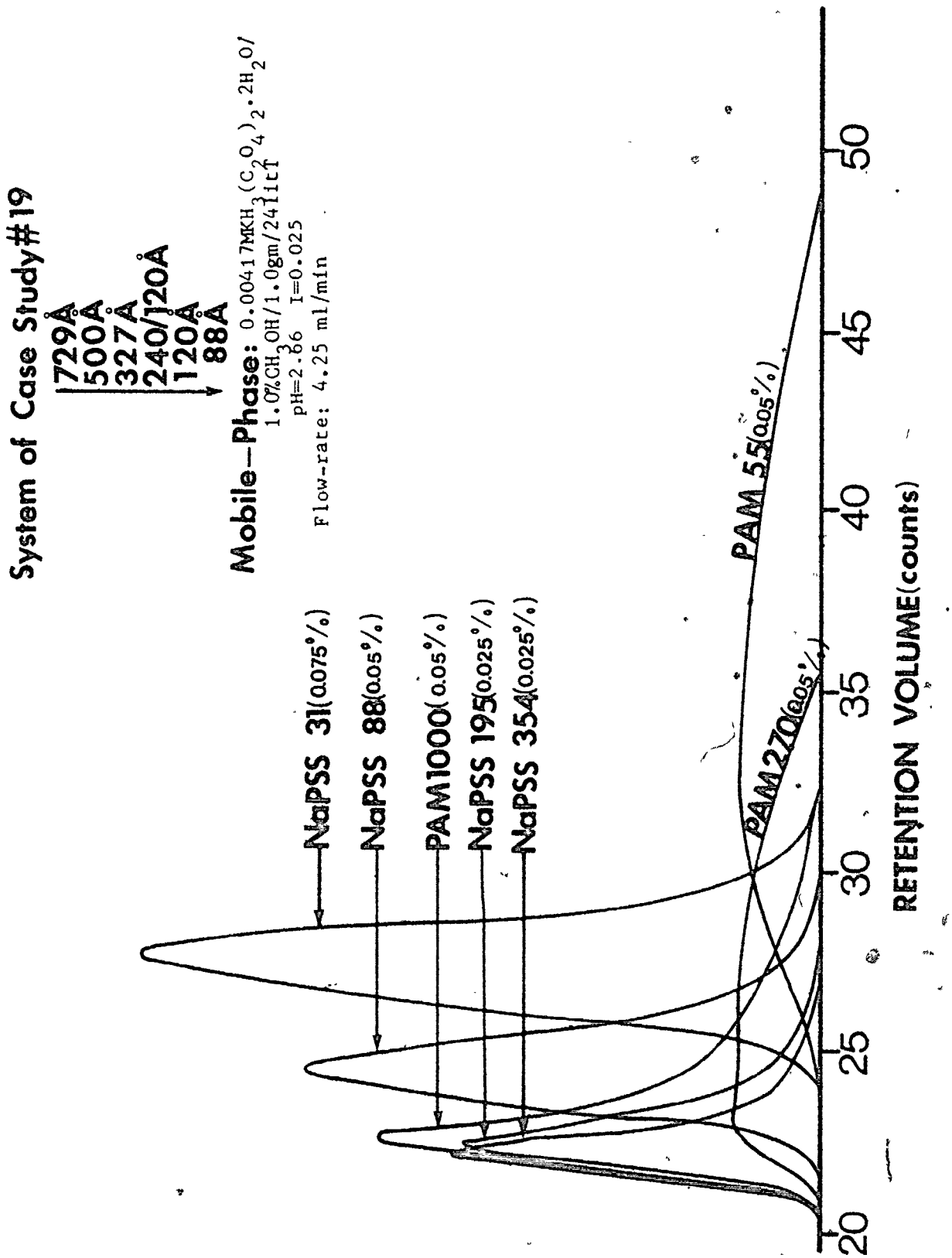

Figure 5-28. Practical limitation of universal concept for system well suited for dextran analysis up to 1×10^6 MW

because of the low pH. The effect of the poorly selected mobile-phase, which enhances polymer-surface interaction, is to broaden the chromatogram of the permeating sample.

In evaluation of mobile-phases, Equation (2.4.14a) for axial dispersion definition was used. For the case where the instrumental spreading function is symmetric as proposed, axial dispersion coefficient as defined is independent of D2 and can be obtained without the knowledge of the MW averages of the sample concerned. In extending the concept to the other water-soluble polymers, it was necessary first to assume that their individual species's shape functions were symmetric or that Equation (2.4.14a) was applicable. Case-Study #33, the only polyacrylamide system with a non-linear $\bar{M}_w$ calibration curve was used along with the highest MW dextran T2000. The results of its application using different linear calibration curves on the samples unimodal and bimodal (T2000) chromatograms are shown in Table 5-28 for polyacrylamide and Table 5-29 for dextran T2000, from which the validity of the equation is difficult to question. In this manner axial dispersion

Table 5-28. Application of σ^{-2} equation for polyacrylamide

Case Study #33

For M(V)=	0.617×10^{10}EXP(-0.289V)		0.381×10^{11}EXP(-0.333V)		0.150×10^{11}EXP(-0.309V)	
Sample	P(GPC)	σ^{-2}	P(GPC)	σ^{-2}	P(GPC)	σ^{-2}
PAM55	2.397	10.47	3.189	10.46	2.713	10.46
PAM270	2.302	9.98	2.985	9.87	2.579	9.92
PAM500	2.811	12.37	3.868	12.21	3.231	12.28
PAM1000	2.450	10.73	3.257	10.66	2.773	10.68
PAM2000	1.664	6.10	1.963	6.09	1.788	6.08

Table 5-29. Their corresponding calculated σ^{-2}** values and errors involved

D2 of linear MW* Calibration Curve	6 0.308	7 0.312	21 0.284	10 0.288	11 0.288	16 0.284	17 0.286	18 0.316	19 0.280	20 0.281	Avg σ^{-2}
T2000 from Case Study #		Axial Dispersion Coefficient, σ^{-2}									
6	7.85	7.85	7.89	7.77	7.89	7.89	7.89	7.84	7.90	7.90	7.87±0.04
7	10.09	10.08	10.16	9.95	10.15	10.16	10.16	10.07	10.18	10.17	10.12±0.07
8	6.95	6.95	6.99	6.86	7.00	6.99	6.99	6.94	7.00	7.00	6.97±0.04
10	7.09	7.08	7.14	7.00	7.13	7.14	7.13	7.07	7.15	7.15	7.11±0.05
12	11.04	11.02	11.12	10.87	11.11	11.12	11.11	11.01	11.13	11.13	11.07±0.08
16	9.44	9.43	9.52	9.29	9.51	9.52	9.51	9.41	9.53	9.53	9.47±0.07
17	10.08	10.07	10.15	9.95	10.14	10.15	10.15	10.06	10.16	10.16	10.11±0.07
18	8.87	8.86	8.91	8.79	8.91	8.91	8.91	8.86	8.92	8.92	8.89±0.04
19	8.86	8.85	8.92	8.74	8.92	8.92	8.92	8.84	8.94	8.93	8.88±0.06
20	9.05	9.04	9.12	8.92	9.11	9.12	9.11	9.03	9.13	9.13	9.08±0.07
21	9.26	9.25	9.34	9.11	9.32	9.34	9.33	9.24	9.35	9.35	9.29±0.07

* The linear MW calibration curves obtained using the TBS method for the different systems

** $\sigma^{-2} = \frac{\ln P(GPC)}{D2^2}$

coefficients for the selected systems and mobile-phases for polyacrylamide and sodium polystyrene sulfonate, were obtained. These are listed in Tables 5-30 and 31 along with their corresponding approximate MW resolution corrections. Again, this phenomenon is shown to be inherent, with less corrections for the narrow MWD polystyrene sulfonate standards than the broad MWD polyacrylamide standards. The latter conclusion has been qualitatively alluded to using the measured widths (W_d) in conjunction with the D2s of each system.

As shown in Table 5-32, where W_d is compared with σ^2 for ten of polydextran systems, there is indeed a relationship between them. The relationship which was found to fit based on the form of Equation (2.4.14a) and was used in assessing the suitability of the selected mobile-phases is given by

$$\ln(W_d D2) = S_N \sigma_T^2 + \ln(W_d D2)_{INF} \qquad (A1\text{-}1)$$

where S_N is the slope of the plot of $\ln(W_d D2)$ versus σ_T^2 and $\ln(W_d D2)_{INF}$ the corresponding value of $\ln(W_d D2)$ at infinite resolution, is the intercept. For each system studied, these plots were obtained. They were found to be linear for all the dextran systems, hydrolysed and non-hydrolysed polyacrylamide systems, pH containing mobile-phase sodium polystyrene systems, but not the non-pH mobile-phase sodium polystyrene systems. Figs. 5-29 to 33 are plots of such cases, in which the non-linear figures are typical of improperly selected mobile-phases.

In updating the TBS method, it was applied to four dextran blends prepared from the standards. Case-Study #19 was used for the analysis of these blends. To obtain the MW averages of these blends using the true MW

Table 5-30. Measured σ_T^2 and σ_T^2 resolution correction for PAM

Case Study # / Sample	26		27		28		29		30	
	σ_T^2	$\exp(\frac{-D2^2\sigma_T^2}{2})$	σ_T^2	$\exp(\frac{-D2^2\sigma_T^2}{2})$	σ_T^2	$\exp(\frac{-D2^2\sigma_T^2}{2})$	σ_T^2	$\exp(\frac{-D2^2\sigma_T^2}{2})$	σ_T^2	$\exp(\frac{-D2^2\sigma_T^2}{2})$
PAM55	6.63	0.604	9.24	0.754	5.85	0.805	4.09	0.769	7.55	0.696
PAM100	10.99	0.433	17.54	0.586	12.37	0.633	7.72	0.610	16.18	0.460
PAM270	--	--	19.03	0.560	12.50	0.630	7.68	0.611	--	--
PAM500	6.10	0.630	14.68	0.639	9.76	0.697	6.28	0.669	9.45	--
PAM1000	6.26	0.621	15.90	0.616	12.08	0.640	6.67	0.652	7.82	0.635
PAM2000	4.38	0.716	12.71	0.679	10.99	0.666	6.92	0.642	6.30	0.687
PAM5000	4.41	0.715	4.66	0.867	--	--	6.50	0.659	--	0.739
	31		32		33		34		35	
PAM55	10.18	0.380	4.03	0.809	10.46	0.646	7.30	0.737	9.36	0.677
PAM100	10.46	0.370	9.13	0.619	--	--	--	--	--	--
PAM 270	--	--	9.18	0.618	9.92	0.661	--	--	--	--
PAM500	7.15	0.507	9.73	0.600	12.28	0.600	10.12	0.655	12.00	0.606
PAM1000	7.30	0.500	8.53	0.639	10.68	0.640	9.64	0.669	10.32	0.650
PAM2000	5.77	0.578	5.14	0.763	6.08	0.776	9.06	0.685	6.10	0.775
PAM5000	5.67	0.584	3.86	0.817	--	--	--	--	--	--
Std B	--	--	--	--	2.88	0.887	5.81	0.785	4.00	0.846

Table 5-31. Measured σ^2 and σ^2 resolution correction for NaPSS

Case Study # Sample	36		37		38		39		40	
	σ_T^2	$\exp(\frac{-D2^2\sigma^2}{2}T)$	σ_T^2	$\exp(\frac{-D2^2\sigma^2}{2}T)$	σ_T^2	$\exp(\frac{-D2^2\sigma^2}{2}T)$	σ_T^2	$\exp(\frac{-D2^2\sigma^2}{2}T)$	σ_T^2	$\exp(\frac{-D2^2\sigma^2}{2}T)$
NaPSS31	--	--	--	--	--	--	6.89	0.925	6.64	0.923
NaPSS88	4.80	0.917	3.74	0.933	3.82	0.909	5.28	0.942	5.16	0.940
NaPSS195	4.42	0.923	3.67	0.934	3.37	0.919	5.67	0.937	5.05	0.941
NaPSS354	4.59	0.885	4.06	0.927	2.87	0.931	4.89	0.946	4.42	0.948
NaPSS690	6.75	0.921	4.01	0.928	4.76	0.887	11.17	0.881	8.04	0.908
NaPSS1060	6.14	0.895	3.46	0.937	3.27	0.921	7.59	0.917	8.04	0.908
	41		42		43		44		45	
NaPSS31	5.08	0.929	2.10	0.919	1.99	0.950	2.84	0.929	2.90	0.927
NaPSS88	4.78	0.933	2.44	0.907	2.23	0.944	3.70	0.908	3.60	0.911
NaPSS195	4.60	0.936	2.13	0.918	2.85	0.929	4.82	0.882	5.59	0.865
NaPSS354	4.66	0.935	2.35	0.910	3.65	0.910	9.40	0.783	8.53	0.801
NaPSS690	10.08	0.865	3.71	0.862	7.83	0.817	8.65	0.799	--	--
NaPSS1060	8.35	0.886	4.72	0.828	8.89	0.795	8.16	0.809	8.27	0.807

Table 5-32. Comparison of W_d and σ^2 of samples from various systems

Case Study #	7		9		11		13		15	
Sample	W_d	σ_T^2	W_d	σ_T^2	W_d	σ_T^2	W_d	σ_T^2	W_d	σ_T^2
T10	7.40	3.04	6.70	2.64	8.30	3.84	8.60	4.16	11.10	6.86
T20	--	--	7.10	3.08	8.60	4.17	8.90	4.60	11.15	7.10
T40	9.50	4.74	8.90	4.78	9.90	5.67	10.50	5.89	11.60	7.71
T70	10.75	5.70	9.90	5.58	10.40	6.35	11.50	7.74	11.70	7.86
T110	9.30	4.51	8.75	4.46	9.50	5.03	9.70	5.33	10.63	6.55
T150	--	--	10.30	6.21	10.70	6.71	11.00	6.74	11.80	8.03
T250	12.40	7.20	12.00	7.55	12.60	8.22	12.90	8.47	12.70	8.76
T500	13.10	8.45	12.95	9.93	12.75	8.82	13.65	10.80	13.60	10.08
	16		17		18		24		25	
T10	8.50	4.04	8.50	4.08	7.80	3.95	5.45	2.05	5.15	1.77
T20	8.60	4.07	8.80	4.57	8.20	4.43	5.30	1.88	5.30	1.53
T40	9.50	4.97	9.60	5.40	9.25	5.40	5.80	2.38	5.85	2.15
T70	10.50	6.13	9.70	5.72	9.40	5.79	7.20	2.97	6.75	2.79
T110	7.90	3.66	8.50	4.10	8.10	4.44	6.30	2.83	6.40	2.70
T150	9.20	4.75	9.40	5.61	9.30	5.63	7.70	4.02	7.70	3.74
T250	11.50	6.50	11.00	6.50	11.40	7.22	9.70	4.84	9.80	4.90
T500	12:10	7.35	12.10	7.35	11.70	7.35	10.10	5.41	10.10	5.27

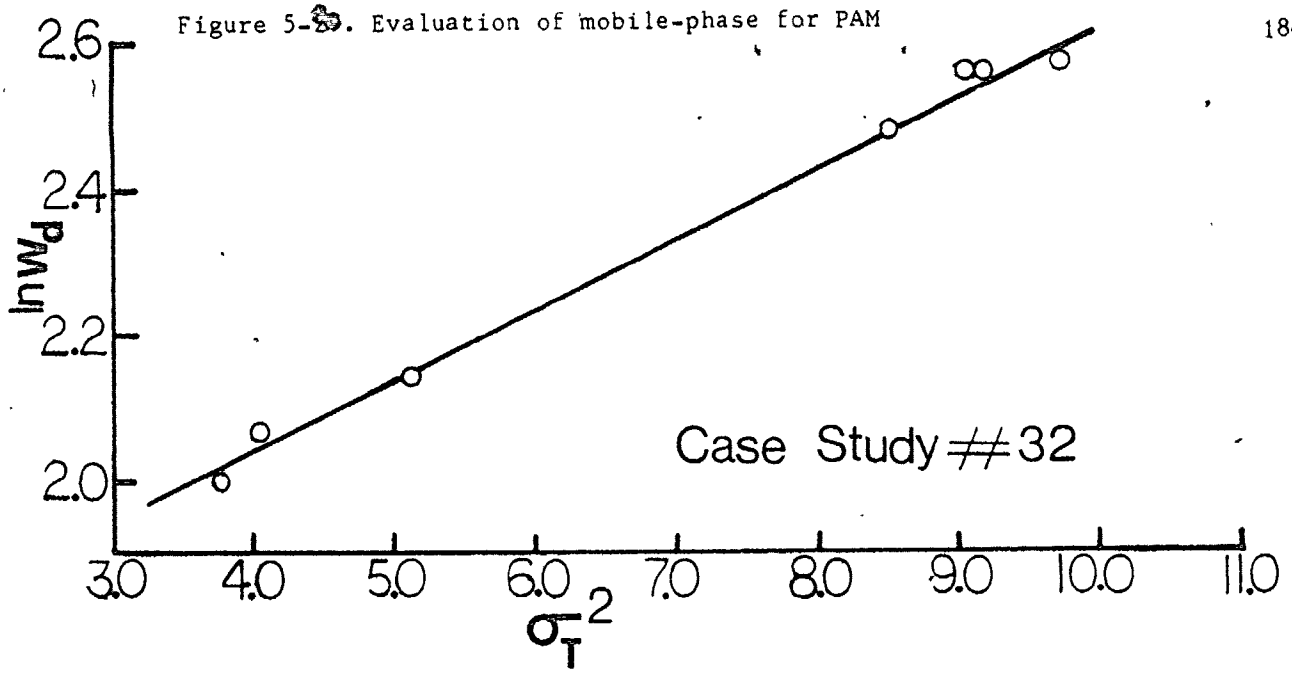

Figure 5-30. Evaluation of mobile-phase for PAM

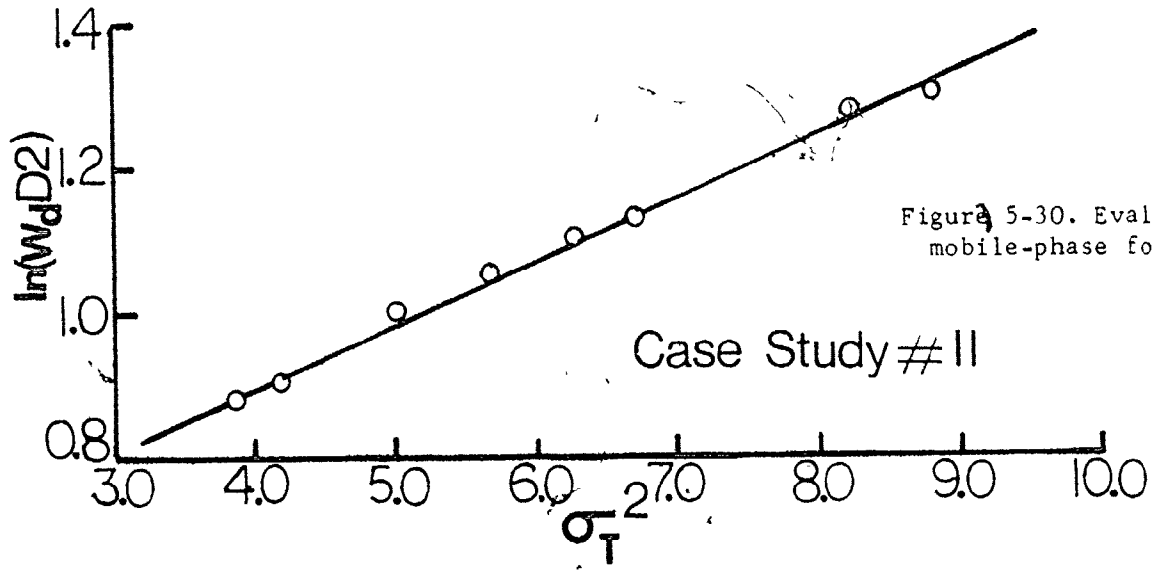

Figure 5-30. Evaluation of mobile-phase for dextran

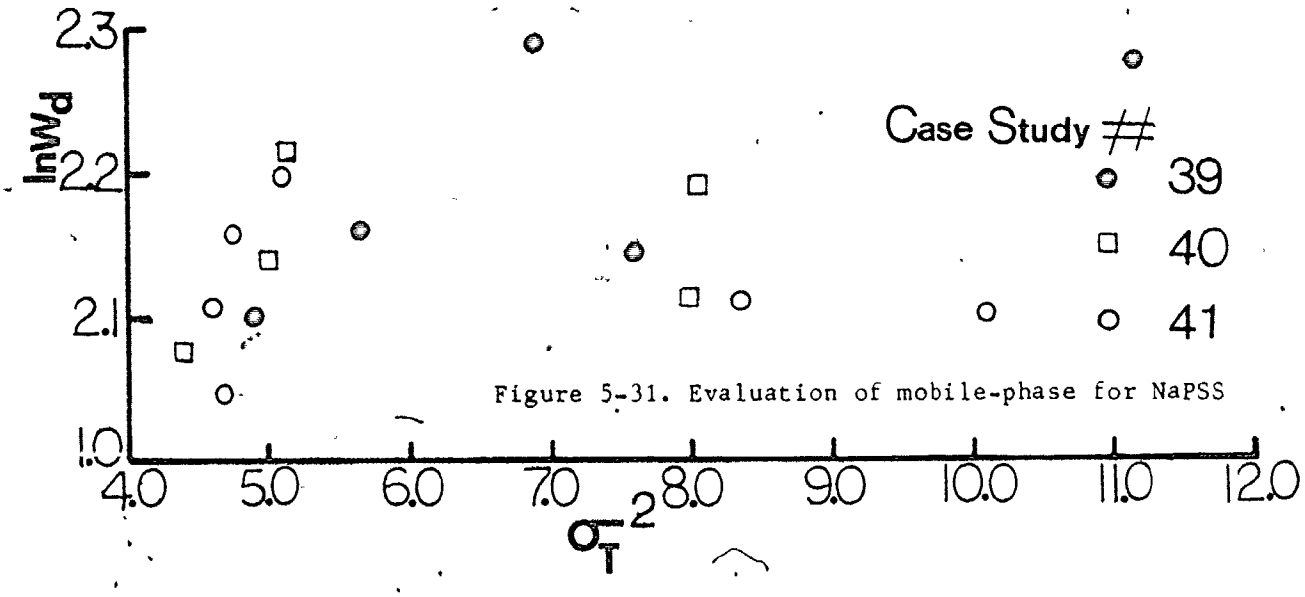

Figure 5-31. Evaluation of mobile-phase for NaPSS

Figure 5-32. Evaluation of mobile-phase for NaPSS

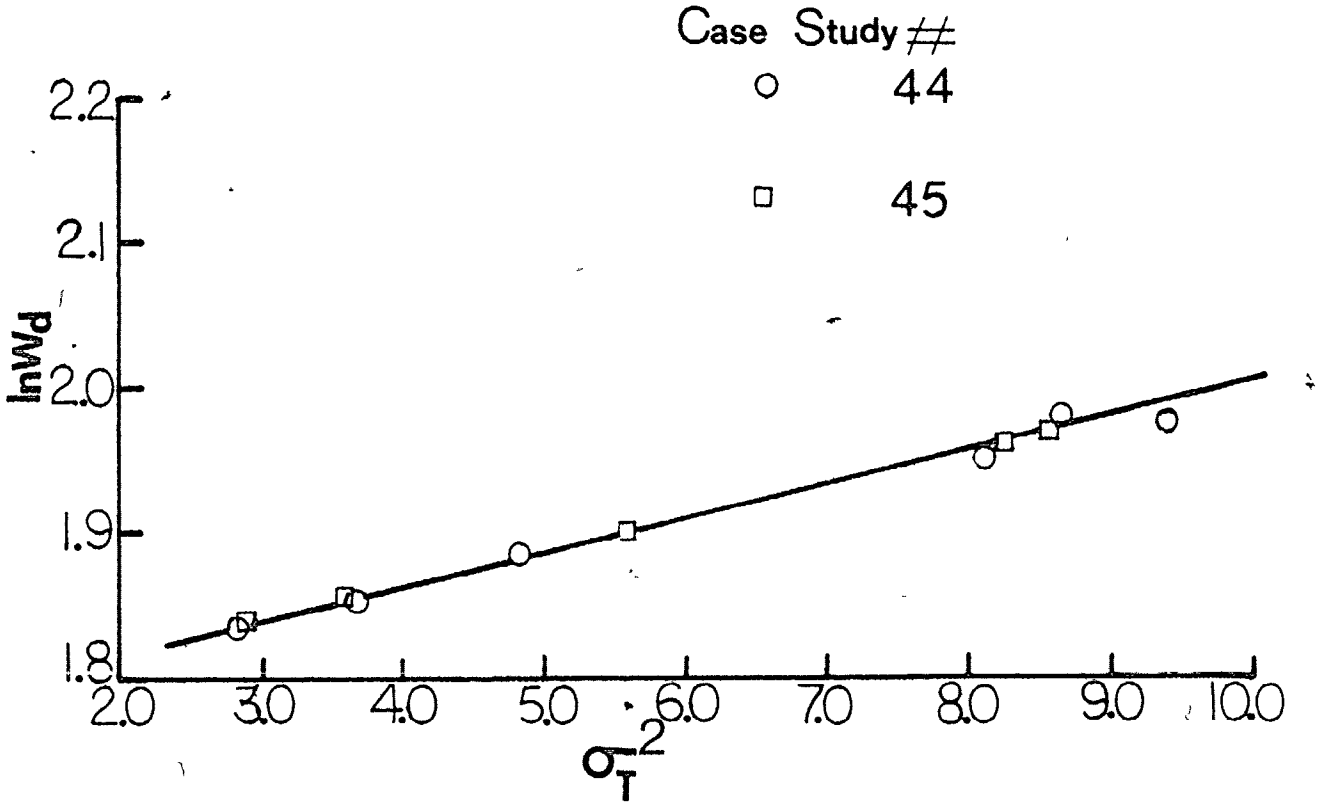

Figure 5-33. Evaluation of mobile-phase for hydrolysed PAM

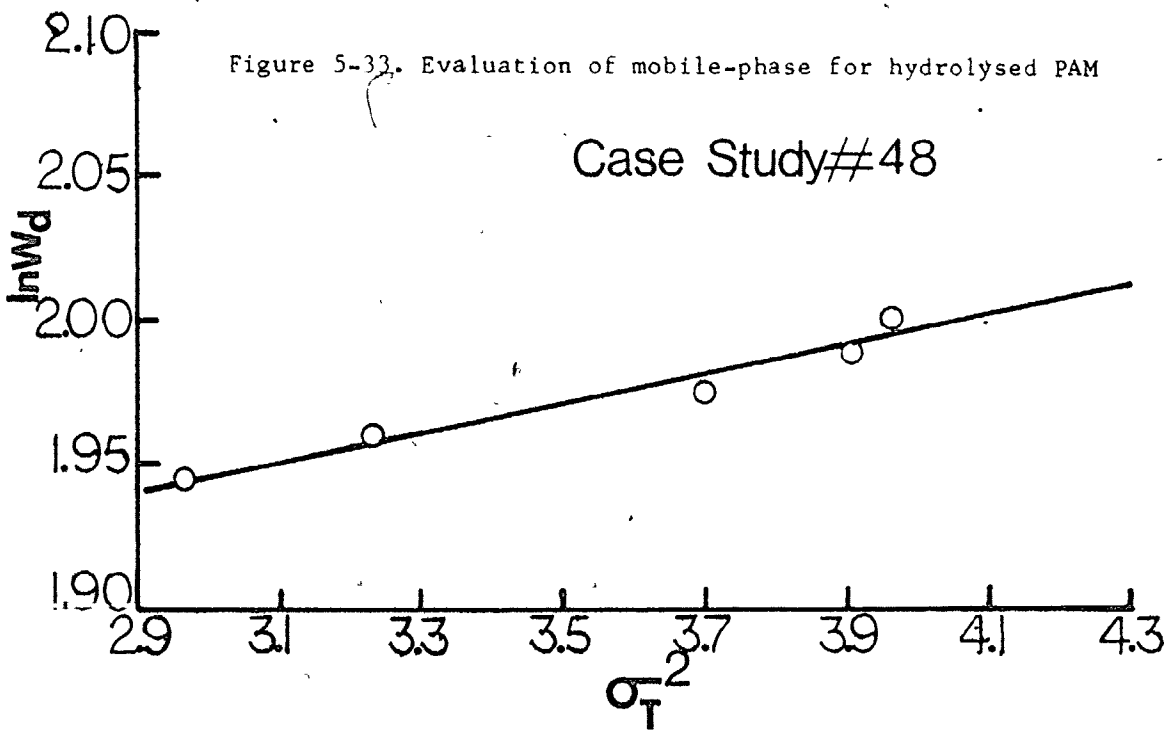

calibration curve of this system, it was necessary to obtain the A_K values for each blend. The MW resolution correction with respect to polyplatykurtosis was found to be independent of the system, but dependent on polydispersity and careful observation has shown that the A_K values are functions of MW and therefore retention volumes. Such dependence is shown in Fig. 5-34 for one of the flow-rate systems (Case-Studies 24 and 25). Using such plots, the A_K values of the blends were obtained and the characteristics of the blends and the chromatograms and the estimated true or corrected MW averages are compared with the true values in Table 5-33.

Table 5-33. Application of TBS Method and proposed instrumental spreading function

Unknown Sample	T20/T40	T110/T250	T250/T500	T110/T200
Ratio of Standards	(1:1)	(1:1)	(1:1)	(3:1)
W_d	10.30	10.50	12.30	14.00
σ^{-2*}	6.65	6.80	8.23	10.00
σ^{-2**}	6.60	6.70	8.25	10.08
PRV	35.70	30.00	27.60	29.40
A_K	-29.00	-24.50	-30.00	-26.00
$\bar{M}_W(t)$	33.35	168.50	340.00	--
$\bar{M}_n(t)$	19.75	90.72	120.30	--
$\bar{M}_W(corr)$	32.85	163.86	333.14	251.05
$\bar{M}_n(corr)$	19.59	93.34	117.06	64.88
$EXP(-D2^2\sigma_4^2/2)$	0.772	0.769	0.724	0.674
$EXP(\frac{-A_K\sigma_4 D2}{24})$	1.380	1.325	1.687	1.967
P(t)	1.689	1.857	2.826	--
P(corr)	1.677	1.756	2.845	3.870
% Error in $\bar{M}_W$	1.50	2.75	2.02	--

* Using equation (2.4.14a)

** Using plot of $\ln W_d$ versus σ_T^2

Figure 5-34. Polyplatykurtic coefficient (A_K) versus peak retention volume for one of the dextran systems

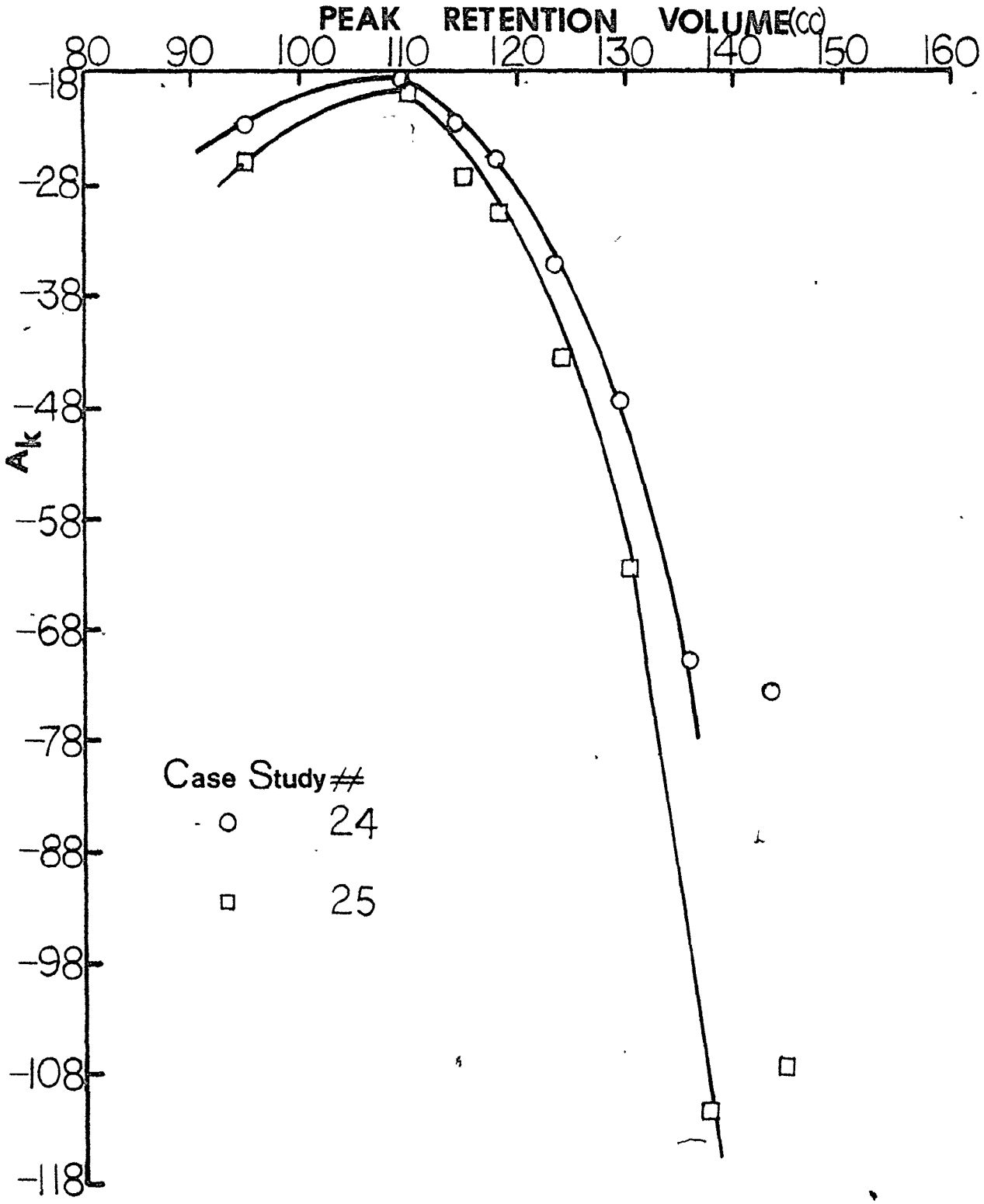

5.5. Relation of Present Results to existing Literature

Two recent attempts to develop aqueous SEC for the characterisation of non-ionic polyacrylamide have been reported (61)(62). The first employed CPG-10 with formamide containing KCL (0.005 M) as the mobile-phase. The investigation was not comprehensive and the final separations achieved were not impressive. Contraction of the polyacrylamide molecules were reported with viscosity data, when salt was added to the polymer in formamide solution, and the chromatograms were reported to shift on addition of salt to the formamide mobile-phase. Four 4 ft. columns containing 3125, 486, 255 and 75 Å packing gave a 19.4 ml separation for $\bar{M}_W$ in the range of about 120,000 to 5×10^6. The use of 255 Å and 75 Å packing for high MW polyacrylamides is not recommended based on the present results. No discussion was made of peak broadening. The only attempt on the analysis of hydrolysed polyacrylamide (7.0 - 37%) was also contained in this investigation. Abnormal elution behaviours were observed depending on the degree of hydrolysis for the formamide mobile-phase with and without salt. No quantitative measurements were possible.

The second study on polyacrylamide (62) employed a newly commercialized organic gel packing TSK-GEL type PW (Toyo Soda Manufacturing Co., Japan). The packing particles were 15 microns in diameter. A 0.08 M tris-HCl buffer solution (pH = 7.94) was used as mobile-phase. The peak separation obtained with a three column set (G 3000 PW + 2G5000 PW) is comparable to the peak separation obtained in the present study for the $\bar{M}_W$ range, 120,000 to 3.6×10^6. Peak broadening of the chromatograms were however reported to be larger than expected although no calculations of single-species variance were done.

Studies involving the SEC analysis of sodium polystyrene sulfonate have also been sparse. Several authors have reported its dependence on the I and pH of mobile-phase (8)(9)(10) using CPG-10, but no comprehensive qualitative studies have been reported. In one of the publications (10), the universal concept was proven to be valid for the sodium polystyrene sulfonate and polydextran. 0.2 M and 0.8 M Na_2SO_4 solutions were investigated as mobile-phases and five-columns 1250, 670, 500, 190 and 75 Å each 5 ft long (0.17 in ID) were used. Characterisation of the NaPSS standards were reported to be complicated by the presence of impurities and no corrections for single-species variances were done. Several attempts (8)(9) have been made to validate the universal concept, but in vain.

Many investigations of the aqueous SEC of dextrans have been published (8, 9, 10, 14, 31, 38, 39, 33, 63, 64, 65, 66). One of the earliest studies was that of Bombaugh et al (65) who used water at 65°C and 1 ml/min as mobile-phase and deactivated Porasil as packing. Qualitatively the chromatograms indicated excellent peak separation of the MW range of 11,000-150,000. The chromatograms for the higher MW standards had shoulders near the void volume, which were first misconceived to be due to polymer surface interaction, but were later confirmed to be caused by the actual distribution of the polymers. Cooper and Matzinger (8) found using CPG-10 packing and phosphate solutions (pH = 7.0) at three Is, that the MW calibration curve was independent of I. They showed that CPG packing materials can exhibit ion-exclusion for polyelectrolytes in low ionic strength media. Though Spatorico and Beyer (10) made almost similar observation at 0.2 M and 0.8 M Na_2SO_4, they reported the dependence of the intrinsic viscosity of dextran on I, which could mean that their

narrow dextran standards were highly charged. Peak separations were good and the corrections to $\bar{M}_n$ and $\bar{M}_w$ for imperfect resolution were appreciably small although data were not presented. Buytenhuys and Vander Maeden (64) chromatographed dextrans on Lichrospher packings (untreated silica micropacking with particle diameter of about 10 microns and 100 Å, 300 Å and 500 Å pores) using water and also 0.5 M sodium acetate (pH = 5.0) as mobile-phases. The use of the salt eliminated the high MW shoulder peak caused by ion-exclusion. These authors suggested that dextrans may have a few negative charges. This was also confirmed in the present study using CPG-10.

Hashimoto et al (62) using the newly commercialized TSK GEL type PW, for three columns combined in series and 0.08 M tric-HCl buffer solutions as mobile-phase, reported bimodal chromatograms for three different batches of $2x10^6$ MW dextran. They suggested the higher branching of the high MW standard to be responsible for the bimodality. These were suggestions previously made by Wu et al (67) and Chow (68), using other packing materials and mobile-phases. However, no references were made by Hashimoto et al (62) of the pictorial bimodal chromatograms of other lower MW standards on single columns of different pore-sizes, reported in their study. For the three single columns studied individually, the samples were bimodal depending on the MW exclusion limit of the pore-sizes, and the MWD of the standard. In the present investigation, the same observations were made not only for dextran but also polyacrylamide. For the broad $2x10^6$ MW dextran standard, and for a system where a part of the polymer was always permeating the pores, leaving another fraction not permeating at all, bimodal chromatograms were observed, the sharpness of the second peak depending on the new slope within the non-linear region.

In a recent study by Ogawa et al (69), using non-aqueous SEC system, the bimodalities were explained on the basis of the non-linearity of the MW calibration curve.

Of all the complex phenomena, ion-inclusion of salt could not be eliminated by increasing addition of salt, as it is believed to be (9)(6). As was recently reported (8), the size of the included salt peaks were found to increase with additional amount of salt. The phenomenon was also found to be stronger with single columns, than multicolumn combinations where sometimes, they were not observed.

For many years, dextrans have been used for developing MW calibration curves for aqueous SEC. In most such reported cases distilled water and deactivated porasil were used. The linear low MW range of separation and other unique features of the MW calibration curves have recently been attributed to the more branching of the high MW standards (38). In the present investigations, in the absence of the newly proposed instrumental spreading function, similar conclusions could have been made. The newly proposed shape function falls very much within the expectations of the observations of several authors including Figini (24), Tung and Runyon (60), Kotaka (70)(71), Yau, Stoklosa and Bly (23), Ouano, Home and Greggs (72), Ouano and Kave (73).

6.1 CONCLUSIONS

A summary of the accomplishments in meeting the three objectives of the thesis now follows, each taken one at a time, in the order specified in Chapter 1.

To develop an effective mobile-phase and packing for the SEC of a polymer, the first major step is the measurement of intrinsic viscosities for the polymer in different mobile-phases. These data reveal how the polar coil size is affected by additives. This greatly simplifies the interpretation of the behaviour of the polymer during chromatographic separation. The changes in polymer coil size of the polymers investigated revealed from viscosity data are summarized below.

(i) Dextran was the only polymer for which the intrinsic viscosities were not affected by addition of salt, acid and surfactant or cosurfactant to distilled water. The very small intrinsic viscosities compared to large values for PAM and NaPSS, confirms their branched structure and compact size in solution (10, 62).

(ii) The intrinsic viscosities of NaPSS in distilled water were much larger than in solutions containing salt or acid or both. This was interpreted to mean that NaPSS in water is highly expanded due to negative charges on the chain. With increasing addition of salt or acid or both, decreasing values of intrinsic viscosities were obtained. Small limiting values were observed in the range I = 0.1-0.3 (Fig. 4.4), the value of I varying with MW of the sample. The addition of salt was more effective than the addition of acid, in suppressing the negative charges and reducing the intrinsic viscosities.

(iii) Two of the non-ionic polyacrylamide samples showed 'anomalous behaviour' in distilled water, giving excessively large viscosities much like NaPSS in water. On addition of salt or acid or both, the Mark-Houwink relationship obtained was independent of I and pH but different from that in water. The anomalous behaviour in distilled water raises some questions about the validity of the Mark-Houwink relationship in the literature (51, 52). These are known to be in substantial disagreement.

(iv) In water, the viscosities of hydrolysed PAM were too large to measure with the available viscometer. Unlike NaPSS, addition of acid was found to considerably reduce the intrinsic viscosities more so than addition of salt. In the absence of acid (pH = 7.0), the intrinsic viscosities were to a large extent independent of I.

(v) The addition of small concentrations of surfactant or co-surfactant to the solvents does not affect the intrinsic viscosities of these polymers.

Based on the intrinsic viscosity data, it was clear that

(a) the MW calibration curve of Dextran is independent of I, pH over the ranges covered.

(b) the MW calibration curve of non-hydrolysed PAM is independent of I and pH, over the ranges covered.

(c) the MW calibration curve of NaPSS is highly dependent on pH and I of the mobile-phase.

(d) the MW calibration curve of hydrolysed PAM is independent of I at pH = 7.0, but dependent on pH of the mobile-phase.

In applying the mobile-phase of choice for the SEC of the polymers in question, complications do arise due to polymer solute/packing interactions and other factors. These include:

(i) complications due to the active sites present in most porous

packing materials suited for the SEC of water-soluble polymers,

(ii) procedures used for column packing,

(iii) the order in which the columns of different pore-sizes have to be arranged,

(iv) the type of pore-sizes which have to be selected for a particular polymer, and

(v) the chemistry of the polymer in solution at various I, pH and surfactant levels.

In eliminating the complications above, the following results were obtained:

(a) A new additive was found, which in the presence of salt or acid or both, considerably reduced the adverse effect of the active sites. This additive was a neutral surfactant and Tergitol was effective.

(b) Reproducibility of separation of a packed column is very important in SEC, and this is only possible when the columns are well packed. The recommended method of packing for macro-particles such as CPG-10 and most others suited for aqueous SEC applications, is dry packing.

(c) Due to large surface areas of small-pore size packing materials, the traditional method of column arrangement is not recommended. Instead the arrangement should be reversed.

(d) The type of pore-sizes selected for the SEC of any polymer is very important. In this respect, it is recommended that each pore-size (single columns) be individually calibrated. In this manner, peak-broadening can be greatly minimized and peak-separation maximized. No common single SEC system (mobile-phase and packing) could be selected which was optimal for the four water-soluble polymers investigated. This suggests that universal calibration may not be a useful concept in aqueous SEC.

(c) Viscosity data may reveal the possible use of a wide range of I or pH or both, but for polymers such as NaPSS, complete adsorption occurred when very high I were used in the presence of tergitol. The addition of acid reduced the adsorption. Whereas for polymers such as PAM, the presence of acid was found to also encourage adsorption, the differences attributed to the chemical differences of the polymers. On the whole, the following are the recommended mobile-phases found for the polymers investigated:

(i) For Dextran: To distilled water, any I of salt or pH can be employed. While addition of salt is very important, the use of Tergitol may depend on the batch of Dextran analysed or degree of active sites present on the stationary-phase.

(ii) For PAM hydrolysed or non-hydrolysed: With I ranging from 0.01-0.2, the pH of mobile-phase should be kept at 7.0 ± 0.5, in the presence of neutral surfactants.

(iii) For NaPSS: Addition of acid is most important ($pH < 4.5$), while keeping the I at intermediate levels ($I = 0.01\text{-}0.1$), in the presence of neutral surfactants.

Two of the more important and least understood phenomena in aqueous SEC, include ion-exclusion and adsorption. Two degrees of ion-exclusion have been identified in the present study - "partial" and "total". Partial ion-exclusion occurs where part of the polymer is excluded from the pores, usually the larger chains. The proposed mechanism for both phenomena is charge repulsion. With distilled water as mobile-phase, total exclusion of polymer solute from the pores was observed. Dextrans have been considered neutral polymers until recently (64). The present work confirms the presence of a small amount of negative charge on some of the chains. This is the cause of partial exclusion with Dextrans. With addition of a

very small amount of salt, partial ion-exclusion is completely eliminated. Unlike dextran, the other polymers are totally excluded from the pores with pure water as mobile phase. Addition of a considerable amount of salt ($I > 0.01$) is needed to eliminate total ion-exclusion. The use of surfactants or co-surfactants alone did not eliminate any of these phenomena.

Adsorption phenomena in SEC are not well understood and very few quantitative details are known. With the aid of viscosity data, some simple basic knowledge of the chemistry of the polymer, and with the use of certain additives, adsorption can be reduced or eliminated. Reversible and irreversible adsorption phenomena were observed. These were eliminated or reduced by the addition of a neutral surfactant to the mobile-phase, with the appropriate pH and/or I, depending on the polymer under investigation. There has been no general agreement on how to eliminate adsorption since the subject matter has never been addressed by carefully planned systematic studies, requiring a wide range of additives. Rather, a few experiments, based on one or two SEC systems are available.

From this research investigation, the following are the new theoretical developments for MW calibration and chromatogram interpretation:

(i) Several methods of MW calibration of SEC were proposed, of which the TBS methods - the linear version was shown to provide a true MW calibration curve. This true calibration curve was identified as a plot of $\bar{M}_{rms}$ versus peak retention volume. This makes SEC very easy to calibrate, although it requires knowledge of the $\bar{M}_w$ of the two standards, and one other average MW (eg. $\bar{M}_n$). This suggests that one MW average is never sufficient to fully characterise a polymer, a misconception in the past.

(ii) A new shape of instrumental spreading function was proposed. This shape function is consistent with chromatographic theories, due to its symmetric form. The proposed shape function is a two-parameter model:

axial dispersion coefficient, σ^{-2} and a new polyplatykurtic coefficient, A_K.

(iii) As a result of the newly proposed shape function, a new definition in the theory of axial dispersion was developed. It was shown to be a function of the polydispersity of the experimental chromatogram obtained from any linear MW calibration curve and the slope of the corresponding calibration curve. It was also shown not to be a function of MW or retention volume as it has been conceived in the past, but a direct function of the width of the chromatograms, W_d.

(iv) Also as a result of the newly proposed shape function, a definition in theory of the "polyplatykurtic" coefficient, A_K, was found. It is a function of the true polydispersity of the polymer, σ^{-2} and D2. In the expression, A_K can only be negative in the range 0 for an infinitely broad standard to $-\infty$ for a monodisperse standard. It was shown to be the most important fundamental parameter in SEC, contrary to past ideas. To obtain A_K for a sample, a calibration curve of A_K versus peak retention volume is used. This curve is similar in shape to previously used plots of σ^{-2} versus retention volume.

(v) From the new definition of axial dispersion, a new method of evaluating the suitability of a mobile-phase was found. In the absence of adsorption, a plot of $\ln(W_d D2)$ versus σ^{-2} was linear.

(vi) A new method of evaluation of true linear MW calibration methods was proposed. This involves a plot of sets of lnD1 versus D2 obtained using different samples in the linear or non-linear regions of the true MW calibration. When the method is adequate, for samples in the linear region, a single point is obtained; whereas for samples in the non-linear region, the plot is linear. When the method is inadequate, for samples in the linear or non-linear regions of the true MW calibration

curve, the plot is also linear, covering a wide range of D2.

(vii) From the newly proposed instrumental spreading function, an expression which contains both σ^2 and A_K was obtained. This expression which is linear, provides a means of checking if the polydispersities of the samples used as standards are the true values. It also provides another means where σ^2 can be obtained (the intercept of the plot).

(viii) Additional sources of peak broadening in SEC were found. These include in decreasing order of contribution:

(a) pore dispersion

(b) improper selection of mobile-phase and packing

(c) polymer/surface interaction resulting from traditional order of column arrangement

(d) flow-rate.

(ix) Finally the true MW calibration curve was shown to be independent of flow-rate. When correction of the siphon dump counter (cc per count) was applied, the same calibration curve was obtained in the flow-rate range of 1.4 ml/min to 7.8 ml/min. This reduces the problem of slow analysis time by the use of high moble phase flow-rates with appropriate peak broadening corrections.

6.2. NOMENCLATURE

A_n	coefficients in the statistical shape function, n=3,4,5
A_3	skewing coefficient in the statistical shape function
A_4	flattening or kurtosis coefficient in the statistical shape function
A_K	flattening or kurtosis coefficient in the newly proposed Instrumental Spreading function
a	a constant (exponent) in Mark-Houwink intrinsic viscosity-molecular weight relation
c	concentration of polymer in a solution (100 cc or 1 litre)
c1, c2	Parameters of a linear molecular weight calibration curve of molecular weight versus retention volume
D1, D2	Intercept and slope of $\log_e$ (Molecular weight) versus retention volume respectively
$\frac{dM}{dV}$, D2'	the slope, D2 of the true linear calibration curve
ELC	Effective Linear calibration method
F(V)	GPC elution chromatogram
$F_W(M)$	Weight-based molecular weight distribution (with respect to molecular weight)
G(v,y)	Instrumental spreading function
G(v-y)	Uniform instrumental spreading function
$G_s(v-y)$	symmetric instrumental spreading function (newly proposed)
GPC	Gel permeation chromatography
h	total Gaussian resolution factor
H_3, H_4	3rd and 4th order Hermite polynomials
I	Ionic strength ($= \frac{1}{2} \sum_{c=1}^{n} c_i z_i^2$, where c_i is concentration of ionic species and z_i is the corresponding valency)
J1*, J2* J3*	Parameters of the transformed true linear molecular weight calibration curve
K_s	the $\log_e$ of the true polydispersity of a sample

M	Molecular weight
$\bar{M}_K(t)$, $\bar{M}_K(oo)$	K-th spreading corrected (or true) and uncorrected molecular weight averages
$\bar{M}_n$, $\bar{M}_W$	number - , weight - average molecular weights
$\bar{M}_n(t)$, $\bar{M}_n(oo)$	spreading corrected (or true) and uncorrected number - average molecular weights
$\bar{M}_{rms}$	root mean square average molecular weight
$\bar{M}_K(app) = \bar{M}_K(oo)$	
$\bar{M}_{n_{mixture}}$, $\bar{M}_{W_{mixture}}$	number - , weight - average molecular weights of mixture or blend
M(V)	true molecular weight calibration curve
MW, MWD	Molecular weight, molecular weight distribution
P(t), P(app) or P(SEC)	true and apparent or SEC polydispersity
pH	strength of acid
PRV	peak retention volume
PAM	polyacrylamide (non-hydrolysed)
R_s	Effectiveness of column resolution
s	bilateral Laplace transform variable
SK	skewing factor
S_N	the slope of the axial dispersion resolution calibration curve
TBS	Two broad standard method
V	retention volume
W_1, W_2 / W_A W_B	peak widths of chromatograms 1 and 2 or A and B
W_d	peak width of chromatograms of any sample
$W_{d_{INF}}$	peak width of chromatograms under condition of 100% resolution
W(y)	the true chromatogram or MWD of a sample or spreading corrected chromatogram
W(v)	normalised spreading corrected chromatogram
x	a variable (see equation (2.4.9c))

Greek Symbols

$[\eta](t)$, $[\eta](oo)$ spreading corrected (or true) and uncorrected intrinsic viscosities dL/g

η_{sp}, $\eta_{solution}$, $\eta_{solvent}$ specific viscosity, viscosity of solution and solvent respectively

μ_o, μ_1, μ_2, μ_3, μ_n zero, first, second, third and n-th moments of chromatogram

σ_T^2 Overall variance

$\phi(v-y)$ Gaussian instrumental spreading function

γ, $\gamma_{\overline{M}_W}$, $\gamma_{\overline{M}_n}$, γ_{D2} Overall molecular weight instrumental spreading function correction factor, total, weight -, number - average and true molecular weight calibration curve based factors

REFERENCES

1. N.M. Bikales, Ed., "Water-soluble Polymers", in Polymer Science and Technology, v.2, Flenum Press, New York (1973).

2. Chemical and Engineering News, March 8 (1976) p.10.

3. E.F. Herbeck, R.C. Heintz and J.R. Hastings, Petroleum Technol, July, 48 (1976).

4 W.B. Gogarty and W.C. Tosch, J. Petroleum Technol., December, 1407 (1968).

5. J.C. Giddings, Separation Sci., 8, 567, (1973).

6. P.A. Neddermeyer and L.B. Rogers, Anal. Chem., 41(1), 94(1969); P.A. Neddermeyer and L.B. Rogers, ibid, 40(4), 755 (1969).

7. K.G. Forss and B.G. Stenlund, J. Polym. Sci., Symp. No. 42, 951 (1973).

8. A.R. Cooper and D.P. Matzinger, J. Appl. Polym. Sci., 23, 419-427 (1979).

9. A.R. Cooper and D.S. Van Derveer, J. Liq. Chrom., 1(5), 693-726 (1978).

10. A.L. Spatorico and G.L. Beyer, J. Appl. Polym. Sci., 19(11), 2933 (1975).

11. R. Epton, C. Holloway and J.V. Mclaren, J. Chromatogr., 117, 245, (1976).

12. H.D. Crone, J. Chromatogr., 107, 25 (1975).

13. H.D. Crone, R.M. Dawson and E.M. Smith, J. Chromatogr., 103, 71 (1975).

14. A.R. Cooper and D.P. Matzinger, Am. Lab., 9(1), 13, (1977).

15. M. Kato, T. Makagawa and H. Akamatu, J. Phys. Chem., 33(3), 322 (1959).

16. P. Chong and G. Curthoys, J. Appl. Polym. Sci., 23, 1563-1575 (1979).

17. N. Onda, K. Furusawa, N. Yamaguchi and S. Komuro, J. Appl. Polym. Sci., 23, 3631-3638 (1979).

18. E. Almof, M. Larsson-RazniKiewicz, I. Lindquist and J. Munyua, J. Prep. Biochem., 7, 1 (1977).

19. Sephadex Gel Filteration in Theory and Practice (Pharmacia Fine Chemicals).

20. Pharmacia Fine Chemicals, Literature references, 1959-1972, 1973, 1974 and 1975.

21. A.E. Hamielec and W.H. Ray, J. Appl. Polym. Sci., 13(1317), 1969.

22. L.H. Tung, J. Appl. Polym. Sci., 10, 375 (1966).

23(a). W.W. Yau, H.J. Stoklosa and D.D. Bly, J. Appl. Polym. Sci., 21, 1911-1920 (1977); (b) A.E. Hamielec, J. Liq. Chrom., 3(3), 381-392 (1980).

24. R.V. Figini, Poly. Bulletin 1, 619-623 (1979).

25. S.T. Balke, A.E. Hamielec, B.P. LeClair, and S.L. Pearce, Ind. Eng. Chem., Prod. Res. Develop., 8, 54 (1969).

26. M.J.R. Cantow, R.S. Porter and J.F. Johnson, J. Polym. Sci., A-1, 5, 1391 (1967).

27. A.R. Weiss and E. Cohn-Ginsberg, J. Polym. Sci., A-2, 8, 148 (1970).

28. L. Wild, R. Ranganath and T. Ryle, J. Polym. Sci., A-2, 2137 (1971).

29. T.D. Swartz, D.D. Bly and A.S. Edwards, J. Appl. Polym. Sci., 16, 3353 (1972).

30. A.H. Abdel-Alim and A.E. Hamielec, J. Appl. Polym. Sci., 18, 297 (1974).

31. J.A.P.P. Van Dijk, W.C.M. Henkens, and J.A.M. Smit, J. Polym. Sci., Poly. Phys. Ed., 14, 1485 (1976).

32. K.A. Granath and B.E. Kvist, J. Chrom., 28, 69 (1967).

33. T. Hashimoto, H. Sasaki, M. Aiura and Y. Kato, J. Polym. Sci., Polym. Phys. Ed., 16, 1789-1800 (1978).

34. F. Rodriguez, R.A. Kulakowski, and O.K. Clarke, Ind. Eng. Chem., Prod. Res. Dev., 5, 121 (1966).

35. F.C. Frank, I.M. Ward and T. Williams, J. Polym. Sci., A-2, 6, 1357 (1968).

36. F.L. McCrackin, J. Appl. Polym. Sci., 21, 191-198 (1977).

37. K.J. Bombaugh, W.A. Dark, and R.N. King, J. Polym. Sci., Part C, 21, 131 (1968).

38. A.A. Soeteman, J.P.M. Roels, J.A.P.P. Van Dijk, and J.A.M. Smit, J. Polym. Sci., Polym. Phys. Ed., 16, 2147-2155 (1978).

39. J.R. Vrijbergen, A.A. Soetman and J.A.M. Smit, J. Appl. Polym. Sci., 22, 1267 (1978).

40. T. Provder, J.C. Woodbrey and J.H. Clark, Separation Sci., 6, 101 (1971).

41. A.H. Abdel-Alim and A.E. Hamielec, J. Appl. Polym. Sci., 16, 783 (1972).

42. T. Provder and E.M. Rosen, Sep. Sci., 5(4), 437-484 (1970).

43. M. Hess and R.F. Kratz, J. Polym. Sci., A-2, 4, 731 (1966).

44. S.T. Balke and A.E. Hamielec, J. Appl. Polym. Sci., 13, 1381-1420 (1969).

45. W.N. Smith, J. Appl. Poly. Sci., 11, 639 (1967).

46. A.E. Hamielec, J. Appl. Polym. Sci., 14, 1519-1529 (1970).

47. H.E. Pickett, M.J.R. Cantow, and J.F. Johnson, J. Polym. Sci., C, 21, 67 (1968).

48. P.E. Pierce and J.E. Armonas, J. Polym. Sci., Part C, 11.21, 23 (1968).

49. S.T.E. Aldhouse and D.M. Stanford, Paper Presented at the 5th International GPC seminar, London, May 1968.

50. A.E. Hamielec and S.N.E. Omorodion, "Recent Advances in Size Exclusion Chromatography", ACS Symposium Proceeding, Washington (1979).

51. T. Ishige, PhD Thesis, McMaster University, Hamilton, Ont., 1972.

52. S.M. Shawki, PhD Thesis, McMaster University, Hamilton, Ont., 1978.

53. W.R. Cabaness, T. Yen-Chin Lin, C. Parkanyi, J. Poly. Sci., Part A-1, 9, 2155-2170 (1971).

54. A.L. Spatorico and G.L. Beyer, J. Appl. Polym. Sci., 19 (11), 2933, (1975).

55. A. Takahashi, T. Kato and M. Nagasawa, J. Phy. Chem., 71, 2001 (1967).

56. J. Lecourtier, R. Audebert and C. Quivoron, J. Liq. Chrom., 1(3), 367 (1978).

57. S.M. Shawki, M.Eng. Thesis, McMaster University, Hamilton, Ont., 1974.

58. D.D. Bly, Physical Methods of Macromolecular Chemistry, Vol. 2, B, Carrol, Ed., Dekkar, New York, 1971.

59. J.R. Purdon, Jr., and R.D. Mate, J. Polym. Sci., A-1, 243 (1968).

60. L.H. Tung and J.R. Runyon, J. Appl. Polym. Sci., 13, 2397-2409 (1969).

61. N. Onda, K. Fuyusawa, N. Yamaguchi and S. Komuro, J. Appl. Poly. Sci., 23, 3631-3638 (1979).

62. T. Haskimoto, H. Sasaki, M. Aiura and Y. Kato, J. Poly. Sci., Polym. Phys. Ed., 16, 1789-1800 (1978).

63. A.R. Cooper and D.P. Matzinger, J. Liq. Chrom., 1, 745, 1978.

64. F.A. Buytenhuys and F.P.S. Van der Maeden, J. Chrom., 149, 489 (1978).

65. K.J. Bombaugh, W.A. Dark and J.N. Little, Analytical Chem., 41, 1337 (1969).

66. A,M. Basedew, K.H. Ebert, H.J. Ederer and E. Fosshag, J. Chrom., 192, 259-274 (1980).

67. A.C.M. Wu and W.A. Bough, J. Chrom., 128, 87 (1976).

68. C.D. Chow, J. Chrom., 114, 486-487 (1975).

69. T. Ogawa, M. Sakai, W. Ishitobi, J. Liq. Chrom., 1(2), 151-162 (1978).

70. T. Kotaka, J. Appl. Polym. Sci., 21, 501-514 (1977).

71. T. Kotaka, Die Angewandte MaKromolekulare Chemic., 56, 77-97 (1976).

72. A.C. Ouano, D.L. Home and A.R. Gregges, J. Polym. Sci., Polym. Chem. Ed., 12, 307 (1974).

73. A.C. Ouano and W. Kaye, ibid., 12, 1151 (1974).